FORSCHUNGSZENTRUM JÜLICH GmbH

KFA

Projektträger Biologie, Energie, Ökologie (BEO)
International Energy Agency IEA

Implementing Agreement for a Programme of Research and Development on Wind Energy Conversion Systems

20th Meeting of Experts – Wind Characteristics of Relevance for Wind Turbine Design

Stockholm, March 7-8, 1991

Organized by:
Project Management for Biology, Energy, Ecology (BEO)
Research Centre Jülich (KFA)

On behalf of the
Federal Minister of Research and Technology,
The Fluid Mechanics Department
of the Technical University of Denmark

Scientific Coordination:
M. Pedersen (Techn. Univ. of Denmark)
R. Windheim (BEO-KFA Jülich)

Implementing Agreement for a Programme of Research and Development on Wind Energy Conversion Systems

20th Meeting of Experts – Wind Characteristics of Relevance for Wind Turbine Design

Stockholm, March 7-8, 1991

Organized by:
Project Management for Biology, Energy, Ecology (BEO)
Research Centre Jülich (KFA)

On behalf of the
Federal Minister of Research and Technology,
The Fluid Mechanics Department
of the Technical University of Denmark

Scientific Coordination:
M. Pedersen (Techn. Univ. of Denmark)
R. Windheim (BEO-KFA Jülich)

C O N T E N T S

Further contributions of the 20 th Expert Meeting without a written paper:

Teknikgruppen AB

Hans Ganander, Teknikgruppen AB, Box 21, S-19121 Sollentuna

Introductory Note

Wind Characteristics of Relevance for Wind Turbine Design.

Development of wind turbines has now been going on for 10 - 15 years and we do not yet really know what life time we could expect of them. Will they last for 20-30 years, which they normally are designed for, without increasing costs of maintenance and repair? Due to increasing interest in wind energy there are tendencies for larger turbines, putting them into wind farms and utilizing windy but complex areas. Questions of load conditions and design load spectrum to get reliable economical machines with required life time therefore becomes more and more important. A very important part of these load conditions are relevant wind descriptions, which take all normal, as well as, extreme phenomenas into account.

Wind Description.

Up till now wind descriptions normally are based on wind duration distribution and so called turbulence models. Is this enough? Do they answer questions like:

- how large
- how fast
- how often

does wind variations in time and space occur, not only in one point but over the whole rotor area, not only as wind speed variations at chosen mean situations, but also regarding changes between them.

What is wind shear and what is turbulence and how do they contribute to the structure of wind speed distribution over the rotor area? This also includes direction changes as well as horisontal shear. To what extent are different meteorological conditions (neutral, stable,..) important and what do we know about influence of complex terrains?

Concerning "normal situations" it must be emphazised that 0.1% of life time, say 5e8 rotational cycles, may correspond to 0.5e6 - 1.e6 cycles on the structure. Regarding material fatigue properties this may be a very important part to take into consideration. Do we have enough data of 4 to 5 standard deviation statistics of the wind, including time as well as space variations?

These are questions the designer has to answer to make as good a design as possible. It is important for static design, but even more for fatigue design and life time estimations. What the designer actually needs is not just a wind gust model, but a wind description that takes the whole wind

situation into account, variations in time, in space, normal conditions and extremes during life time.

These aspects of a relevant wind description may be summarized as:

- **time variations** relevant for the whole rotor area, long term as well as short term variations. Does frequency representation correctly describe how fast these time variations are?
- **space variation** of wind distribution over the rotor area, for example in terms of vertical and horisontal distributions as well as direction. How important is the vertical (w) wind speed component?
- wind **direction changes.** A relevant definition which takes different yaw systemes into account?
- what **extremes** of time and space wind variations may occur, during turbine operation as well as in parked mode ?
- in what way does **wakes** and different **meteorological** and **terrain** conditions influence the wind description, especially space distribution over the rotor area and its time variation.

Methods.

This is what the designer in general wants to know about the wind. But in what way does he want this description? This is an important question about what methods are relevent? From theoretical and practical points of view, what are the differences, possibilities and limits between time and frequency domain wind descriptions? The answer is not unique and it depends on many factors such as :

- type of turbine; size, number of blades, soft or stiff design, variable speed, etc.
- what kind of structural model does he have?
- adding loads to calculate stresses in any point of the structure?
- it is amplitudes (variations) of loads he wants, not standard deviations.
- due to fatigue properties of the material not only variations are of importance but also mean levels.
- non linearities as control system, aerodynamics, structural dynamics,etc.
- generating time series out of spectrum, is that possible?
- long term behaviour of wind variations?

- extreme wind conditions and situations?
- space distribution of wind speed over the rotor area?
- wind direction changes?
- special meteorological as well as terrain conditions?
- wakes?

Measurements.

What are the demands on wind measurements in order to fulfill these wind description requirements that the designer needs, compared to what we have today. Improvements concerning

- space distribution, not to forget horisontal variations and direction changes
- long time measurements
- sample rate

have to be regarded. What available measurements do fulfill these requirements?

Miscellaneous.

When having these wind descriptions further questions arise. What wind conditions does the wind turbine company use when designing turbines? Are generalized descriptions necessary which make it possible to judge wind situations at the actual location? Or is it acceptable to have different types (classes) of descriptions representing different topological and meteorological conditions?

These are some questions to discuss in order to exchange ideas and experiences and thoughts. Of course there are a lot of other related aspects of wind characteristics, but we hope this introduction may inspire you to join an interesting wind meeting.

THE RELEVANCE OF DIFFERENT GUST COMPONENTS FOR THE LOADSPECTRUM

M.J.C.M. Berkelmans
F.J. Follings

Intron
Institute for material and environmental research

Abstract

The effect of several aspects of the wind, as given by the "Handbook Wind Data for Wind Turbine Design; version 3", on the wind- and loadspectrum of several wind turbines is examined.
With a rather simple wind turbine model, to describe the conversion of the wind spectrum to the loadspectrum, the influence of the gust and wind speed classes and of rotational sampling effects is demonstrated. The calculated spectra are also compared with measured spectra.
The results indicate that the wind classes around the rated wind speed contribute most to the load spectrum and that by omitting the sampling effects the predicted life time is over estimated more than twice, further more it appears that at least three gust classes are needed to obtain a satisfiable spectrum.

1.0 Introduction

The aerodynamic loads on a wind turbine or wind turbine components often determine the structural design of the wind turbine or components.
Designing a wind turbine therefore requires detailed information of the mean wind speeds and wind speed fluctuations to be expected during the life-time of a wind turbine.
To support wind turbine designers and manufacturers a Handbook has been developed that provides the necessary information for the structural design calculations in the time domain. Just recently version 3 of the "Handbook Wind Data for Wind Turbine Design" has been published [1]. The paper of Verhey [2] focuses on the theoretical background of this handbook.
The key aspects used to describe the wind in this handbook are:

- (hourly) mean wind speeds
- large scale longitudinal wind speed fluctuations
- small scale longitudinal wind speed fluctuations
- wind shear
- oblique wind

The deterministic winddata are obtained by analysing series of (dutch) wind measurements. To get a broad spectrum of winddata the gusts were classified. This paper describes the effects of the classification on the windspectrum and the resulting loadspectrum.
Chapter 2 deals with the classification of large and small scale gusts. In chapter 3 the related loads are presented and in chapter 4 the results of the verification. Some final conclusions are drawn in chapter 5.

2.0 Winddata

2.1 Mean wind speed and gust duration

The range of mean windspeeds at hub height (mean windspeeds from 4 to 25 m/s) is divided in eight classes. Each class is represented by the maximum value of that class. The chance of occurence of the wind classes is according to the Weibull probability distribution.
The deterministic gust data of the Handbook are presented in the time domain by means of the amplitude, duration and number of gusts in a certain period.
In case of the large scale gusts the gust duration is divided in three classes: from 2 to 7 sec, 7 to 16 sec and from 16 to 30 sec (half a sinus). The chance of occurence of each class is one third. For the determination of the number of gusts the representative durations are 4, 10 and 20 sec respectively. For the determination of the amplitudes the conservative values within each class are being used (7, 16 and 30 sec).

2.2 Gust amplitudes

The amplitudes of the gusts in a certain wind and duration class are distributed according to a Weibull probability function (shape factor 1,8). To determine the necessary number of classes for a satisfiable load spectrum the wind data are presented in a special way. The amplitude of the gusts were plotted versus number of gusts. Presenting the winddata in this manner appears to be instructive with respect to the load spectrum. Table 1 gives the gust amplitude classifications that have been examined.

case	amplitudes	chance of occurence
1	$A_{10\%}$	100%
2	$A_{10\%}$	98%
	$A_{1\%}$	2%
3	$A_{10\%}$	80%
	$A_{1\%}$	18%
	$A_{0.01\%}$	2%

Table 1: Gust amplitude classification

First the gusts were represented by one amplitude corresponding to an exceedance level of 10 % and a chance of occurence of 100 % (figure 1a). The resulting windspectrum of the considered wind turbine is plotted in figure 2 along with the 1P to 4P-modes. The considered wind turbine (HAT25) has a rotordiameter of 25 m, hub height of 22 m and is sited in a terrain with an estimate roughness of 0.1 m. The winddata show that the higher amplitudes are not represented, so a second class of gusts is defined with an amplitude corresponding to an exceedance level of 1% and with a chance of occurence of 2% (figure 1b and figure 2). Still the higher ranges were

not represented satisfiable and the "10%-" and "1%-gusts" did not overlap qua number of gusts, so a third class of gustamplitudes was defined representing 2 % of the gusts with an amplitude of 0.01 % and the other two amplitude classes are redefined (figure 1c).
So three classes of wind gusts are defined. One class representing amplitudes smaller than the amplitude corresponding to an exceedance level of 10 %. This class has a chance of occurence of 80 %. Then a class of gusts with their amplitudes between the amplitudes corresponding with exceedance levels of 10 and 1%. These gusts are represented by the latter exceedance level and have a chance of occurence of 18 %. The rest of the gusts (2 %) are represented by an amplitude corresponding with an exceedance level of 0.01 %. So the classes of the 1% and 10% gusts are represented by more or less conservative values. The resulting windspectrum is rather smooth as illustrated by figure 3. The higher numbers correspond to the 1P to 4P rotational sampling effects. Beside the gusts and 1P to 4P effects equivalent wind fluctuations because of wind shear and oblique wind are incorporated in the spectrum.

2.3 Terrain roughness

An important parameter is the terrain roughness. In figure 4 an example of the effect of the terrain roughness on the winddata is demonstrated. Despite the significant difference in terrain roughness (0.25 m instead of 0.03 m) the effect is modest.

3.0 Loads

3.1 Model

The influence of different parameters on the winddata spectrum can not directly be translated to the load spectrum because of the non linear character of the transmission. The loads are calculated with a simple model. The fluctuations in the wind are transformed via a precalculated power and thrust versus wind speed curve to fluctuations in power or thrust as illustrated in figure 5. With this the resulting lagmoment and flapmoment for one blade can be derived. Doing so one can obtain all relevant loads B resulting from the winddata as indicated by figure 7 . Dynamic effects are taken into account by multiplying the static load B with a dynamic multiplication factor O. In case of the HAT 25 wind turbine, a pitch regulated turbine, a factor of 1,5 has been used. The final load of a certain mode can be found be combining higher order modes according to the rain flow counting method. The formulas of this operation are presented in figure 6. It is a global approach but for first order parameter analysis sufficient. The used thrust and power curves are shown in figure 7a and 7b.

3.2 Contribution of windgusts to load-spectrum

The thus calculated cumulative load spectra are presented in figure 8a and 8b. The calculated spectra agree reasonably with the measured data. It looks like an acceptable method to examine the influence of several gust parameters on the load spectra.
Figure 9 shows the contribution on the cumulative loadspectra of different

aspects of the winddata. One can see that specific windaspects determine the loads in a certain range. The presented loads are of the loads B* (see figure 6), which means that effects of higher modes are taken into account as well as the dynamic multiplication factor.
Figure 10 shows the influence of the wind classes on the loadspectra. The contribution of the high wind speeds to the loadspectra is modest. The same trend was observed with two other turbines but of course this depends very much on the used thrust curve.
Figure 11 shows the effect of omitting rotational sampling.

4.0 Verification of handbook winddata

In order to find out how well the fatique loads based on the handbook are predicted the handbook has been verified by the Netherlands Energy Research Foundation (E.C.N.) by comparing measured load spectra with calculated load spectra on three different windturbines by using the more sophisticated model PHATAS [3]. The load calculation method is presented in figure 12. The large scale wind gusts are combined with the higher modes to one windsignal. Vertical windshear, tower passage and oblique windfluctuations are part of the aerodynamical model of the turbine. After rain flow counting the loads, one gets the load spectrum of figure 13a and 13b. There is a good agreement with the measured data. Verification on two other turbines shows an even better agreement with measurements.

5.0 Conclusions

It appears to be possible with rather simple aerodynamical models of the wind turbine to assess the influence of several parameters of the wind data on the wind loads. The spectra show that about three gust duration and amplitude classes are necessary for an adequate wind and load spectrum. The influence of the terrain roughness on the load spectrum is modest. The wind speeds around V_{rated} contibute most to the load spectrum. Omitting rotational sampling effects can lead to an over estimation of the life time of the wind turbine (component) of more than a factor of two.

Literature

[1] F.J. Verhey, F.J. Follings, A.P.W.M. Curvers
Handbook Wind Data for Wind Turbine Design, version 3
TNO-IMET, INTRON, ECN
1991

[2] F.J. Verhey
Gust Modelling for the Dutch Handbook on Wind loads
TNO (IMET)
Workshop Stockholm
1991

[3] L.W.M.M. Rademakers
Verificatie van het "Handboek Ontwerpwindgegevens windturbines, versie 2"
Netherlands Energy Research Foundation (ECN)
1991
to be published in dutch

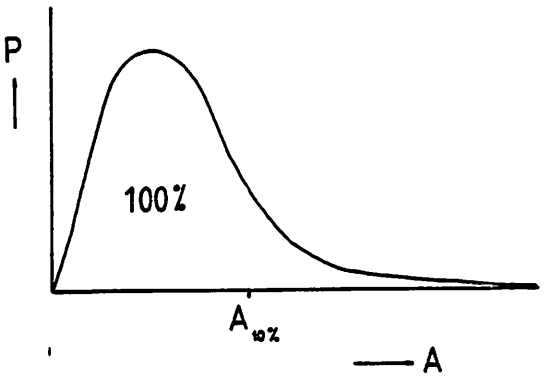

figure 1a: Classification of large scale windgust in amplitude classes (case 1).

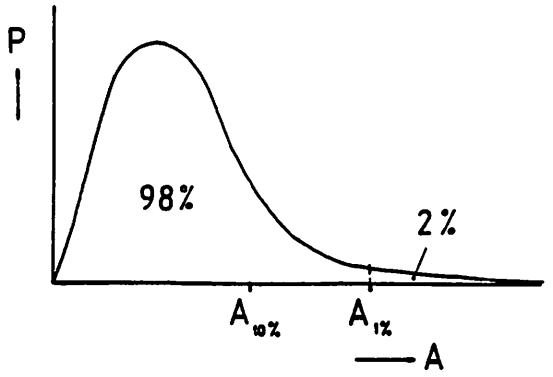

figure 1b: Classification of large scale windgust in amplitude classes (case 2).

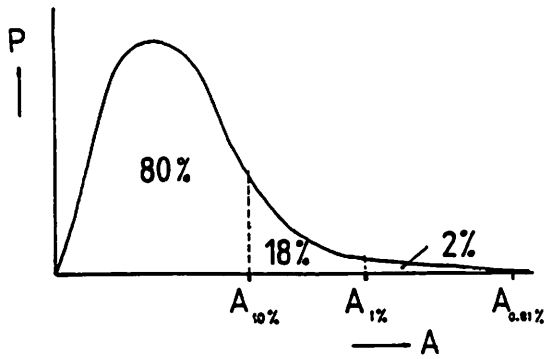

figure 1c: Classification of large scale windgust in amplitude classes (case 3).

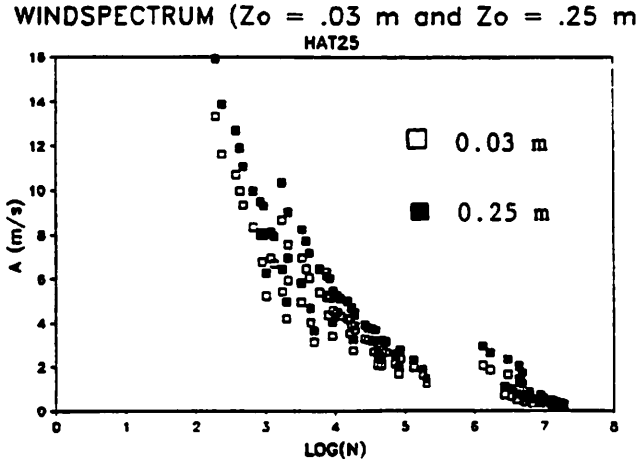

Figure 4: Windspectrum HAT25 with terrain roughness 0.03 m and 0.25 m.

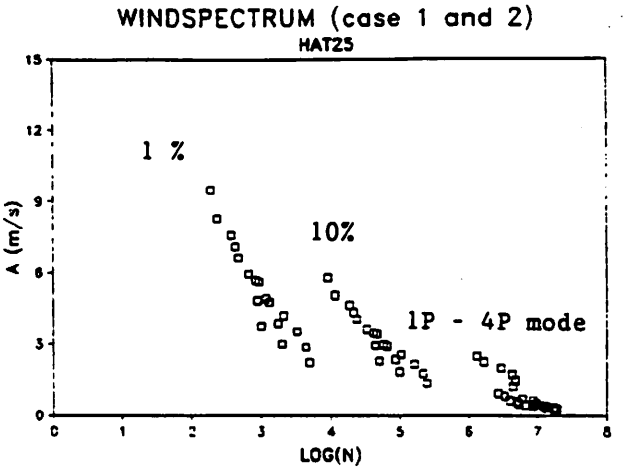

Figure 2: Windspectrum HAT25 according to case 1 and 2.

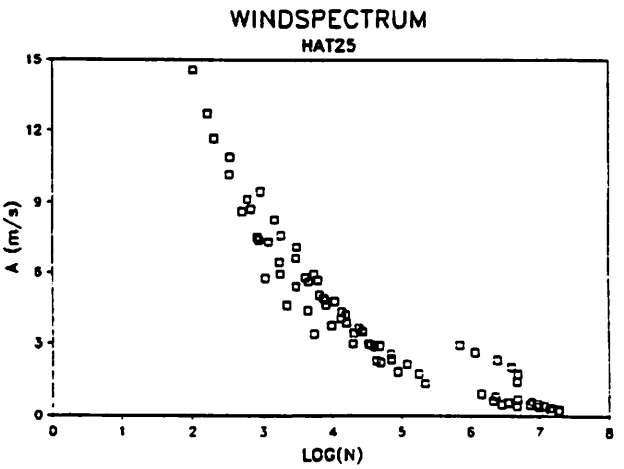

Figure 3: Windspectrum HAT25 according to final classification.

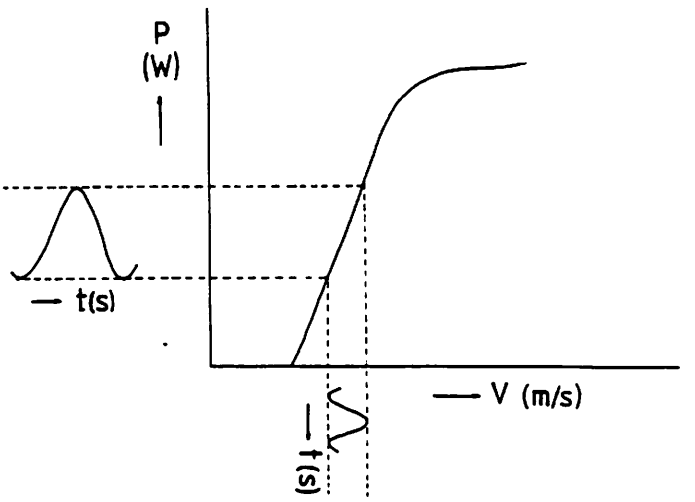

Figure 5: Calculation of loads according to global model

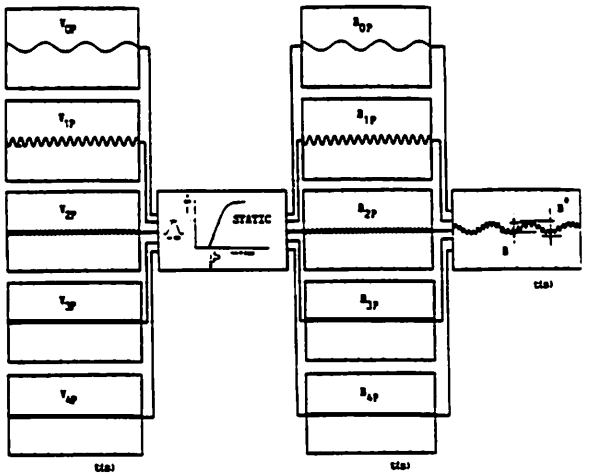

$$B_{4P}^{*} = O_{4P}B_{4P} + C_{4P}$$
$$B_{3P}^{*} = O_{3P}B_{3P} + O_{4P}B_{4P} + C_{3P}$$
$$B_{2P}^{*} = O_{2P}B_{2P} + O_{3P}B_{3P} + O_{4P}B_{4P} + C_{2P}$$
$$B_{1P}^{*} = O_{1P}B_{1P} + O_{2P}B_{2P} + O_{3P}B_{3P} + O_{4P}B_{4P} + C_{1P}$$
$$B_{0P}^{*} = O_{0P}B_{0P} + O_{1P}B_{1P} + O_{2P}B_{2P} + O_{3P}B_{3P} + O_{4P}B_{4P}$$

Figure 6: Calculation method used by the global model.

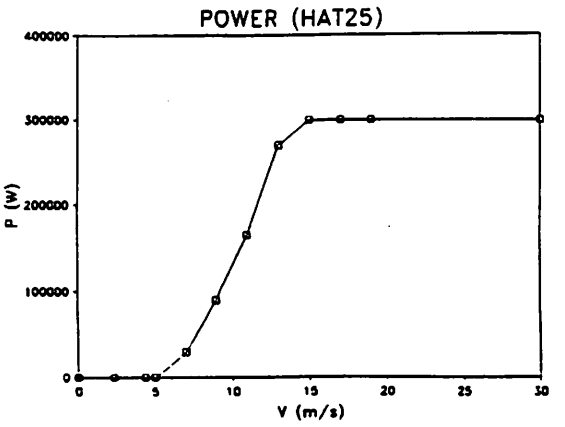

Figure 7a: Power versus windspeed curve.

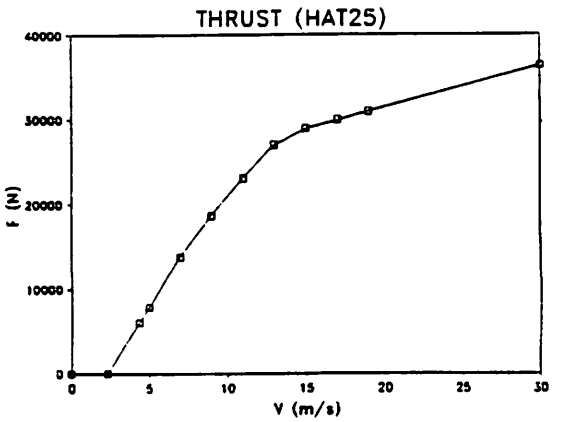

Figure 7b: Thrust versus windspeed curve.

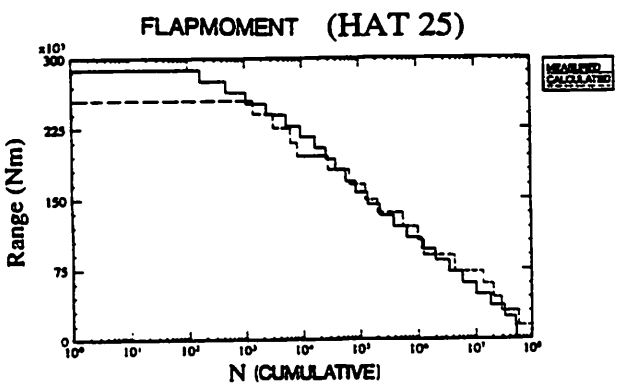

Figure 8a: Loadspectrum (flap moment) HAT25 according global model.

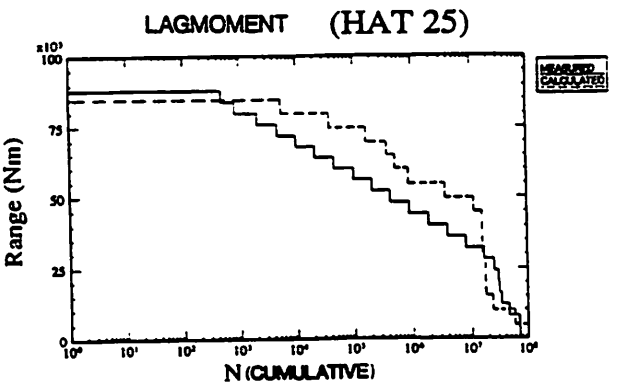

Figure 8b: Loadspectrum (lag moment) HAT25 according global model.

FLAPMOMENT (HAT 25)

(CALCULATED)

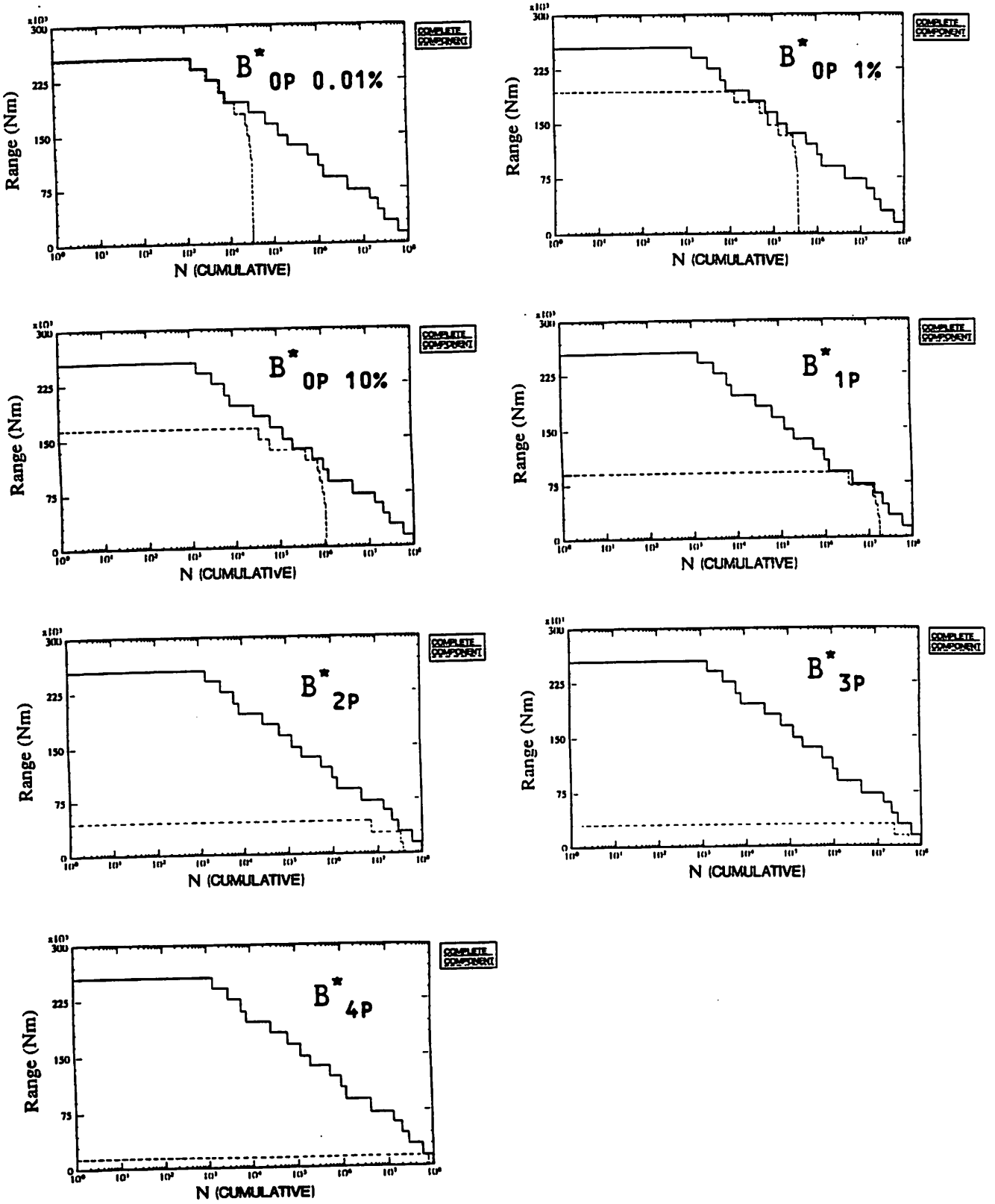

Figure 9: Contributions large scale gusts and higher order modes.

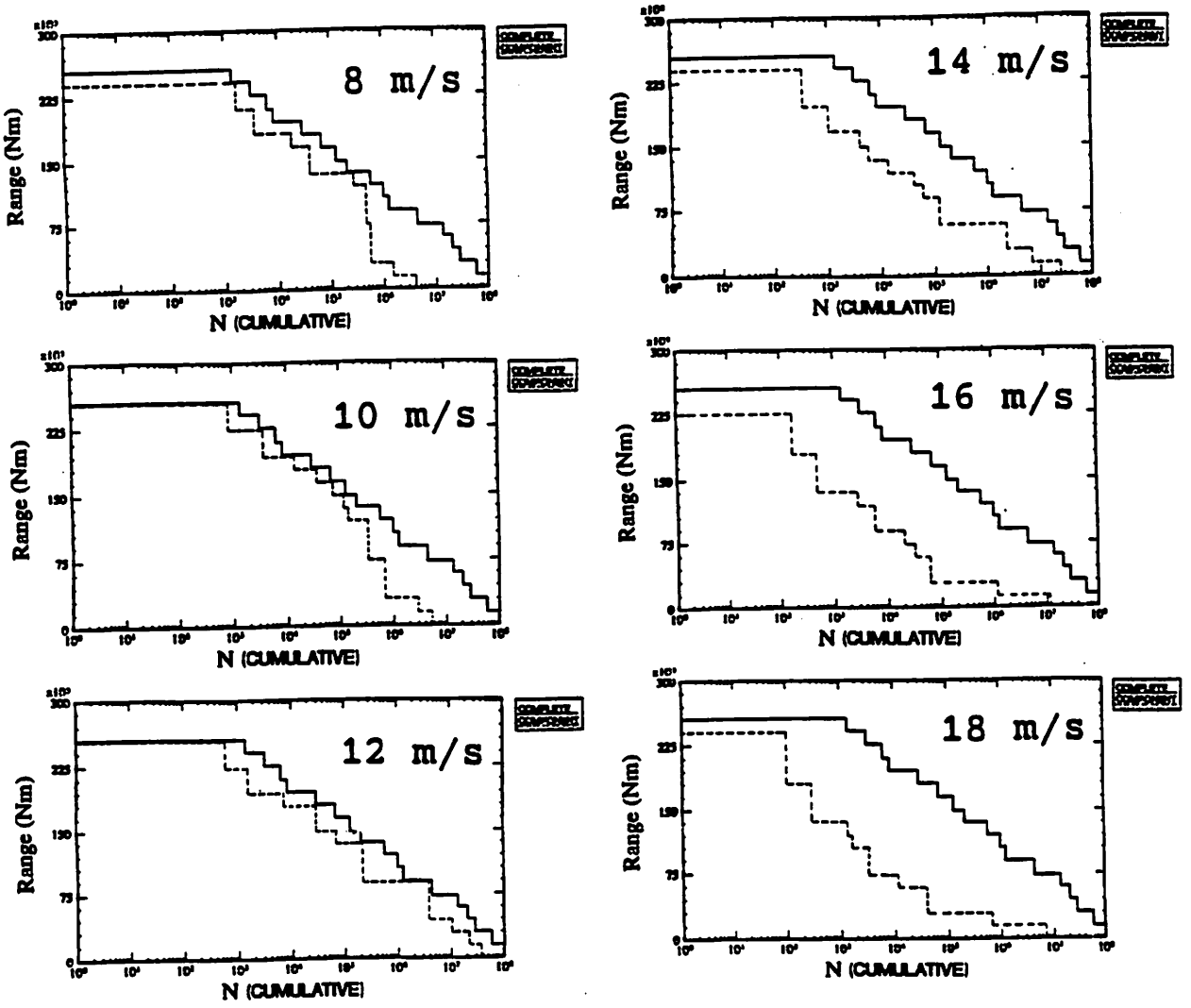

Figure 10: Contributions of the windclasses on the loadspectrum HAT25 (flapmoment).

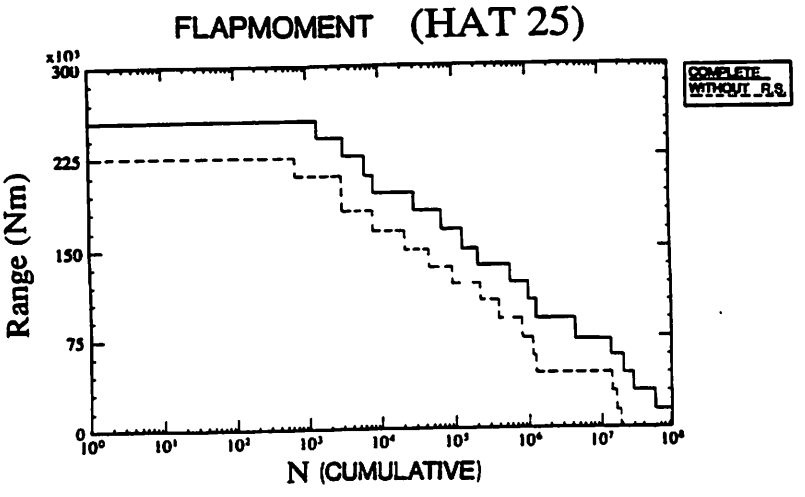

Figure 11: Effect of rotational sampling on the loadspectrum HAT 25 (flapmoment).

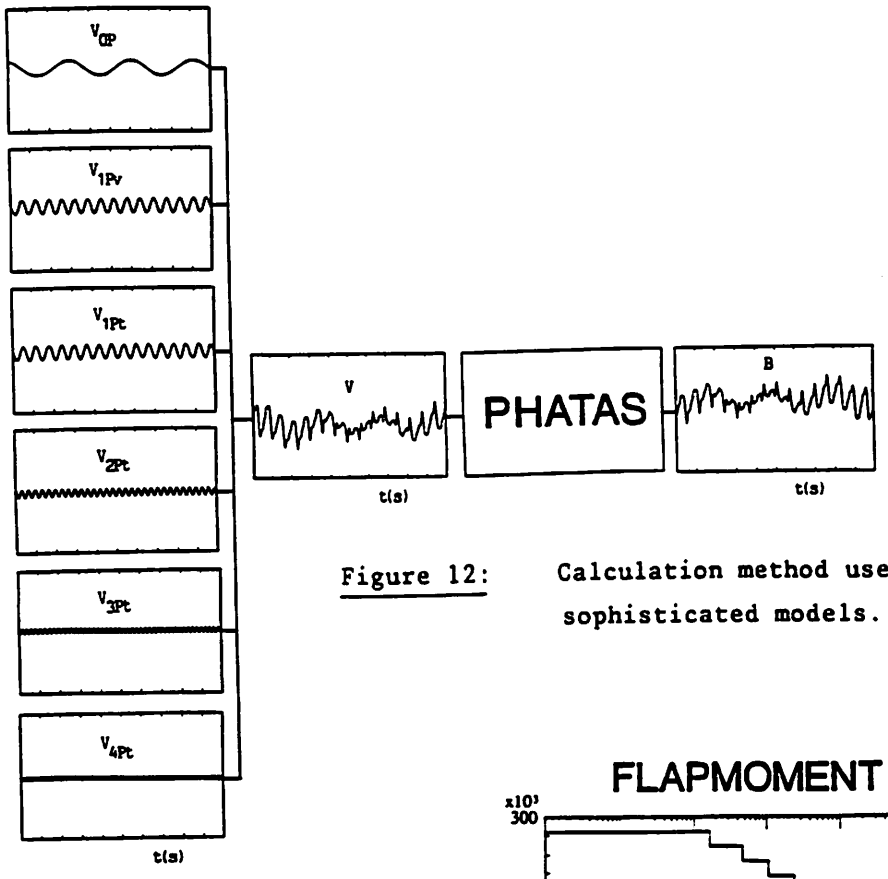

Figure 12: Calculation method used with more sophisticated models.

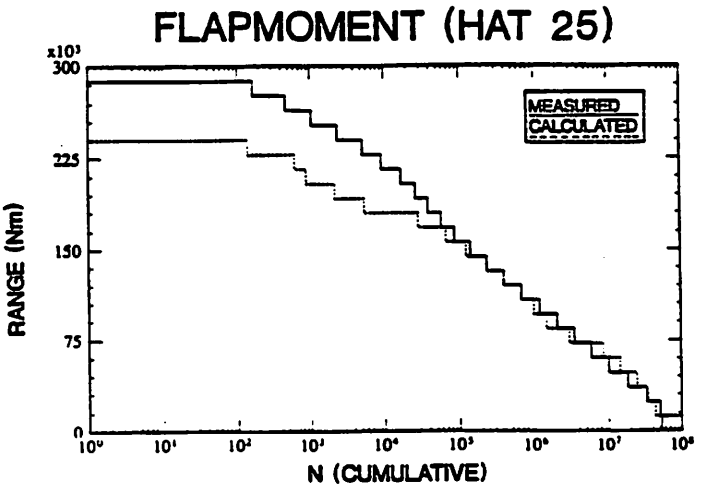

Figure 13a: Loadspectrum (flapmoment) HAT25 according to sophisticated model.

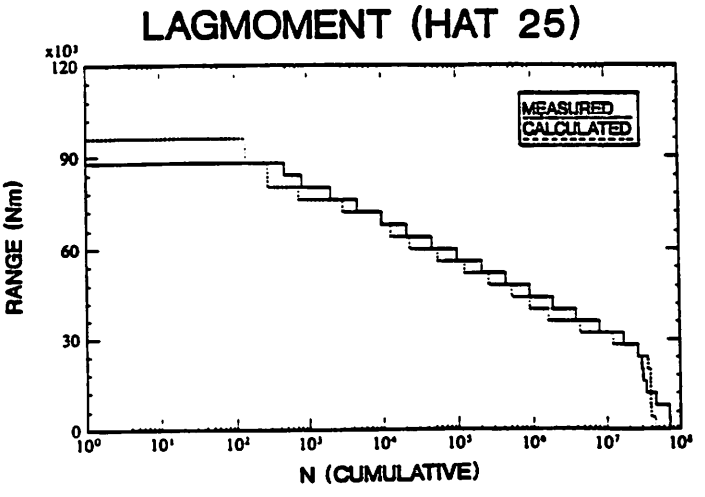

Figure 13b: Loadspectrum (lagmoment) HAT25 according to sophisticated model.

IEA Annex XI
Stockholm 7-8 March 1991

RISØ

Probability structure of turbulence in a windfarm

Jørgen Højstrup
Department of Meteorology and Wind Energy
Risø National Laboratory
Roskilde, Denmark

1 INTRODUCTION

It is well known that turbulent velocity fluctuations cannot be described as a Gaussian process i.e. see Wyngaard 1973, Dutton and Højstrup 1979, Busch and Jensen 1982, Panofsky and Dutton 1985, just to mention a few. In many cases it is nevertheless possible to use the normal distribution as a good approximation to velocity distributions, it is not until we get out on the tails of the distribution that the differences show up. The deviations from gaussianity become particularly obvious when we look at the time derivative of velocity, which have much wider tails in the distribution than a Gaussian has. In many cases this fact is of no consequence, but if we start looking for extreme turbulent wind loads, then we must treat models using normal distribution with some caution.

In the wake of a wind turbine and particularly in a windfarm we know that turbulence levels are high (Højstrup 1990) which of course will make extreme values of wind fluctuations large. It is of some interest to see whether the normal distribution for these cases is a reasonable approximation, or if the distributions in the windfarms look significantly differently than they do in the free flow.

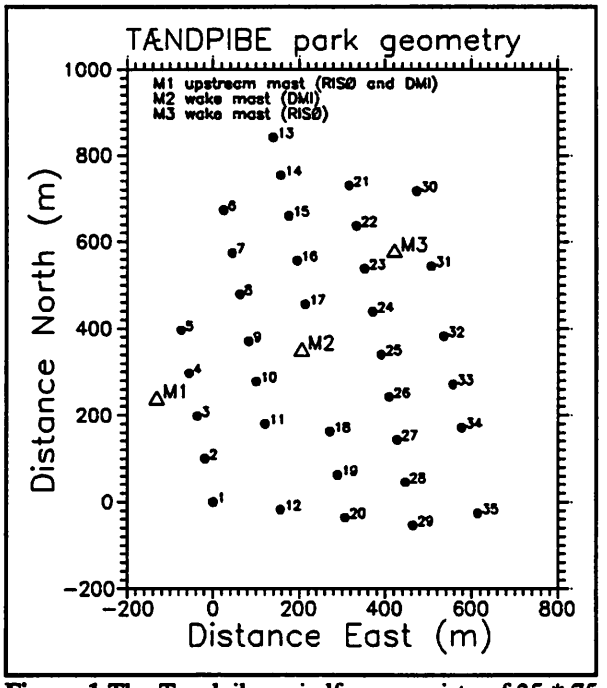

Figure 1 The Tændpibe windfarm consists of 35 * 75 kW VESTAS machines situated in flat terrain near the coast. Each of the turbines is denoted by a filled circle. The two masts used by Risø are denoted by open triangles M1 and M3.

2 MOMENTS OF VELOCITY FLUCTUATIONS

We will look at statistics from four runs from the Tændpibe windfarm (Højstrup and Nørgård 1990), with windspeeds of 6-7 m/s and a wind direction of approx. 240 degrees. The data is presented as profiles of statistics (averaged over the four runs) measured inside the windfarm (mast M3) normalized by measurements at the upstream mast (M1). Three curves are shown in each plot: In full line the average value over the four runs, and in dashed line the average value ± one std. error of the average value.

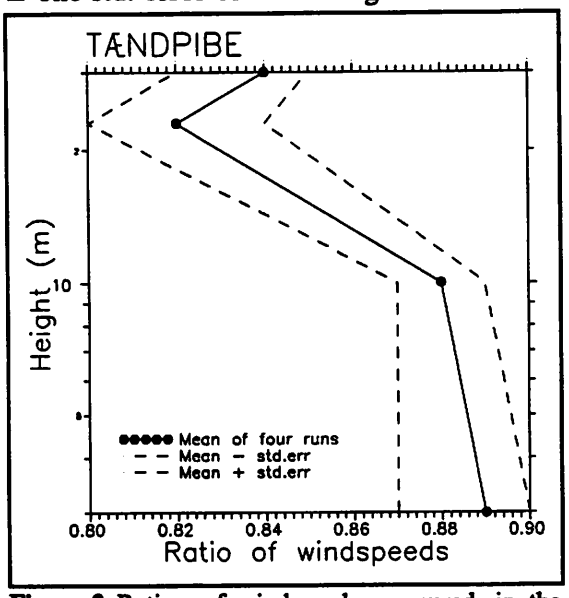

Figure 2 Ratios of windspeeds measured in the farm to upstream values. The full line denotes the average values. The dashed lines denote ± one std. err. on the mean value.

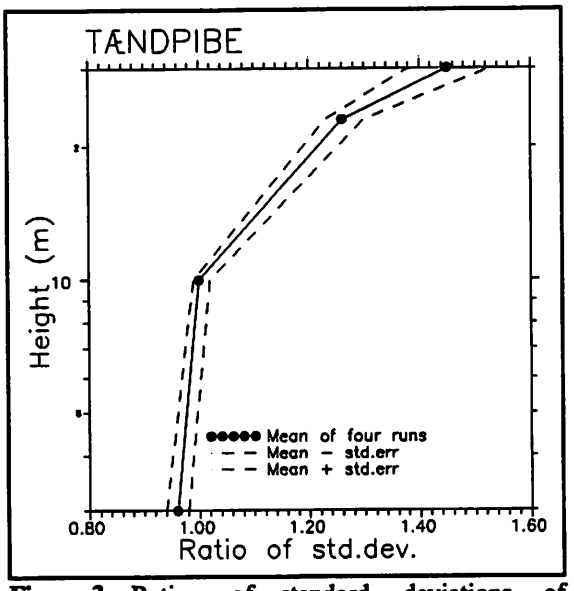

Figure 3 Ratios of standard deviations of windspeeds measured in the farm to upstream values.

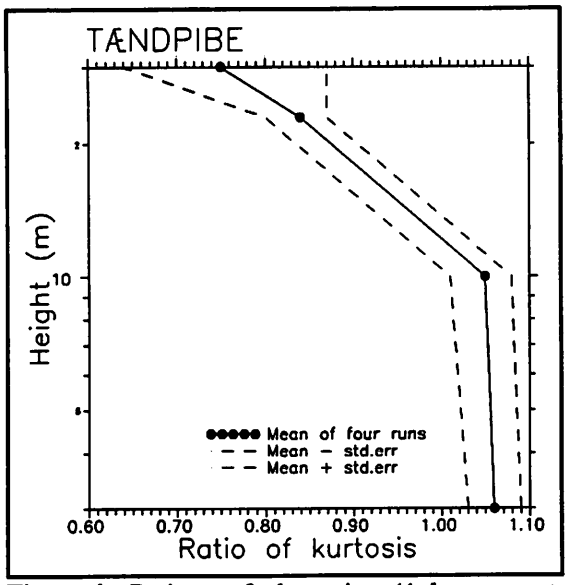

Figure 4 Ratios of kurtosis (4.th moment normalized by variance squared). Average value upstream was 3.0 for the four runs, in the farm 2.7. (Gaussian: 3.0).

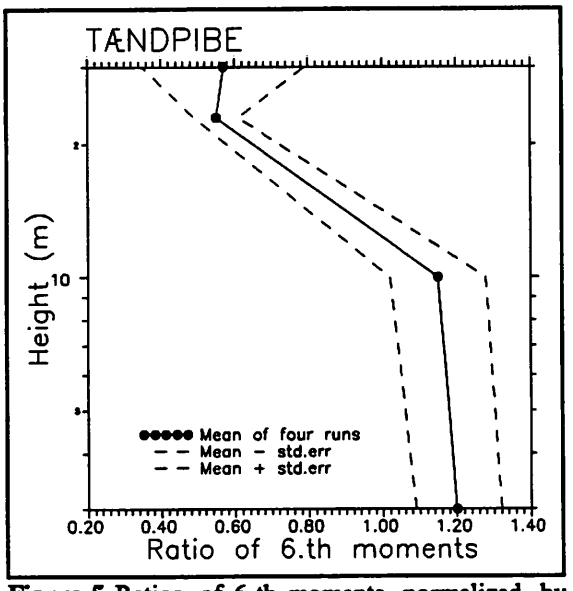

Figure 5 Ratios of 6.th moments normalized by variance cubed. Upstream average value was 15.2, in the farm 10.9 (Gaussian: 15.0).

There emerges a fairly clear picture from these plots: Std. Deviations increasing with height, higher order moments decreasing with height, indicating that increased variance results in wider distributions of course, but these are well behaved in the sense that they exhibit smaller excursions from the average value than a gaussian distribution with the same variance.

3 PROBABILITY DENSITIES

We will now take a closer look at the actual probability density distributions of windspeed fluctuations, exemplified by one run where distributions at two heights (3m and 30m) are shown, compared with normal distributions with the same mean and variance.

In figure 6 at the 3m level we see very little difference between measurements upstream and measurements inside the farm. The measured distributions are shown as curves whereas the normal distributions are denoted by symbols. In figure 7 is shown sonic anemometer measurements at 32m in addition to the cupanemometer results. Several things are worth noting here:

- The velocity distribution inside the farm is indeed considerably more narrow than the corresponding normal distribution.

- The distributions resulting from cup at 30m and sonic at 32m are very similar except in one respect: The cupanemometer distribution shows smaller excursions towards low windspeeds than does the sonic data. This is obviously a result of slight cupanemometer overspeeding i.e. the fact that any cupanemometer will respond to variations in speed faster than the cutoff frequency of the anemometer in a nonlinear fashion, such that it adjusts more rapidly to increasing windspeed fluctuations than to decreasing fluctuations.

- The upstream distribution is slightly skewed which is of no consequence for this purpose.

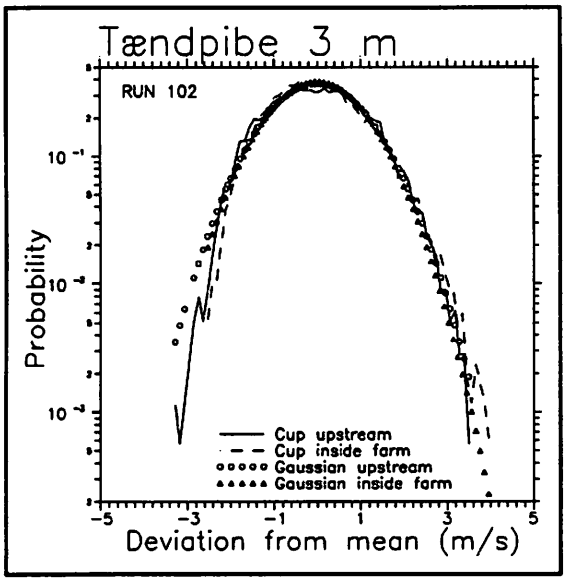

Figure 6 Probability density distributions at 3 m height, upstream and inside the windfarm. Normal distributions with the same variances as the data are shown as open circles and open triangles.

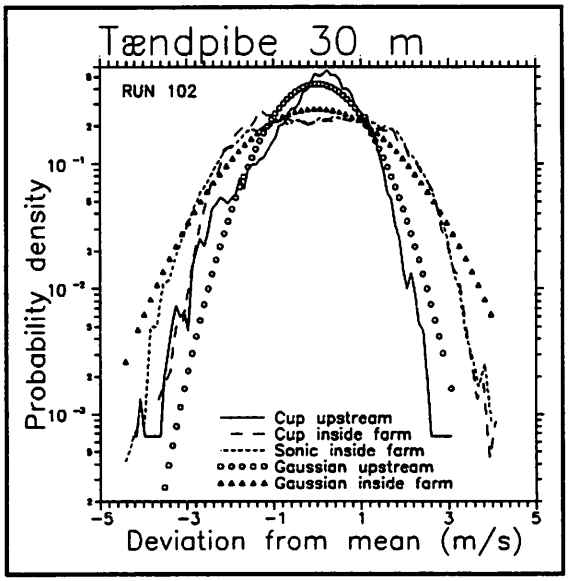

Figure 7 Probability density distributions at 30 m. Data shown upstream (cupanemometer) and inside the windfarm (cupanemometer and sonic at approx. same height). Normal distributions shown for comparison.

4 SONIC ANEMOMETER STATISTICS

The sonic anemometer is capable of making rapid response measurements of the total wind vector, and we can calculate statistics of the individual components: U alongwind, V laterally and W vertically, to compare the structure of the turbulence inside the farm with our knowledge about free stream turbulence.

We use the same four 4000 second runs as we did above, and compare the standard deviations of the three components. In uniform terrain we normally normalize the values by u_*, which is $\sqrt{-<uw>}$, where the brackets denote averaging (after the mean value has been subtracted). This is not possible here, since the turbulence is so disturbed that the uw-correlation has a positive sign at 18m height. Instead we have chosen to normalize the values by σ_w:

	σ_U/σ_W	σ_V/σ_W	σ_W/u_*
Uniform terrain	1.91	1.54	1.25
Tændpibe 18 m	1.67±.14	1.49±.05	
Tændpibe 32 m	1.64±.14	1.17±.08	1.22±.02

We see that the U- and V-components show values far from their uniform terrain equilibrium values, especially at 32m, whereas the W-component seems to be close to equilibrium values. Looking at the actual velocity spectra (Højstrup and Nørgård 1990) confirms this observation. Another important feature of the spectra is the fact that the excess energy appears at scales of the order 1-2 rotor diameters (the wake diameter), which make the spectra look as if they were measured at a height 10 times lower than the actual height. The values for uniform terrain have been taken from Panofsky and Dutton (1984).

CONCLUSIONS

- Large turbulence levels in windfarm (25 %)

- Probability distributions of velocity fluctuations inside windfarm not normally distributed. Tails of distribution are shorter than for Gaussian distribution.

- Vertical velocity fluctuations appear to be in local equilibrium in windfarm. Horizontal components far from equilibrium.

- Velocity spectra of U-component have received the excess energy at a scale of order 1-2 rotor diameters, which means that the U-spectra look as if they were measured at a height 10 times lower than they actually were.

References:

Busch, N.E., and N.O.Jensen, 1982: Atmospheric turbulence. **Engineering Meteorology**, E.J. Plate, Ed., Elsevier Scientific Publishing Company, Amsterdam.

Dutton, J.A, and J. Højstrup, 1979: A model for the probability structure of atmospheric turbulence, **Proceedings of the Conference and Workshop on Wind Characteristics and Wind Energy Siting 1979.** Portland, Oregon. Sponsored by the U.S. Department of Energy and Amer. Meteor. Soc., coordinated by Pacific Northwest Laboratory. PNL-3214.

Højstrup, J., 1990: Turbulence measurements in a windfarm. **Proceedings of BWEA12, Norwich, UK, March 28-30 1990.** Ed. by T.D.Davies, J.A.Halliday, J.P.Palutikof.

Højstrup, J., and P.Nørgård, 1990: Tændpibe Wind Farm Measurements. **Risø M-Report.** M-2894.

Panofsky, H.A., and J.A. Dutton, 1984: Atmospheric turbulence. Models and methods for engineering applications. John Wiley & Sons Inc., New York.

Wyngaard, J.C. 1973: On surface layer turbulence. **Workshop on Micrometeorology,** D.A. Haugen, Ed., Amer. Meteor. Soc., pp. 101-149.

APPLICATION OF WIND INFORMATION IN THE DESIGN OF A VARIABLE SPEED HAWT

A. Aliberti, Alenia, Rome, Italy

and

B. Montgomerie, WEST, Taranto, Italy

ALENIA
AERITALIA & SELENIA
VIA VITORCHIANO 81
00 189 ROMA
ITALIA
TEL (06) 333 90 40
FAX (06) 333 90 59

WEST
WIND ENERGY SYSTEMS TARANTO S. p. A.
VIA ARCHIMEDE, ZONA INDUSTRIALE
741 00 TARANTO
ITALIA
PHONE (099) 476 91
FAX (099) 471 85 64

INTRODUCTION

The following text and charts does not follow the normal report format. What the reader will see is the view graphs as they were presented at the "WINDS WITH RELEVANCE FOR WIND TURBINE DESIGN" conference in Stockholm, Sweden in march 7 - 8, 1991. Preceeding most view graphs a text page has been added for explanation.

VIEW GRAPH 1

The following chart is an overview of the Aeritalia's total wind turbine program. Our focus in this presentation is on the **Medit Mark III**. But first a summary of the Medit Mark II main characteristics.

- Diameter = 33 m
- Number of blades = 2
- Axis approximately horizontal (uptilted 6°)
- Upwind
- Stiff hub
- Whole blades pitch control
- Coning angle = 4°
- Hub height = 26 m
- Fixed RPM = 40
- Asynchronous generator

The Medit Mk III is a product development of the Mk II. This development follows closely the ideas implemented in the Gamma project. The main deviation between Mk II and Mk III is that the Mk III has:

- Variable RPM
- Original Windane 34 blades (perhaps to be tip clipped)
- Fixed pitch
- Turn out of wind (instead of pitch control)
- Teetered hub
- Hub height approximately 34 m

In November of 1989 Aeritalia created a subsidiary company called WEST - Wind Energy Systems Taranto

In 1990 Aeritalia changed its name to ALENIA, after a marger with formerly Selenia.

WEST is a company of Alenia (IRI FINMECCANICA GROUP), committed to develope and commercialize W.E.C.S. in Taranto in southern Italy.

WEST is able to supply complete wind farms, made by several W.E.C.S. delivering energy to the existing network.

The two product lines of WEST deal with medium and large size W.E.C.S. called MEDIT MARK 2 (320 Kw) and GAMMA 60 (1500 Kw).

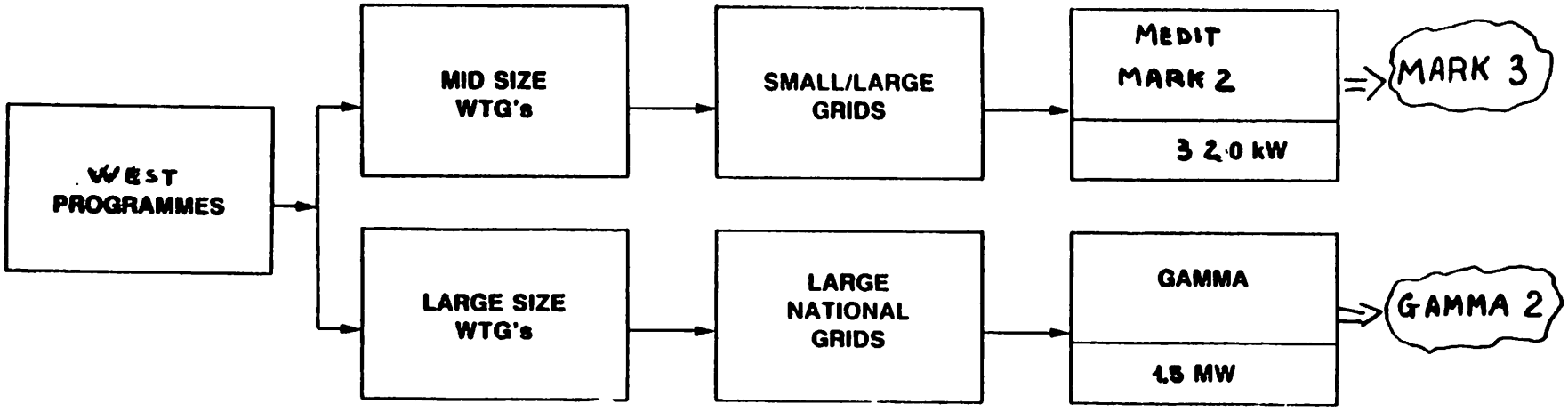


THE WAY WE WISH
WE COULD DO IT

THE IDEAL BASE WORK

Our preferred foundation for the utilisation of the wind is seen in the next graph. The upper left part has already been carried out in several places. The comparison was generally found to be good.

The RFC comparison has not yet been made. But if this work is carried out soon enough we will perhaps utilise this technique.

DESCRIPTION OF THE GANANDER/JOHANSSON RAIN FLOW COUNT ON THE WIND

The suggestion to apply the Rain Flow Count method on the wind (WRFC) was first proposed by H. Ganander and H. Johansson, TEKNIKGRUPPEN, Sweden in 1985. The basis for the idea is that wind can be correlated to structural stress. In the context of fatigue the RFC method, applied to a stress signal in a monitored point, is generally accepted to be the best in order to define what a structural load cycle is.

It is possible to first simulate the wind and then calculate the stress and then carry out the RFC on the stress signal. All of this can be done in a simulation program. However, the computer time needed may be forbidding. A direct RFC on the wind will save a tremendous amont of computer time. The reason is that "gusts" will be identified. These gusts start from a certain level and transfer to another level (selfexplanatory). All gusts are collected in bins whereby a number of finite gust combinations are established. Then the gusts are grouped into bin for descretisation. All of these *separate* descrete gusts can be used to "drive" a simulated wind turbine structure. During the simulation a load/stress change can be recorded in a number of monitoring points throughout the structure. This simulation may involve the control system and acceleration of the rotor. Somewhere along the time axis the stress deviates most from the starting stress. The difference is taken to be the *stress excursion.*

In this manner all combinations of gusts defined as WRFC "from/to" gusts will be used to calculate the corresponding stress excursions. But, each one will only be calculated once. To carry through all these simulations does *not* require any knowledge whatsoever of the wind statistics!

In a *separate* effort the number of each excursion is calculated. This is done using the information extracted from the wind statistics (using the WRFC technique). Then a standard Palmgren-Miner linear fatigue damage analysis can be carried out.

The technique allows a *non-linear* structure to be analysed. The active control system together with the variable RPM makes the Medit Mk III turbine highly non-linear! A direct spectral analysis (wind spectrum in -> stress spectrum out) would have little value in the case of our machine.

WRFC ON *SIMULATED* WIND

As pointed out above, the simulation technique used to simulate a wind time signal is quit good. It is therefore not too far fetched to imagine the WRFC to made on the simulated wind rather than the measured one. This gives a very attractive freedom of analysis. In brevity: - No wind measurement is taken exactly where the intended wind turbine is going to be located. Even if the wind at the same site is measured the meteorologists will erect a met. tower where the anemometers are at some height which is not at hub height. Therefore, the wind information will have to be manipulated to fit the right hub height under all circumstances. This means that an WRFC directly on the measured wind signal is not useful for turbine design. Hopefully the reader now appreciates the idea of performing the WRFC on the *simulated* wind rather than on the *measured* wind.

The future development, that the authors would appreciate, is touched upon in the very low part of the chart. A certain curve fit is mentioned. Before this topic is addressed the reader is adviced to view the next graph first.

THE IDEAL BASE WORK

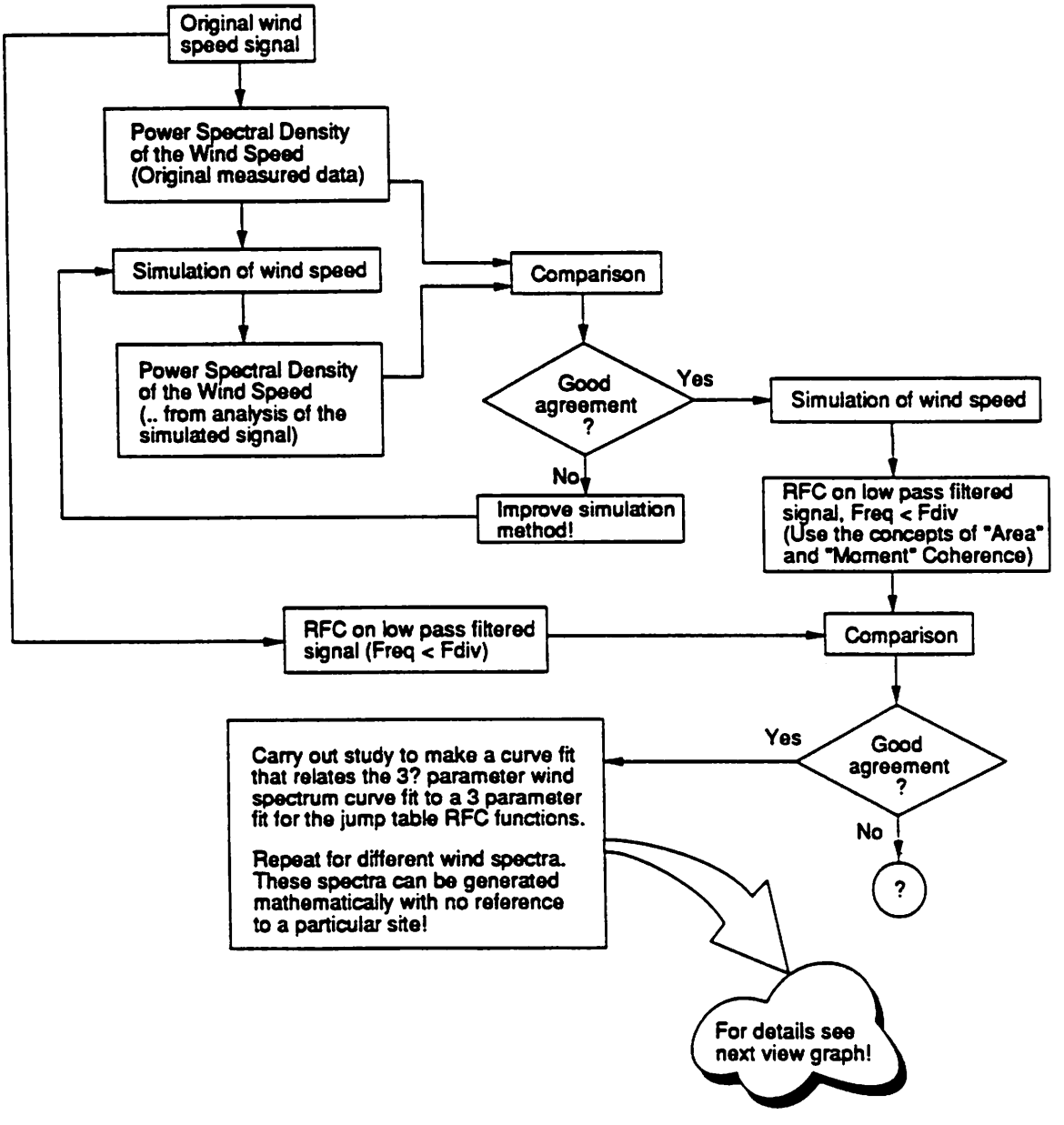

FUTURE WORK SEQUENCE (?)

This view graph should clarify the work sequence described in the previous chart. The type of WRFC information that can be extracted is placed in paper sheets like those sketched or (perhaps more likely) in computer storage.

The curve fit mentioned in the text about the previous chart should be described here:

The S(n) curve seen in this chart can be constructed from three basic parameters only. They are

1. Annual mean wind speed
2. Site average roughness length
3. Hub height

In fact, using this simple information, the measurements of the wind can be reduced to 10 min average information just to find the annual average (standard meteorological practice in many locations over the years). Perhaps even the wind atlas of Europe (or US or other) can be used together with a terrain model.

If the calculations depicted in the graph have been carried out many times it is perhaps possible to identify the pattern that connects the three basic parameters to the jump matrices. Then, ever after into the future, no simulation will be necessary. Some inventive "curve" fit technique can be applied to directly generate the jump matrices (tables). Better yet, the jump tables can be calculated once for all times for a number of combinations of the three basic parameters. Then the wind turbine designer will have a hand book containing this information to fit his design to any standardized type of site.

This concludes our lofty views of this topic. All the rest of our presentation should be viewed with the perspective provided in this and the previous chart.

For lack of the research suggested we must make do with what is actually available today. - So, back to reality (i.e. next chart).

FUTURE WORK SEQUENCE (?)

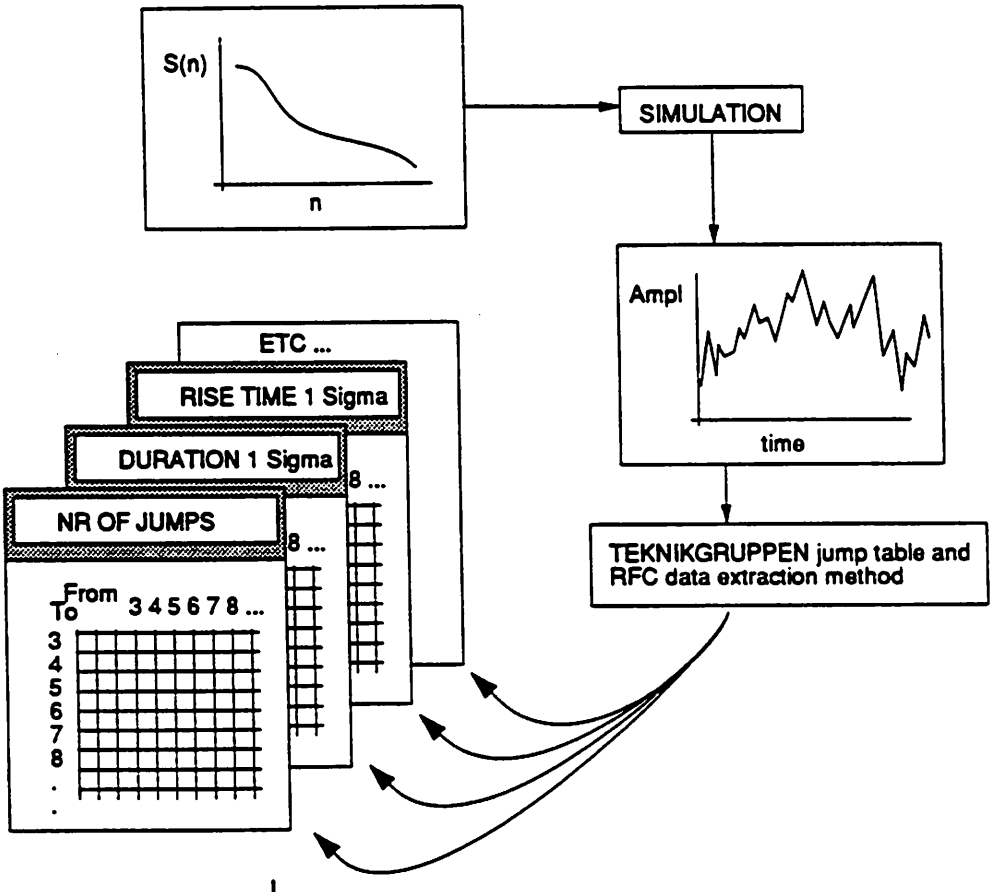

Each jump is simulated using a model of the turbine inertia and the control system.

Final cycle counting for either of:

- Analysis of existing machine
- Design of new machine
- Mixture of both (Medit Mk II prototype)


THE WAY WE MUST DO IT ?

MAJOR WIND CONCEPTS

This view graph shows how the information in the wind can be coarsely subdivided in order to clary-fy to the reader/viewer what topic we are addressing. This presentation only deals with fatigue driv-ing winds of frequencies below a certain dividing frequency. This frequency is closely associated with the difference between part disk gusts and full disk gusts.

In our presentation we are only concerned with "Fatigue, f < Fdiv" as seen in the graph.

WINDS FOR WIND TURBINE DESIGN AND ANALYSIS				
	Fatigue		Extreme	
	f > Fdiv	f < Fdiv	Ultimate strength	Extreme gust
Structural response ->	Eigenmode exitation	Quasi steady (with some control action)	Eigenmode exitation Quasi steady	Quasi steady (with some control action)

DISCRETISATION OF "BASE SPEEDS"

We propose to use a definition of "gusts" as being dispatched from certain "base speeds". The curve, as seen sketched in the view graph, represents the annual (long time) exceedance distribution of wind velocities. Vm is the median wind speed which can be calculated from the mean wind speed and the beta value. (We do not explain how to do it in this context.)

Our basic wind material consists of data of the type described in H. Bergstrom's paper in the Madrid EWEC 90 conference. A distribution of gust sizes is availble from WRFC analysis. But, the complete information (as in the Ganander/Johansson WRFC technique) is not available. Instead an assumption will have to be made *from which speed to which speed.* This is accomplished by starting all wind/machine simulations from the base speeds. Then the WRFC gusts (Bergstrom model) are applied as one positive gust from the base speed and one negative gust. The gust distribution later is used to figure out how many such cycles the turbine will experience during its intended life.

Gust excursions will be made from the "Base Speeds".

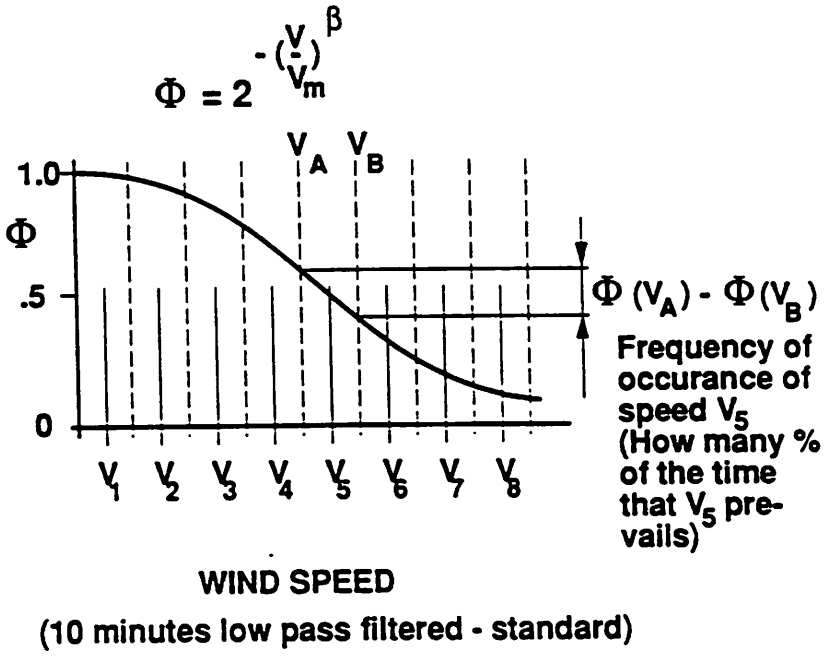

RFC NASUDDEN, 77 m

This graph shows that there is a connection between gust amplitude and gust duration although the spread is large.

This particular diagram is based upon a wind signal that has first been 10 min prefiltered for high frequency passage. This has as one consequence that the right upper part of the scatter is more unreliable than the swarm of points down to the left. More likely the upper right (unreliable) part should be even higher. That would have been the result if the wind signal had not been prefiltered in the described way. It is beleived that the trend, sketched into the diagram as two curves (one low esitimate and one high), could be near doubled in height for a duration equal to the filtering time.

Although the number of points is relatively low another interesting trend seems to present itself: The higher the duration the smaller the amplitude spread. This is a tentative conclusion awaiting the arrival of a more densely populated scatter plot from more extensive measurement campaigns.

→P. 34

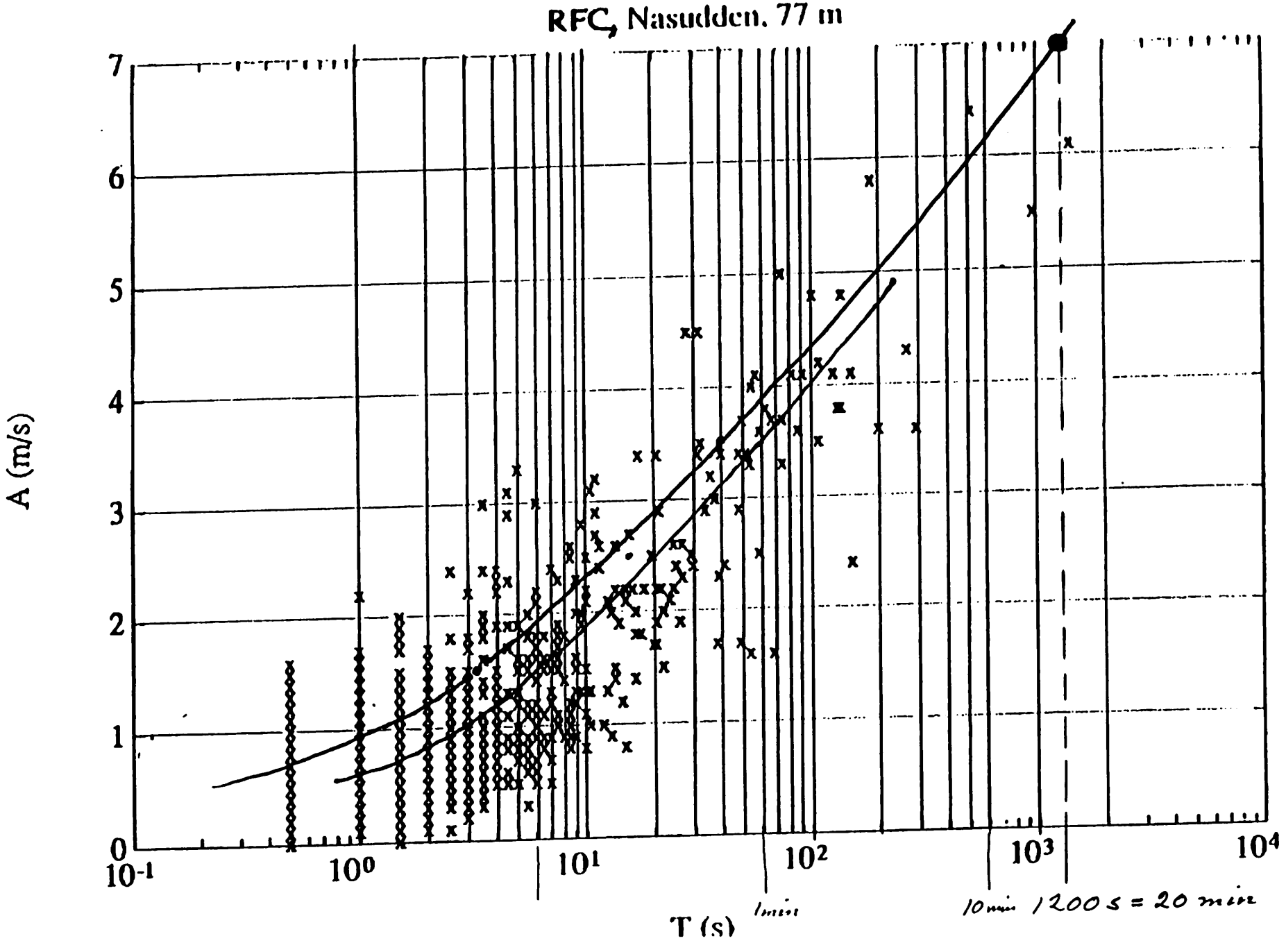
RFC, Nasudden. 77 m
A (m/s)
0
1
2
3
4
5
6
7
10-1
10⁰
10¹
10²
10³
10⁴
T (s)
1min
10min 1200 s = 20 min

CORRELATION BETWEEN AMPLITUDE & DURATION

In order to be able to make the previous scatter diagram useful only a duration interval is of real interest. In the diagram sketch two shadowed regions are excluded from consideration. The left region represents gusts of short duration. It is judged to be short enough to represent gusts that do not cover the whole disk. Such small gusts are not interesting for the scope of analysis laid out for this presentation. In fact, they are not interesting in the context of a total fatigue analysis of the machine either. The reason is that the Medit Mk III has a teetered hub and relatively flexible blades (the soft Gamma concept). The limit is 1/Fdiv as seen in the diagram. Fdiv is found from certain considerations explained in another presentation during the Stockholm conference. The title of that paper is: "FULL DISK GUST DIVIDING FREQUENCY" by B. Montgomerie.

The shadowed band to the right represents gust duration times that can not be represented well by the method behind the diagram. Therefore it must be excluded from useage. This does not mean that this area is not interesting. It is. But, its influence is treated separately as the curious reader will discover toward the end of this presentation.

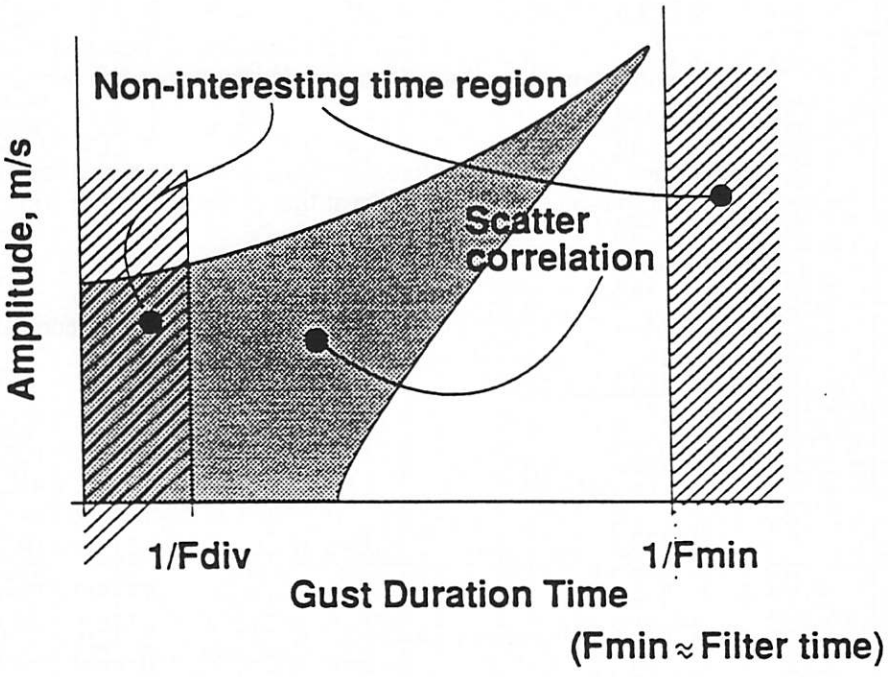

Data from Hans Bergstrom paper from EWEC 90 in Madrid includes measuring series from several very different sites. Although it covers a limited amount of data interesting trends are visible. Some of these trends were not part of the Madrid paper but they appear here after private communication with H. Bergstrom.

GUST DURATION DISTRIBUTION FOR DIFFERENT GUST AMPLITUDES

The same diagram as seen in the previous view graph is repeated. The aspects that are emphasized here are:

- Discretisation of the gust amplitudes.
- Statistical distribution of gust duration for each discretised gust amplitude.

The very basis of our method for fatigue calculation is seen in this diagram. To repeat what has been said already and expand somewhat on the same topic:

- Each fatigue load change in the structure is created from a simulation. This simulation is carried out using a simplified model of the turbine (no elasic modes). The simplified model includes the important aspecs of the control system and the total rotor inertia. Thus a variation of both RPM and yaw angle will in principle result from the gusts as they are defined.
- A gust simulation starts with the turbine in equilibrium at the "base wind speed" (see 3 graphs before this one!) The wind is then increased (and decreased in another run) in accordance with a Fichtl gust shape. (More about Fichtl gusts later.)
- The Fichtl gusts are defined by two parameters amplitude and duration. The given (discretised) amplitudes are applied for several gust durations.
- The most severe deviation from the initial conditions appear somewhere along the simulation, one can not know where until after the simulation output has been scrutinized. By "most severe" we refer to

  - The largest thrust variation to be applied to the tower as a load cycle.
  - The combination of RPM and thrust that gives the largest strain variation in the blades.

  The two do not necessarily occur at the same time.

- As a separate exercise, after all load/strain calculations have been carried out, the number of occurances is calculated using

  - Occurance of gust amplitudes
  - Occurance of gust duration

We must have access to information about both types of occurances. The next few graphs will explain how.

→ P. 37

GUST DURATION DISTRIBUTION FOR DIFFERENT GUST AMPLITUDES

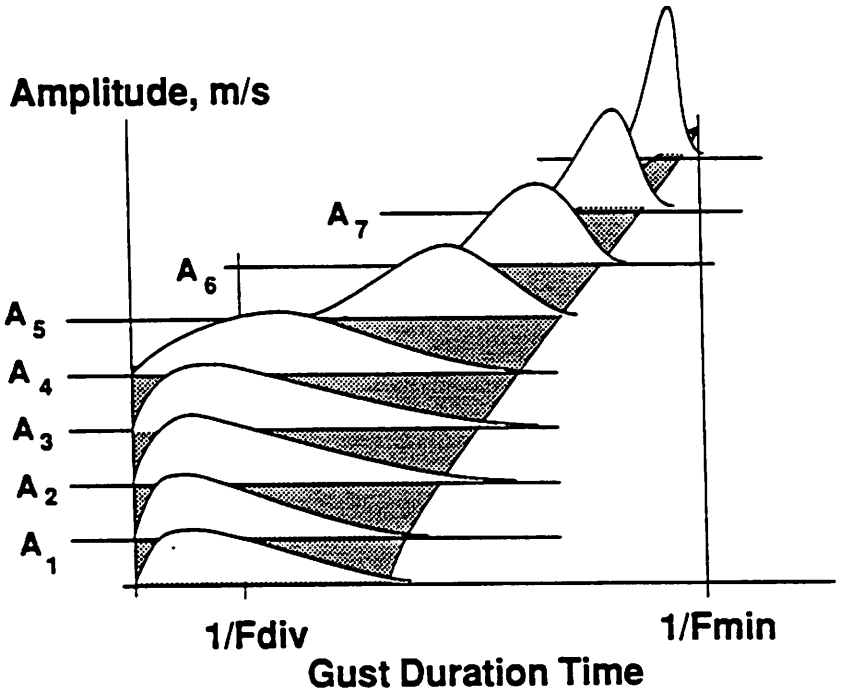

EXAMPLES OF ACTUAL OCCURANCE DISTRIBUTIONS FOR DURATION

The upper diagram would typically be used to represent a descretised gust amplitude of 1.5 m/s.The lower diagram would typically be used to represent a descretised gust amplitude of 2.5 m/s.

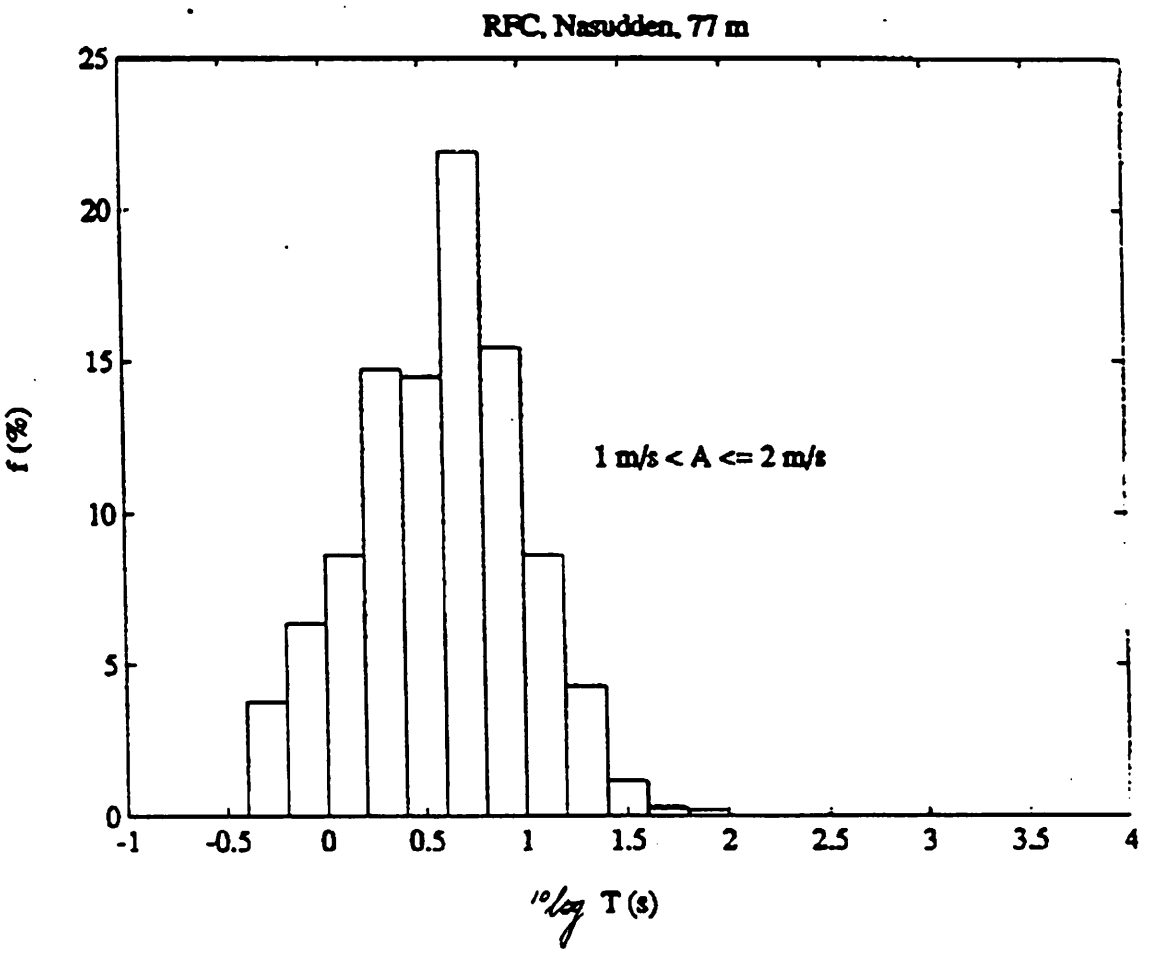

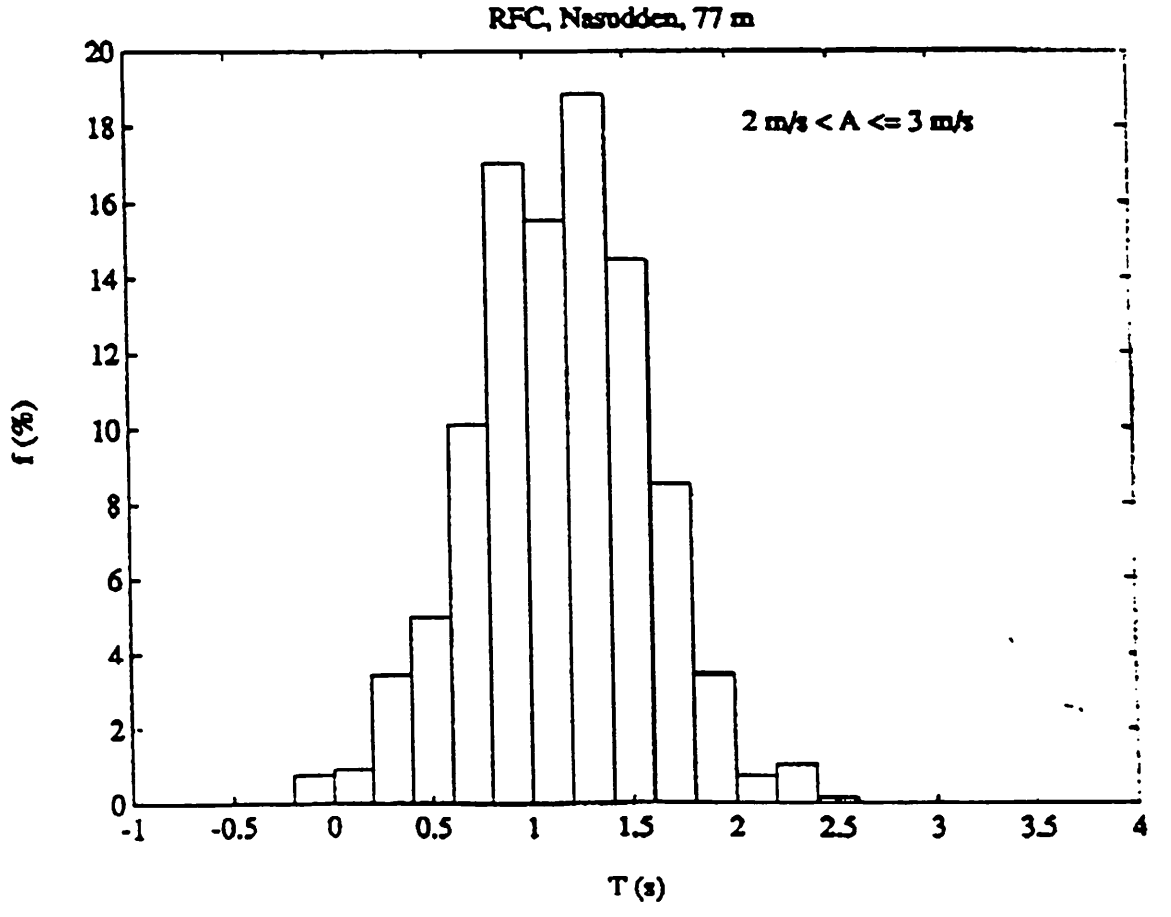

CUMULATIVE GUST DISTRIBUTION

The diagram looks very similar to the duration diagram for "base wind speeds" on a previous view graph. There is, however, a significant difference between the two.

The previously described "base wind" distribution tells the analyst how large a portion of the total calendar time that the wind exceeds a certain value (that is chosen on the x axis).

In the case of the cumulative gust distribution the interpretation is that a certain value on the x axis has a probability of exceedance, among gusts discovered in the RFC. In this case nothing can be said about calendar time. The reason is that gusts occur contemporarily. Base wind speeds can not happen at the same time.

In this diagram the quantity on the x axis is amplitude divided by the gust average amplitude (1 sigma). To be able to use the information in the diagram we must know sigma. The next graph shows how.

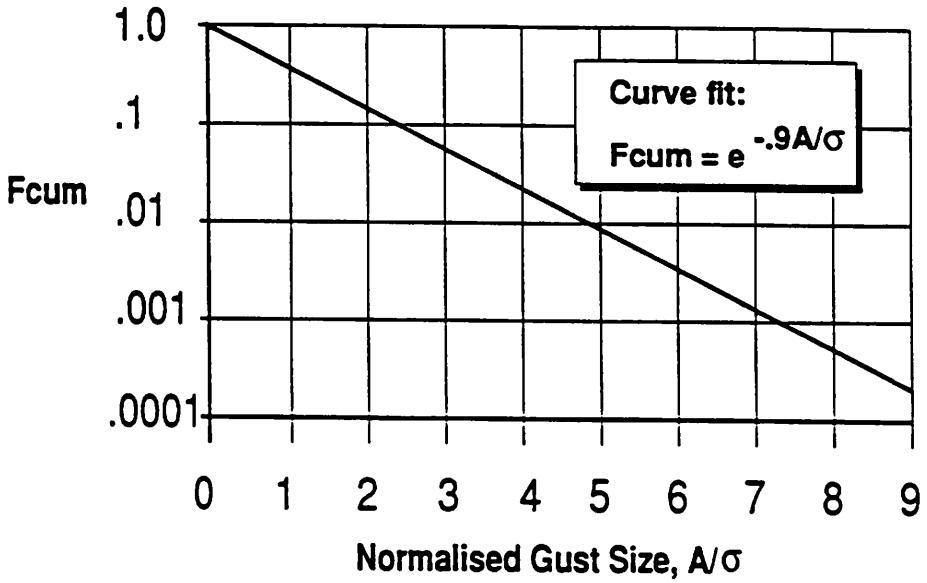

Data taken from Bergstrom's Madrid -90 paper.- The interpretation of the cumulative distribution is: "The relative number of gusts that exceed a certain size A/σ"

In addition the number of gusts registered per time unit (Fg) must also be available to facilitate fatigue cycle counting.

TURBULENCE

Two methods how to find the one sigma turbulence are available to us. Either the general set of formulae shown first is used. ENEL also has advice concerning the siting circumstances. This information appears further down the graph.

If no or little measured data are available for an intended wind turbine site the following expressions can be used. (See the Swedish wind definition for the specification of WTS-3 and WTS-75 - Document: "Vindunderlag for kravspecification", 78-06-15)

$\sigma^2 = 10.25\, u_*^2$ variance at neutral stratification, where

$u_* = \frac{k\,\bar{u}(z)}{\ln (z/z_0)}$ where

k = von Karman's constant, approx. .35 or .40

z = height above ground

$\bar{u}$ = Annual mean (not median) velocity at height z.

z_0 = "Roughness length" (=.1 open country, =.3 for intermediate undulating, =.6 for forest)

ENEL, the Italian national power distributor, proposes a turbulence level as a function of the standard 10 min average wind speed. Data from a mountain site, referred to as "site B", was used as a base for this table. (Annual mean wind speed is 6.7 m/s)

Wind speed bin	1 σ turbulence in % of wind
.5 < V < 5.0	24
5 < V < 10	19
10 < V < 15	18
15 < V < 20	17
20 < V	16

CYCLE COUNT

To calculate the cycle count of different types of circumstances three types of inputs are required. In the view graph this is stated without proof. Proof will appear in following graphs.

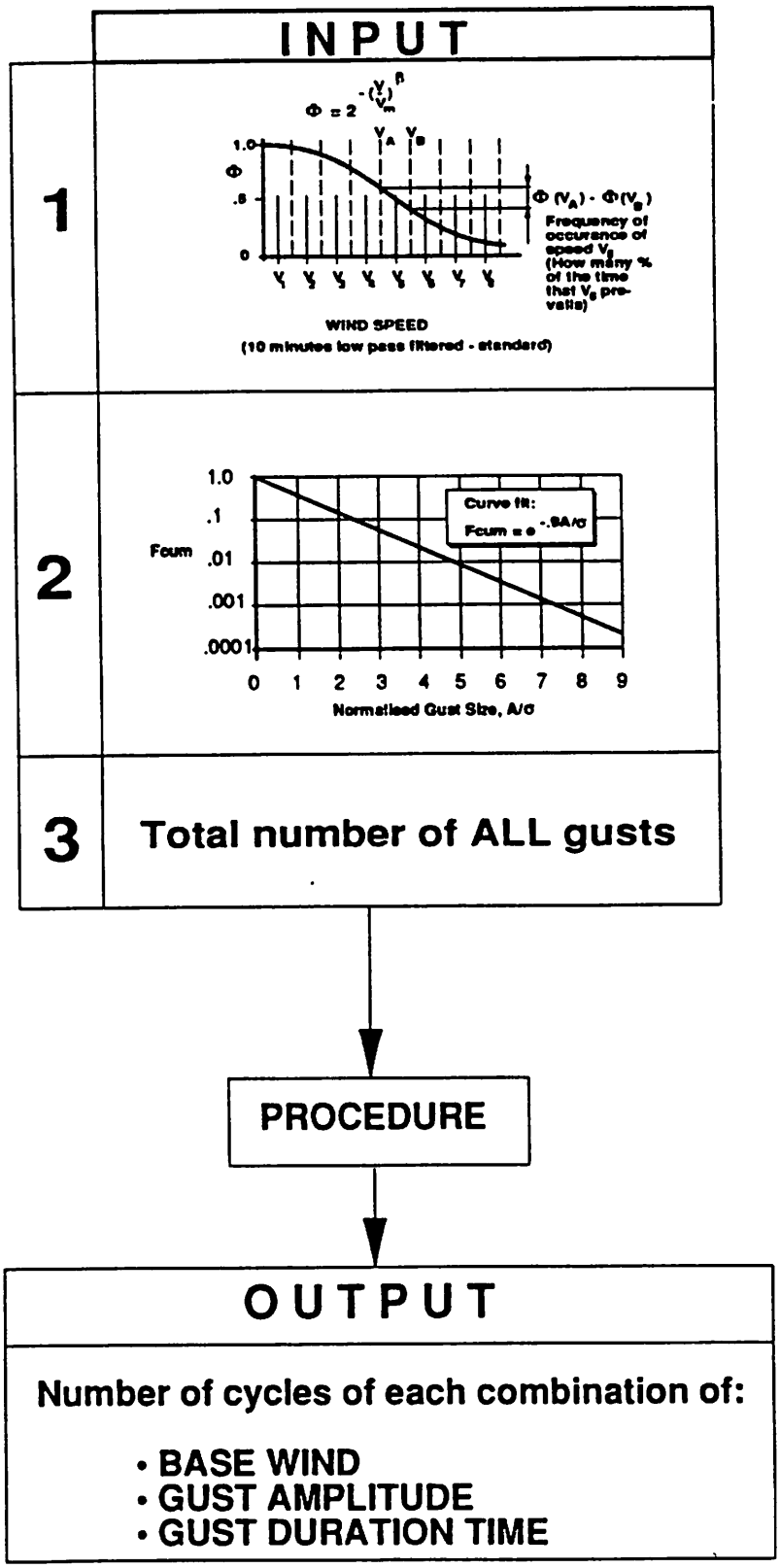

GUST BUDGETING
FOR FATIGUE CYCLE COUNTING

The different gusts are allotted their place in the life of the wind turbine according to the chart. This chart also attests to the statement of the previous graph. Thus, in the example, the allotted time for V4 is taken from the base speed exceedance function (input 1). In the expansion of Ai delta-F-cum is taken from the gust exceedance diagram (input 2). Finally the information from the WRFC must contain the number for gusts/(time unit) or total number of gusts.

f_o= Frequency of occurance of ALL gusts.
N_{tot}= (Total number of gusts) = $f_o T_o$

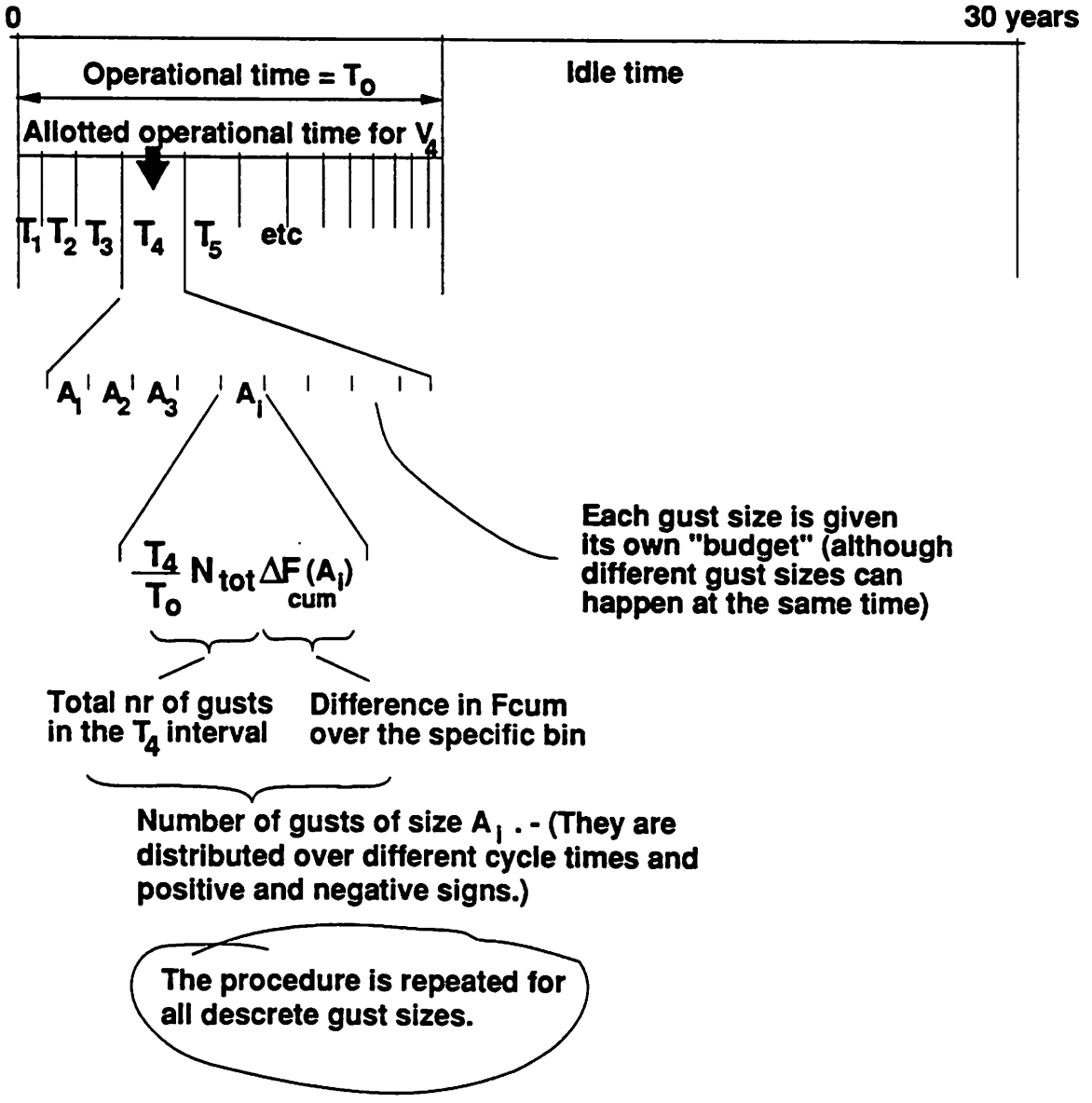

FUNDAMENTAL INSIGHT

The separation of meaning between the wind distribution and the gust distribution is emphasized again. One consequence of this insight is that the sum of the times of the base speeds must be equal to the total operating time, whereas the sum of all gust times by far exceeds the total operating time. (Hence, it would not be possible to use the gust times for a check sum.)

- **Base winds happen one at a time!**
- **Gusts happen contemporarily (overlapping)!**

FICHTL GUSTS

This cartoon is only meant to spark the idea that a distribution of gust lengths must be applied in a discrete way. It is pointed out that the longer duration gusts need not be simulated! - We remind you of our technique:

1. The gust and its consequences are simulated.

2. A scrutiny of the output helps decide what and where the worst fatigue excursion occurred.

3. A performance program is used to calculate the detailed forces along the rotor blades for the critical combination of RPM and wind speed (found in step 2).

4. Another program calculates the strain maximum on the suction and pressure sides of the blades. this is accomplished by balancing the external aero forces against centrifugal and elastic spring forces.

5. We refrain from our temptation to delve into the problem of tower fatigue calculation. It can be done using the same (perhaps similar) methods. Or, the tower can be treated by a direct spectral method. But this topic is well beyond "Winds with Relevance to Wind Turbine Design" which is the head line of the conference.

So, back to why no simulation of the long duration gust is needed. - If the duration is as long as to permit the slow RPM variation to adapt to the "new" wind, then we can simply assume that the Tip Speed Ratio (TSR) is constant. Then we know from the beginning that such a simulation will have its extreme where the wind has its extreme. No dynamic of the rotor speed need be considered.

The reader is suggested to remind himself of this statement two view graphs after this.

For turbine simulation purposes a time history description of the gusts is necessary. The gusts always start from the base velocity with the machine in equilibrium. - Half of the gusts are positive, half are negative.

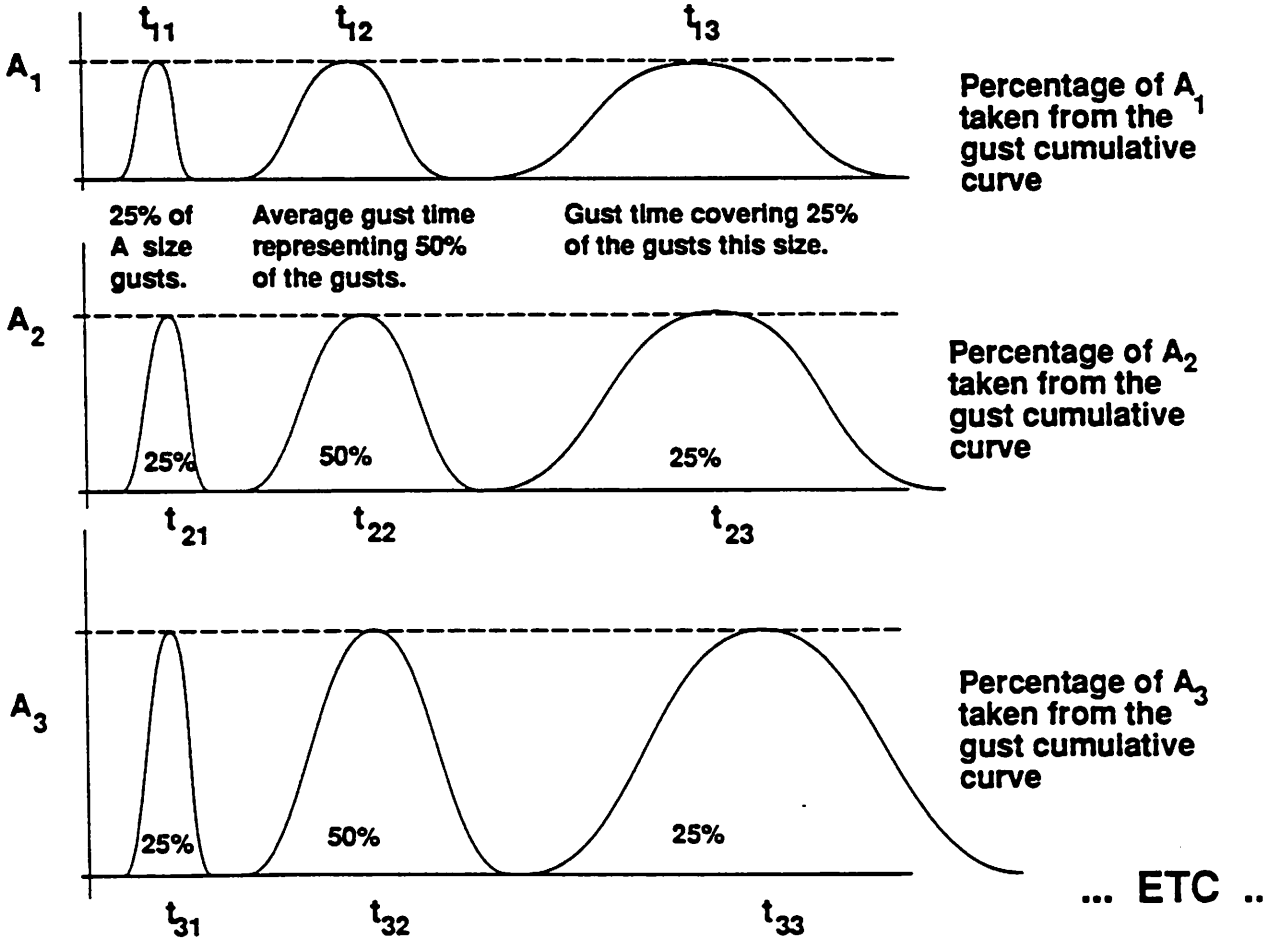

Medit mk III, Standard DWT Rotor

The result of one gust simulation can be plotted in an RPM vs wind speed diagram. This type of diagram is nowadays referred to as the "Lawson-Tancred" diagram. It looks repellantly busy to the unused eye. But for the purpose of overview of a variable speed machine it is very attractive once you have digested its principle contents. (Incidently the whole diagram can be constructed from only four inputs. They are: air density, rotor radius, Cp vs TSR table and a CT table.)

The simulation was done for a Fichtl gust starting from 8 m/s going to 12 and back again. The corresponding graph appears as a loop drawn by hand. For different durations of the gust the loop will assume different shapes. In this dia gram it is clear to see how the rotor, because of inertia and control system, never reaches its ideal value of 59 RPM (riding up the TSR=9 beam). The reader can see that the worst thrust appears at about the coordinates (11.9; 51).

With a much longer duration of the same amplitude gust the coordinate (12; 59) would have been approached. That would have exceeded the 60 kN thrust line (dotted). It must be concluded that the modelling of the gust duration is very important.

Medit Mk III, Standard DWT Rotor

Air density = 1.225
Rotor radius = 17.400

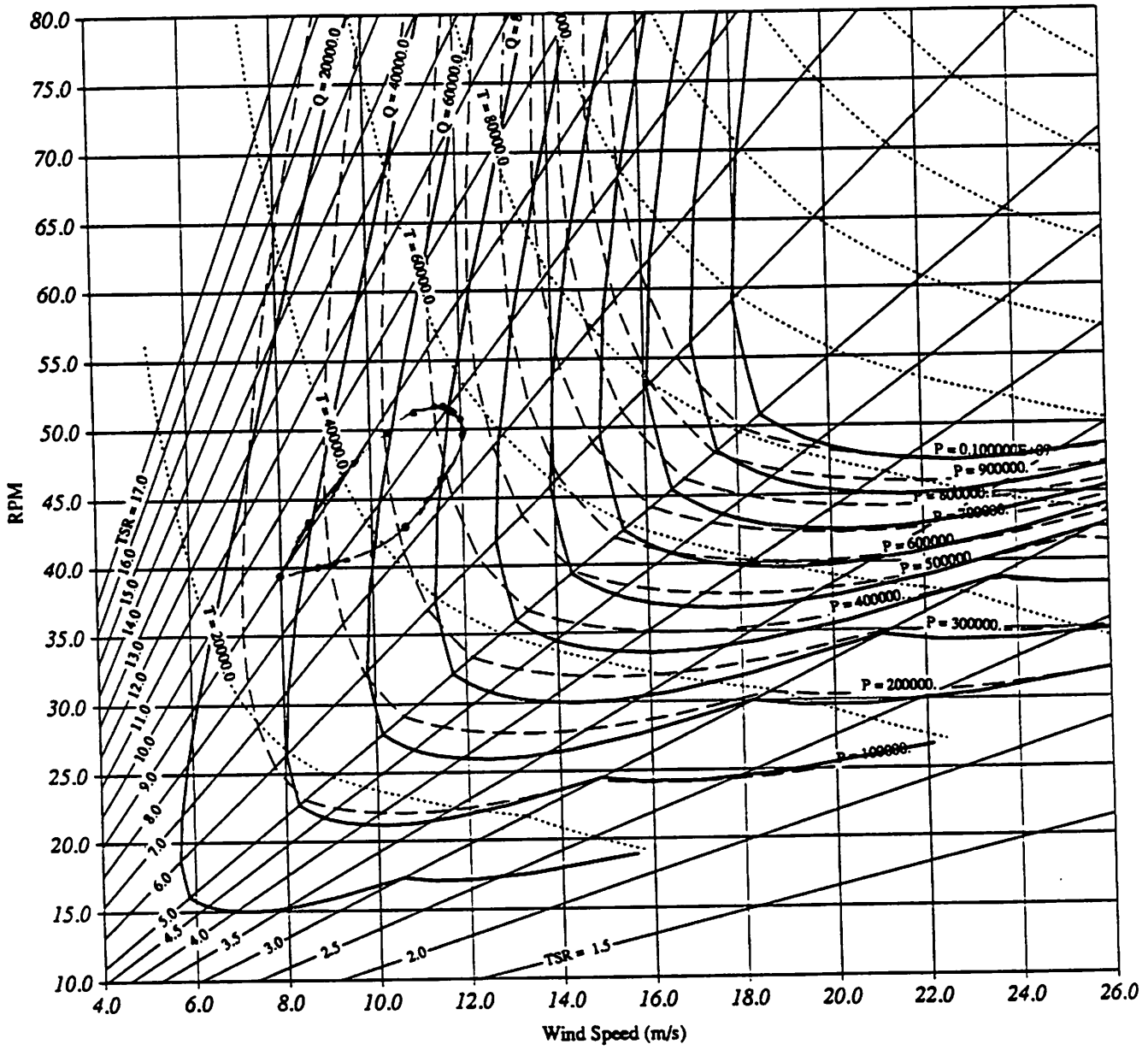

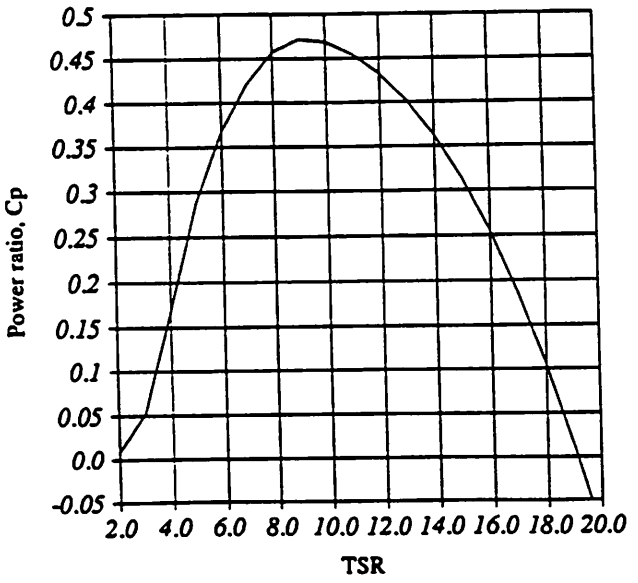

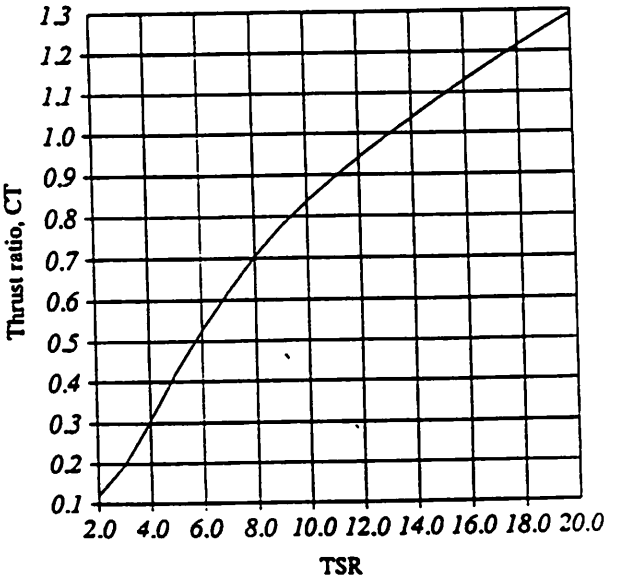

SUMMARY AND PERSPECTIVE

The reader is reminded that the analysis so far starts from a gust definition. This gust definition is a Fichtl gust on top of some selected "base wind speed". But base speeds also vary. This variation has not been considered so far.

- **We have covered the higher part of the spectrum, that part of the spectrum that is normally referred to as "gusts".**
- **What about the lower frequency part? - How does the variation of the 10-min low pass filtered "mean" wind vary? - That variation certainly also contributes to fatigue!**

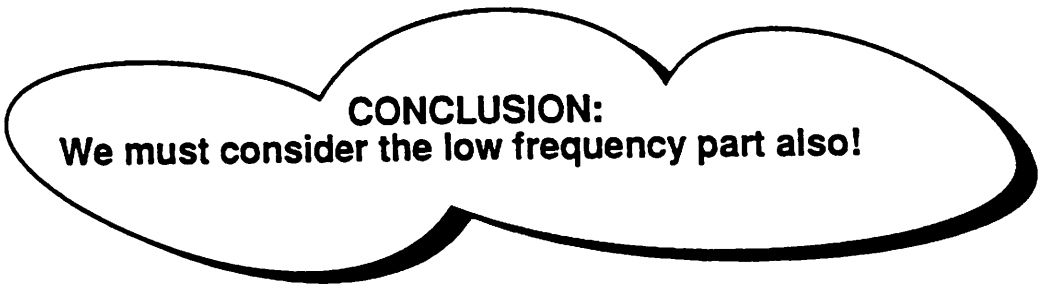

LOW FREQUENCY GUSTS

An additional fatigue cycle counting technique is constructed by using the *base wind* variation. In the low frequency regime we have all gusts of longer duration than about 10 min. One important feature in this algorithm is to find the total number of these low frequency gusts. The next graph explains how this is accomplished.

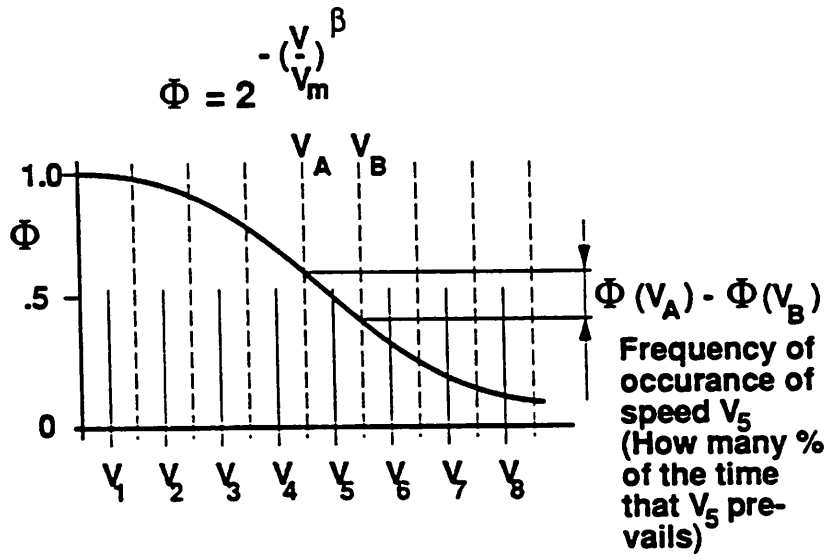

- The information seen here was shown previously. Now we will be using this distribution for the

LOW FREQUENCY *GUSTS!*

HOW?

- Find out how many gusts!
- Pretend the base velocity = annual mean velocity!
- Let all gusts be excursions from the base velocity!
- Use the distribution curve above to distribute the gust sizes!
- Enjoy the comfort of knowing that no dynamic effects need be considered!

NUMBER OF LOW FREQUENCY GUSTS

The formula can be interpreted to mean the weighted average of the frequency squared. S is the power spectral density of the wind.

$$n_{AVE}^2 = \frac{\int_0^{F\min} S(n)n^2 dn}{\int_0^{F\min} S(n)dn}$$

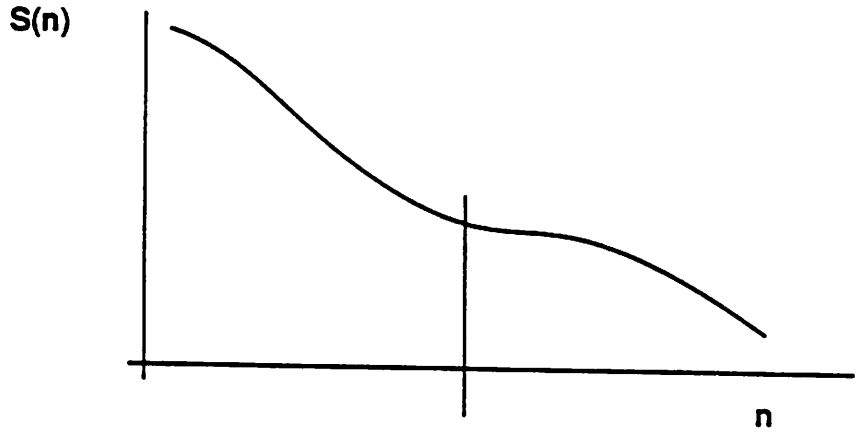

Finally:

Nr of gusts = (Operating time) • n_{AVE}

THE EFFECTS of SLOW GUSTS and QUICK GUSTS are NON-ADDITIVE

In this view graph we admit to the weakness of the proposed method and we try to make up for it.

The stress/strain cycles from high frequency gusting and low frequency gusting will be used as *SEPARATE* contributions to the part damage fatigue calculation. But we know that the RFC method does not allow superposition of gusts!

EXCUSES

- The number of cycles of the low frequency gusts is much lower than that of the high frequency gusts. (Hence we commit an error to a small proportion)

- A separate conservative set of cycles are added by assuming that:

  - The wind increases from zero to that wind which creates maximum thrust and back again once every day
  - There are ten complete starts and stops from and to cut in speed every day (of operating time).
  - There is one stop and start cycle at cut out speed every day.

EXTREME MEAN WIND SPEEDS AND GUSTS IN NORTHERN GERMANY

by

Heiner Schmidt

Abstract

The method of determination of "extreme" mean wind speeds and gusts from shorter time series of the wind with a mean recurrence around "once in 50 years" is discussed. Results are given for the coastal areas of Northern Germany. The climate of the western European coasts is such that the extreme wind speeds mentioned before are always connected to normal storm events. For these cases relations between hourly mean wind, turbulence intensity, and gust factor and further a relation between hourly mean wind direction and the momentary direction of the peak 1 sec wind is given. Gusts generated by convective situations (i.e. thunderstorms, sqall lines) are less frequent and of lesser intensity than during storms. In other climates this may be distinctly different.

Introduction

The construction of wind energy converters depends on the knowledge of many meteorological parameters. A few of them, which were investigated for the more general application in building design, are discussed here. The gust speed (peak momentary wind speed, averaged over 1, 2 or 5 seconds) at a certain height with a mean recurrence period of 10 or 50 years is used in many building design codes as a measure of the maximum static wind load ("design wind speed"). The ratio between this gust speed and the hourly mean wind speed at the same level of probability is often used as a simple parametric measure of the wind variations. Especially in wind turbine design other necessary load assumptions may already lead to far stronger buildings so that the before mentioned wind loads only serve as minimum load cases.

Wind values with a recurrence period of 50 years

For the renewal of the design wind speeds in German building design codes (e.g. DIN 1055) in investigation of the regional distribution of "extreme" winds was made in 1982. In figures 1 and 2 the extreme values of the 10 min mean and 2 sec wind speeds, respectively, with a mean recurrence of "once in 50 years" at a height of 10 m above ground level are shown. The word "extreme" in this context does not mean an upper limit, which does not exist, but corresponds to a specified probability of exceedance, which can less exactly be transformed to a mean recurrence period. Thus "once in 50 years" really means "$2*10^{-2}$ events per year".

In order to investigate only the regional variability of the wind, the data have to be taken from the same time period for all stations. Otherwise possible climatic variations can obscure the regional effects. The simplest way of analysis would be to take the annual maxima of hourly mean wind and gust speed from 20 years or preferably many more for each station, fit the distribution to a theoretical extreme value distribution (Gumbel or other) and extrapolate down to "once per 50 years". Unfortunately this does not work properly in most cases.

The reason generally is a violation of basic requirements. Often only about 10 years' extremes are availible, which is definitely not enough for an extreme

value analysis. Other reasons are less obvious. The basic assumption for the estimation of extremes is that the time series of events be a realisation of an underlying stationary and homogeneous stochastic process. For the wind itself the validity of this assumption cannot be shown to be true, it has to be taken as granted. But very often it can be shown from a thorough investigation of the station history, that the technical realisation (i.e. the measurements) did not produce a homogeneous time series.

This is due to many reasons, e.g. gradual or abrupt changes: in measuring equipment, in the measuring height or location, in the surrounding surface roughness, in nearby obstacles (trees, buildings), or other. In Northern Germany there is another severe reason which makes the extreme value analysis technique impossible. All of the older wind recording systems stop at 80 knots = 41 m/s in gust speed, a value which near the coast is exceeded in many years. This means that a considerable part of the data is equal to 41 m/s instead of having their true value.

Therefore the more tedious way of determination of the extremes from the distribution of all measurements (the whole sample) was chosen. The frequency distribution has to be generated from the time series, is then transformed to frequencies of exceedance, normalized to the number of possible events N per year, and fitted to a theoretical distribution. In this case most often the Weibull distribution is chosen, which is in the integraded formulation as a frequency of exceedance F(U) of all wind speeds greater than or equal to U given by

$$F(U) = N * \exp\left(-\left(\frac{U-d}{A} \right)^{k} \right)$$

with the "scale" parameter A (which is related to the annual mean wind speed), the "shape" parameter k (k=1 is an exponential type, k=2 the Rayleigh distribution, k=3.6 almost a Gaussian distribution), and a "displacement" d. In westwind climates d can be chosen as 0. In climates with a considerable portion C of calms per year (Saudi Arabia for example) these have to be kept separate, and the Weibull function can only be fitted to the rest of the distribution with wind speeds above, say, d=1 m/s. In this case the normalizing number of possible events per year has to be reduced from N to (N- C).

The method of fitting a Weibull distribution to the whole sample, and extrapolating it down to "once per 50 years" was used for the generation of fig. 1 and 2. The method is subjekt to the same statistical restrictions as the extreme value analysis (stationarity and homogeneity), but the results already begin to stabilize at shorter time intervals (7-10 years data). This obviously is due to the fact that the whole sample contains more information about the underlying stochastic process "wind" than only the annual extremes. The method has the further advantage that the fitting can be restricted to all values below some upper limit in wind speed (41 m/s in our case) with only a slight loss in the accuracy of the results. In our case about 8 years of homogeneous wind data were used per station from the period 1970-80. The possible number of events per year here was 52596, as 10 min intervals were used (would be 8766 in the case of hourly values).

Fig. 1 and 2 highest values at sea (38 and 52 m/s, resp.) rapidly decreasing inland of the coast with increasing aerodynamical roughness of the surface. The confidence level of the data is estimated to be about $\pm$ 3 m/s for the statistical method. Variations of the same order are superimposed, induced by local effects in single stations. For a recurrence period of 50 years, 50-55 m/s in 2 sec gusts and 35-40 m/s in 10 min mean speed can be considered as typical all along the continental European west coast from Denmark to Northern Portugal. Higher values will occur at the coasts of Great Britain and Ireland.

For intercomparison with other investigations note the following rules: At the

same level of probability extremes of hourly mean winds are 10% lower than those of 10 min mean winds, due to a loss of variance by averaging. For the same reason 5 sec extreme gusts are 5% lower than 2 sec gusts. Finally extreme winds with a mean recurrence period of 10 years are about 10% lower than those with 50 years return period.

Differences between storm gusts and thunderstorm gusts

All over the coastal areas of western and northern Europe "gusts" with a mean recurrence period of 10 years or more are always found to be generated by normal storm situations. Storms come and go in a typical time scale of a day. During storms generally hourly averages and standard deviations of both wind speed and direction are well defined. The momentary wind fluctuates in a more or less random way around the mean wind. On the average the hourly peak momentary wind (hourly "gust") Umax is found to be by a factor of about 1.5 greater than the hourly mean wind speed U. The factor (called the "gust factor", G) is depending on the height above ground, the mean wind, the atmosperic stability, the roughness of the surface and the averaging time of the momentary wind. A numerical formulation is given by Wieringa () and others.

For these typical storm situations in a special investigation in Northern Germany we found a rather stable relation between the gust factor G, the mean wind speed U, the standard deviation s on the basis of hourly means and 1 sec averages as momentary winds. s divided by U is the so called "turbulence intensity" I of the wind speed. On the average it was found that

$$I = C * (G - 1) \quad \text{or} \quad (Umax - U) = C * s$$

with a constant (for wind speeds > 10 m/s) C = 3.1 $\pm$ 0.3 for hourly averages U, and C = 2.5 $\pm$ 0.3 for 10 min averages. This means that the turbulence intensity at a location can be approximately calculated from routine (weather service) data, where most often Umax and U are known, but s is unknown. From an investigation of the wind vectors it could be shown that (for gust factors up to 2) the standard deviation, turbulence intensity and gust factor for the along wind component u are practically identical to those of the wind speed U. The turbulence intensity of the cross wind component v was found to be by 10% lower.

Further the relation between the direction of the hourly peak 1 sec wind and the hourly mean wind direction was investigated. It was felt, that there should exist a systematic difference in directions due to the assumed origin of "gusts" from higher altitudes. The result for storm "gusts" was negative, as shown in fig 3, the peak 1 sec wind on the average has the same wind direction as the hourly mean wind. From a lot of time histories of storm gusts we found that this is caused by a lack of correlation between the variations in wind speed and direction on the time scale of a few seconds.

Fig 4 gives a typical example. (Note the scaling of direction: axis value = (degrees - 200)/10 !) The smooth curves are 80 seconds low pass filtered. On that time scale the "gust" clearly comes out, speed rises from 10 to 18 m/s and goes back to 11. The direction shows a distinct right turn from 280 to 310 degrees and back to 290, as is often seen with storm gusts on wind recorders. But the speed peak and the maximum right turn of direction are somewhat out of phase (50 seconds in this case), which normally cannot be detected on routine wind recorders. On the 1 sec time scale hardly any correlation between speed and directional changes can be detected. The 1 sec peak wind (with a speed of almost 21 m/s) is situated randomly somewhere on top of the 80 sec "gust" and therefore connected to some wind direction value randomly deviating from the hourly average direction.

Quite the contrary of all this is true for gusts which are generated by strongly convective situations of the atmospere (like thunderstorms, sqall lines). For the coastal areas of Western and Northern Europe this type of gusts was found to be far less frequent and of lesser intensity than the storm type gusts described before. In other climates this is distinctly different. But generally the convective gust type are felt to be very hazardous for wind energy converters.

A typical example of the passage of a sqall line is shown in figure 5. The time series of 10 second averages (sampled every 250 s) of wind speed and direction were measured at a high mast near Hamburg by the Meteorological Institute of the University of Hamburg. Measurements of three levels (50, 150 and 250 m) are shown. Before the squall line there is a light easterly wind with a relatively large vertical shear in speed U and direction R. Then the squall line passes with a sudden wind turning to the south west and a sharp increase in wind speed from near zero to 15 m/s within a minute. The gust would hit a wind converter exactly from the rear. The vertical wind shear afterwards is small.

In cases like this hourly averages of speed and direction are meaningless and the calculation of standard deviations and turbulence intensities results in something arbitrary. The whole concept does not work in the instationary convective cases because these "gusts" are highly organized and are not generated by a more or less random turbulent process as in the case of storm gusts. Note that the onset of the sqall line in this case first begins in the lowest level (50 m) and only a minute later hits the highest level (250 m).

Geostrophic wind in the German Bight during the last 100 years

Long time series of measurements of the wind in the order of 100 years do not exist. There are series of estimations of the wind, but the methods of estimation have changed considerably, and the time time series therefore cannot be regarded as homogeneous. We therefore chose an indirect method to develop a long time series of the wind. The driving force of the wind near the earth's surface is the horizontal air pressure at that height. Force and direction of the gradient can be calculated from the simultaneous pressure readings at three stations in a triangle assuming linear pressure variation between them.

As a measure of the wind the so called "geostrophic" wind is calculated. It is directly proportional to the pressure gradient and (at a minor rate) varies with air density and latitude. The relation between the actual wind at 10 m height and the surface geostrophic wind is nonlinear. The ratio decreases from 0.7 at 10 m/s to 0.5 at 60 m/s geostrophic wind speed.

The 08.00 LT pressure readings (reduced to the sea level) of the three stations Fanoe (Denmark), Hamburg and Borkum (both Germany) were available as basic data for most of the days in the period 1876 to 1989. The stations are arranged in a nearly equilateral triangle of 200 km side length, the center of which is located in the German Bight. The resulting time series of the geostrophic wind again consists of one sample per day.

The annual mean geostrophic wind speeds (scalar averages) for 1876 to 1989 are shown in figure 6. No statistically significant trend can be seen, but only long time variations superimposed by strong shorttime variations. The analysis of geostrophic wind speeds greater than the mean wind and of geostrophic wind direction essentially reveils the same picture, i.e. no linear trend, but relatively strong variations in all time scales. This is a further indication that the wind can be assumed to be a stationary stochastic process.

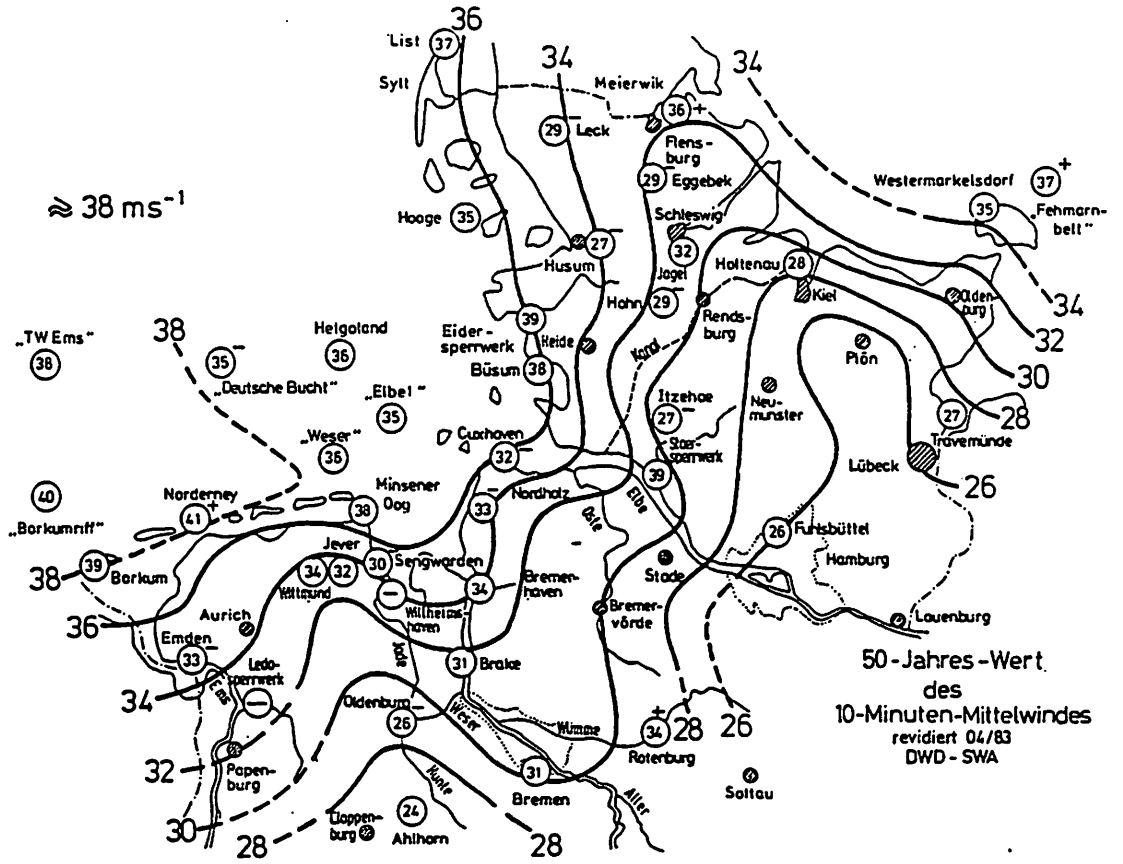

Fig. 1 10-min-mean wind speed with a mean recurrence period of 50 years in Northern Germany

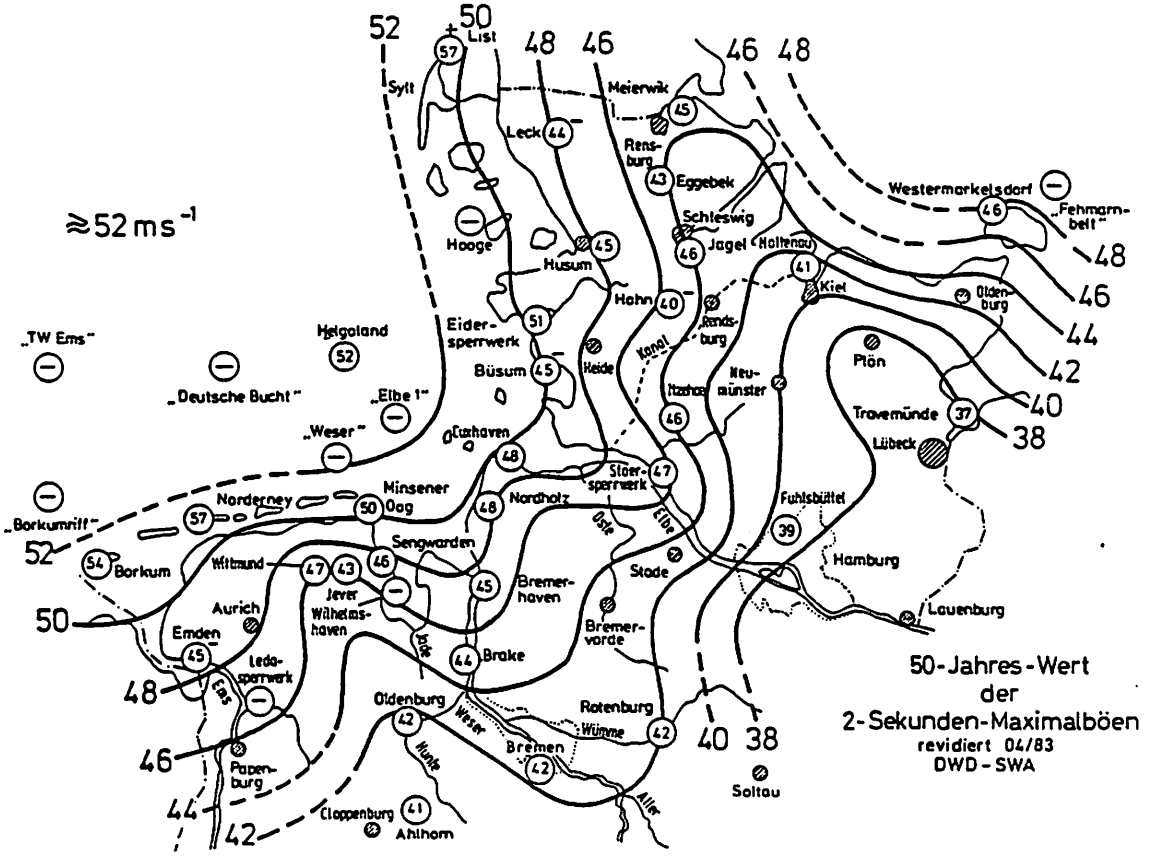

Fig. 2 2-sec-gust speed with a mean recurrence period of 50 years in Northern Germany

Fig. 3 Direction of 1 sec peak winds

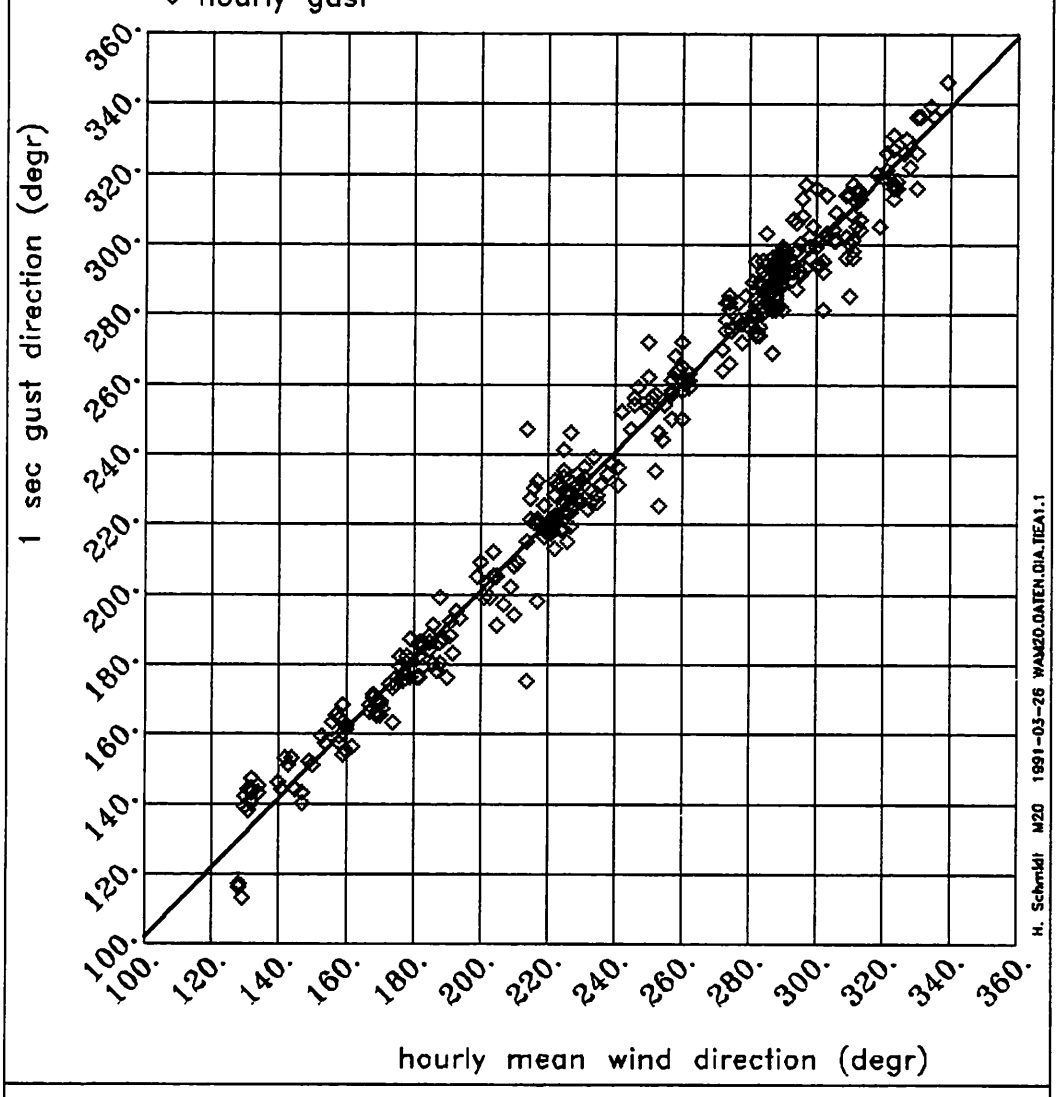

Wind direction of storm gusts (1 sec peak winds) vs hourly mean wind direction. 387 hours of measurement at the island Sylt (Northern Germany) for hourly mean wind speeds > 10 m/s. Effective heights 24–54 m. Deutscher Wetterdienst – Seewetteramt

Fig. 4 Time history of a storm gust

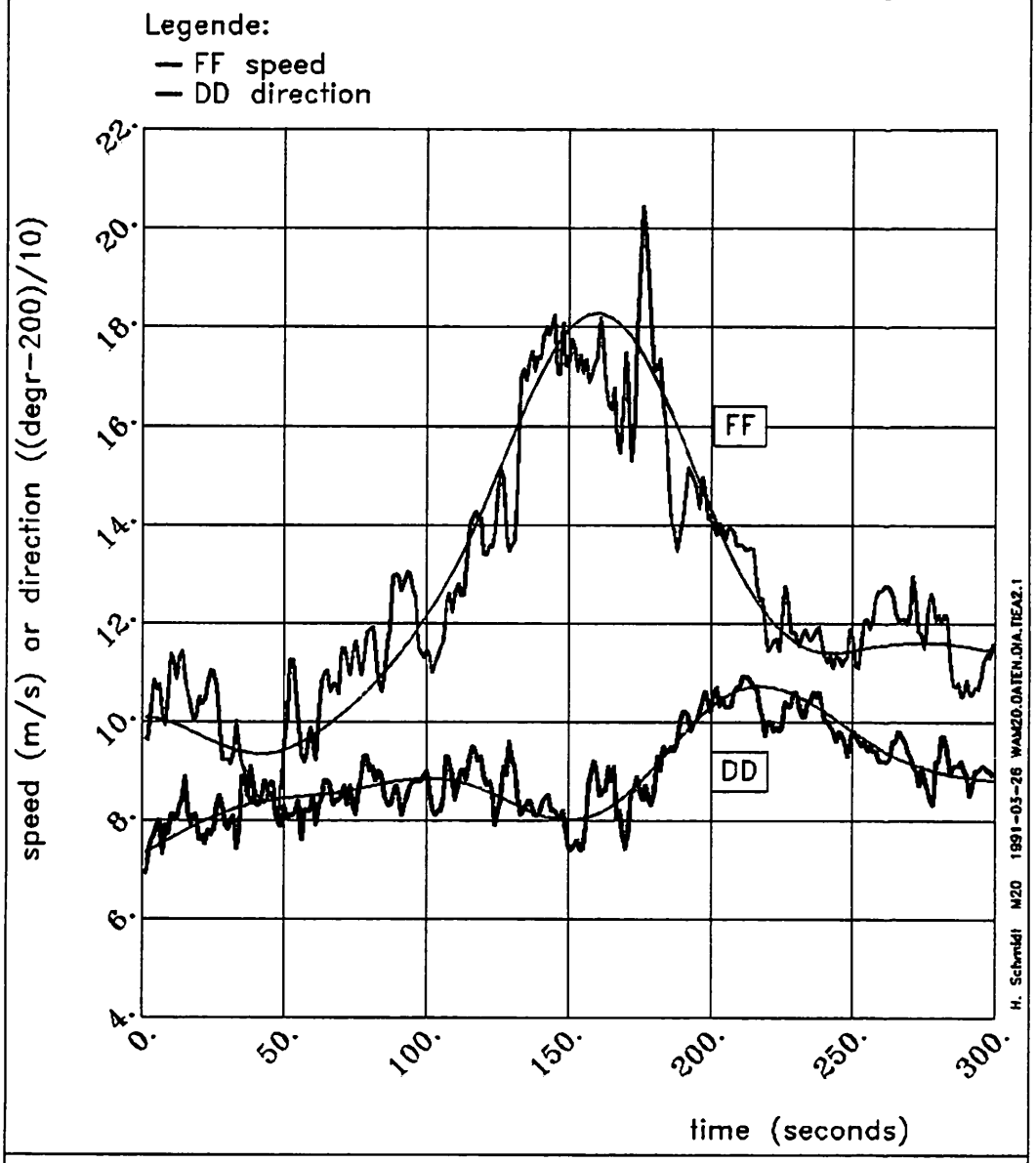

Wind speed and wind direction of a storm gust.
Time series of 1 second averages (and low pass 80 sec)
measured on the island Sylt (Northern Germany)
in an effective height of 54 m. Date 13−11−1982.
Deutscher Wetterdienst − Seewetteramt

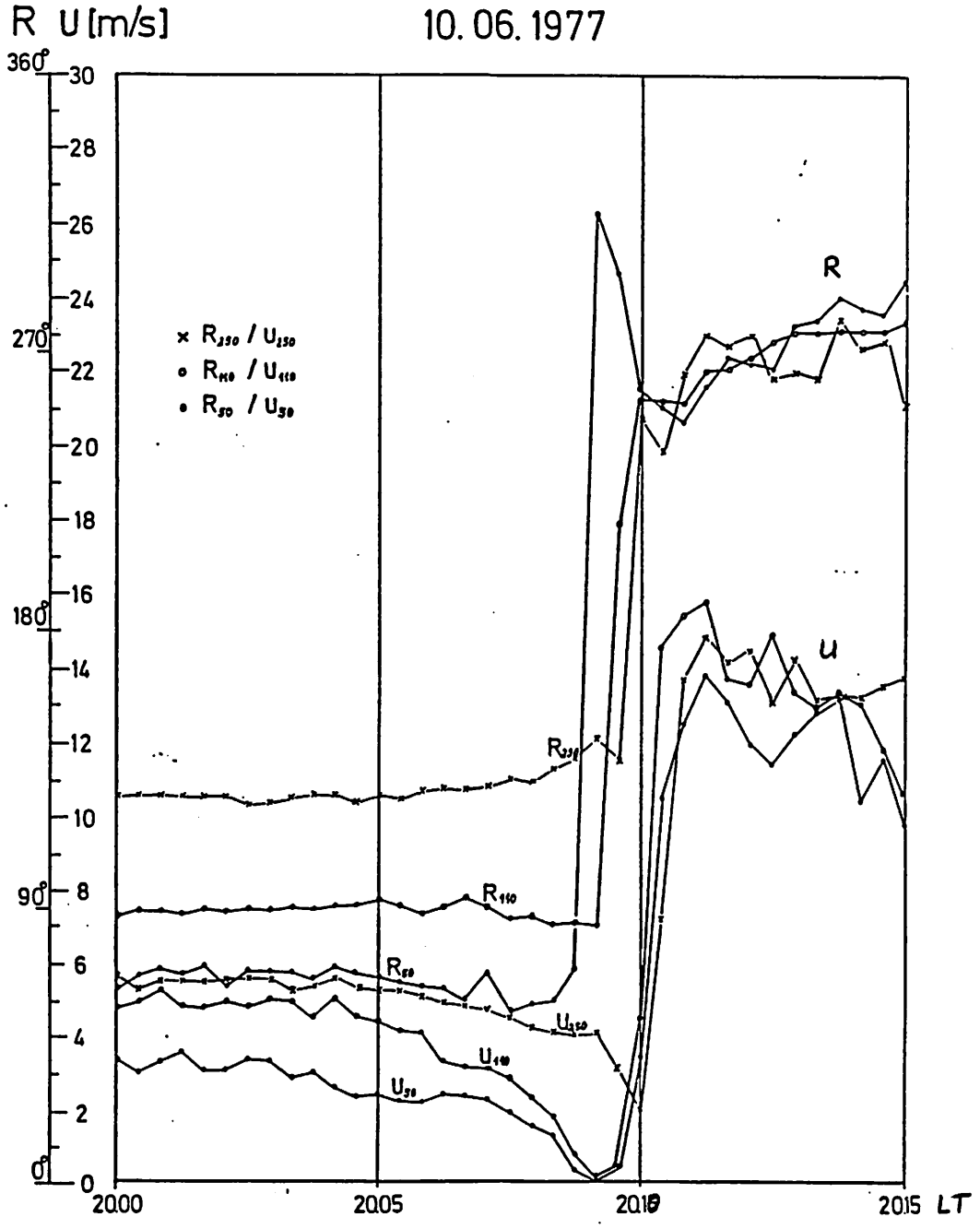

Fig. 5 Passage of a squall line.
Time series if 10 sec averages (sampled every 250 sec) of wind speed U and wind direction R, measured at 3 levels (50, 150, and 250 m) at a high mast near Hamburg (Germany). Measurements by Meteorological Institute, University of Hamburg.

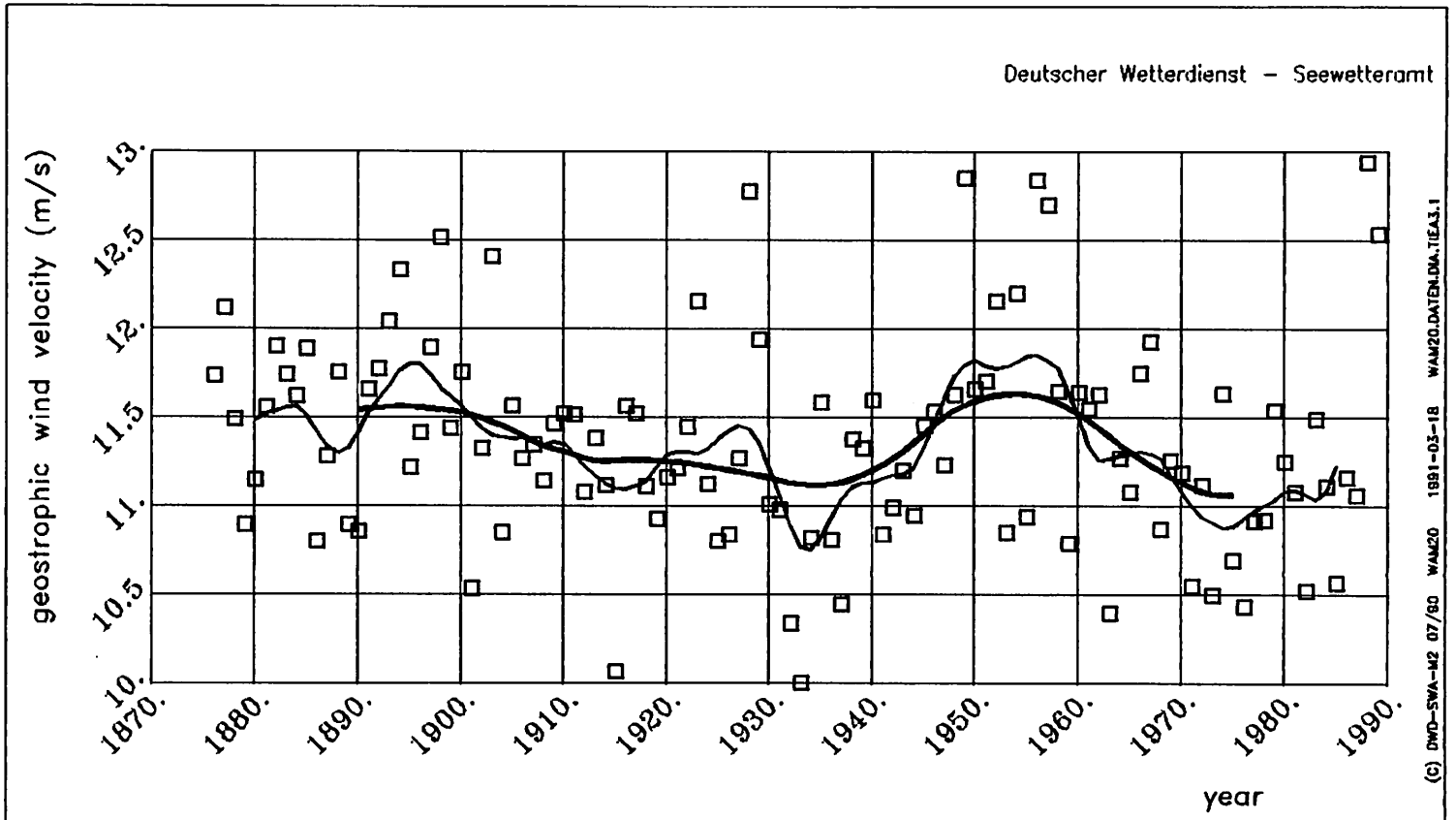

Fig. 6 GEOSTROPHIC WIND from pressure triangle "BORKUM"–"HAMBURG"–"FANÖ".
Annual mean scalar wind velocity.
Lines: low pass filtered (thin: 10, bold: 30 years cut off period).
For more information see text.

Measurements of Turbulent Parameters at Twin Towers in Northern Germany.

G. Tetzlaff and K.-J. Schreiber

Institut für Meteorologie und Klimatologie
Universität Hannover

Summary

During a period of slightly more than one year data were taken at the twin tower system designed to supply wind data allowing to trace load cases on the wind turbine once called GROWIAN. The data were coded in a unfavourable manner what made it difficult to evaluate more than a small portion of the total wealth of data available. It is the results of a selected number of intervals that is presented here. Due to shortness of time for the evaluation only a glimpse can be taken on the potential of knowledge that is still to be gained from these data. Wind shear estimates in the vertical and the horizontal as well as wind coherence functions and coherences of wind machine reactions were evaluated for a limited number of data sets missing the representativity required to translate them into design or certification criteria.

1. Introduction.

This report summarises results presented in form comprehensive volumes reported in the the years 1987 and 1988 to the GROWIAN manufacturer. The data contained in these reports cover only a fraction of the total amount of wind and machine data taken in the active period of the measuring program designed for GROWIAN and they again represent only a small fraction of the data that initially had been planned to be taken. After the dismantling of the worldwide unique measuring system of the twin 170 m towers no perspective was developped to make any use of the unique data set however limited mainly by administrative restrictions within the measuring program.

Turbulence is a critical constituent of the wind, and wind is essential in wind power. Therefore, many efforts were made to

quantify the turbulent fluctions effecting wind turbines. A rather early attempt was made when GROWIAN was built. It was mainly in the planning phase that the importance of wind measurements was stressed. However, all three planned towers were properly deployed and later on partially eqipped with wind sensors. Figure 1a gives details of the site and the situation relative to GROWIAN. The coast line is oriented NNW-SSE at a distance of about 1600 m from the wind machine. The wind measuring tower 1 is sited between the coast and the wind turbine. The twin towers with a total height of 170 m are only 70 m from the wind turbine on its western side. With an air flow from 244° the GROWIAN wind turbine is exactly in the lee of the towers.

2. Measuring strategy and technique.

The 12 m long booms of the twin towers (figure 1b) were equipped with wind sensors. The total number of 16 wind sensors was meant to give a full coverage of the rotor swept area. To supply a reference value sensors were also installed at 10 m height. As main turbulence wind sensors a combination of a propeller anemometer and a wind vane was selected giving the two horizontal wind components. The vertical spacing of these sensors was 25 m, the horizontal one close to that value (about 24 m). In addition, air temperature and relative humidity were measured at 10 m, 100 m, and 150 m. The propeller-vanes were used in well defined measuring campaigns only. The routine temporal coverage relied on cup anemomters mounted at 10 m, 50 m, 100 m, and 150 m. All sensors were sampled at 12 Hz. The cup anemoter data were routinely reduced to 30 minute averages as well as the temperature and humidity data. The propeller-vane data were saved as raw data in the full temporal discretisation of 12.5 Hz.

The standard routine data should give an estimate of the long term conditions at the site. Therefore, the data were summarized to hourly, daily and monthly sets of data. They give some insight in the energy output of the machine on the long run, possible freqencies of flow types, and subsequently on some engineering considerations.

The measuring campaigns based on the propeller vanes were selected to suffice the reqirement of presenting all important atmospheric flow situations in particular to give the multifold turbulent conditions. They were combined with synchronously taken

machine data. In principle this would allow to win information on load cases and the corresponding general atmospheric flow conditions.

The installation of the measuring system was terminated as early as 1984, it took some time to make all components operational, i.e. the machine sensors. Due to these technical considerations the time interval with full machine and meteorological data coverage concentrated on the period from august 1986 to august 1987. In this period a total of 39 campaigns with a duration of about 25 minutes each was collected. These campaigns were launched to fill in a matrix of meteorological conditions. The sorting criteria were the wind direction (onshore and offshore flow), the stability of the stratification (day and night, clear and cloudy skies), and the wind speed itself. It was for several technical reasons that the number of data sets could not be enlarged beyond the number mentioned above, in particular the time interval did not contain situations with wind speeds of more than 15 m/s. Therefore, a climatological coverage was not directly achievable.

3. Exemplaric data sets.

Among the data sets several proved to be particularly adequate to be analysed in more detail. Two of these were looked at in more detail than at the others. These two data sets were taken under onshore flow conditons with almost perpendicular flow with respect to the twin towers. The first data set (campaign 10) was taken under unstable atmospheric conditions on 21 october 1986, from 12.45 to 13.15 local time, the mean wind direction was 245°, the mean wind speed at 10 m was 10.8 m/s. The campaign 28 stands for stable atmospheric flow conditions. The data were taken on 22 january 1987 between 12.45 and 13.15 local time with a mean wind direction of 240°, the mean wind speed at 10 m was 3.5 m/s. The data sets differed to large extent in their turbulence characteristics i.e. the turbulence intensities at 10 m were 0.24 and 0.10 respectively.

Before any detailed analysis could be performed a quality control of the data proved to be useful. Beforehand the sampling rate was transformed from 12.5 Hz to 2.5 Hz. Different transformation techniques exhibited virtually no significant differences even in the higher frequency range. Furthermore, some of the mean values

needed corrections. Their quantities were derived using the theoretical vertical wind profile and the redundant wind information in the different levels. The actual amount of the corrections did not exceed 0.4 m/s. The data matrix of the temporal changes of the wind speed from one time step to the following one allowed to check the technical availability of the wind sensors.

4. Results of wind shear.

The data sets were used to analyse the wind shear, both the vertical and the horizontal one. The wind shear S_v is a vectorial quantity and defined by equation 1.

$$S_v = \delta v / \delta z \qquad (1)$$

with v the wind vector and z the vertical cordinate.

The vertical shear of the wind speed then is defined according to equation 2.

$$\delta v / \delta z = ((u^2(z_2)+v^2(z_2))^{1/2} - (u^2(z_1)+v^2(z_1))^{1/2}) / z \qquad (2)$$

In this equation u and v denote the horizontal wind components in a cartesian system with u being the zonal and v the meridional wind component.

The wind shear is a function of the distance between sensors, taken in both directions horizontally and vertically. The figures 2a, 2b, 2c and 2d show the wind shear in units of 0.01 s^{-1}. The logarithmic shape of the vertical wind profile shows itself dinstintly in figures 2a and 2b. With increasing distance from the surface the average as well as the extreme values of the vertical wind shear decrease. The data included in the figures comprise the data of 23 data blocks. Most interesting is the question whether the vertical and the horizontal wind shear exhibit different properties. The results for all 23 data blocks are shown in the figures 2c and 2d. In figure 2c the vertical

shear is taken between the sensors in 50 m and 150 m height, in figure 2d the horizontal wind shear is taken between the most distant sensors in 100 m height (76 m). While 0.03 s^{-1} is most frequent in the vertical case, the 0 value occurs most frequently in the horizontal case. However, the scatter of the shear value around the maximum frequency is rather similar in both cases. Thus, the extreme values are of similar occurrence levels in either case.

To show the effect of atmospheric stability two data sets were selected. Figures 3a and 3b exhibit the effect of the density gradient on the vertical and the horizontal flows. In the unstable air flow the vertical flow is dislocated against the 0-shear (figure 3b), the horizontal one (figure 3b) shows a slight asymmetry. This asymmetry may be caused by a systematic inhomogeneity in the air flow possibly connected to a surface structure. The stable flow conditions in represented in figure 4a and 4b emphasize the similar magnitudes of the vertical and the horizontal shear.

On the basis of the 2.5 Hz-data extreme values of the wind shear were evaluated. The maximum values for the vertical shear were observed to be 0.091 s^{-1} between 50 m and 150 m. This means a speed difference of 9.1 m/s between top and bottom of the rotor swept area. Reducing the distance to 25 m in the vertical enlarges the maximum value of the shear to 0.338 s^{-1} between 50 m and 75 m. The corresponding wind speed difference amounts to 8.5 m/s. In greater heights (125 m to 150 m) the maximum shear reduces to 0.235 s^{-1}, or a wind speed difference of 5.9 m/s. The maximum observed horizontal shear values in 100 m height were 0.238 s^{-1} for a distance of 24 m, with a horizontally taken wind speed difference of 5.9 m/s. Taking the longest possible horizontal distance in 100 m height (76 m) the maximum observed shear was 0.100 s^{-1} resulting in a wind speed difference of 10.0 m/s for a 100 m distance (or 7.6 m/s for 76 m). The basic structure already found in the complete data sets for the vertical wind shear is confirmed. Vertical and horizontal shear are rather similarly distributed. However, the 0-crossing is different for the two directions.

Applying an extreme value statistical method relying on the Gumbel-distribution of the extreme values the return period of the extreme shear events was considered. It showed that the

events detected in the very short measuring periods indeed does not exceed return periods of about half a year. An extrapolation resulted in a 100 year event of 0.180 s^{-1} for a distance of 100 m in the vertical and of 0.190 s^{-1} for a distance of 76 m in the horizontal. These values result in a wind shear of about 18 m/s for a distance of 100 m both in the vertical and the horizontal. The extension of the averaging period to longer intervals reduces the shear values, however, results are not yet available here.

Energy transfer P to the blades is proportional to third power of the wind speed. Therefore, the wind shear analysis is extended to power differences. These differences δP are evaluated according to equation 3.

$$\delta P(dt) = \tfrac{1}{2}\,\alpha\,\{\,u(ane1)^3 - (u(ane2)\,\cos\beta)^3\,\} \qquad (3)$$

The values of δP(dt) are given in the units of kg/s^2 or W/m^2, dt in s denotes the time interval over which the wind speed is integrated, α is the air density, β the angular difference between the two anemometers, here ane1 and ane2. This applies for vertical as well as for horizontal differences. The coincidence between the averaging time interval and the extension of the gusts is not heeded here. Due to the third power in the equation the numerical values exhibit stronger variation than the wind shear itself. Vertical differences are taken from top to bottom, i.e. ane1 is the one in 150m, ane2 the one in 50m.

A detailed analysis was performed for two data sets both for vertical and for horizontal differences, one in unstable stratification (21.10.86, 12h45 to 13h15) and one in stable stratification (22.1.87, 12h45-13h15). A simple statistical analysis shows the mean values of the differences.

In the set of data with the unstable stratification the mean values are u(150m)= 16.7m/s, u(50m)=14.2m/s with an average angular difference of 7° between the two levels. The average value of the power difference then amounts to 1200 W/m^2. However, the unstable conditions also evoke a strong variability. The standard deviation reaches 950 W/m^2, the maximum value 4667 W/m^2 and the minimum value -1405 W/m^2 (figure 5a). It is in about 5 % of the time interval that the differences become negative. The

average value of the horizontal power differences at 100 m between the most distant anemometers in this level (76m) amounts to 50 W/m², the standard deviation however rising to 660 W/m². The extreme values vary between 3262 W/m² and -2677 W/m²(figure 5b). This asymmetry is result of the shortness of the time interval. The total range of the differences is equal both for the horizontal and the vertical differences. There is however a slight unlikeness of the vertical and the horizontal figures as to be expected.

The data taken in stable stratification show the expected features. The average wind speeds were u(150m)=9.9 m/s and u(50m)=6.7 m/s with a wind direction difference of 24° between the two levels. The mean difference is 500 W/m² in the vertical and 0 W/m² in the horizontal case. Even the maximum values do not exceed 850 W/m²in the vertical and 350 W/m² in the horizontal case (figures 6a and 6b).

5. Time series analysis of the wind data.

To look into the structure of the wind data a power spectrum analysis was performed. In addition a coherence analysis gave information on the interrelation between the wind at different locations and machine oriented parameters. The time series were given in the form of the functions x(t) and y(t). The spectrum then gives the fraction of the total variance σ^2 for a certain frequency interval. As wind variance and kinetic energy have the same physical dimension a connection between the turbulence kinetic energy and the turbulent eddies can be derived. The interrelation between two time series can be investigated with the cross spectrum analysis. The Fourier transform of the cross covariation gives the complex cross spectrum. This shows whether there does indeed exist an interrelation between two time series as a function of frequency. The quadratic covariance is the normalised cross spectrum (consisting of the cospectrum and the quadratic part, denoting the real and the imginary part of the cross spectrum), which mathematically results from the variance spectra of the two time series and the cospectrum and the quad-spectrum. The coherence thus gives the frequency-dependent quadratic correlation-coefficient between the two time series x(t) and y(t) (i.e. Panofsky and Brier 1965, Chatfield and Watts 1968, Taubenheim 1969, Walk 1970, Bath 1974, Richter 1980, Schönwiese

1985). The pretreatment of the data in the time series includes the proper filtering. The frequency ranges from 1.25 Hz to 1/900 Hz in accordance with the filtered sampling rate and the length of the time interval.

The presentation of the power spectra using the axes $f \cdot E(f)$ and ln f allows the conservation of the total variance integrating over all frequencies. The digitization of the data of the windspeed was 0.3 m/s. This results in a white noise the contribution of which reaches a quantity of about 0.005 m^2/s at 2.5 Hz. In most atmospheric conditions this is a neglegible quantity, in some few cases with very strong turbulence reduction the white noise contribution becomes detectable on the high frequency part of the spectrum.

The variance spectrum of the wind and the wind coherence were analysed in detail for a set of data in

-unstable conditions : 21.10.1986, 12h45-13h15,
wind direction 245°,
surface friction velocity u_*=0.93 m/s;
in 10 m average wind speed u=10.8 m/s,
standard deviation σ=2.58 m/s and
turbulence intensity TI=0.24;
in 50 m u=14.2 m/s, σ=3.03 m/s and TI=0.21;
in 100 m u=16.1 m/s, σ=3.15 m/s and TI=0.20;
in 150 m u=16.7 m/s, σ=3.00 m/s and TI=0.19.

The figures 7a-7c give a good impression of the basic structure of the turbulent parameters. The amplitude of the turbulent fluctuations quite distinctly decreases with height, the longer periods occur almost simultaneously through all levels, the shorter ones cannot, however, be easily identified.

In the figures 8a-8c the power spectra of the time series shown in figures 7a-7c are presented. The amplitudes of the higher frequencies decreases with height so that the turbulent energy in the low frequency range increases with height.

The consequently derived coherence values are shown in the figures 9a-9b. In figure 9a the cross spectrum was calculated for the

time series of 50m and 150 m. The coherence in the low frequency range approaches the maximum value 1, then decreases and has a shoulder at about 0.01 Hz (100s). The horizontally taken cross-spectrum at 100 m height, between the maximum possible distance at this level exhibits a similar pattern (figure 9c). It is at about 0.01 Hz that the correlation between the two time series falls under the value of a strong interrelation.

In strongly stable stratification the expected conditions can be detected. The data were taken in january 1987 at noon in warm air advection with the formation of some fog and very low clouds. The main wind direction with 240° again was optimum for the instrument setting. The wind data showed :
10 m wind speed u=3.5 m/s, σ=0.35 m/s, TI=0.10, u_*=0.34 m/s;
50 m : u=6.7 m/s, σ=0.18 m/s, TI=.03;
100 m : u=7.8 m/s, σ=0.22 m/s, TI=0.03;
150 m : u=9.9 m/s, σ=0.17 m/s, TI=0.02.

The turbulence intensity is on a very low level. Figure 10 shows the time series of the wind speed in 150 m height with virtually no detectable turbulence. The corresponding spectrum (figure 11) shows the white noise of the digitisation in the high frequency range. Else there is indeed very little turbulent energy in the classical turbulence range. It is only beyond the 100s threshold that some fluctuations are found, but with almost neglegible energy when compared to the unstable case. The coherence analysis confirmed the overall low frequency levels and the decoupling of the vertical wind speeds through a wide range of frequencies (figure 12). Even in the low frequencies the air flow between 50 m and 150 m height apparently is decoupled. There are hints that a temperature inversion was responsible for this effect. The temperature data themselves were not accurate enough to include them into the investigation. This is emphasised by the the coherence analysis of the 100 m data. The coherence between the two most distant wind sensors showed a coherence close to 1 in the range beyond about 200 s, and no detectable coherence at higher frequencies (figure 13).

The power spectrum analysis was also applied to the power differences between the vertical and the horizontal ones (figure 14a-14b). The vertical power differences were taken between 50 m and 150 m, the horizontal ones between the most dinstant sensors at 100 m height. The power spectra show the maximum of the variance

at about 15 s with a decrease to lower and higher frequencies.

The vertical power differences show contributions to the variance mainly in the low frequency range with a shoulder at about 15 s. This pattern in principle is also valid for stable stratification (figures 15a and 15b). The low energy level of the spectra makes it clear that the digitisation noise dominates the high frequency range at 1 s. The vertical differences go with an average difference to be seen in the low frequency range, the average horizontal differences are very close to 0.

Synchronous to the wind data machine data were taken for some of the time intervals. As indicators to characterize the machine the power output was selected, as well as the strain gage data deployed at three locations in the rotor blade on the windward side. To get a first guess of an integrated wind signal the anemomter data were averaged arithmetically in order to represent one value of the rotor swept area (figures 16a and 16b). Figure 16a shows the wind speed at 100 m height, figure 16b the arithmetically averaged values (data of 10 september 1986, 12h45-13h09, wind direction 260°, cloudy skies, u(10m)=6.6 m/s, TI(100m)=0.09 indicating near neutral stratification). The electric output of the machine is presented in figure 16c. To give insight in the loads on the the machine the most appropriate information seems to be the data of strain gages in the blades.

Figures 17a, 17b and 17c show the time series of the strain gage signals at 11 m, 27 m and 40 m from the hub. The power spectrum of the wind speed at one sensor in 100 m height differs markedly from the spectrum of the arihtmetically averaged wind signal (figures 18a and 18b). The spectrum of the signal of the electrical output follows the pattern of the wind spectra, with some dinstinct deviations at the rotation frequencies of the blade itself (figure 18c). The power spectra of the strain gages are even more subject to the rotation frequency of the rotor. Figure 19a shows three narrow lines with a very high peak energy but a very narrow frequency range at 3.7 s, 1.8 s, and slightly less than 1 s. Filtering the data with a Gaussian filter suppressing frequencies higher than 100 s results in spectrum of figure 19b. The spectral density here agrees rather well with the one of the wind input as taken from the arithmetically averaged wind data. The interaction of the blades and the wind appears in to features. In figure 19c the broadening of the "foot" of the spectral

lines certainly is one form of the reaction, and secondly the spectral reaction in the frequency range of the wind speed itself is wind dependent. In particular the differences in the spectral density allow some insight in the amplitudes of the blades as a reaction on the wind forcing. The strain gage at 40 m from the hub sows much larger values of the variance than the ones closer to the hub.

Considering the coherence between the wind and machine parameters the correlation ceases to exist for frequencies higher than about 0.03 Hz. This applies almost identically for the wind speed taken with one individual wind sensor at 100 m height (figure 20a) or for a the arithmetically averaged wind speed (figure 20b). The strain gages react similarly (figure 20c). The correlation in the low frequncy range is very high breaking down at about 0.03 Hz.

This analysis was performed for a several sets of data showing structurally similar results. Furhter analysis were also performed being not presented here. To fathom this very rich mass of data requires more time and effort than could be invested up to now. However, hope to continue this piece of interesting data analysis never ends.

List of figures.

Figure 1a : Geometrical setting of the measuring towers.

Figure 1b : Positions of sensors on the twin towers (H horizontal wind, R winddirection, T temperature).

Figure 2a : Vertical wind shear for height interval 50-75 m in unstable stratification.

Figure 2b : Vertical wind shear for height interval 125-150 m in unstable stratification.

Figure 2c : Vertical wind shear for height interval 50-150 m for 23 stes of data.

Figure 2d : Horizontal wind shear in 100 m height and 76 m horizontal distance for 23 sets of data.

Figure 3a : Horizontal wind shear in 100 m height in unstable stratification.

Figure 3b : Vertical wind shear in unstable stratification.

Figure 4a : Vertical wind shear in stable stratification.

Figure 4b : Horizontal wind shear in stable stratification.

Figure 5a : Time series of vertical wind shear in unstable stratification.

Figure 5b : Time series of horizontal wind shear in unstable stratification.

Figure 6a : Time series of vertical wind shear in stable stratification.

Figure 6b : Time series of horizontal wind shear in stable stratification.

Figure 7a : Time series of wind speed in 10 m in unstable stratification.

Figure 7b : Time series of wind speed in 50 m in unstable stratification.

Figure 7c : Time series of wind speed in 150 m in unstable stratification.

Figure 8a : Power spectrum of wind speed as shown in figure 7a.

Figure 8b : as figure 8a, but 50 m.

Figure 8c : as figure 8a, but 150 m.

Figure 9a : Quadratic coherence for wind speeds in 50 and 150 m in unstable stratification.

Figure 9b : Quadratic coherence for wind speeds in 100 m and 76 m horizontal distance.

Figure 10 : Time series of wind speed in 150 m in stable stratification.

Figure 11 : Power spectrum of wind data of figure 10.

Figure 12 : Quadratic coherence for wind speeds in 50 and 150 m.

Figure 13 : Quadratic coherence for wind speeds in 100m and 76 m horizontal distance.

Figure 14a : Power spectrum of the vertical power differences in unstable stratification.

Figure 14b : Power spectrum of the horizontal power differences in unstable stratification.

Figure 15a : as figure 14a, but for stable stratification.

Figure 15b : as figure 14b, but for stable stratification.

Figure 16a : Wind speed in 100 m in near neutral conditions.

Figure 16b : Arithmetical average of all wind sensors in near neutral conditions.

Figure 16c : Electrical power output for wind speed of figure 16b.

Figure 17a : Time series of strain gage data in rotor blade 11 m from the hub.

Figure 17b : as figure 17a, but 27 m from the hub.

Figure 17c : as figure 17a, but 40 m from the hub.

Figure 18a : Power spectrum of wind speed taken from figure 16a.

Figure 18b : Power spectrum of wind speed taken from figure 16b.

Figure 18c : Power spectrum of electrical output taken from figure 16c.

Figure 19a : Power spectrum of strain gage taken from figure 17a.

Figure 19b : Power spectrum of strain gage taken from figure 17a, but low-pass filtered.

Figure 19c : Power spectrum of strain gage taken from figure 17c.

Figure 20a : Quadratic coherence between the wind speed in 100 m and the electric output.

Figure 20b : as figure 20a, but for area averaged wind speed.

Figure 20c : as figure 20a, but for the strain gage in 27 m from the hub.

List of References.

Bath 1974, Spectral analysis in geophysics, Elsevier, Amsterdam, pp. 365.

Chatfield 1972, The analysis of time series, Chapman and Hall, London, pp.268.

Müller 1988, Prognose der Niederschlagswahrscheinlichkeit an einer Station (Berlin), Metorol. Abhandl., Freie Uni. Berlin, Neue Folge A 4/2, pp.146.

Panofsky and Brier 1965, Some applications of statistics to meteorology, Pennsylvania State Uni., pp.224.

Richter 1980, Spektralanalyse immisionsklimatischer Messungen im Oberrheintal, Diplom-thesis, Uni. Karlsruhe, Meteterol. Inst., pp 154.

Schönwiese 1985, Praktische Statistik, Gebrüder Bornträger, Stuutgart, pp. 231.

Schreiber and Tetzlaff 1987, Die GROWIAN-Windmessungen; Ansätze zur Zeitreihenanalyse im Rahmen des GROWIAN-Meßprogramms.

Schreiber and Tetzlaff 1988, Die GROWIAN-Windmessungen; Kohärenzuntersuchungen zwischen der Windgeschwindigkeit und ausgewählten Anlagenparametern.

Taubenheim 1969, Statistischwe Auswertungen geophysikalischer und meteorologischer Daten, Akad. Verlagsges., Leipzig, pp. 386.

Tetzlaff, Franke and Linse 1989, Quantitative Bestimmung des klimatologisch gemittelten Windfeldes in der Umgebung von typischen Hindernissen Norddeutschlands, Ber. Inst. Meteorol. und Klimatol. Uni. Hannover, Band 38, pp. 251.

Theunert, Tetzlaff and Bufe 1990, Auswertung der Windmeßdaten von sechs Standorten in Norddeutschland, Ber. Inst. Metorol. u. Klimatol. Uni. Hannover, B1, pp.232.

Walk 1970, Zur Interpretation von Energie-, Ko- und Quadraturspektren meteorologischer Parameter. Wiss. Mitteilungen Meteorol. Inst. Uni. München, 20, pp.37.

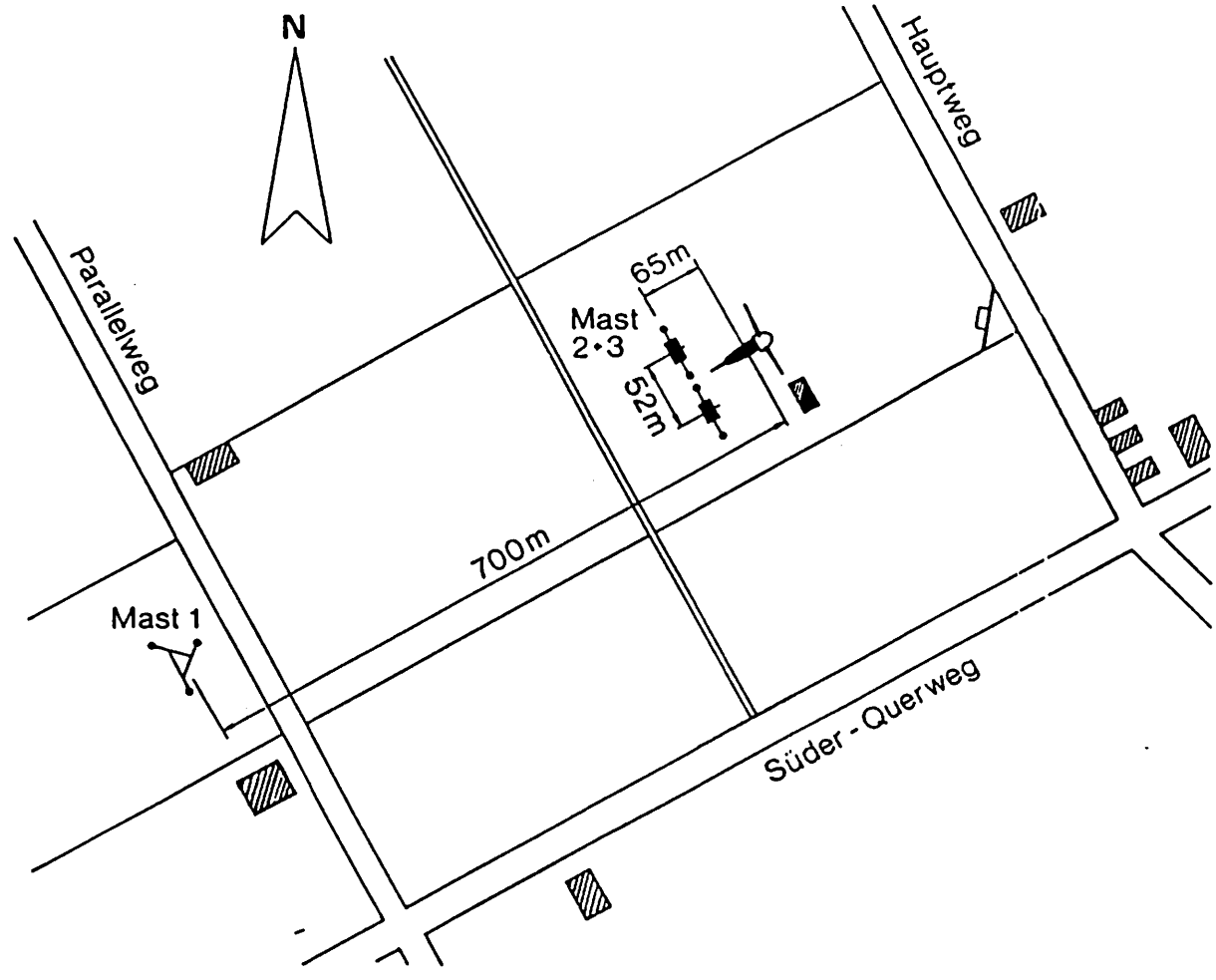

Figure 1a : Geometrical setting of the measuring towers.

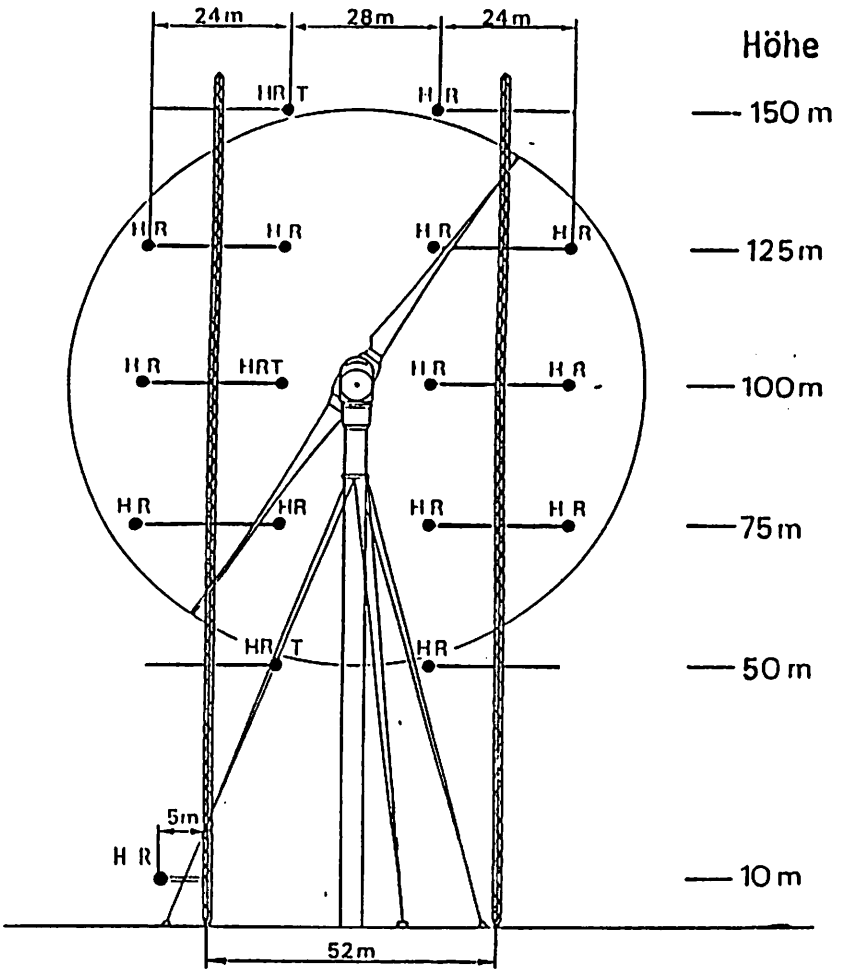

Figure 1b : Positions of sensors on the twin towers (H horizontal wind, R winddirection, T temperature).

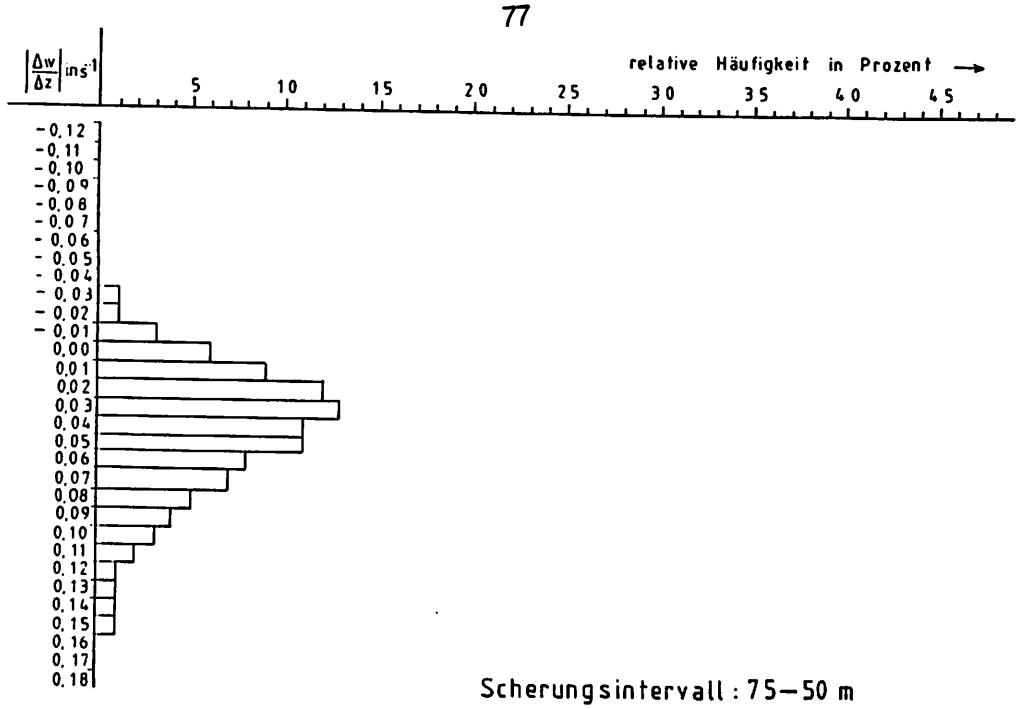

Figure 2a : Vertical wind shear for height interval 50-75 m in unstable stratification.

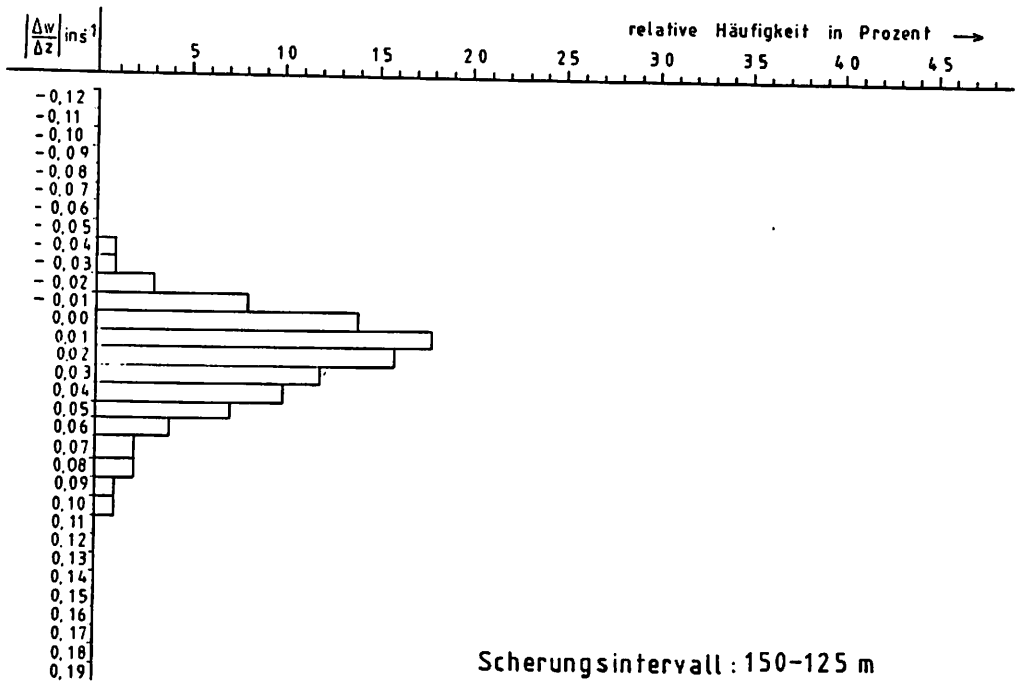

Figure 2b : Vertical wind shear for height interval 125-150 m in unstable stratification.

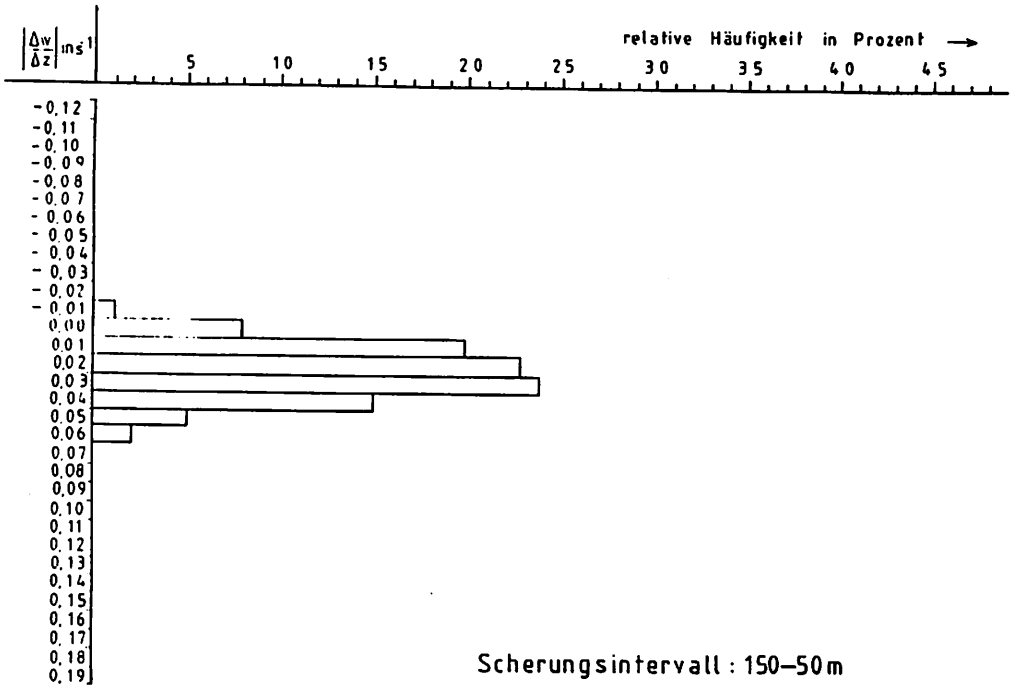

Figure 2c : Vertical wind shear for height interval 50-150 m for 23 stes of data.

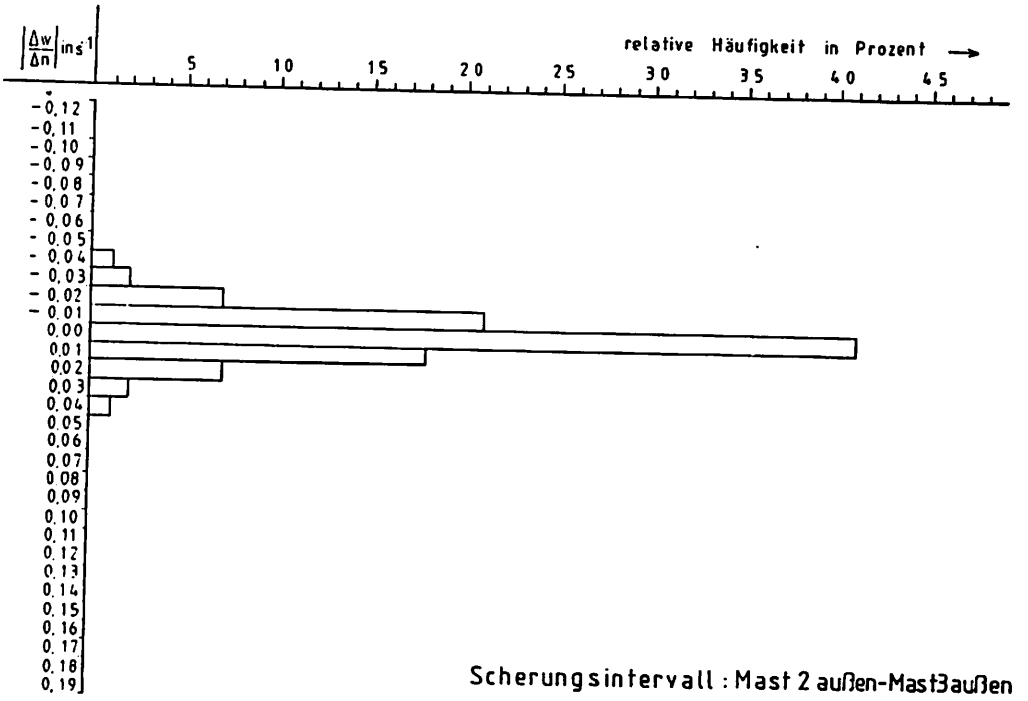

Figure 2d : Horizontal wind shear in 100 m height and 76 m horizontal distance for 23 sets of data.

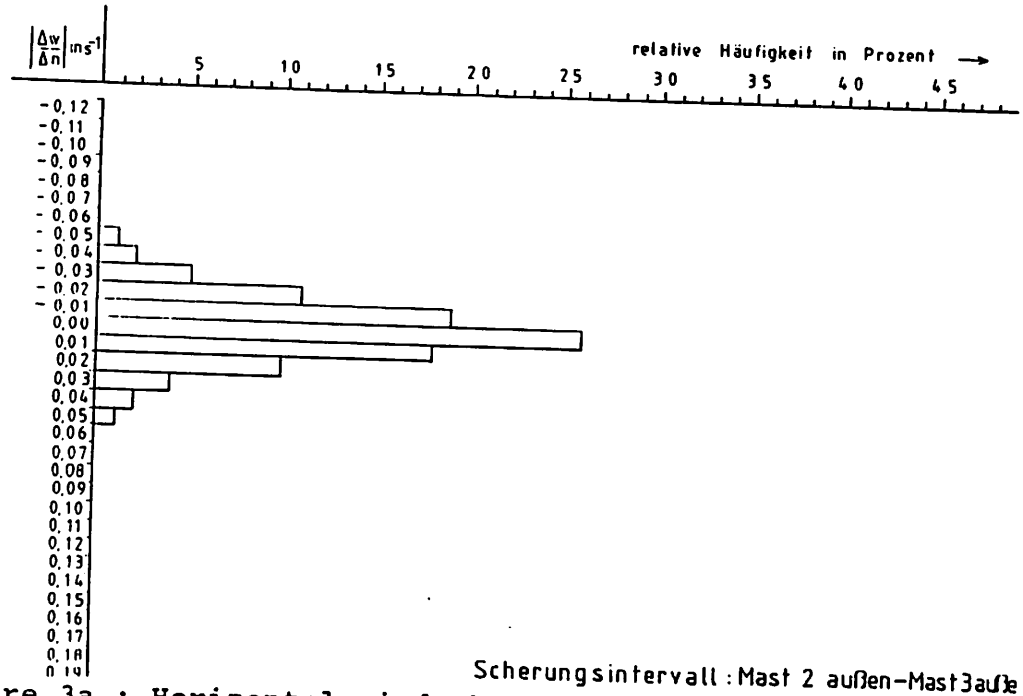

Figure 3a : Horizontal wind shear in 100 m height in unstable stratification.

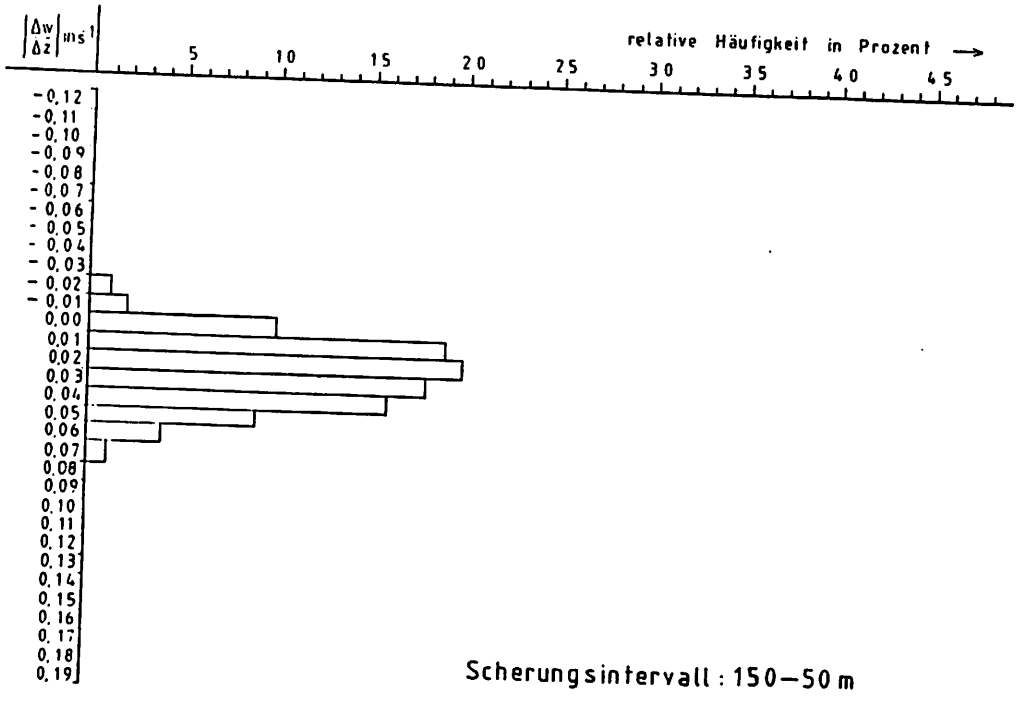

Figure 3b : Vertical wind shear in unstable stratification.

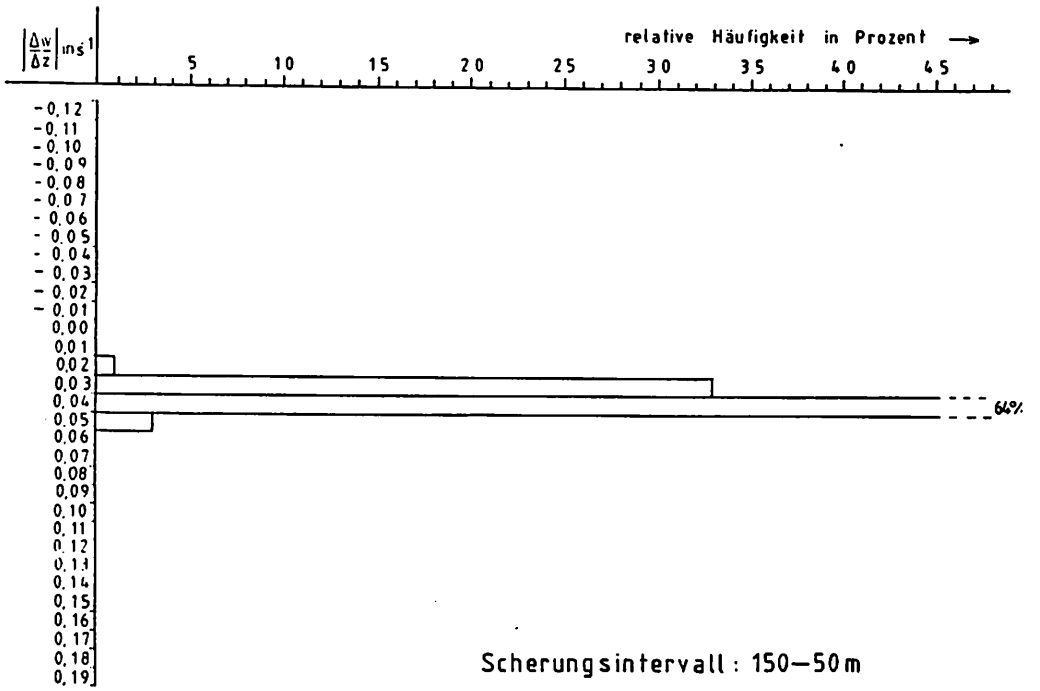

Figure 4a : Vertical wind shear in stable stratification.

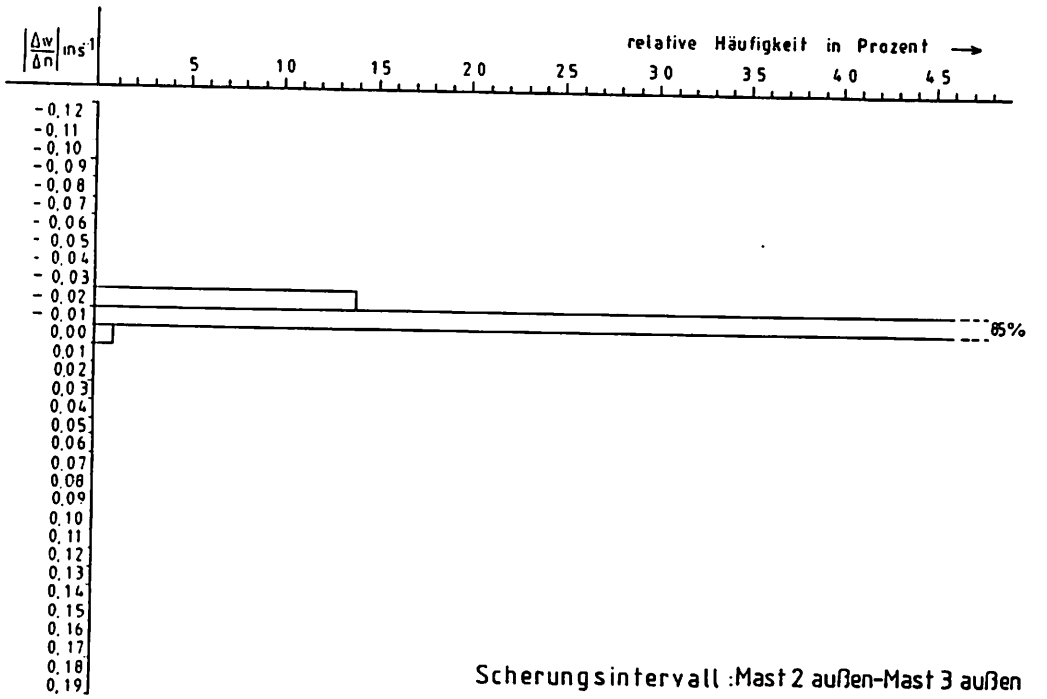

Figure 4b : Horizontal wind shear in stable stratification.

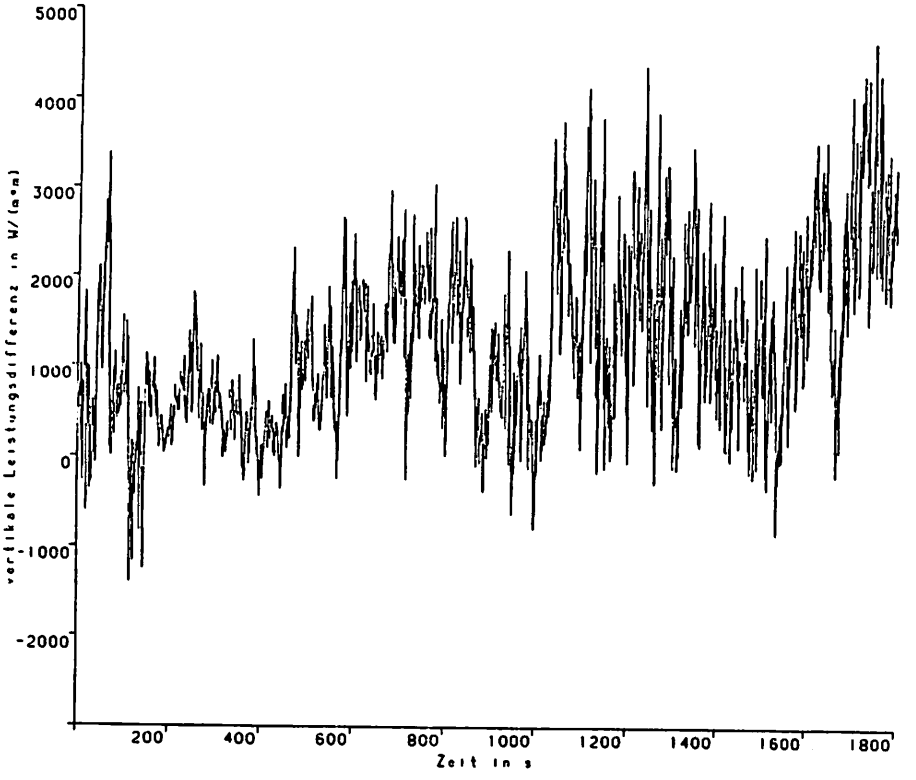

Figure 5a : Time series of vertical wind shear in unstable stratification.

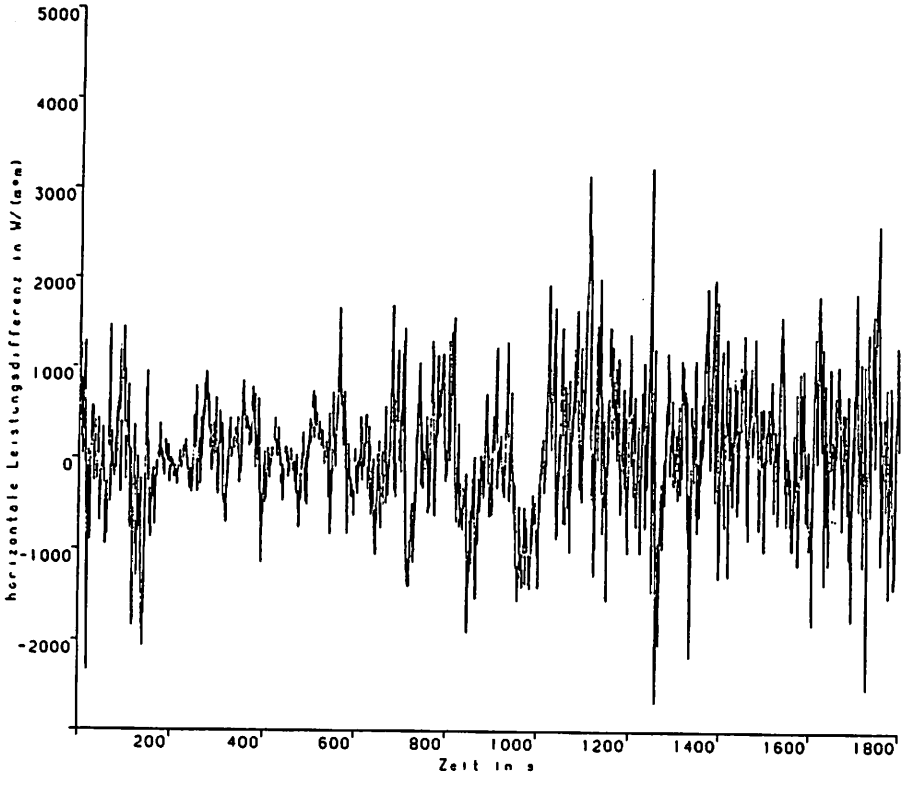

Figure 5b : Time series of horizontal wind shear in unstable stratification.

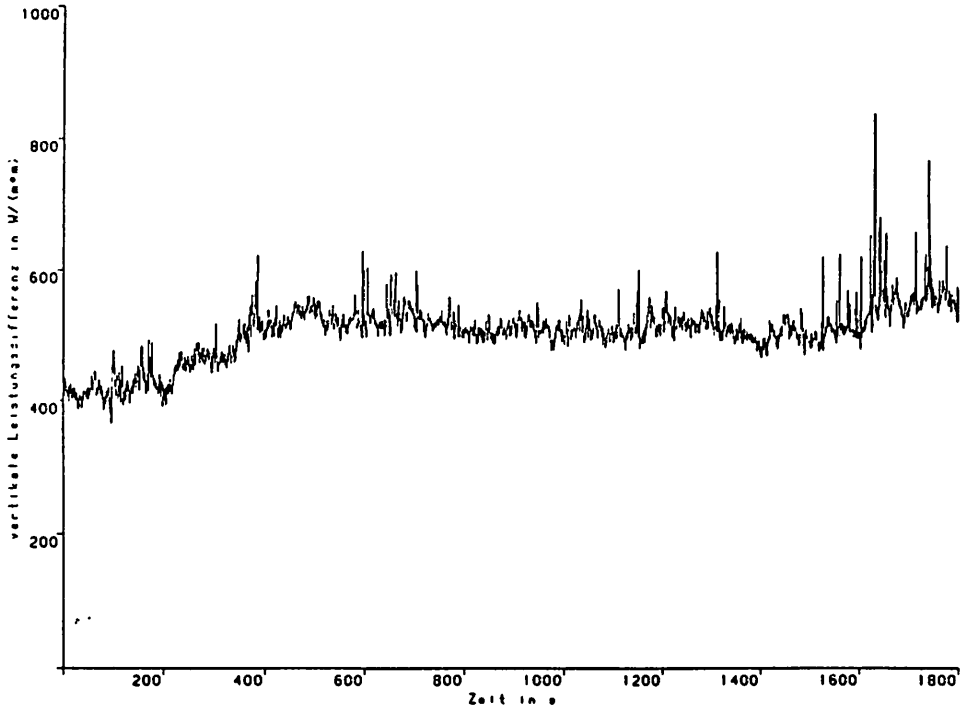

Figure 6a : Time series of vertical wind shear in stable stratification.

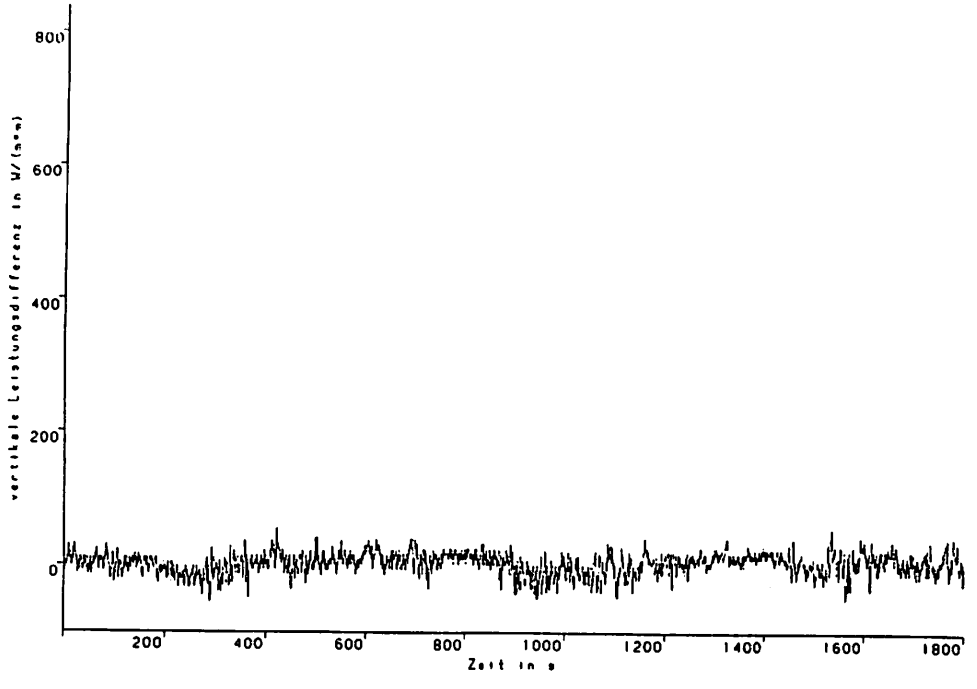

Figure 6b : Time series of horizontal wind shear in stable stratification.

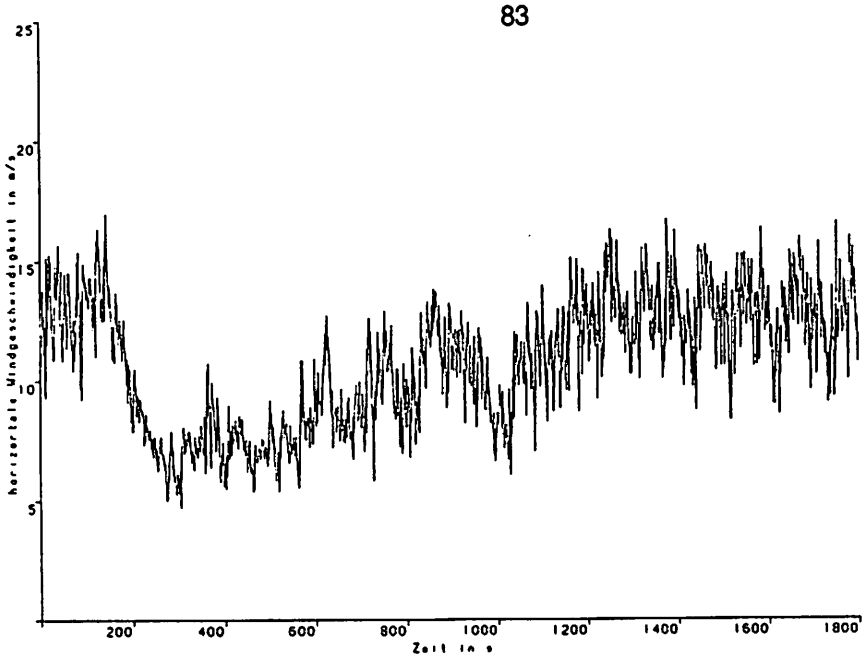

Figure 7a : Time series of wind speed in 10 m in unstable stratification.

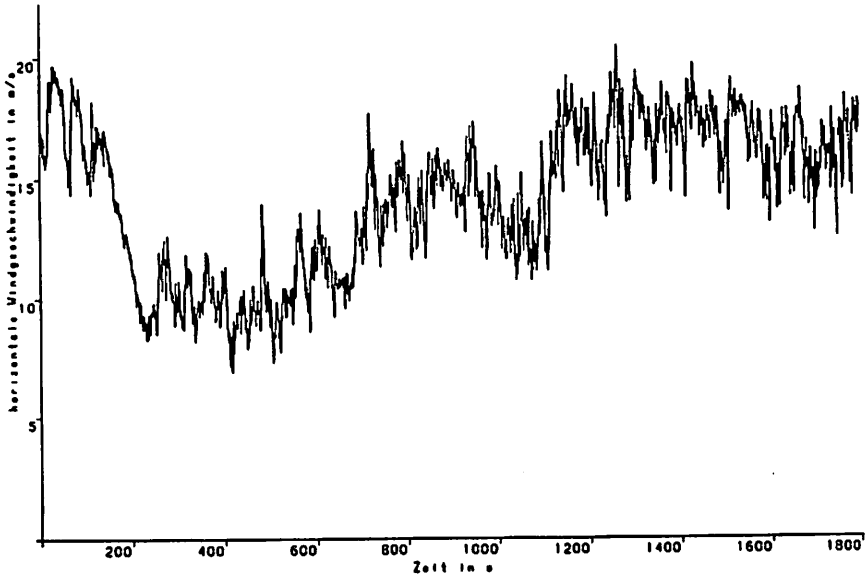

Figure 7b : Time series of wind speed in 50 m in unstable stratification.

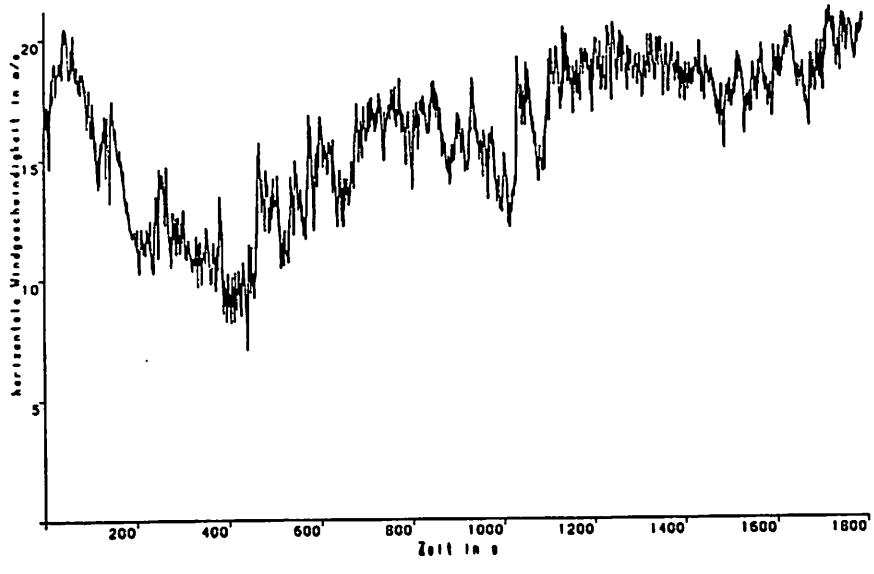

Figure 7c : Time series of wind speed in 150 m in unstable stratification.

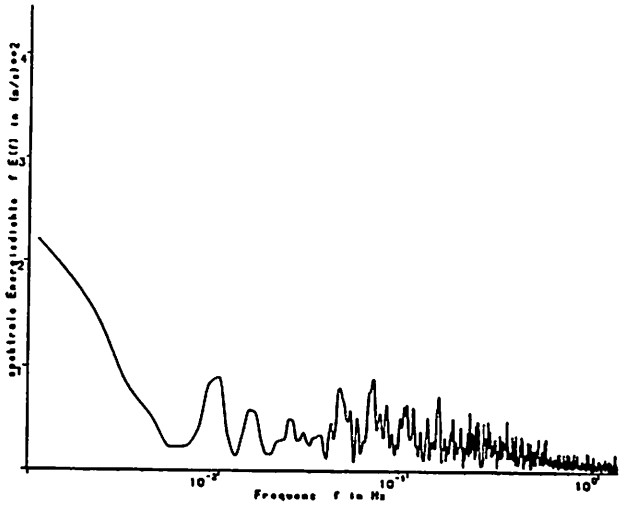

Figure 8a : Power spectrum of wind speed as shown in figure 7a.

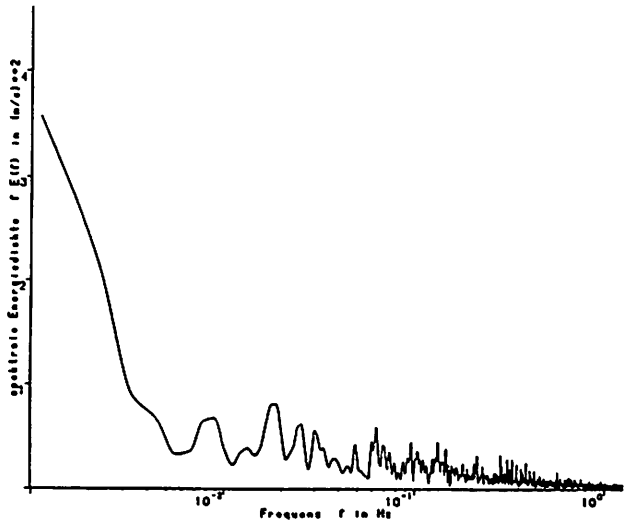

Figure 8b : as figure 8a, but 50 m.

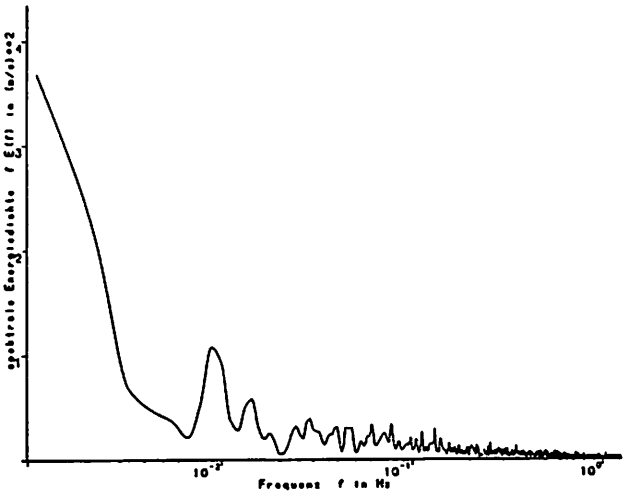

Figure 8c : as figure 8a, but 150 m.

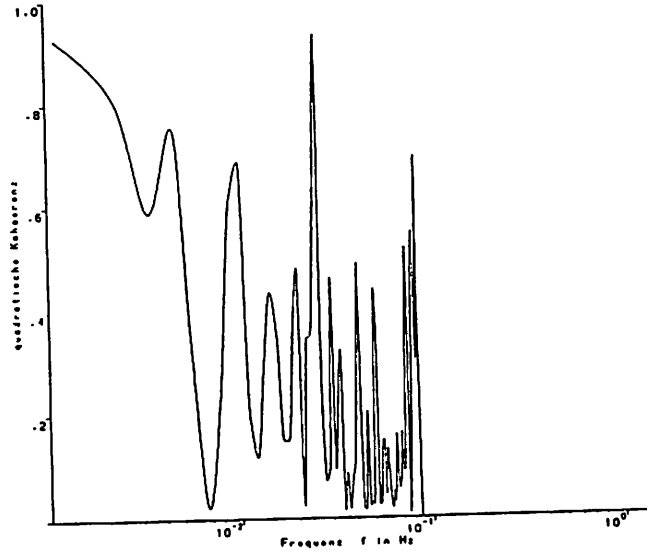

Figure 9a : Quadratic coherence for wind speeds in 50 and 150 m in unstable stratification.

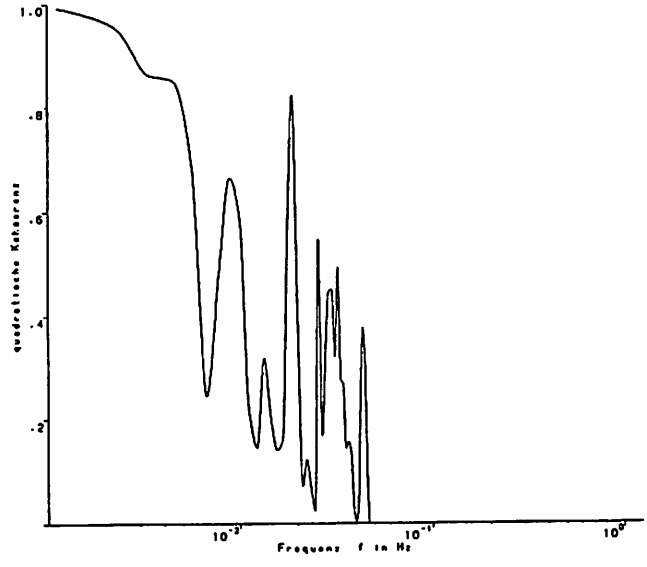

Figure 9b : Quadratic coherence for wind speeds in 100 m and 76 m horizontal distance.

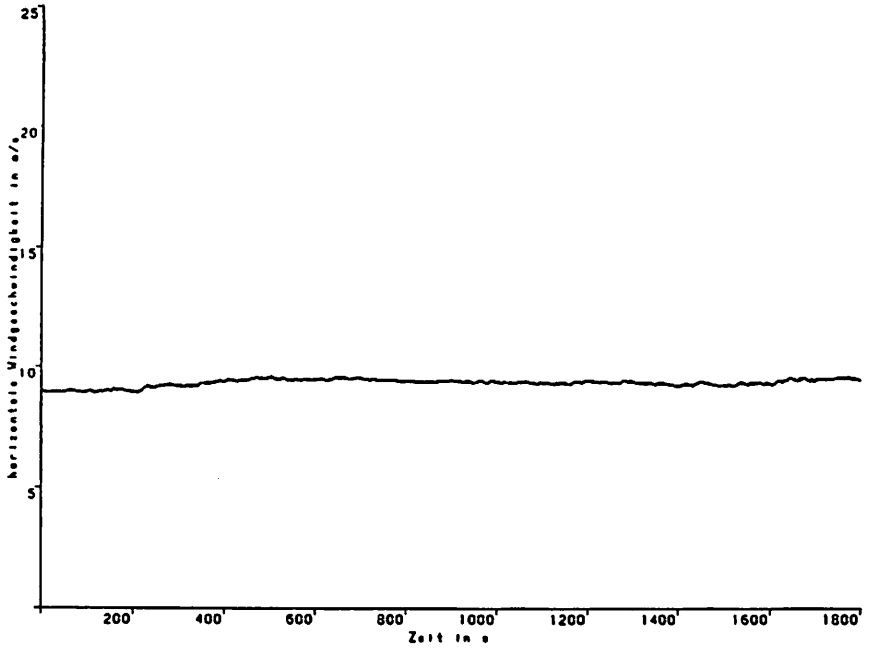

Figure 10 : Time series of wind speed in 150 m in stable stratification.

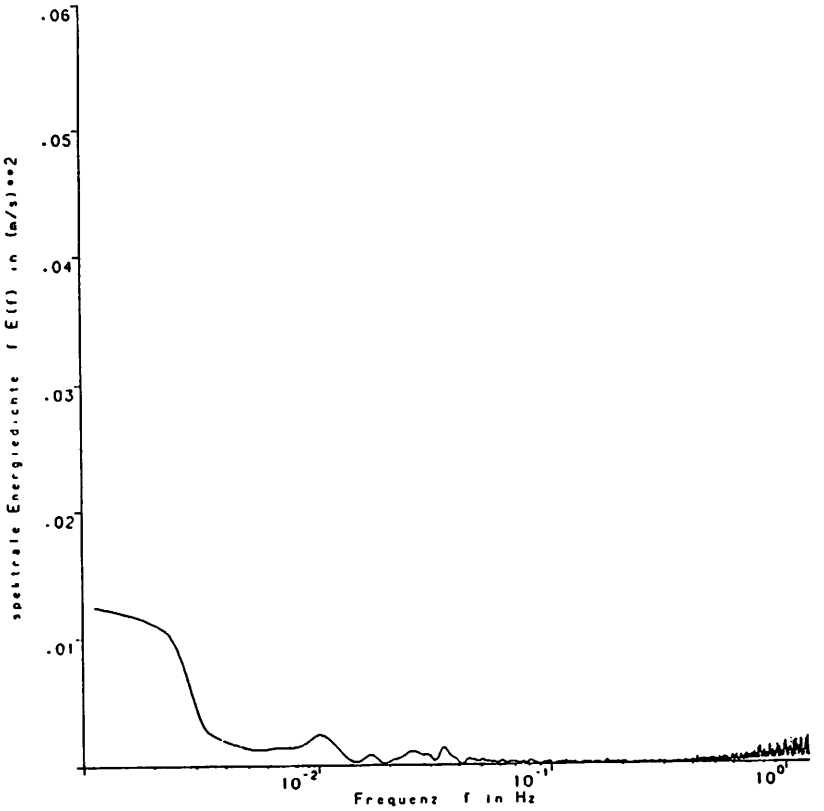

Figure 11 : Power spectrum of wind data of figure 10.

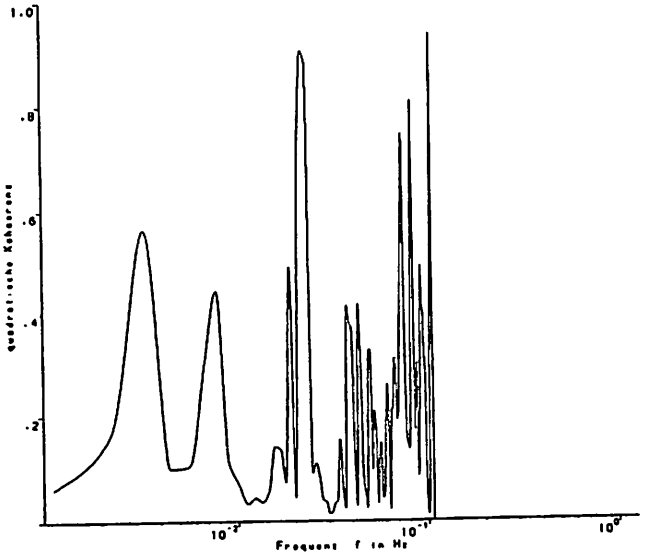

Figure 12 : Quadratic coherence for wind speeds in 50 and 150 m.

Figure 13 : Quadratic coherence for wind speeds in 100m and 76 m horizontal distance.

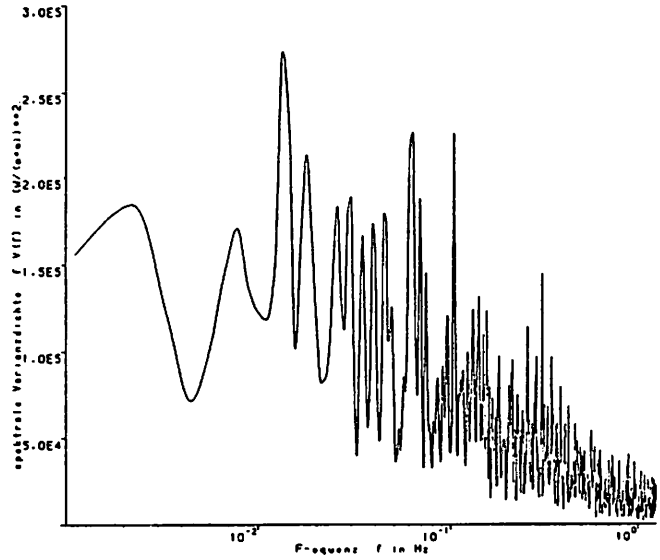

Figure 14a : Power spectrum of the vertical power differences in unstable stratification.

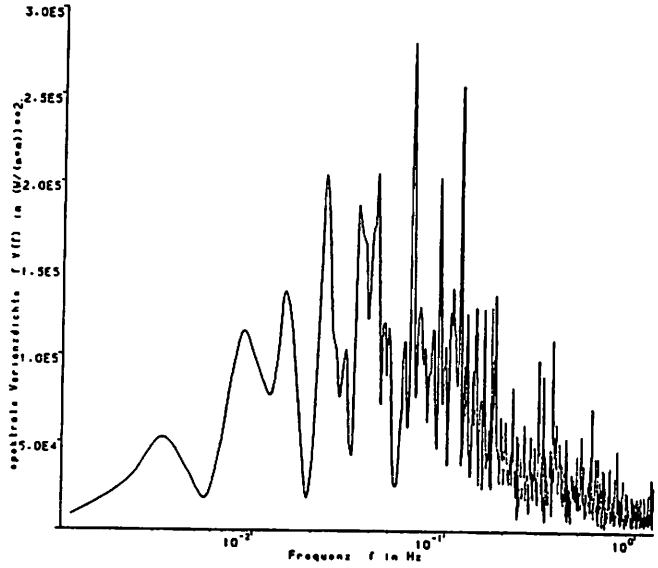

Figure 14b : Power spectrum of the horizontal power differences in unstable stratification.

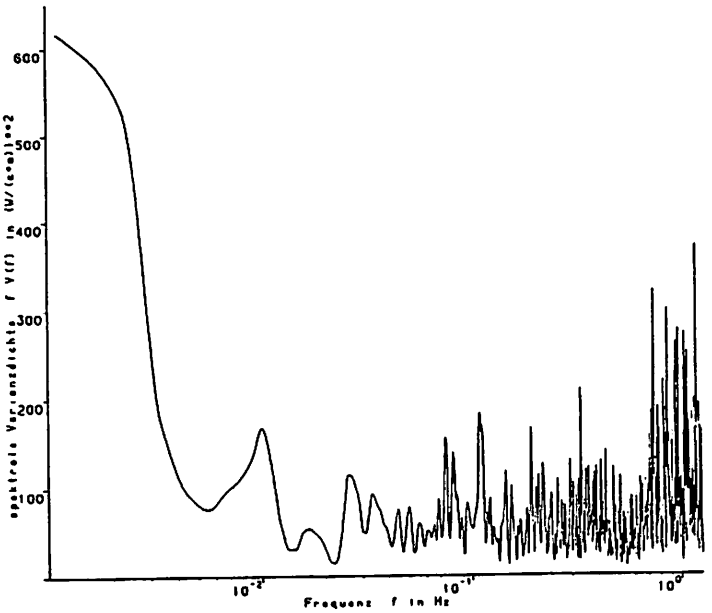

Figure 15a : as figure 14a, but for stable stratification.

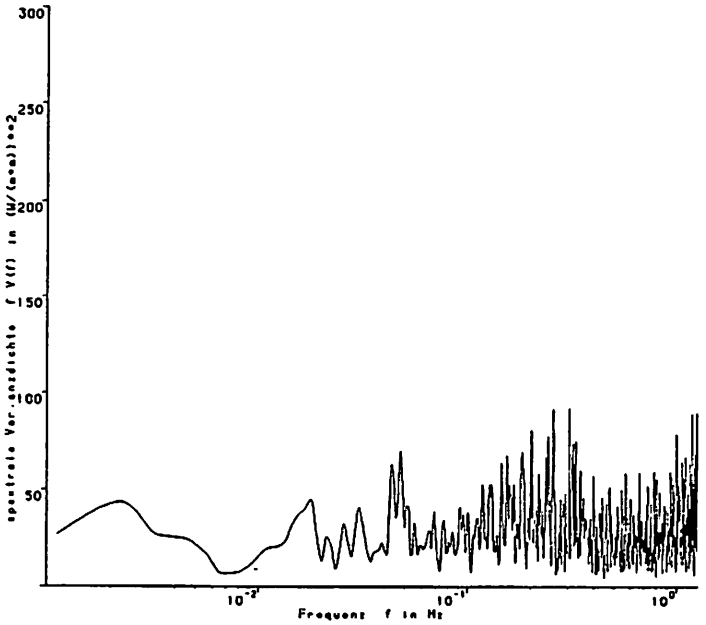

Figure 15b : as figure 14b, but for stable stratification.

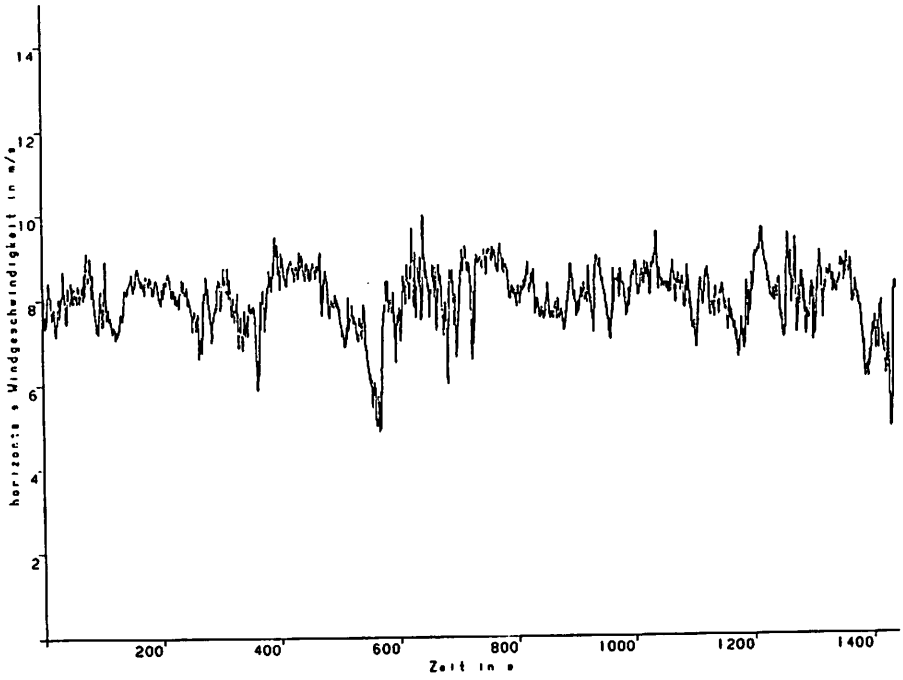

Figure 16a : Wind speed in 100 m in near neutral conditions.

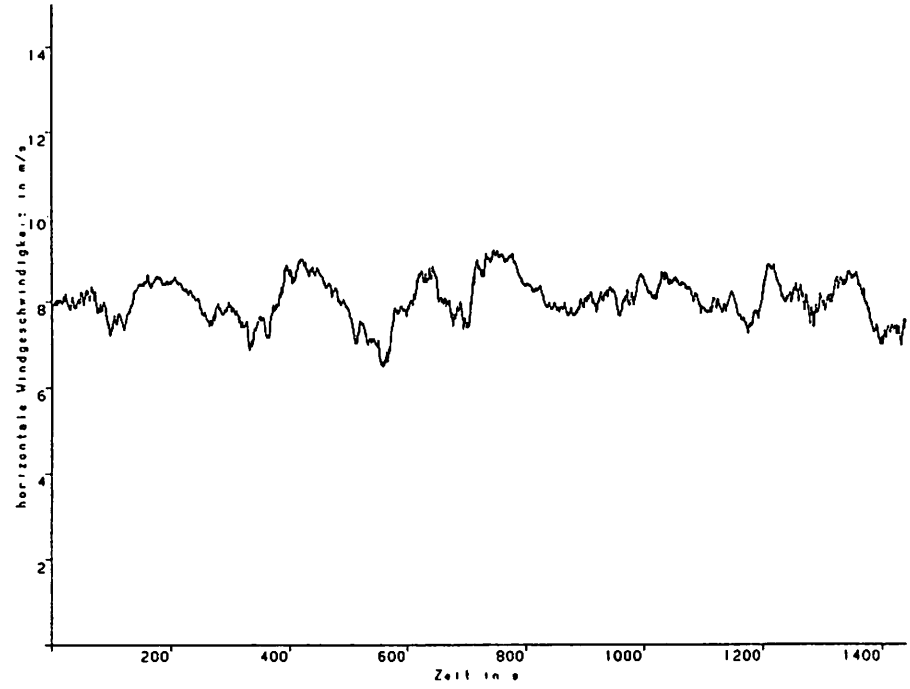

Figure 16b : Arithmetical average of all wind sensors in near neutral conditions.

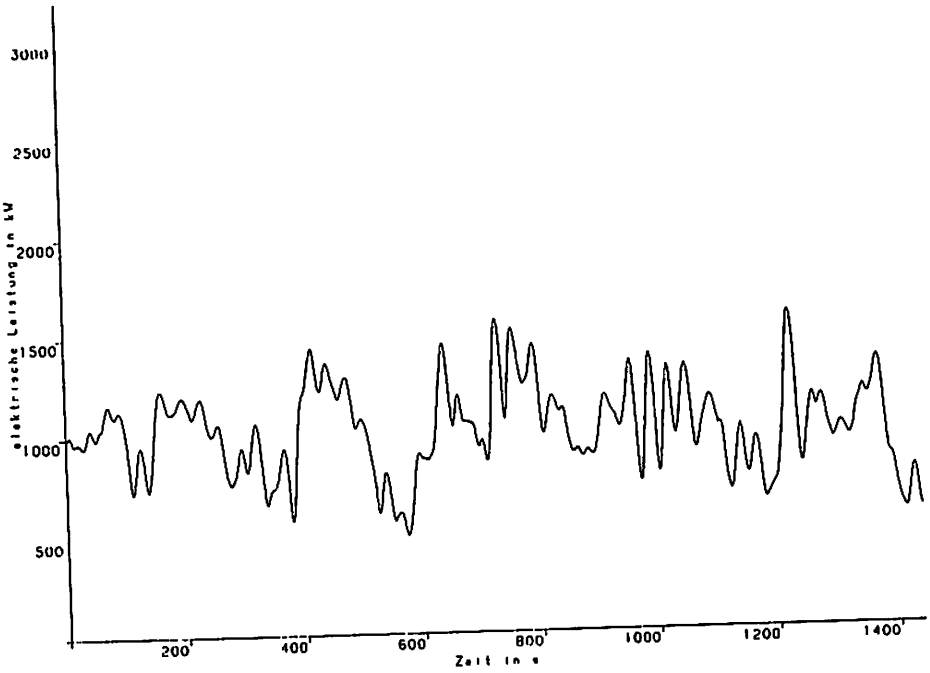

Figure 16c : Electrical power output for wind speed of figure 16b.

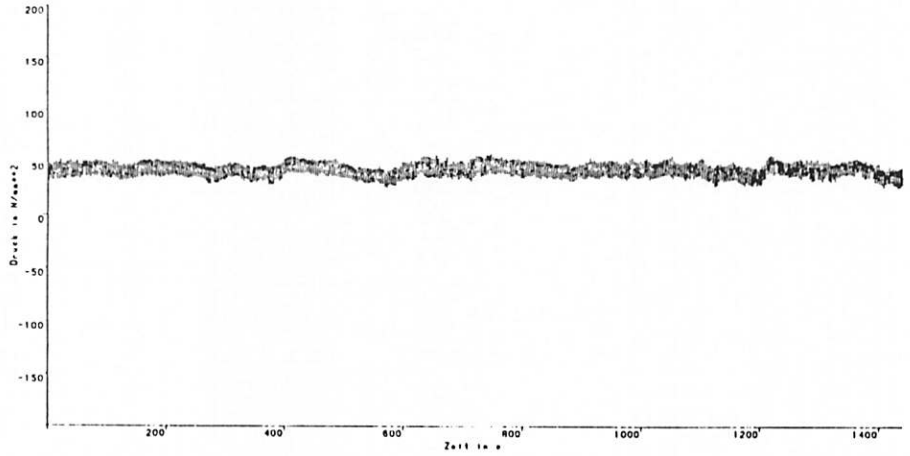

Figure 17a : Time series of strain gage data in rotor blade 11 m from the hub.

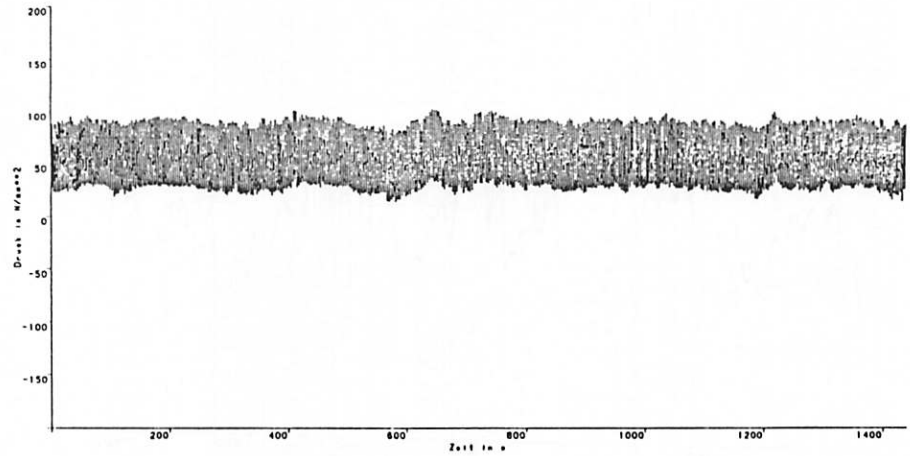

Figure 17b : as figure 17a, but 27 m from the hub.

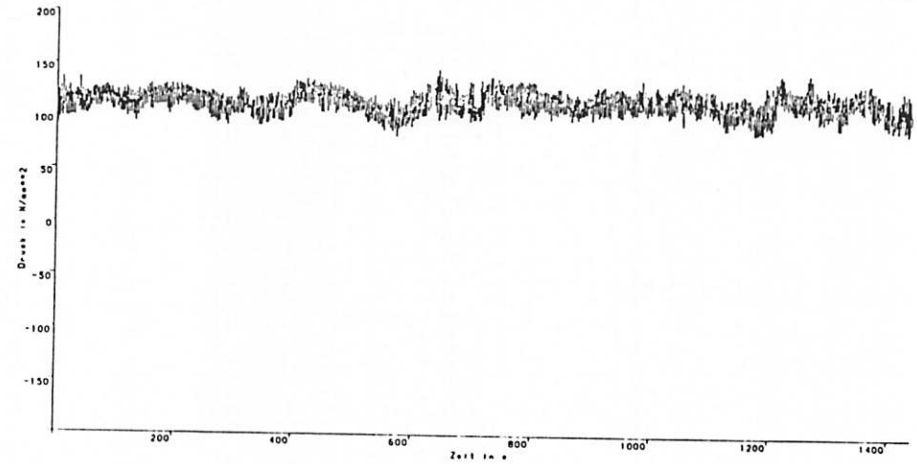

Figure 17c : as figure 17a, but 40 m from the hub.

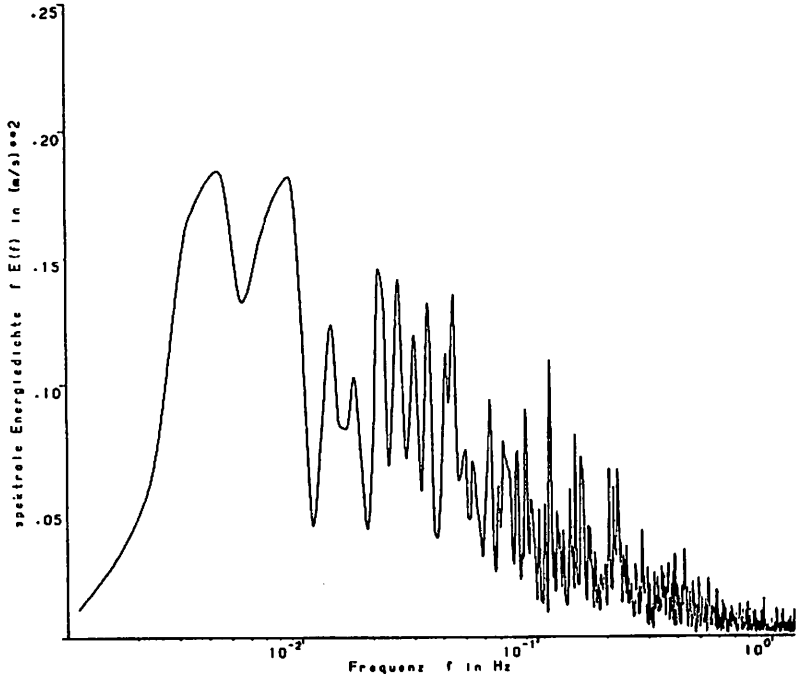

Figure 18a : Power spectrum of wind speed taken from figure 16a.

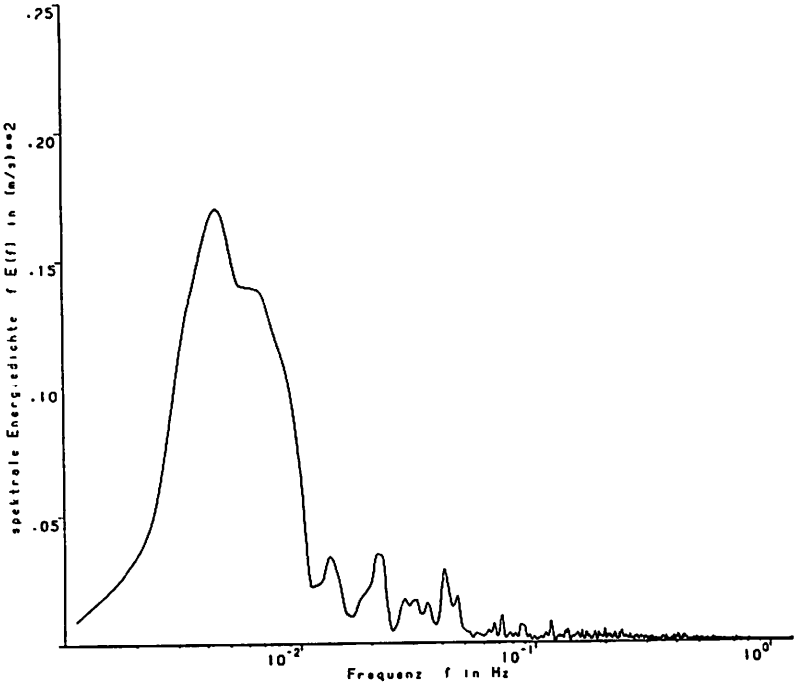

Figure 18b : Power spectrum of wind speed taken from figure 16b.

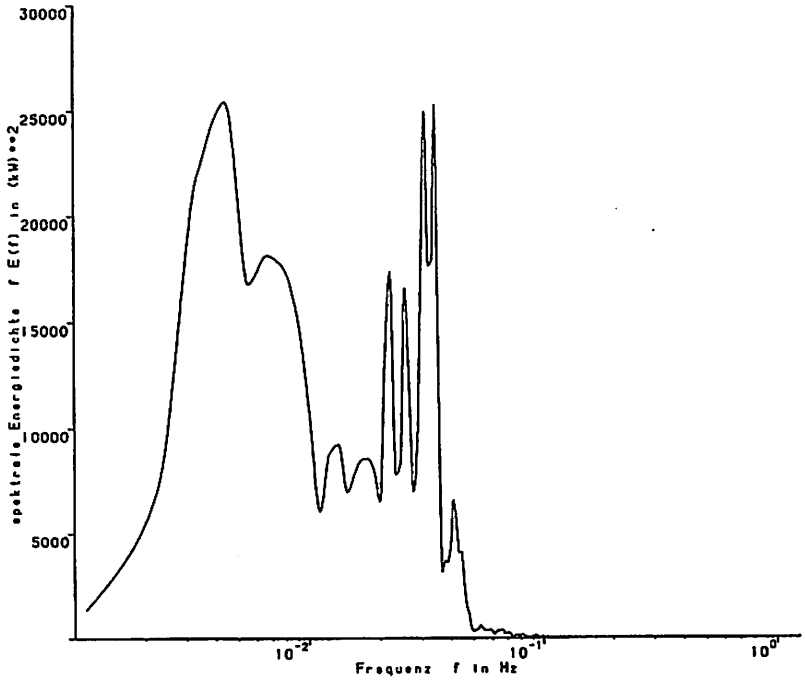

Figure 18c : Power spectrum of electrical output taken from figure 16c.

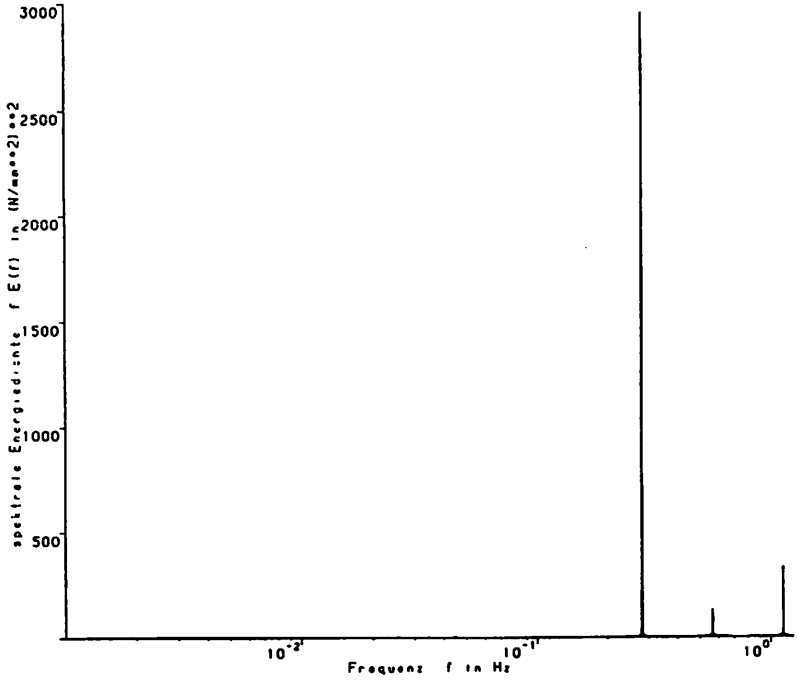

Figure 19a : Power spectrum of strain gage taken from figure 17a.

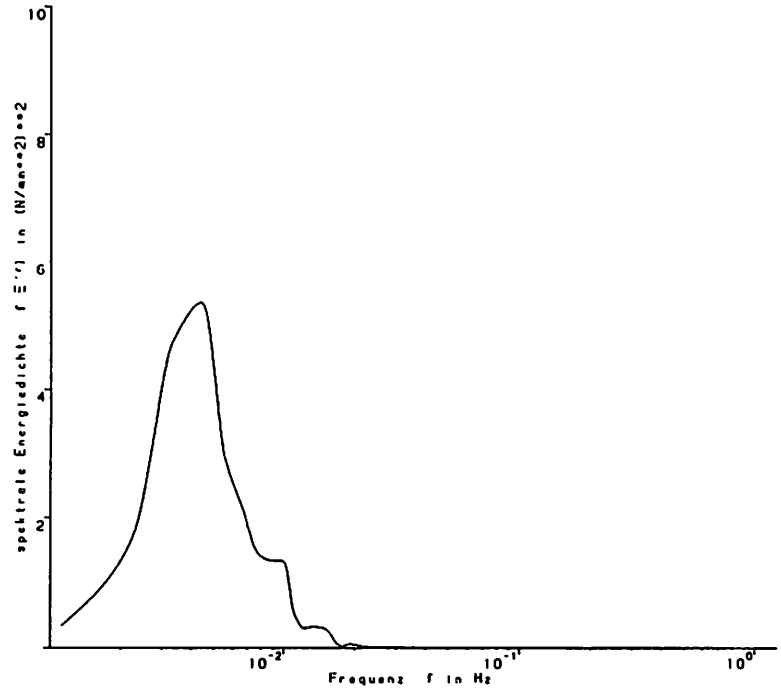

Figure 19b : Power spectrum of strain gage taken from figure 17a, but low-pass filtered.

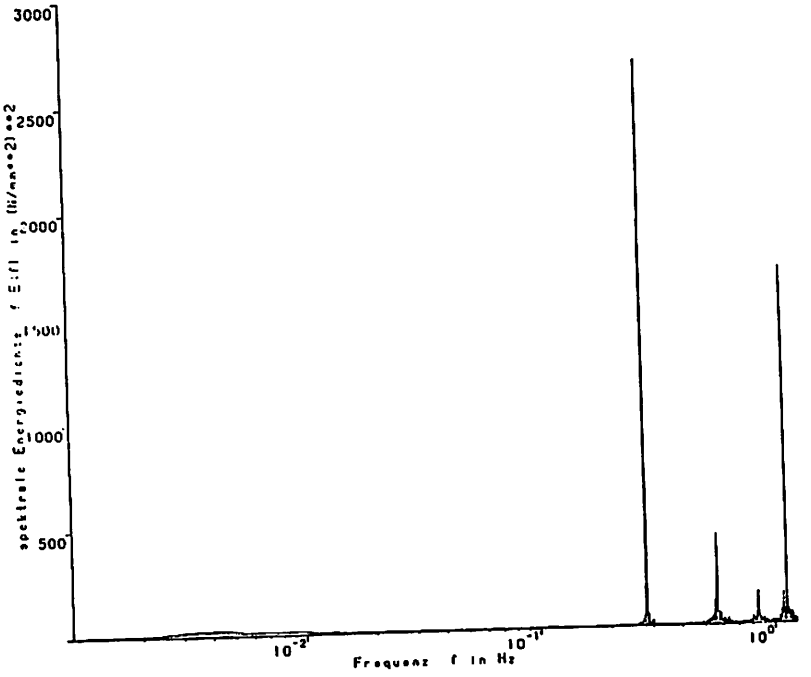

Figure 19c : Power spectrum of strain gage taken from figure 17c.

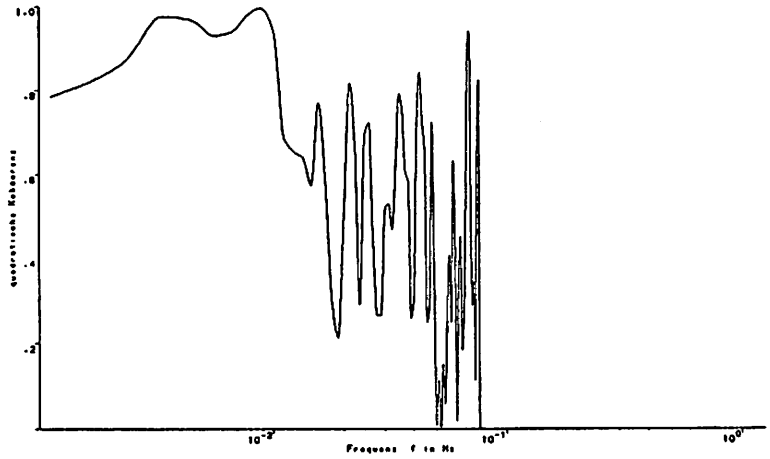

Figure 20a : Quadratic coherence between the wind speed in 100 m and the electric output.

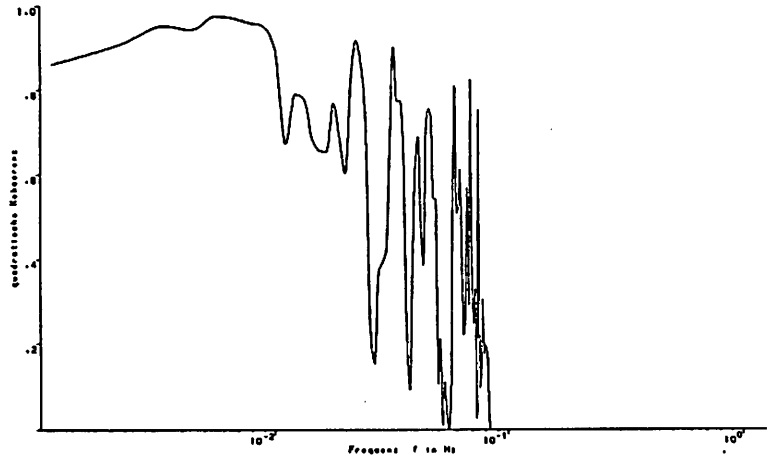

Figure 20b : as figure 20a, but for area averaged wind speed.

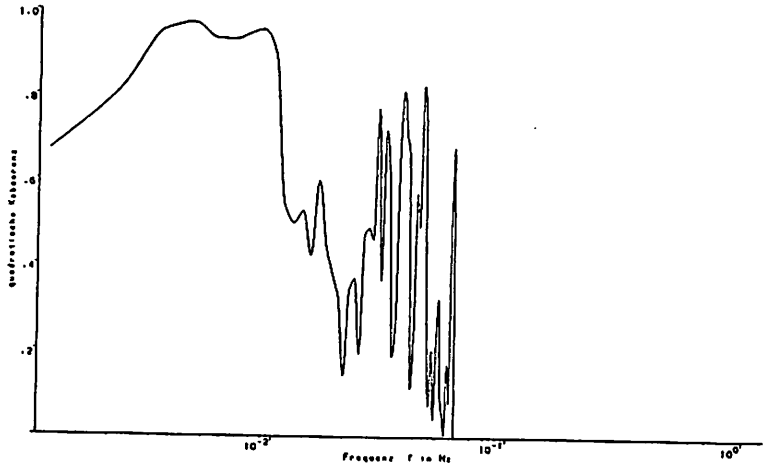

Figure 20c : as figure 20a, but for the strain gage in 27 m from the hub.

Simulation of Loads on a Wind Turbine including Turbulence

by

Stig Øye

Fluid Mechanics Department

Tech. University of Denmark

SIMULATION OF LOADS ON A WIND TURBINE INCLUDING TURBULENCE.

1.Introduction.

This paper presents some initial results from calculations of fatigue loads on the 60 m, 2 MW Tjæreborg Wind Turbine using a recently developed time-domain computer code including a simulation of turbulent wind.

2.Structural dynamics model.

The structural dynamics model "FLEX" uses a relatively limited number of degrees of freedom to describe the rigid body motions and elastic deformations of the turbine. Figure 1 shows the case of a 3 bladed turbine with a maximum of 20 DOF. No. 1 and 2 are the horizontal deflections of the tower top in two directions at right angles to each other. Both DOF can include prescribed rotations of the tower top. (tilt). DOF 3 is tower torsion / yaw drive flexibility, while no. 4 is a tilt angle DOF simulating the nacelle bedplate flexibility in the tilt direction. DOF 5 is the main shaft rotation angle at the front bearing while 6 and 7 are angular deflections of the main shaft in the bending directions simulating main shaft bending flexibility or teeter hinges. No small angle assumptions have been used for any of these 7 rotations. The blade deflections relative to the blade roots are described by a maximum of 2 flapwise and 2 chordwise modes for each blade. Normally only 1 chordwise mode is used. Each blade can be pitched at the root, however the pitch angles are not independent DOF's, but are prescribed by a simulated control system. Finally DOF 20 simulates the shaft torsion between hub and generator.

The aerodynamic loads on the blades are calculated by the traditional blade element momentum method. The mean wind field over the rotor plane includes wind shear, yaw and tower shadow. The generator torque can be modelled to simulate all kinds of characteristics including variable speed operation.

3.Turbulence model.

The turbulent part of the wind is included in the model as time series of simulated turbulence (u-component only) in a large number of points over the rotor plane, figure 2. The simulated turbulence is calculated in advance and stored on disk. During the actual simulation of the turbine response the value of the turbulent wind component at any point and time is calculated from the turbulence time series by interpolation in both space and time.

The simulated turbulence is calculated by the method of Schinozuka & Jan (fig.3). A very instructive description of the method for this particular use is given by Veers. The method is quite general and allows the user to specify the target spectral density functions for all the points and the cross spectral densities between the points. However, one should note that each set of simulated time series is only one of an infinitely large number of possible realizations. Therefore, for each wind condition, several different wind simulations should be used in order to obtain a reliable average result.

4. Results.

The results presented here have been calculated assuming a 10% turbulence intensity, the same Kaimal spectrum at all points in the rotor plane and a constant coherence function with a coherence decay of 8 (fig. 3). Simulations have been made for 6 mean wind speeds from 7 to 22 m/s, but only one turbulence simulation have been used for each. The turbulence has been simulated for the 181 points in figure 2 with a 0.1 sec resolution for 200 sec. The time to calculate each of the 6 turbulence time series is approximately 7 hours on a 16 MHz 386 PC with coprocessor.

Running the "FLEX"-code with the turbulent wind as input produces time series of simulated loads and deflections at a large number of points in the wind turbine. Time steps of 0.025 sec is used producing 200 sec of simulated turbine operation in approximately 2 hours with the same computer as above.

In order to present an example of the results in a condensed

way, the flapwise bending moment in the blade root has been rainflow counted and the equivalent 1P moment range has been calculated for each mean wind speed. The equivalent 1P moment is defined as the constant moment range which at a frequency of 1P (once per rev. of the rotor) produces the same fatigue damage as the actual moment variation assuming a given damage rate exponent m (8 is used here) and linear damage accumulation. The upper line in figure 4 shows the result including turbulence, while the lower line in the same figure are the results calculated without turbulence. The broken lines are also calculated with no turbulence but with plus/minus 10 degree of yaw. In all cases a wind shear exponent of 0.14 has been used. The results clearly show that the turbulence contributes significantly to the flapwise blade root fatigue.

Figure 5 shows a direct comparison with measured data from the Tjæreborg Wind Turbine. Results from a large number of measured time series, each 180 sec long is plotted. The measured time series correspond to a range of turbulence intensities, the major part between 5 and 10%. The agreement between measurements and calculations is very satisfactory at least for wind speeds below 15 m/s. At higher wind speeds the calculated values are rising less with increasing wind than the measured values. The reason for this will be investigated in the future looking into the sensitivity of the results to changes in turbulence length scales and coherence function.

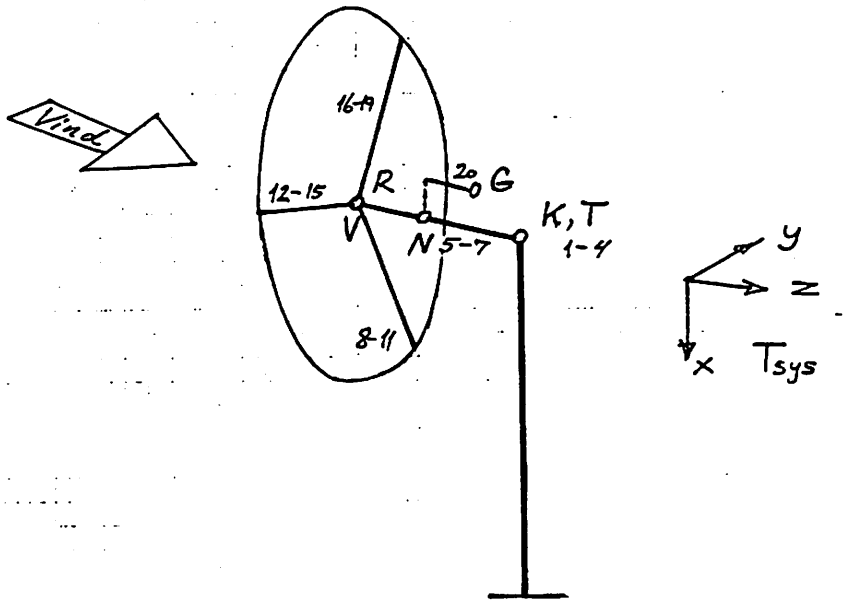

Figure 1. Basic elements of structural dynamics model "FLEX".

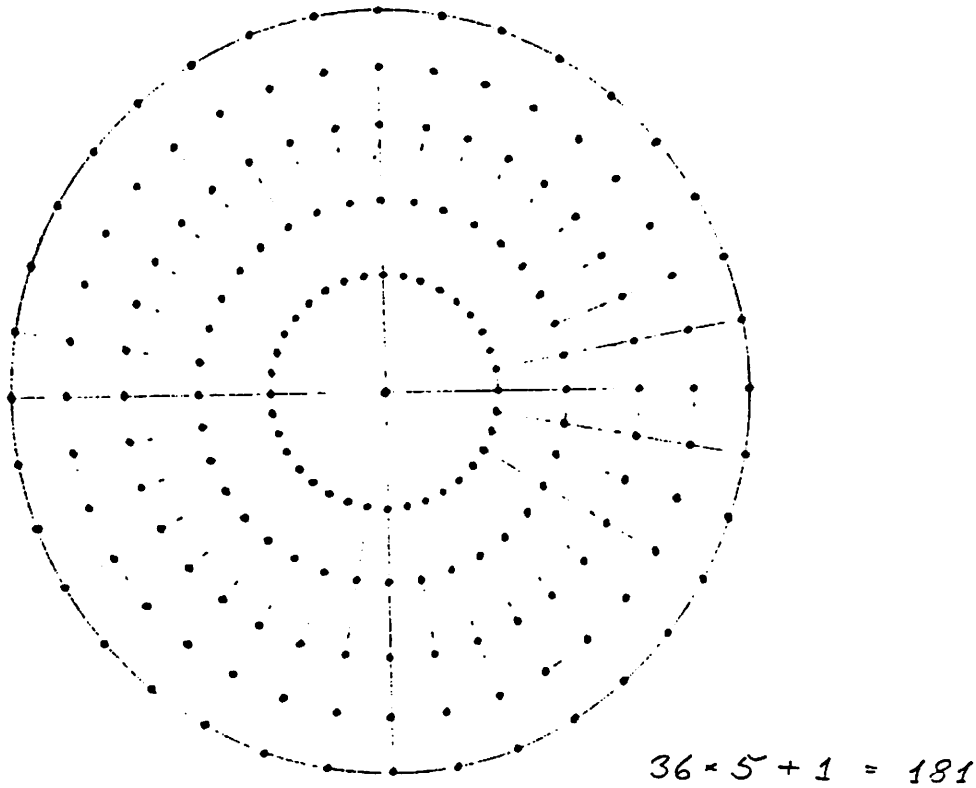

Figure 2. Rotor plane with turbulence simulation points.

Simulation of turbulence (u-comp.):

Shinozuka & Jan : Digital Simulation of Random Processes and its Applications. J. of Sound & Vibration, Vol 25, No1, 1972.

Paul S. Veers : Three-Dimensional Wind Simulation. Sandia Report, SAND88-0152, 1988.

Spectral density :

$$S(n) = \frac{\sigma^2 \cdot l/U}{(1 + 1.5\,\frac{n \cdot l}{U})^{5/3}}$$

Kaimal, $l = 600$ m.

Cross Spectral density :

$$|S_{jk}(n)| = Coh_{jk}(n, d_{jk}, U_{jk}) \cdot S(n)$$

Coherence function

$$Coh_{jk} = \exp\left(-C\,\frac{n \cdot d_{jk}}{U}\right)$$

Coherence decay

$C = 8$ Danish Code

$C = 12\left(\frac{d_{jk}}{z_m}\right)^{0,25}$ Solari

$C = 7.85\sqrt{1 + \left(\frac{U}{n \cdot l}\right)^2}$ P.H.M.

Figure 3.

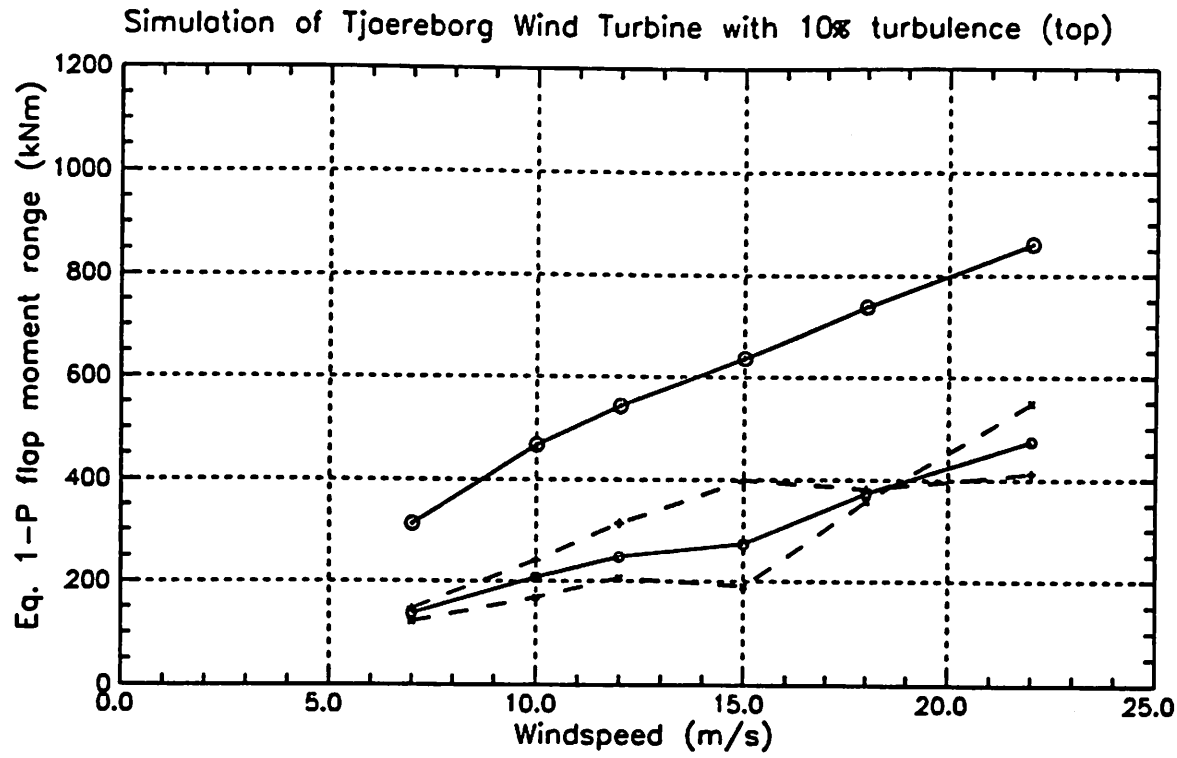

Figure 4.

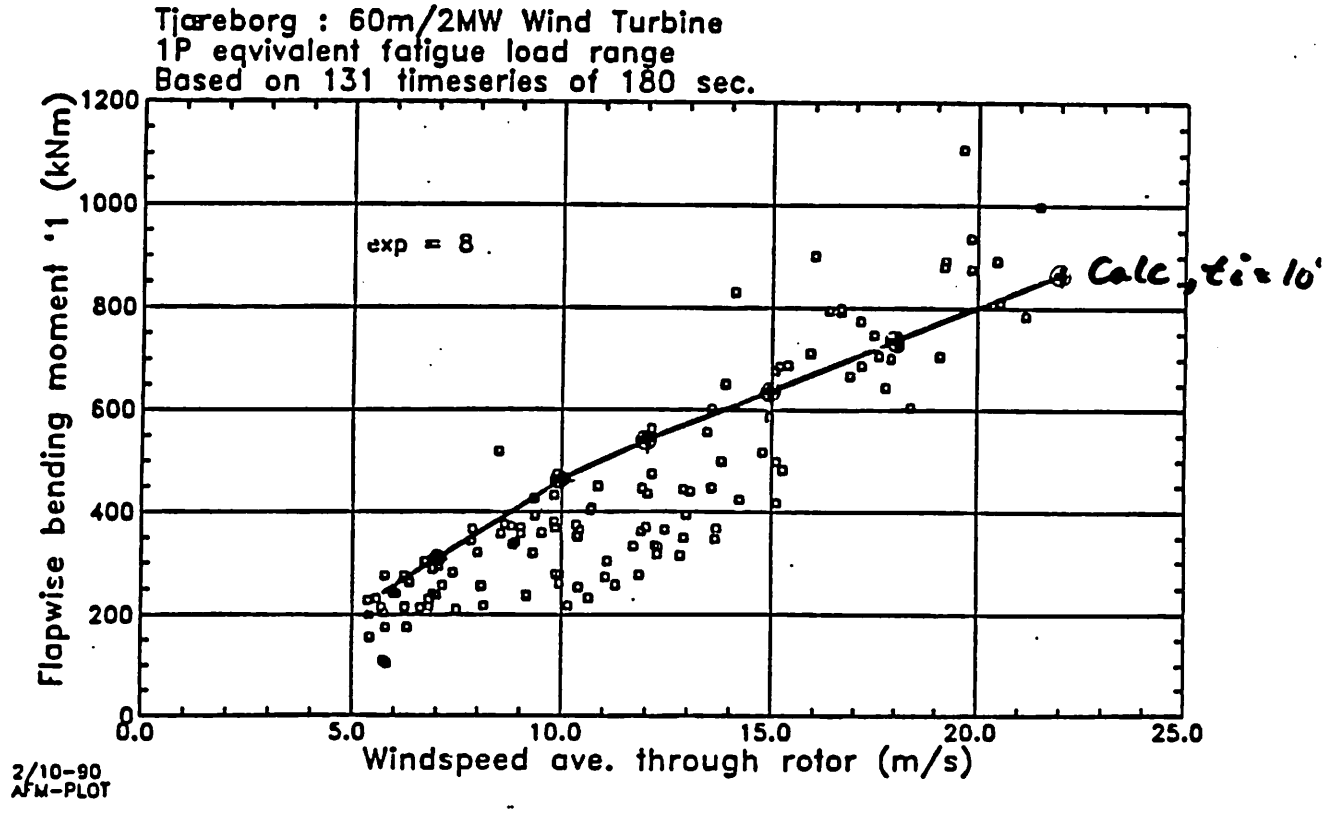

Figure 5.

Kvaerner Turbin AB
Wind Power Dept

RAPPORT / REPORT

EXPERIENCES FROM DIMENSIONING OF NÄSUDDEN II

Report on IEA-meeting

FFA Stockholm 1991-03-07/08

CONTENT

Anders Wickström

Kvaerner Turbin AB
Wind Power Dept
P O Box 1005
S-681 01 Kristinehamn, Sweden

DIMENSIONING LOADS FOR Näsudden II 3MW WIND TURBINE

BACKGROUND

KVAERNER TURBIN AB is a manufacturer of large wind turbines. We are now in the middle of the Näsudden II/Aeolus II project which means delivery, in cooperation with MBB in Germany, of two 3 MW turbines to the electricity boards VATTENFALL in Sweden and PREUSSEN ELEKTRA in Germany.

To design a wind turbine, the accuracy of the loads are very important. Additionally, the loads in the design phase have to be few, preferably only

F_i max — for static dimensioning

F_i middle, $\triangle F_i$, N — for fatigue dimensioning

$i \in$ load component 1, 2, 3, 4, 5, 6
N is corresponding number of load cycles

MBB is responsible for the load specification (and manufacturing of the blades) for the Näsudden II.

MBB's first proposal for dimensioning fatigue loads was:

During all time of operation (=2.3E+8 rotations)

* rated wind speed = 14 m/s at hub height

* constant asymmetric wind speed gradient = 0.25 m/s/m

That would cover all other possible fatigue loads and having the advantage of being easy to calculate (as specified above). That wind assumption was also approved by Germanischer Lloyd for the MBB's one bladed Monopteros machines with flapping hinge.

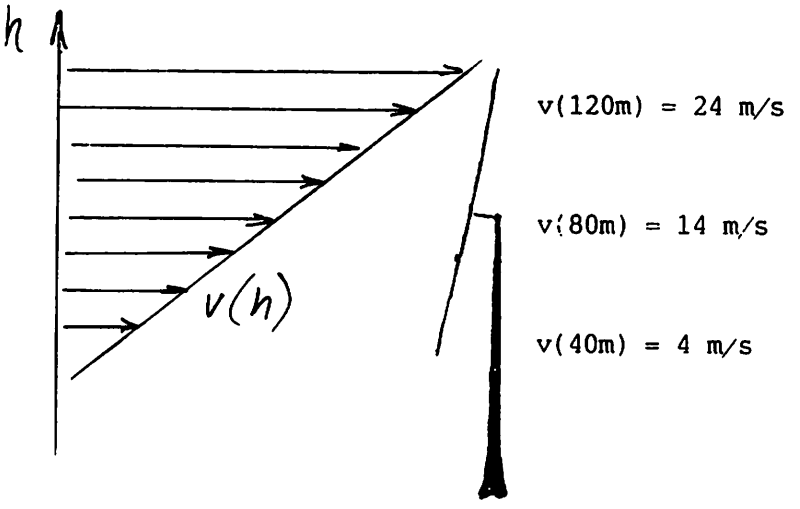

For the twobladed Näsudden machine with rigid hub, the very high wind speed gradient involved unacceptable consequenses for the design.

A comparison with measured wind gradient during 4 years at Näsudden showed gradient values around -0.02 - 0.08 m/s/m for the whole rotor. By assuming a normal distribution of the gradient, a high fictive wind shear distribution was constructed. The median gradient was increased with 4 standard deviations and also the standard deviation was increased with 50 percent. The result was a distribution as the following :

0.20 m/s/m	5E+6	rotations
0.17 m/s/m	35E+6	:
0.12 m/s/m	157E+6	:
-0.04 m/s/m	50E+6	:
-0.08 m/s/m	3E+6	:
	250E+6	

Our customer VATTENFALL wanted to have a verification that this fatigue load assumption did cover what was stated in their TECHNICAL SPECIFICATION.

WIND CHARACTERISTICS

Our customer's TECHNICAL SPECIFICATION specify a lot of different wind characteristics which are supposed to be valid at Näsudden. It states

* the distribution of wind speed
* normal wind speed gradient
* roughness lenght for different wind directions
* extreme wind speeds
* turbulense intesity
* ... (see enclosed extract of TECHNICAL SPECIFICATION)

With these statistical specifications a comparison was carried out against a gust spectrum based on a turbulence model. The theory of that work is presented in enclosed paper.

The result from that paper showed that even with some very conservative assumptions, the load variations in the rotating blade root system is too high for the fictive wind shear distribution. In the nacellefix nonrotating system, the difference is even more obvious. The flapwise bending moment is highly overestimated whereas the thrust variation is underestimated. Later, a "partial gust" was introduced to increase the thrust variation.

The purpose of enclosed work was to show that the used wind assumptions give loads on the safe side. The result showed a significant built-in safety factor.

The design of the Näsudden II unit is almost finished. Therefore KVAERNER is about to start the work to determine the loads for the next generation of large wind turbines. Hopefully, improved wind characteristics relevant for wind turbine design will be available then. Are they to be taken from statistical relationships or extrapolations of the wind measurements?

Is it possibile, from fatigue point of view, to summarize all kinds of wind into a combination of one symmetric and and one asymmetric wind speed gradient? Could the site dependent parameters be the different inclinations of the wind gradients?

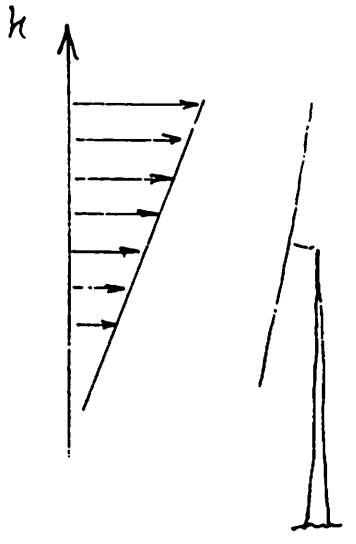

asymmetric wind gradient

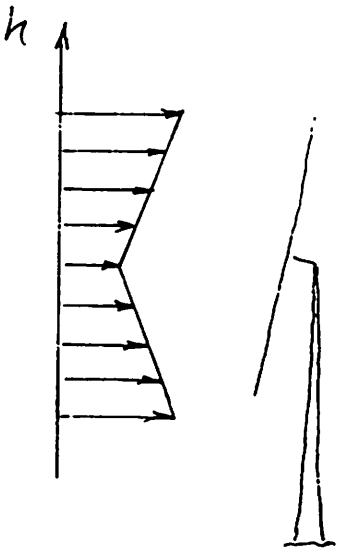

symmetric wind gradient

Extract from Technical Specification 1989-03-06

3 OPERATIONAL CONDITIONS

3.1 Wind characteristics

The WTS shall be designed for a typical site along the a northern European coastline. The site has three sectors with different roughness parameters and different wind data as specified in Table 1.

Table 1 Wind data for a typical site, based on ten minute averages, at 90 m height for each of three sectors, i, respectively.

Sector	Water	Field	Forest
Time for wind in each sector % of total time	40%	30%	30%
Distance and roughness z_0 in each sector:	0-500 m 0.05 m 500-∞ m 0.001 m	0-∞ m 0.2	0-100 m 0.2 100-∞ m 0.8
V_m 90 m	9.0 m/s	8.0 m/s	7.3 m/s
Weibull parameters:			
$A_{90\ m}$	10.6 m/s	9.6 m/s	9.0 m/s
C	2.2	2.0	1.8
$\alpha_{10\text{-}50\ m}$	0.17	0.22	0.29
$\alpha_{60\text{-}100\ m}$	0.10	0.22	0.33

$V_{m\ 90\ m}$ - the median wind speed at 90 m height - for all sectors together will be approximately 8.2 m/s.

3.1.1 Macrometeorological wind speed

(a) Median and mean wind velocity is based on a ten minute average at height h_{ref} = 90 m, in each sector, i, respectively.

(b) Median wind speed profile is expressed as

$$V_m(i,h) = V_m(i,h_{ref}) \left(\frac{h}{h_{ref}}\right)^{\alpha(i,h_{ref})}$$

giving wind velocities at a height h when the velocity at h_{ref} is known. α is the altitude parameter which in turn is a function of the surface roughness length in each sector.

(c) Wind duration

The distribution of wind velocities in each sector, i, during a year is described by the Weibull distribution function

$$f(V) = (C/A)\,(V/A)^{C-1}\,e^{(-(V/A)^C)}$$

with its corresponding duration curve

$$F(>V) = \int_V^\infty f(V)dV = e^{(-(V/A)^C)}$$

where

f(V) is the probability density function

F(>V) is the part of the total sector time when the wind velocity is higher than V

C is a shape parameter

A is a scale parameter

(d) Extreme wind speed

Estimated extreme wind velocities, at 90 m height, to be used in the load calculations, are shown in table 2.

Table 2 Extreme wind velocities for two different mean time values at 90 m height

	10 min	3 sec
V_{E1} (m/s)	58	75
V_{E2} (m/s)	40	52
V_{E3} (m/s)	V_{col}	$V_{col}*f$
V_{E4} (m/s)	25	33

where

V_{E1} is highest wind speed that can occur

V_{E2} is highest wind speed to be considered when the machine is parked in a recommended way with the worst kind of critical fault in the WTS.

V_{E3} is highest wind speed including gusts, to be considered when the WTS is producing power.

V_{E4} is highest wind speed to be considered at the appearence of a critical fault in the WTS when it is producing power or is in a starting or stopping mode.

V_{c01} is the highest wind speed at wich the machine is producing power.

f = gustfactor taken from the turbulence spectrum. (f = 1,7)

(e) Extreme wind speed - height profiles

In the height interval 10-150 m, the following expression is assumed for extreme wind velocities

$$V_E(h) = V_E(h_{ref}) \left(\frac{h}{h_{ref}}\right)^{\alpha}$$

where α is assumed to be 0.13 for 10 minute mean time value and 0.1 for 3 second mean time value. The air density is assumed to be ρ = 1,25 kg/m^3 of extreme wind speeds.

(f) Extreme changes of winddirection

A sudden change of winddirection of 65 degrees during a time of 180 seconds may occur. See also loadcase 3A.

3.1.2 Micrometeorological wind velocity

The micrometeorological wind velocities (or turbulence) shall be superimposed on the sixty minutes mean wind velocity, V. The turbulence is described in the rectangular coordinates

u = longitudinal wind velocity in the main wind velocity direction

v = lateral wind velocity positive to the right

w = vertical wind velocity positive upward

The turbulence is described by the spectral functions during neutral conditions.

$$\sigma_j^2 = \int_0^\infty S_j(n)\, dn \qquad \text{where}$$

$j \in (u, v, w)$

σ_j^2 = the variance

n = the frequency in Hz

(a) Gust spectra

(1) Longitudinal

$$\frac{n\, S_u(n)}{u_*^2} = \frac{105\, f}{(1+33\, f)^{5/3}}$$

(2) Lateral

$$\frac{n\, S_v(n)}{u_*^2} = \frac{17\, f}{(1+9.5\, f)^{5/3}}$$

(3) Vertical

$$\frac{n\, S_w(n)}{u_*^2} = \frac{2\, f}{(1+5.3\, f)^{5/3}}$$

where

$u* = \frac{0{,}4\ u(h)}{\ln(h/z_0)}$ = friction velocity

$f = \frac{n\ h}{u(h)}$ = normalized frequency

z_0 = roughness length for each sector i

u(h) = mean wind velocity at height h.

(b) Probability density function

The three component (u, v, w) of the wind are assumed to be normally distributed.

(c) Cross spectra

The square of the cross-correlation, i.e., coherence, Coh, can be approximated as:

$$Coh = e^{k \frac{n \times D}{V}}$$

where

D = vertical or lateral separation of points in space

n = frequency

V = longitudinal mean wind velocity in the layer D when D/Z < 1

k = -14 for lateral and vertical coherence of u

k = -7 for lateral and vertical coherence of v

Both the lateral and vertical Coh for the vertical component of w is small and negligable for interesting values of z.

3.1.3 Local windshear

(a) A linear windshear of $\frac{dV}{dz}$ = 0.2 (m/s/m) shall be assumed.

(b) This value will be exceeded at the most two permille of the time.

(c) A negative wind shear of $\frac{dV}{dz}$ = -0.1 (m/s/m) can occur.

Kvaerner Turbin AB
Wind Power Dept

RAPPORT/ REPORT

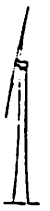

TITEL/TITLE				REG NR
FATIGUE LOADS ON NÄSUDDEN II/AEOLUS II. A COMPARISON BETWEEN GUST SPECTRUM AND WIND SHEAR SPECTRUM.				R-5401-010
PROJEKT/PROJECT				ANT SID/N O PAGES
NÄSUDDEN II/AEOLUS II				
UTFÄRDARE/ISSUED BY		AVD/DEPT	SIGN	TEL
Anders Wickström		KVB		0550-848 39
UTG/ISSUE	DATUM/DATE	KONTR/CHECKED		GODK/APPROVED
2	1989-11-03			891103

DISTRIBUTION

Svensson : SV
Blix : SV
Dahlén : SV
Habib : MBB
Mickeler : MBB
Thor : FFA
KV KVB

REVISIONS

The gust amplitude, defined as deviation from a mean wind velocity, is distributed according to a general relationship defined by Hans Bergström in ref 3 .
In prior issue it was normally distributed.
The normalizing gust frequency, N, is solved for each gust (values between 0.20 and 0.30 Hz). In prior issue, N was assumed as a constant = 0.2.

SAMMANFATTNING/SUMMARY

PLEASE TURN OVER

Kvaerner Turbin AB
Wind Power Dept
P O Box 1005
S-681 01 Kristinehamn Sweden

FATIGUE LOADS ON NASUDDEN II/AEOLUS II. A COMPARISON BETWEEN GUST SPECTRUM AND WIND SHEAR SPECTRUM

CONTENT

1 INTRODUCTION

Most parts in a WECS are dimensioned against fatigue.

With measured or statistically calculated values of turbulence, a gust distribution can be derived. From such a spectrum, loads can be calculated for each gust.

Considering a high fictive wind speed gradient, covering all gusts, normal wind shear and other load cases, can reduce the calculation effort.

To get accurate design loads for a load carrying component, it is very important to know if simplifications in wind assumptions are valid for the studied component. For Nasudden II/Aeolus II, which will be a two bladed WECS with a rigid hub, a fictive high wind speed gradient may be sufficient for dimensioning components in the rotating blade root system, giving load variations on the safe side (provided the gradient is high enough). For design of an offshore steel tower though, where the variation in thrust load is dimensioning, the high wind shear assumption will not give correct values.

In this paper a comparison of partial damage between a gust spectrum (based on statistical assumptions) and a high wind shear spectrum is shown. Load variations (amplitude and number) are calculated in both the rotating blade root system and the non rotating rotor axis system. From these data, corresponding Wohler curves are plotted and compared.

THEORY FOR GUST STATISTICS

The distribution of wind velocities during the year is described by the Weibull distribution function.

f1

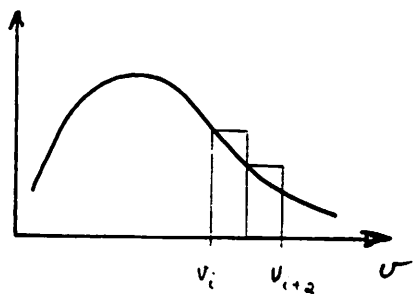

$$f_1(v) = \left(\frac{c}{A}\right)\left(\frac{v}{A}\right)^{c-1} e^{-\left(\frac{v}{A}\right)^c}$$

A and c are the Weibull parameters. At 90 meters height the values are estimated to

$A = 10.6$ m/s

$c = 2.2$ Ref 1

The probability to find a wind velocity in the range $\Delta v_i = v_{i+1} - v_i$ is estimated according to

$$F_1(\Delta v_i) = \text{maximum}\left[f_1(v_{i+1}), f_1(v_i) \right] * \Delta v$$

The turbulence is defined in ref 1. The variance of the longitudinal component is described by

$$\sigma_u^2 = \int_0^\infty S_u(n)\, dn \qquad \text{Ref 1}$$

Solving the integral gives a function

$$\sigma_u = \sigma_u(v, z_0, h)$$

A gust is defined in the figure below, having an amplitude A and a duration T.

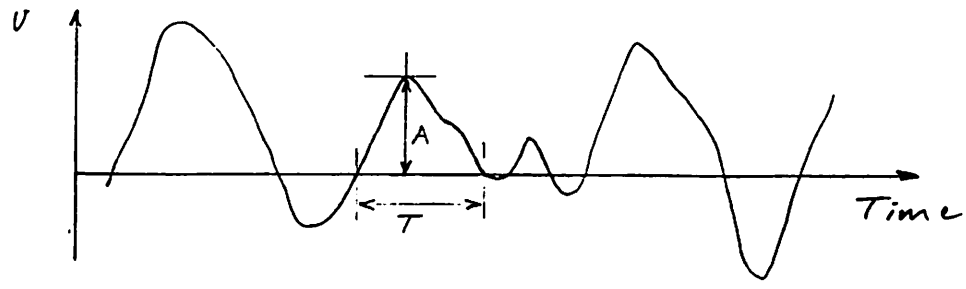

A general relationship between the amplitudes of gusts and the turbulence is shown in ref 3. The cumulative distribution function can be described by

$$F_2(A) = \text{Exp}\left[a \left(\frac{|A|}{\sigma_u}\right)^2 + b \frac{|A|}{\sigma_u} \right] \qquad \text{Ref 3}$$

$a = -0.245 \qquad b = -0.953$

The probability to find a gust amplitude in the range $\Delta A_j = A_j \pm \frac{\Delta A}{2}$ is

$$F_2(\Delta A_j) = \left| F_2\left(A_j + \frac{\Delta A}{2}\right) - F_2\left(A_j - \frac{\Delta A}{2}\right) \right|$$

The total number of gusts hitting the rotor is N_0

$$N_0 = \sum_i \sum_j F_1(\Delta v_i)\, F_2(\Delta A_j)\, \Delta T / T_j$$

ΔT = total estimated time

T_j = duration of gust with amplitude ΔA_j

The duration of the gust T_j can be calculated from

$$T_j = \frac{p}{N} \left(\frac{A_j}{\sigma_u}\right)^q \qquad \text{Ref 3}$$

$p = 0.90 \qquad q = 1.41$

N is the frequency of accurance of all gusts.
N may be estimated from

$$N = 2 \left[\frac{\int n^2 S_u(n)\, d_n}{\int S_u(n)\, d_n} \right]^{\frac{1}{2}} \qquad \text{Ref 3}$$

In ref 1 the coherence of the turbulence is defined, giving a relevant integration frequency range of 10^{-4} - 1 Hz. In appendix 5 the expression is solved and N is calculated for different wind velocities.

From these assumptions, and with knowledge of the Weibull parameters and the roughness length, a statistical gust distribution can be shown for different wind velocities and heights. This is done in a gust matrix. Part of it is written below for ΔT = 24 hours.

A similar gust matrix, based on measurements at Näsudden, is shown in appendix 1.

To \ FROM	6	7	8	9	10	11	12	13	14	15	[m/s]
6	7090	335 5	38 12	5 18	1 25	0	0	0	0	0	
7	335 5	7421	441 4	61 9	11 15	2 20	0	0	0	0	
8	38 12	441 4	7436	537 3	87 7	18 12	4 17	1 21	0	0	
9	5 18	61 9	537 3	7436	620 2	111 6	25 10	6 14	2 18	0	
10	1 25	11 15	87 7	620 2	7166	671 2	129 5	33 9	9 12	2 16	
11	0	2 20	18 12	111 6	671 2	6658	687 2	140 5	38 8	11 11	
12	0	0	4 17	25 10	129 5	687 2	5978	670 2	142 4	41 7	
13	0	0	1 21	6 14	33 9	140 5	670 2	5192	624 1	137 3	
14	0	0	0	2 18	9 12	38 8	142 4	624 1	4368	559 1	
15	0	0	0	0	2 16	11 11	41 7	137 3	559 1	3562	

[m/s]

Element outside diagonal:

1) Number of shifts
2) Meantime for a shift (τ)

Diagonal element:

1) Wind duration (τ)

h = 90 m
z_0 = 0.2 m
A_{90} = 10.6 m/s
c = 2.2

THE NUMBER OF LOAD CYCLES FROM A GUST

With knowledge of the number of gusts occuring during a time period ΔT, the number of load cycles can be derived.

DIfferent ways of calculating the number of load cycles per gust, N_L, are plausible, corresponding to alternative load situations. On next page, three different assumptions are shown.

The first case is assuming the whole rotor uniformly hit by the gust.

The second case corresponds to when half the rotor is hit. This can be the case if the WECS is located in a windfarm, or near the coastline, where a boundary layer builds up as in the figure, resulting in a very sharp turbulence gradient at hub height and almost no turbulence in the lower part.

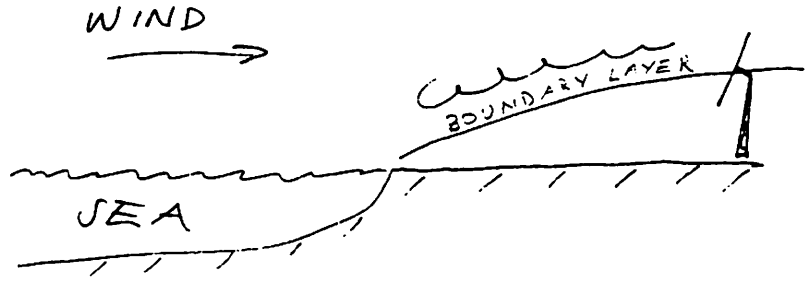

Case 2 is the most realistic. Severe calculating effort is required for that case, because each gust results in several load amplitudes.

Therefore, the load situation is modelled as in case 3. The load gradient is described by a step function, which is more conservative than case 2, and easier to calculate.

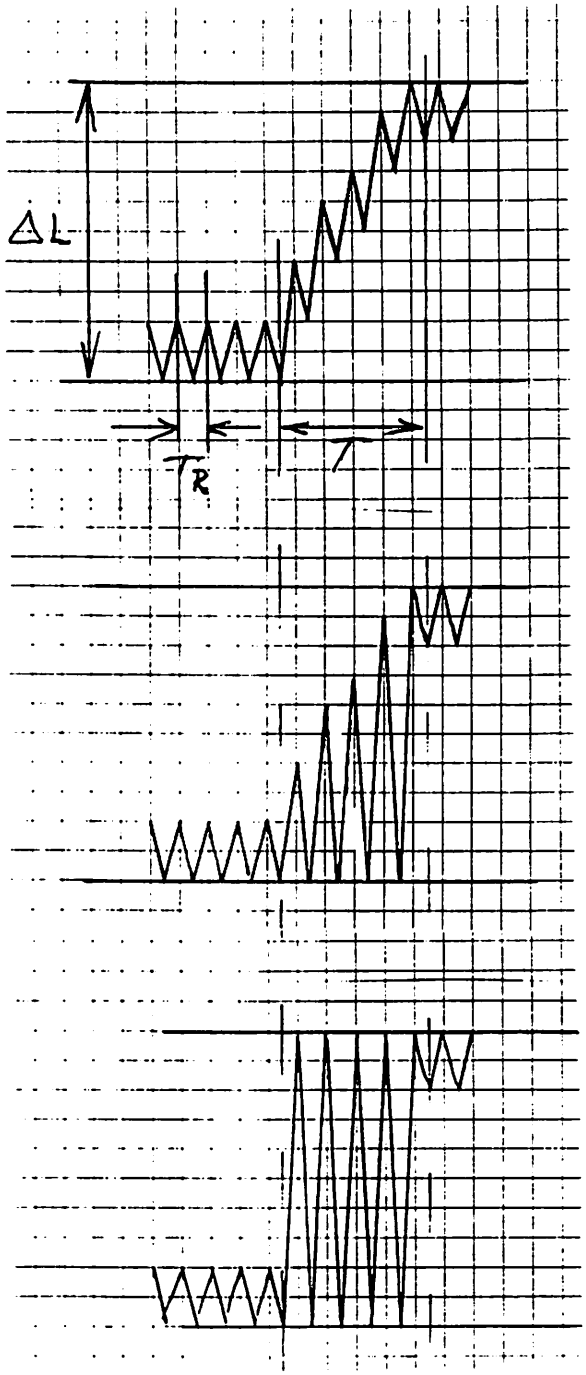

Case 1:

The gust hits the whole rotor uniformly

$N_L = 1$

Case 2:

The gust hits half the rotor only

The load gradient is constant during the gust

Case 3:

The gust hits half the rotor only

The load gradient is described by a step function

$N_L = T/T_R$; $T > T_R$

$N_L = 1$; $T \leq T_R$

T_R = Time for a rotor revolution

T = Mean time for the duration of the gust

ΔL = 2 * load amplitude

LOADS CAUSED BY A GUST

Loads are calculated by WINRO (ref 4), a program designed by FFA, based on two-dimensional blade element theory.

A vertical "normal" wind gradient = 0.04 m/s/m is considered, superimposed on the gusts. Dynamic effects are not considered.

The time constant of the control system is assumed to be infinite. That is, regardless the amplitude or duration of the gusts, the blades are not feathered to reduce the loads.

When the loads are calculated in a desired coordinate system, the gust matrix can be extended with these values. This is done with the middle and amplitude values of each load component L.

$$L_{middle} = \frac{L_{max} + L_{min}}{2}$$

$$L_{amplitude} = \frac{L_{max} - L_{min}}{2}$$

Part of a gust matrix is shown on next page, considering gusts occuring at wind speed 15 m/s in the rotating blade root system.

The resulting complete gust matrix in the rotating blade root system is shown in appendix 7 and the corresponding matrix in the non-rotating rotor axis system in appendix 8.

PART OF COMPLETE GUST MATRIX

LOADS (MIDDLE-/AMPLITUDE VALUE) FOR GUSTS

CALCULATION CONSIDER THE ROTATING BLADE ROOT SYSTEM

WIND SPEED 15.0 m/s WIND SHEAR = 0.04 m/s/m

TO	NUMBER	Fx	Fy	Fz	Mx	My	Mz
6	2.8E+02	542 78	-19 94	-114 70	-31 13	2821 1782	-439 1464
7	4.0E+03	542 78	-20 93	-120 64	-31 13	2973 1630	-461 1442
8	3.0E+04	542 78	-21 92	-126 58	-31 13	3133 1470	-489 1415
9	1.4E+05	542 78	-23 91	-133 51	-31 13	3296 1306	-522 1381
10	4.1E+05	542 78	-24 89	-139 45	-31 13	3460 1142	-561 1342
11	8.9E+05	542 78	-26 87	-146 38	-29 14	3624 979	-605 1298
12	1.4E+06	542 78	-28 85	-153 32	-29 15	3786 817	-654 1250
13	1.9E+06	542 78	-31 82	-159 25	-29 14	3946 657	-707 1196
14	3.7E+06	542 78	-33 80	-165 19	-29 14	4100 503	-762 1141
15	1.4E+07	542 78	-35 78	-171 13	-31 13	4243 360	-815 1088
16	3.1E+06	542 78	-38 81	-176 18	-42 24	4374 491	-879 1152
17	1.1E+06	542 78	-40 83	-180 22	-55		
18	7.6E+05	542					

In the rotating blade root system, a drop of wind from 15 m/s to 11 m/s will give 8.9E + 5 load cycles.

$$8.9E + 5 = N_0 * T/T_R$$

N_0 = number of drops = 1.9E + 5

T = mean gust duration = 14 s

T_R = time for a rotor revolution = 2.9 s

Each load cycle gives for example

$F_{z_{middle}}$ = -146 kN

$F_{z_{amplitude}}$ = $\pm$ 38 kN

$M_{y_{middle}}$ = 3624 kNm

$M_{y_{amplitude}}$ = $\pm$979 kNm

LOADS CAUSED BY HIGH WIND SHEAR

To bring down the extensive dimensioning work, calculating a gust matrix gives a lot of different load cases. One can assume a fictive high wind speed gradient, giving the rotor blade big load variations, depending on rotor position. The number of load cycles are one every rotor revolution in the rotating blade root system, two every rotor revolution in the non-rotating system.

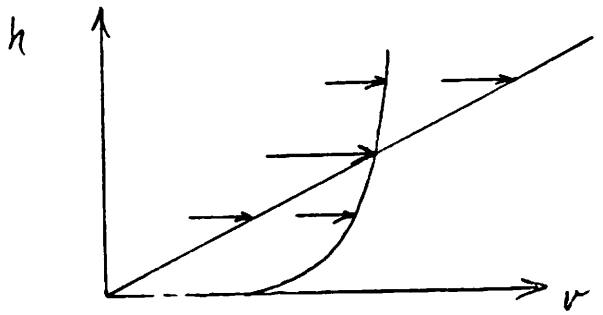

A wind shear spectrum has been evaluated by Kvaerner Turbin for dimensioning purposes (ref 6). From actual wind shear measured at Näsudden during four years (1980-84), a normal distribution has been assumed. By increasing the mean wind shear with 4 standard deviations and also increasing the standard deviation with 50 percent, a wind shear spectrum has been classified:

wind shear gradient =	0.20 m/s/m	2 percent of time
=	0.17 "	14 "
=	0.12 "	63 "
=	-0.04 "	20 "
=	-0.08 "	1 "

The loads from this spectrum is shown in appendix 4.

THEORY FOR COMPARISON OF LIFE BETWEEN DIFFERENT WIND ASSUMPTIONS. DEFINITION OF Q-FACTOR

Most load carrying parts in a WECS are dimensioned against fatigue.

By using the Palmgren's cumulative damage rule, the life can be predicted.

$$D = \sum_{i=1}^{j} \frac{n_i}{N_i}$$

n_i = Actual number of ΔL_i-load cycles

N_i = Number of ΔL_i-load cycles to reach life

$D < 1$; Life is not reached. The safety margin $S = 1/D$.

$D = 1$; Life is reached. No safety margin.

N_i is calculated from the Wöhler curve definition

$$\Delta L_i = c * f(N_i)$$

The function f is defined differently by Germanischer Lloyd (GL) and BSK, Eurocode 3 (see Appendix 2). For dimensioning the most conservative f-function will be used. In this comparison the definition made by GL is used.

To compare different load assumptions regarding their effects on fatigue, the c-value is a useful parameter.

As the c-factor is directly proportional to the load variations ΔL_i, the relation between the c-factors for different wind assumptions gives information of severeness regarding fatigue. For that purpose a Q-factor is defined:

$$Q = \frac{\text{c-factor for Wöhler curve 1}}{\text{c-factor for Wöhler curve 2}}$$

To get equal life for the two load assumptions, all loads in assumption 2 shall be multiplied with Q. Or, the factor Q can be used to calculate the safety margin if the Wöhler curve for load assumption 1 is valid.

$$\Delta L_i = c\,(1_w)\, f(N_i) = c\,(1_w)\, A \left(\frac{\alpha}{N_i}\right)^{\frac{1}{\beta}}$$

$$\Delta L_i * Q = c\,(2_w)\, A \left(\frac{\alpha}{N_i}\right)^{\frac{1}{\beta}} = c\,(1_w)\, A \left(\frac{\alpha}{SN_i}\right)^{\frac{1}{\beta}}$$

Dividing the two equations gives $S = \left(\frac{1}{Q}\right)^{\beta}$

Example

In the loglog diagram below, the loads for two assumptions are plotted.

1) Statistic gust spectrum
2) Wind shear spectrum

In the same diagram the corresponding Wöhler curves giving D = 1 are shown.

1_w) Wöhler curve (Germanischer Lloyd) gust spectrum
2_w) Wöhler curve (Germanischer Lloyd) wind shear spectrum

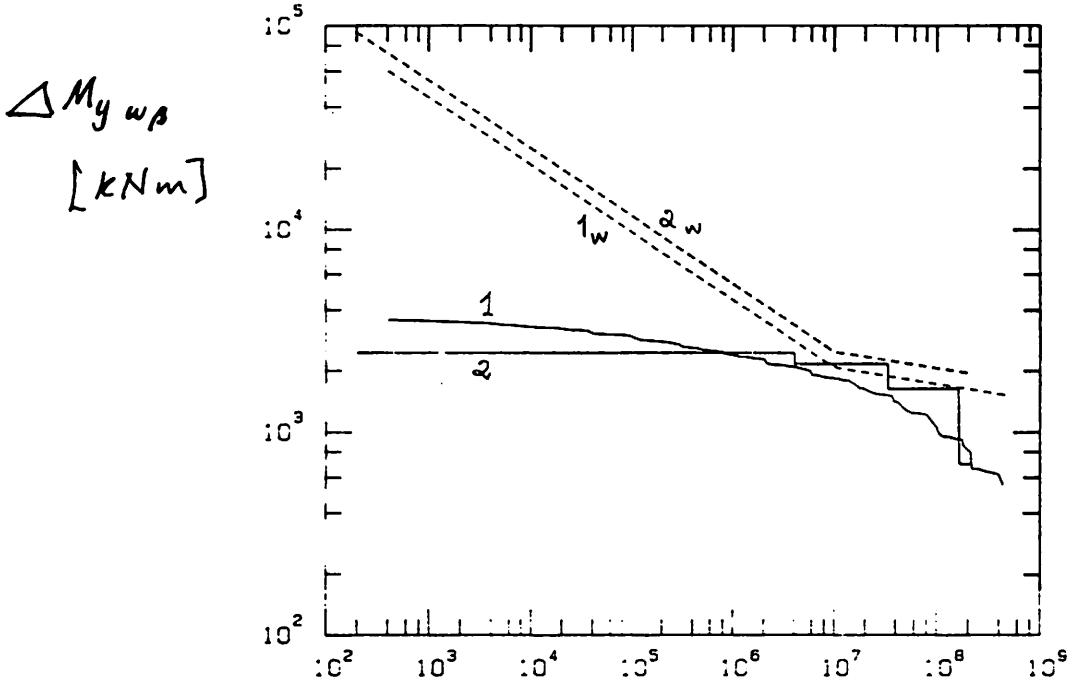

The c-factor for 1_w-curve

$$c\ (1_w) = 3542$$

and the c-factor for 2_w-curve

$$c\ (2_w) = 4289$$

The quotient of the two c-factors gives a factor Q

$$Q = \frac{c\ (1_w)}{c\ (2_w)} = 0.83$$

In the example, Q = 0.83, β = 12

S = .9

In appendix 5, the Wöhler curves are plotted for load components in both the rotating blade root system and for the non-rotating rotor axis system.

9 REFERECES

1 : TECHNICAL SPECIFICATION
1989-03-06

2 : GUSTS. A STATISTICAL ANALYSIS

by Hans Bergstrom
Dept. of meteology, Uppsala Univerity

Prepared for IEA-LS-WECS 14 th meeting in
Stockholm 4-5 dec 1985

3 : A STUDY OF ATMOSPHERIC BOUNDARY LAYER WIND STRUCTURE

by Hans Bergstrom
Dept. of meteology, Uppsala Univerity

Doctoral dissertation 1988-04-19

4 : WINRO Computional program for load and performance calculations

by The Aeronautical Research Institute of Sweden
Described in Technical Note AU-1499

5 : BESTAMMELSER FOR STAL KONSTRUKTIONER (BSK)
(translated to REGULATIONS FOR STEEL CONSTRUCTIONS)
Swedish edition

by STATENS PLANVERK 1987

6 : Evaluation of preliminary load spectrum
"Wind shear spectrum 890213" Nr R-5401-001

by Kvaerner Turbin

7 : Eurocode 3
Entwurf sept. 85 from MBB 890116

8 : Wohler curves defined by Germanischer Lloyd
Message from MBB 890901

Calculation of total loadspectrum and component dimensions of Wecs based on wind matrix and simulation.

presented at IEA R&D Wecs Annex XI Meeting at FFA 7-8 of march 1991, by Hans Ganander, Teknikgruppen AB, Box 21, S-19121 Sollentuna, Sweden

Designing wind turbines is very extensive. It comprises static as well as fatigue design. The static part depends on extreme conditions due to wind conditions and turbine situations. Fatigue loads may be divided in high cycle and low cycle fatigue. Load variations due to turbine rotation, space distribution of wind and dynamic respons of turbine structure contribute to high cycle fatigue loads. Low cycle loads are dominated by mean wind speed variations. Wakes, yawing and start/stopp situations also contribute to these fatigue loads. A total load spectrum applicable for design has to consider all these parts.

The aim of the presented method is to take this whole load spectrum into account. Main parts of the method are the Rain Flow Count (RFC) wind matrix [1] containing wind data and a time simulation program (VIDYN) capable of calculating loads at different parts of the turbine system. Key point of the method are shown in fig 1.

The method is from the beginning based on time and space behaviour of wind and from frequency point of view, what is essential for fatigue cycles and damage. This background is shown i fig 2.

The wind matrix is based on long term wind measurements and contains at every mean wind speed statistical information of wind structures covering the turbine area. It also describes variations of mean wind speed, how often and how fast these variations occur. For the purpose of fatigue design these variations are also evaluated according the RFC-method. See fig 3-5.

Loads of different parts of the turbine system are calculated by the simulation program. The calculations are arranged in a special way, see fig 6-8. Mean wind speed is increased step-wise and at each mean wind speed different conditions are introduced, e.g. different space distribution of wind over the turbine area. Results from this only calculation are the relation of loads, levels as well as variations, due to all normal wind conditions. Loads at special turbine situations as e.g. start/stopp, yawing and wakas are calculated seperately.

Load spectrum in the "RFC sense" is then easily created by using frequencies of wind situations in the RFC wind matrix in combination with calculated loads at these wind situations, see fig 9-12. Thus this load spectrum is based on spacial wind conditions at different mean wind speed as well as changes of the mean wind speed itself. Variabel speed of turbine rotation and influence of power control may also be treated directly in this way.

Load spectra are calculated for representative quantities of main parts of the turbine, e.g. blade, hub, nacelle and tower, fig 13. Introduction of material properties, as allowed static and fatigue stresses makes, it possible to calculate what dimensions are required to fullfill these stress requirements, see fig 14-15. In case of a total load spectrum the method takes static as well as fatigue demands in to account and even tells the designer what design drivers there are.

The whole system is presented in fig 16.

Reference:

[1] :Fatigue Design by using a modified RFC description of the wind. Hans Ganander and Hjalmar Johansson, AWEA, Honolulu, Hawaii 1988.

Calculation of total loadspectrum and component dimensions of Wecs based on wind matrix and simulation.

- **wind matrix**
- **simulation => loads and variations as function of situation**
- **loadspectrum at points of interest by combining wind matrix and loads**
- **dimensions of components regarding static as well as fatigue requirements**

Why this method?

- **basics**
- **used in fatigue evaluation**
- **levels of loads and variations due changes of levels as well**
- **no restrictions on aerodynamics, structural dynamics, power control, variable speed, etc conserning linearities**
- **answer questions the designer asks**
- **time and space describtion of wind**
- **total load spectrum**

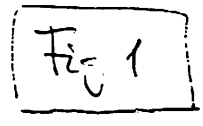

Basic about wind, dynamics and fatigue

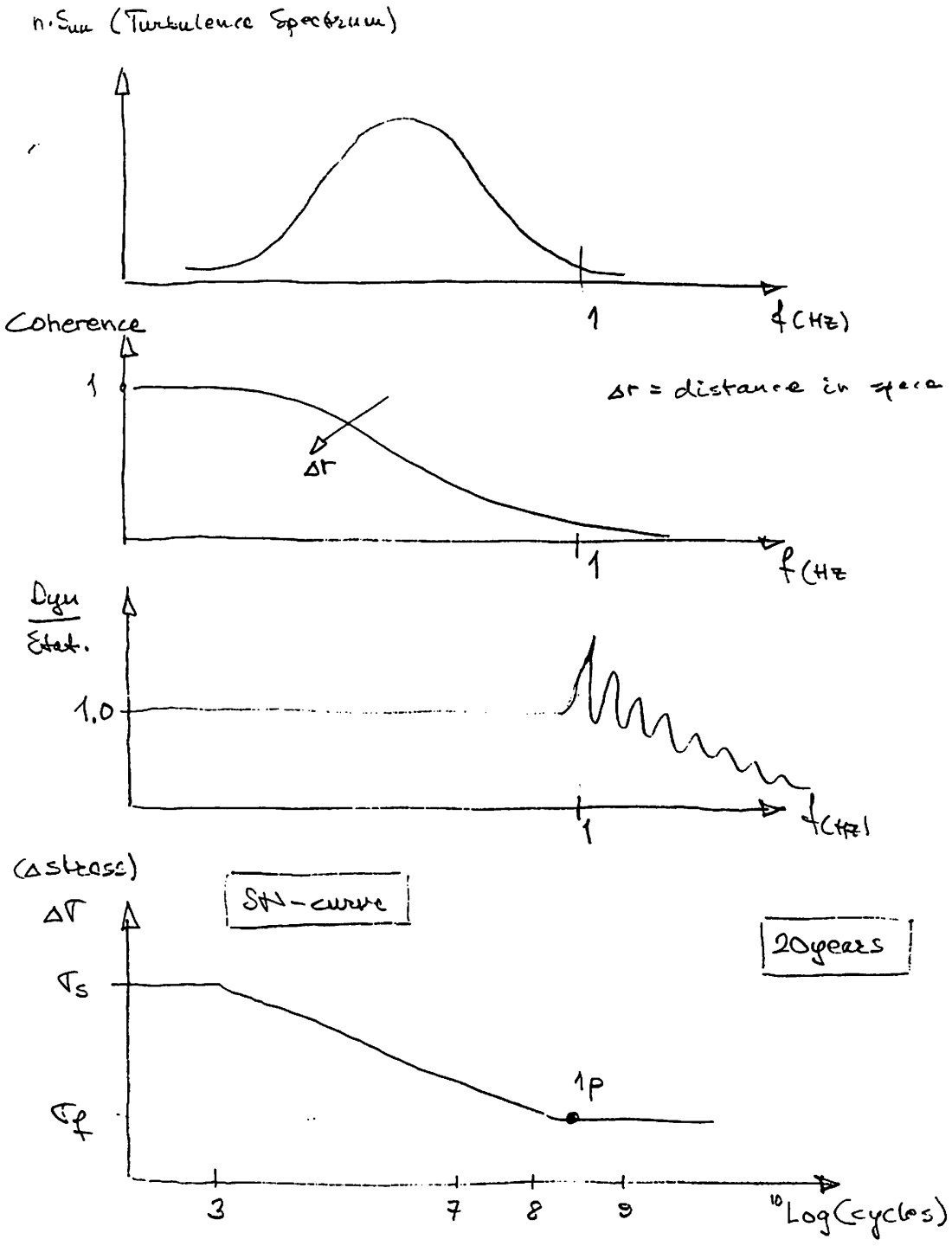

Static | Wind speed variations + 1°/₀₀ cases + + starts/stops +... | Wind speed space distribution

Fig 2

Representative wind speed signal

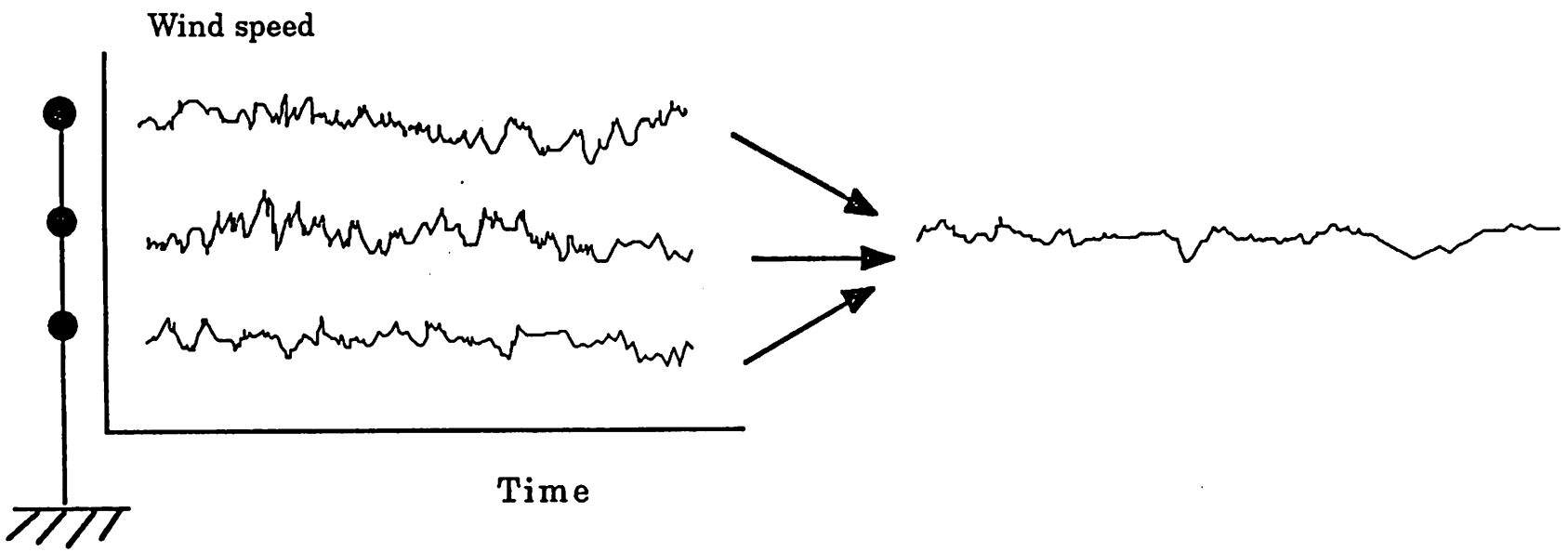

Fig 3

Peak Valley -> RFC wind matrix

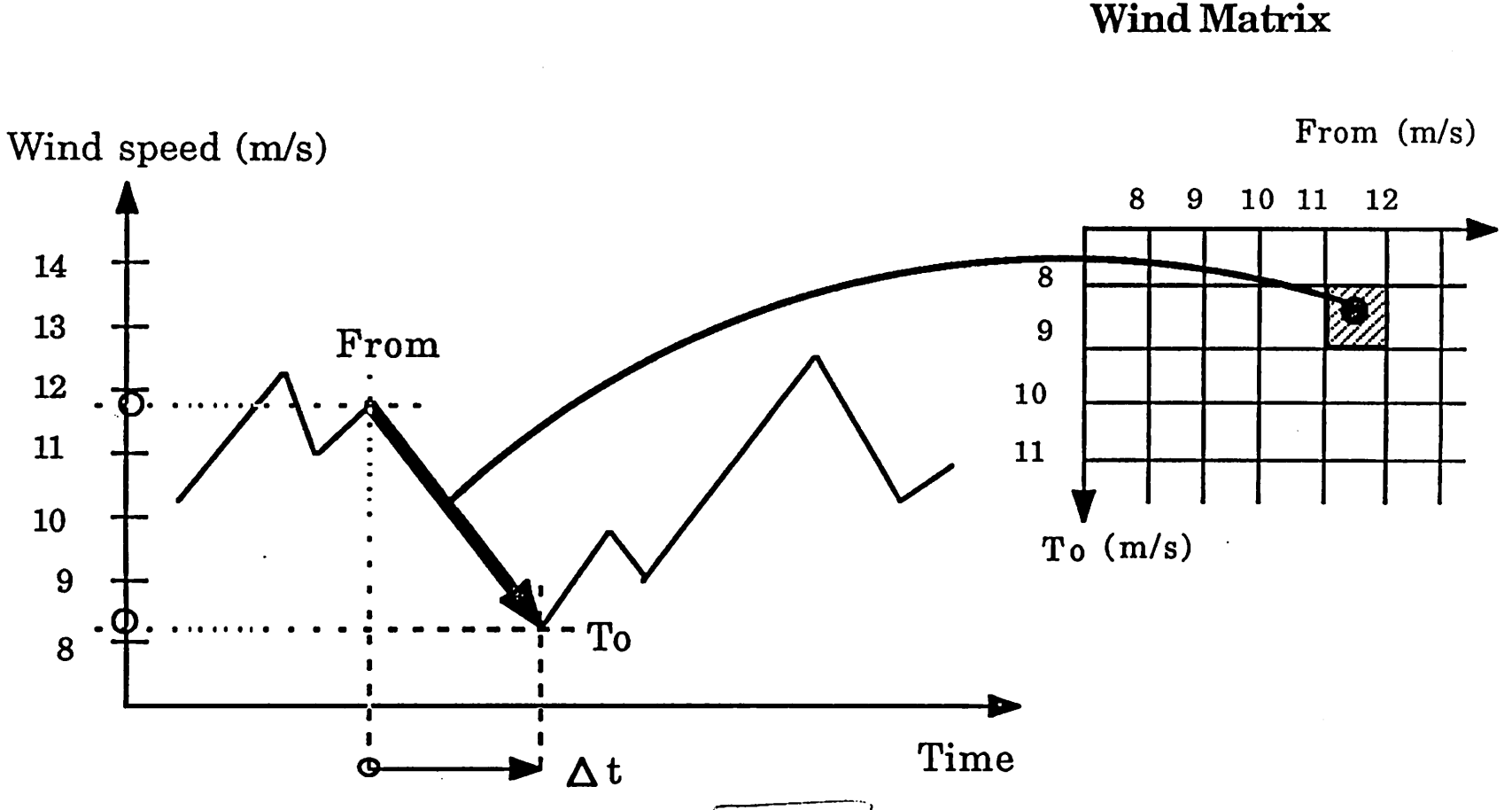

Fig 4

Example of a Wind Matrix

NASUDDEN 821006, H=77 m, dT=1s. Anemometers at 135, 77 and 11 m.
Total reg. time 52464 sec = 14.57 h. Sym. and asym. gradient related to H=77 m.

Elements outside diagonal:

Peak-Valley:
- Number of shifts
- Mean time per shift
- Min. time per shift

RFC:
- Number of half cycles
- Mean time per half cycle
- Min. time per half cycle

Diagonal elements:

- Wind speed duration
- Mean of asym. gradient
- Std.dev. of asym. gradient
- -
- Mean of sym. gradient
- Std. dev. of sym gradient

$\left[\frac{\Delta V}{\Delta z}\right] = (\text{m/s})/\text{cc}$

To (m/s) \ From (m/s)	6	7	8	9	10	11	12	13
7	0	3	0	0	0	1	1	0
7	0	51	0	0	0	30	41	0
7	0	10	0	0	0	30	41	0
7	0	-	0	0	0	0	0	0
7	0	38	0	0	0	0	0	0
7	0	13	0	0	0	0	0	0
8	0	0	384	8	62	62	15	1
8	0	0	43	6	11	18	22	31
8	0	0	10	2	1	2	2	31
8	0	0	-	0	0	2	12	2
8	0	0	12	0	0	9	96	114
8	0	0	12	0	0	9	33	114
9	0	0	8	4506	179	308	133	29
9	0	0	5	42	6	9	13	18
9	0	0	2	11	1	1	1	6
9	0	0	16	-	116	200	66	50
9	0	0	5	2	7	17	55	85
9	0	0	2	12	1	2	7	6
10	0	1	61	179	11125	263	392	187
10	0	2	8	7	41	5	9	13
10	0	2	1	1	12	1	1	1
10	0	0	54	312	-	316	246	144
10	0	0	16	6	-5	5	10	28
10	0	0	1	1	13	1	1	2
11	0	1	61	312	260	13736	305	368
11	0	13	13	9	5	41	5	8
11	0	13	3	1	1	13	1	1
11	0	0	108	316	326	-	394	307
11	0	0	54	11	4	-12	5	5
11	0	0	3	1	1	14	1	1

Fig 5

Loads calculated for increasing wind speed with two superimposed windshears.

Wind speed (m/s)

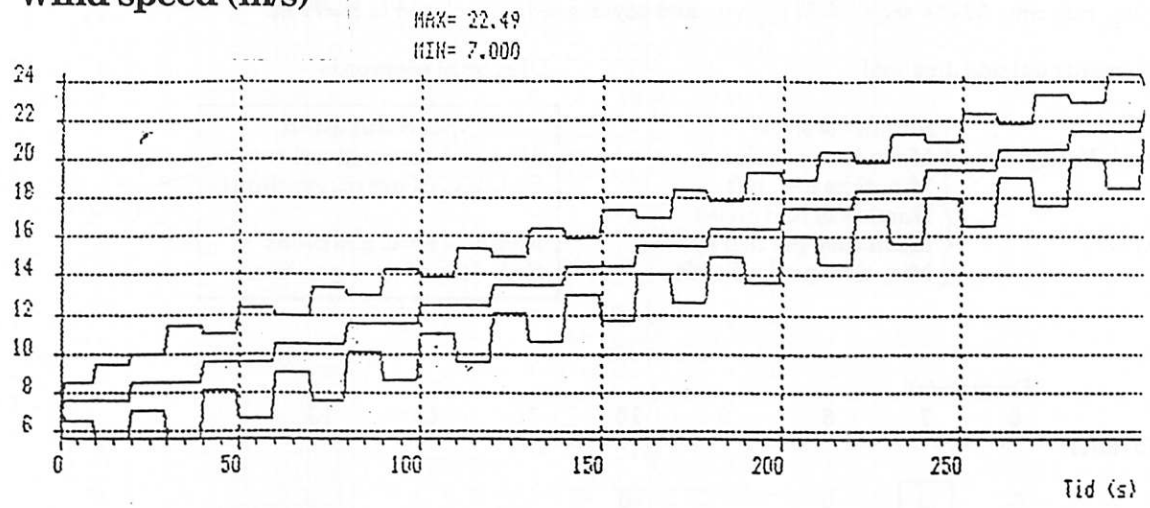

Thrustload (N)

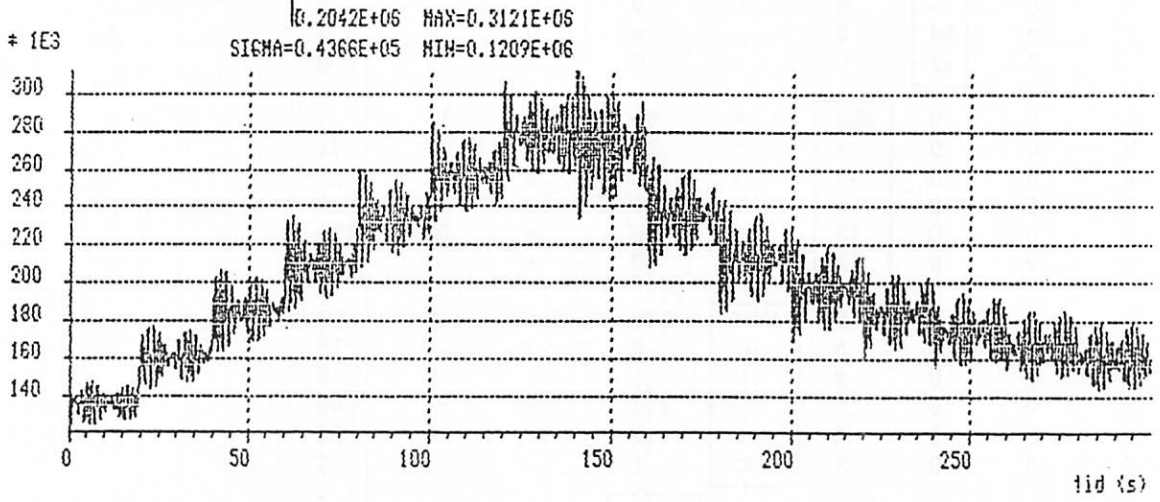

Yaw moment (Nm)

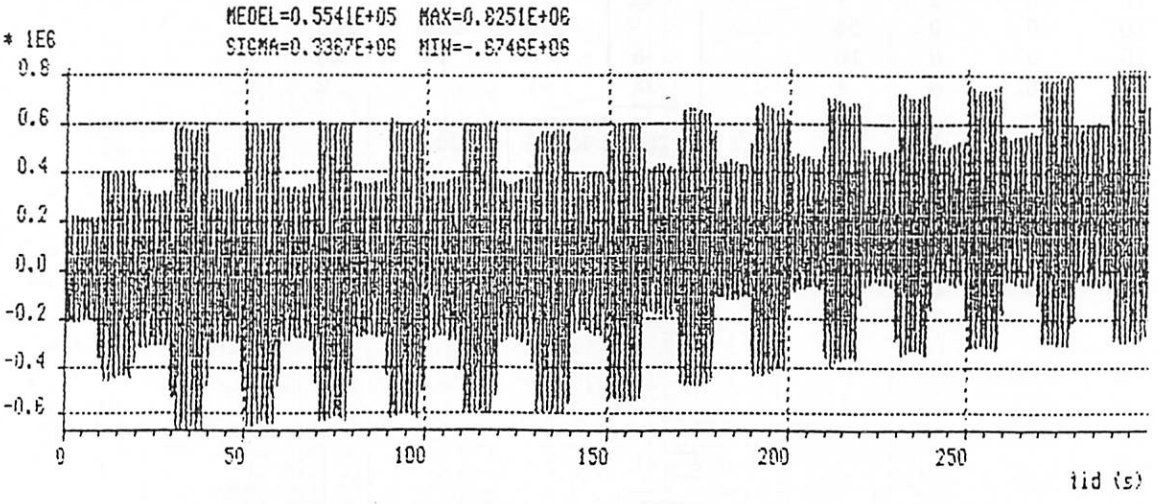

Fig 6

Loads calculated for increasing wind speed with two superimposed windshears.

Vindhast (m/s)

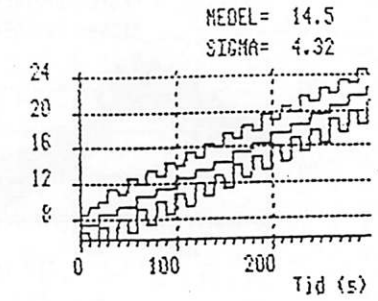

Girmoment (Nm)

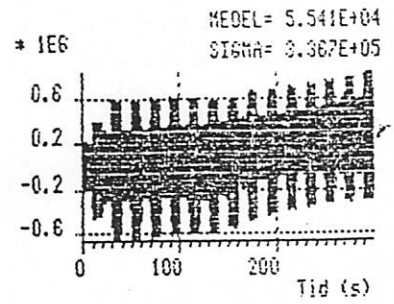

Dämpmoment (Nm)

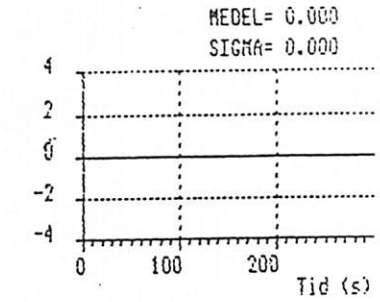

Effekt (kW)

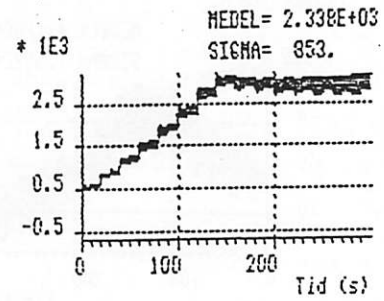

Gir-, vindrikt (gr)

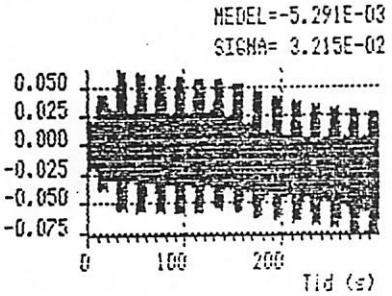

Axialkraft torn (N)

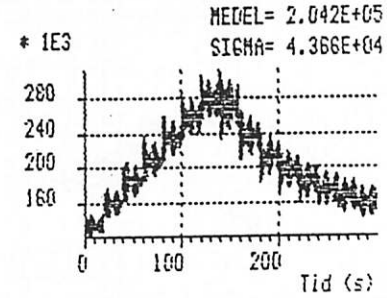

Vridmoment (Nm)

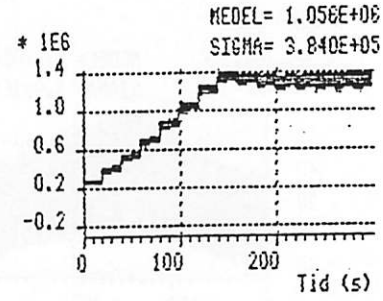

Gungvinkel (grad)

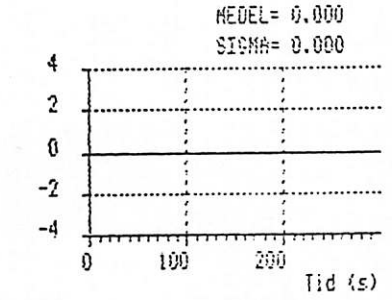

Tornutbojning Xt (m)

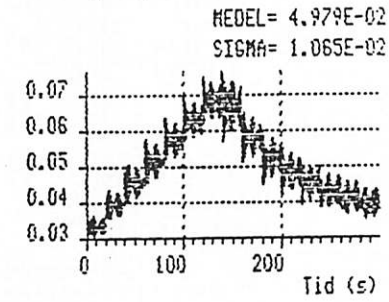

Turbin (rpm)

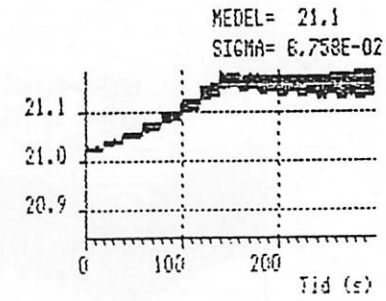

Generator (rpm)

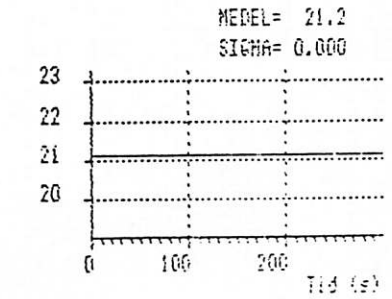

Tornutbojning Yt (m)

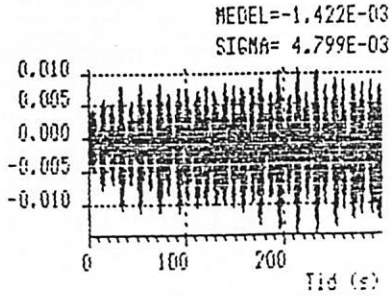

Pitch (grad)

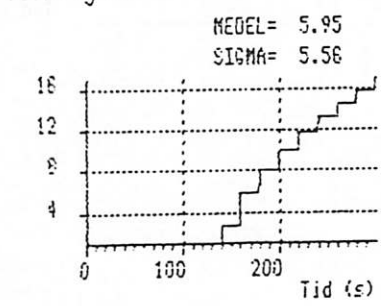

Pitchmoment (Nm)

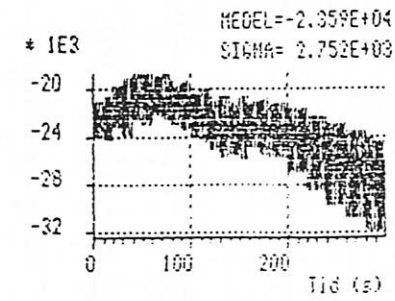

Rotorcentrum vert(m)

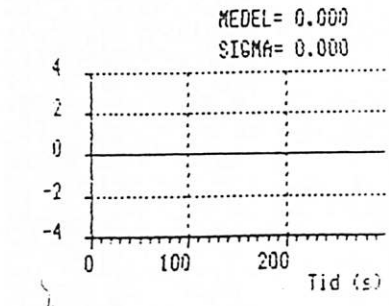

Fig 7

Loads calculated for increasing wind speed with two superimposed windshears.

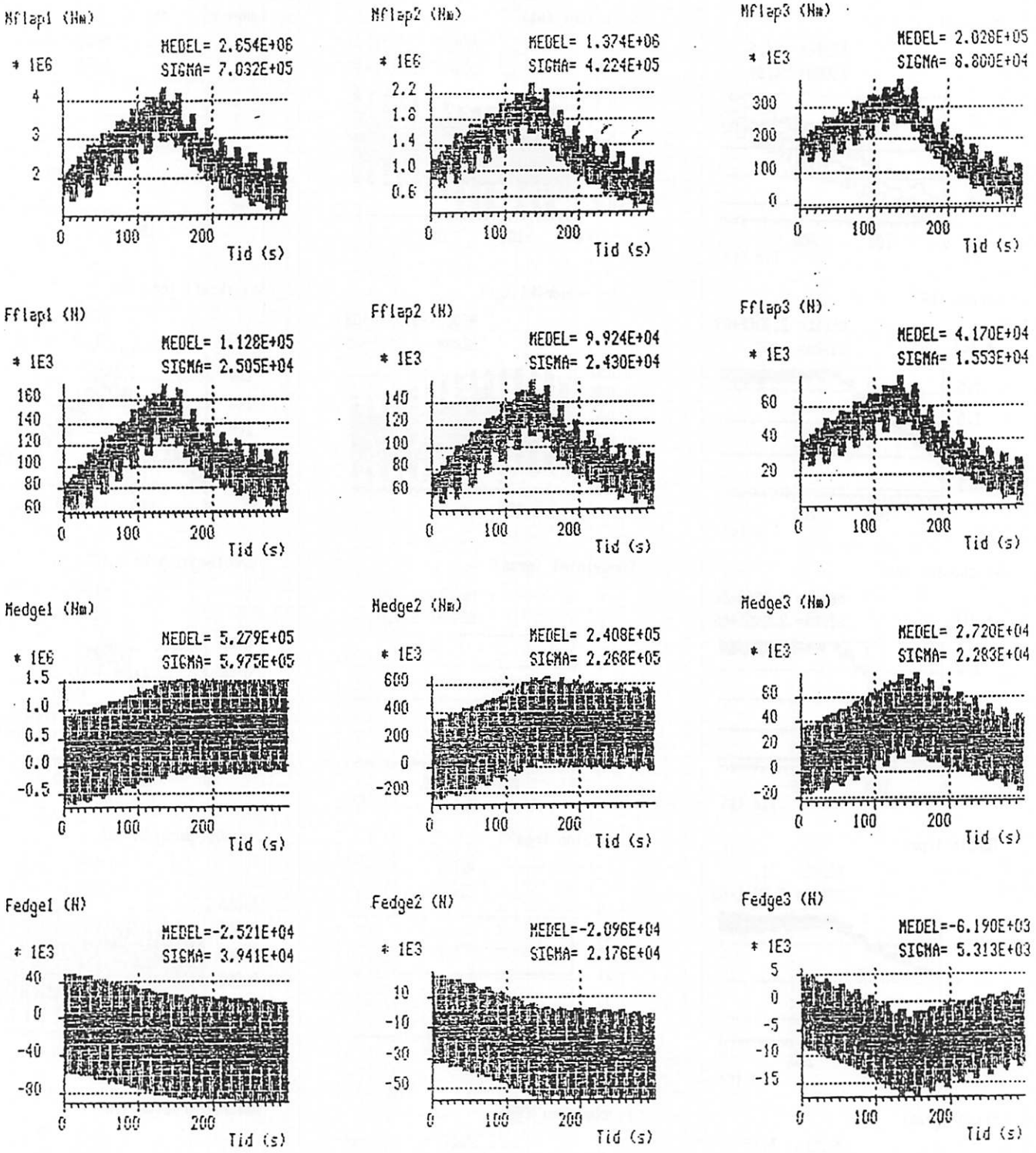

Fig 8

Load spectrum calculation

Load calculation

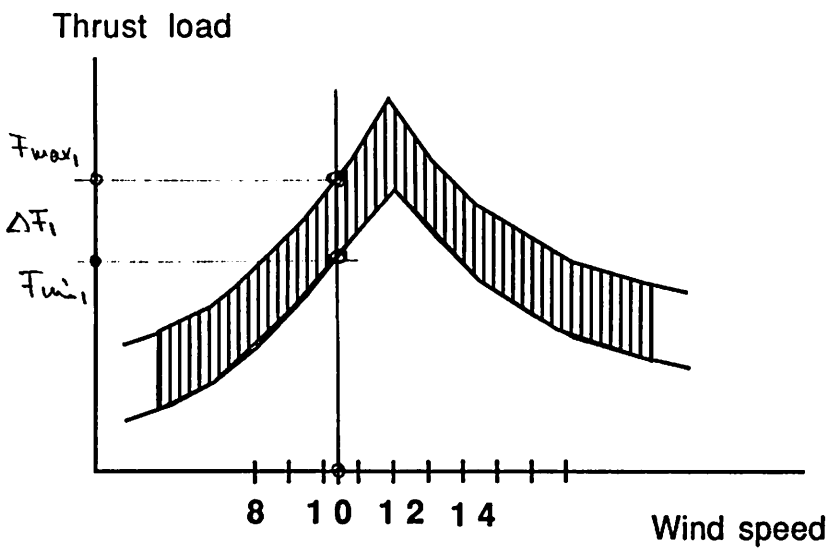

Wind matrix

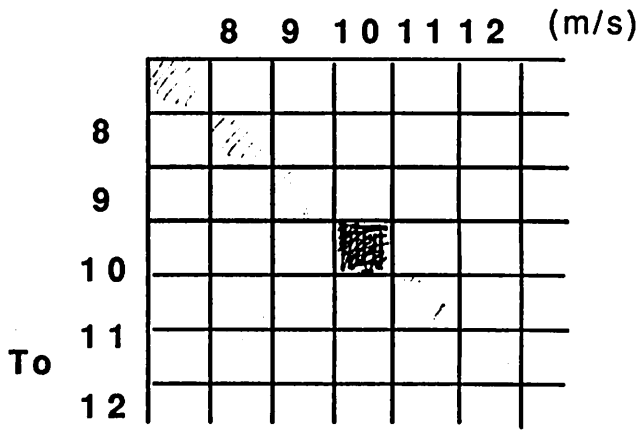

Number of cycles (n_i): operating time * rotational speed.

F_{max_i}
F_{min_i}
ΔF_i
n_i

Fig 9

Distribution of asymmetric gradient

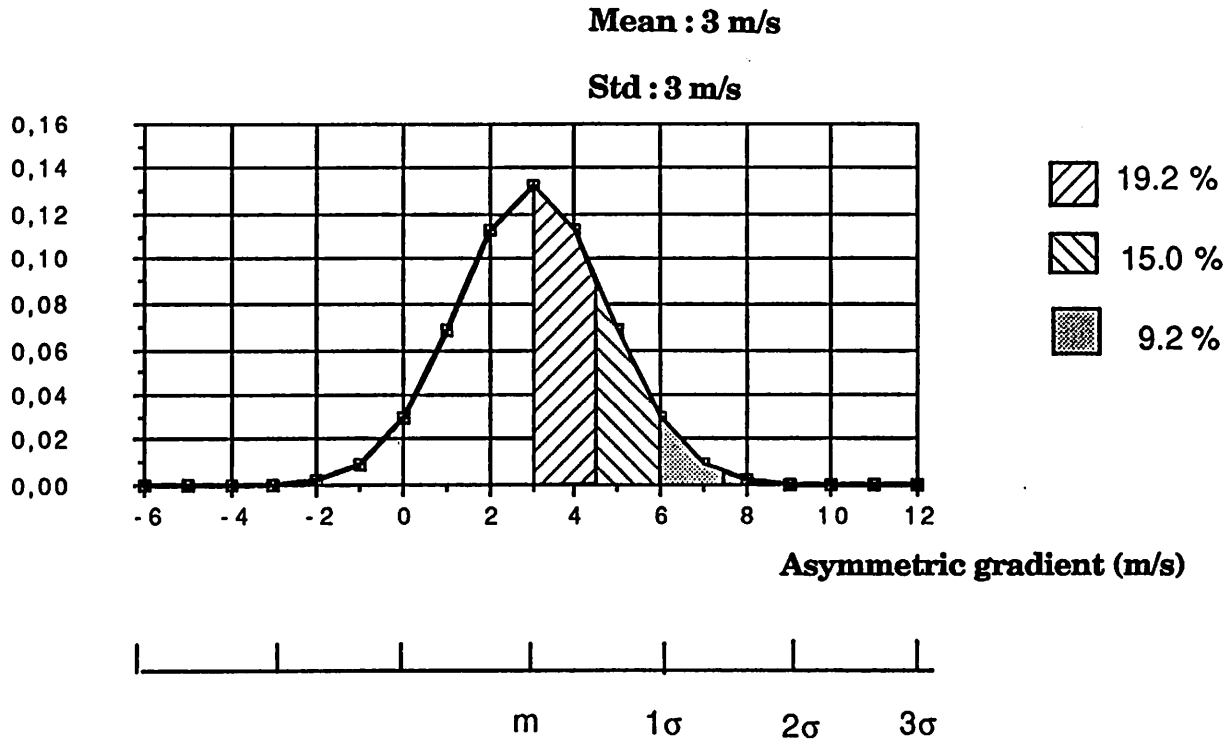

Fig 10

Load spectrum calculation

Load calculation

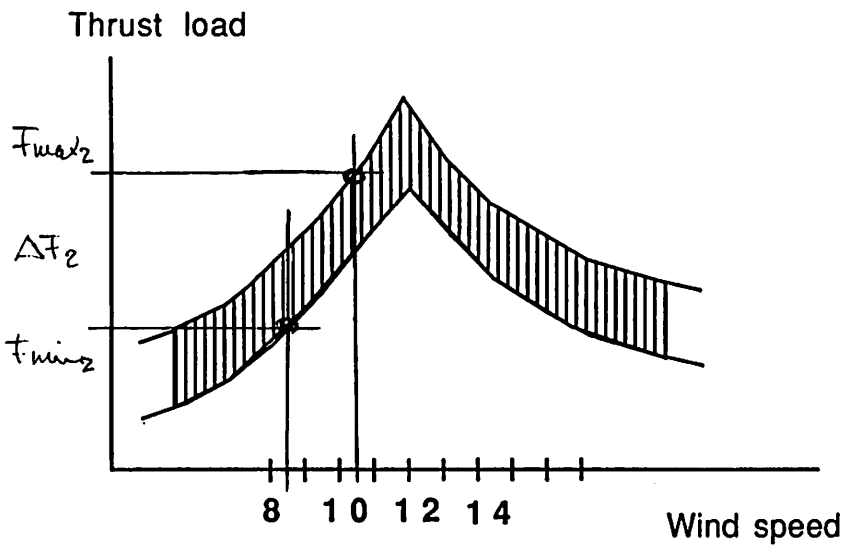

Wind matrix

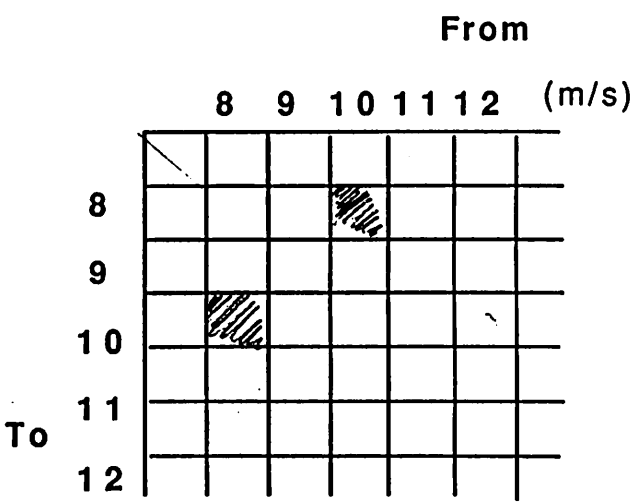

Number of cycles (n_2): number of changes

F_{max_2}
F_{min_2}
ΔF_2
n_2

Fig 11

Load spectrum calculation

Load calculation

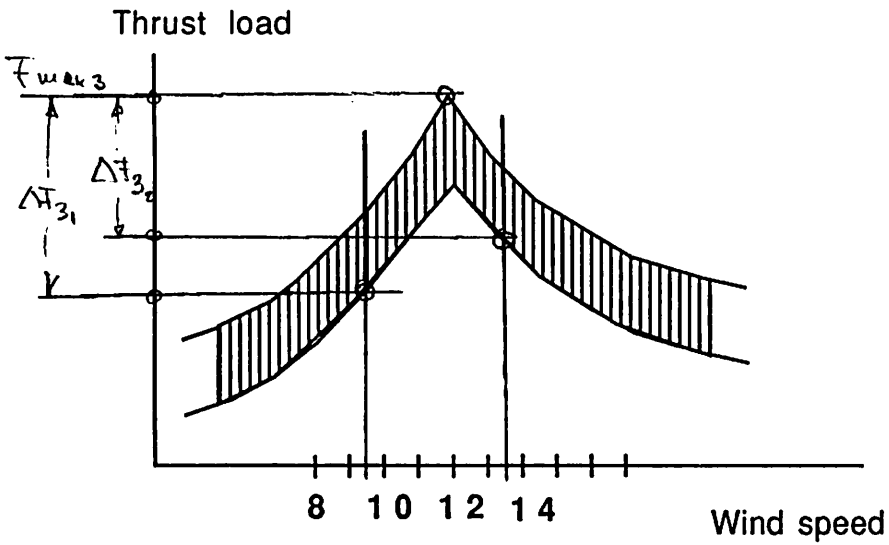

Wind matrix

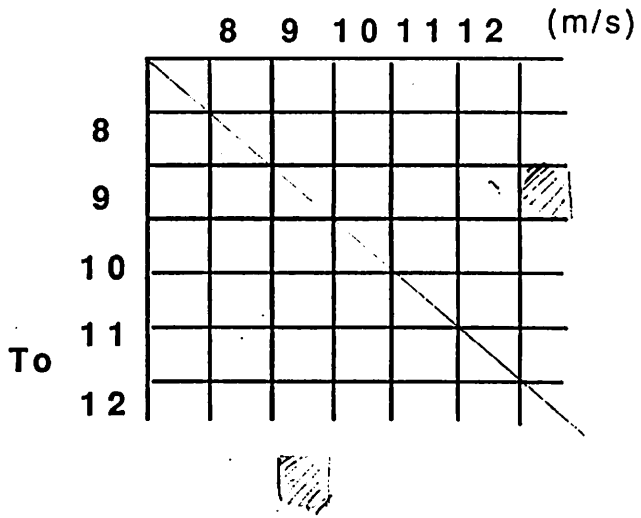

F_{max3}
F_{min3_1}
F_{min3_2}
ΔF_{3_1}
ΔF_{3_2}
n_3

Fig 12

Load spectrum for other points of interest than originally calculated.

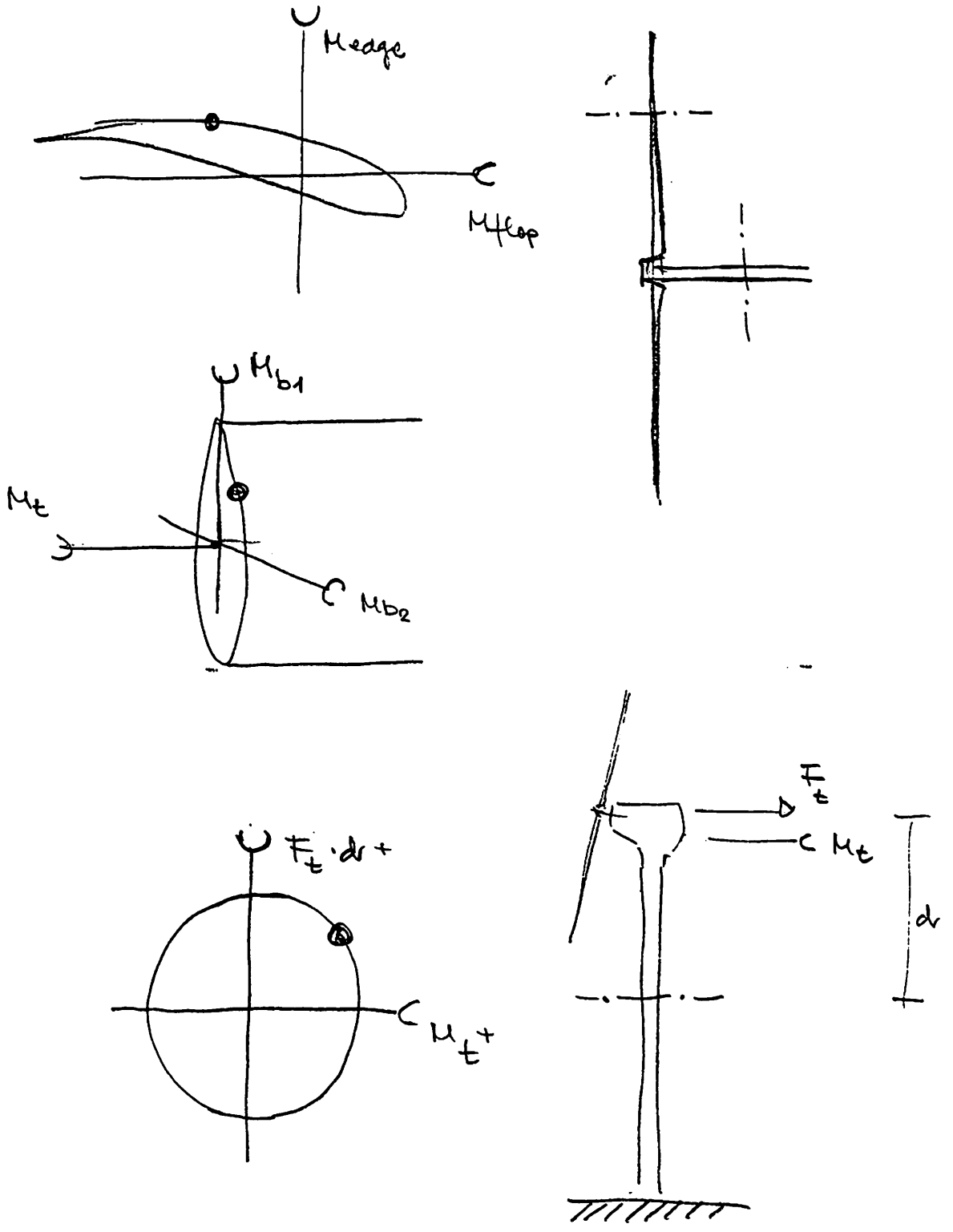

Fig 13

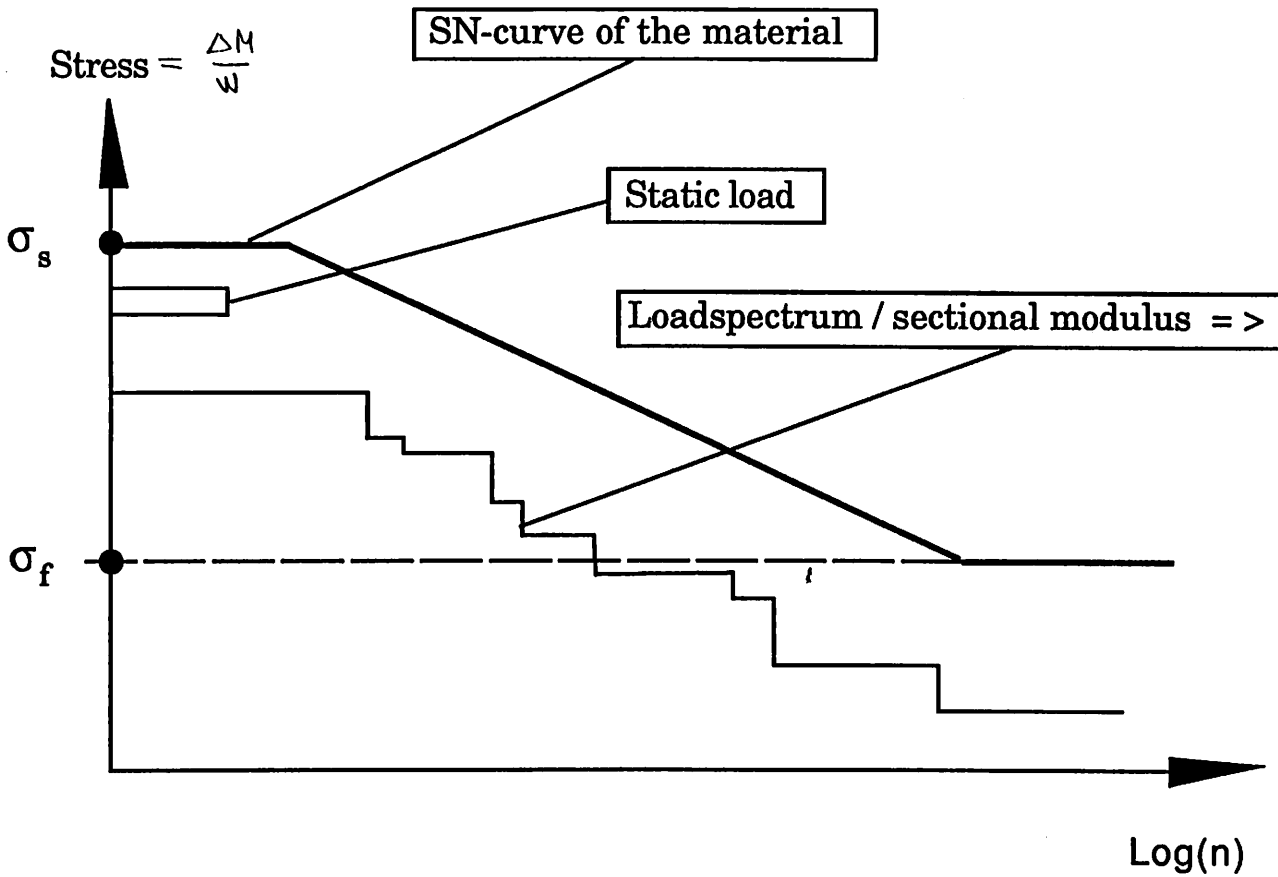

$= \sigma = \frac{M}{W}$; W?

Satisfy:

$\sigma_{static} \rightarrow W_s$

$\sigma_{fatigue} \rightarrow W_f$

$\sigma_{damage} \rightarrow W_{dt}$

Fig 14

Final choise of section modulus (I/c = W)
Comparison of stress spectrum and SN curve (steel)

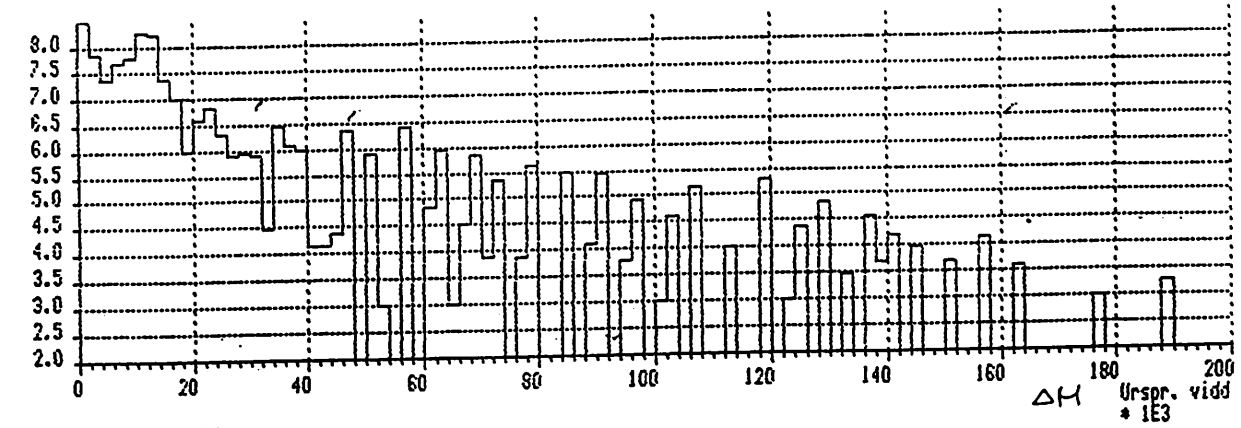

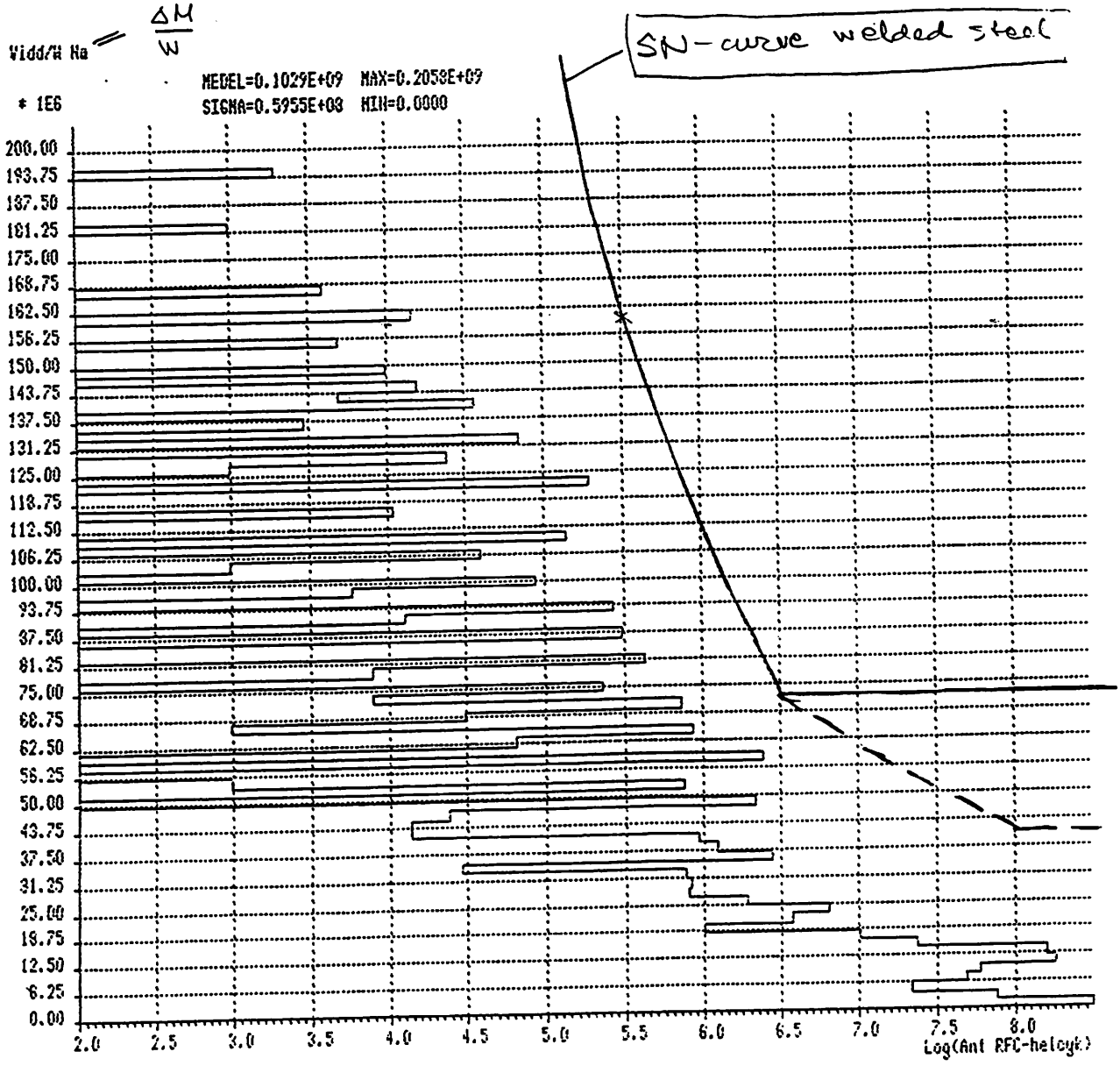

Fig 15

Vidyn system for loadspectrum and fatigue design calculations

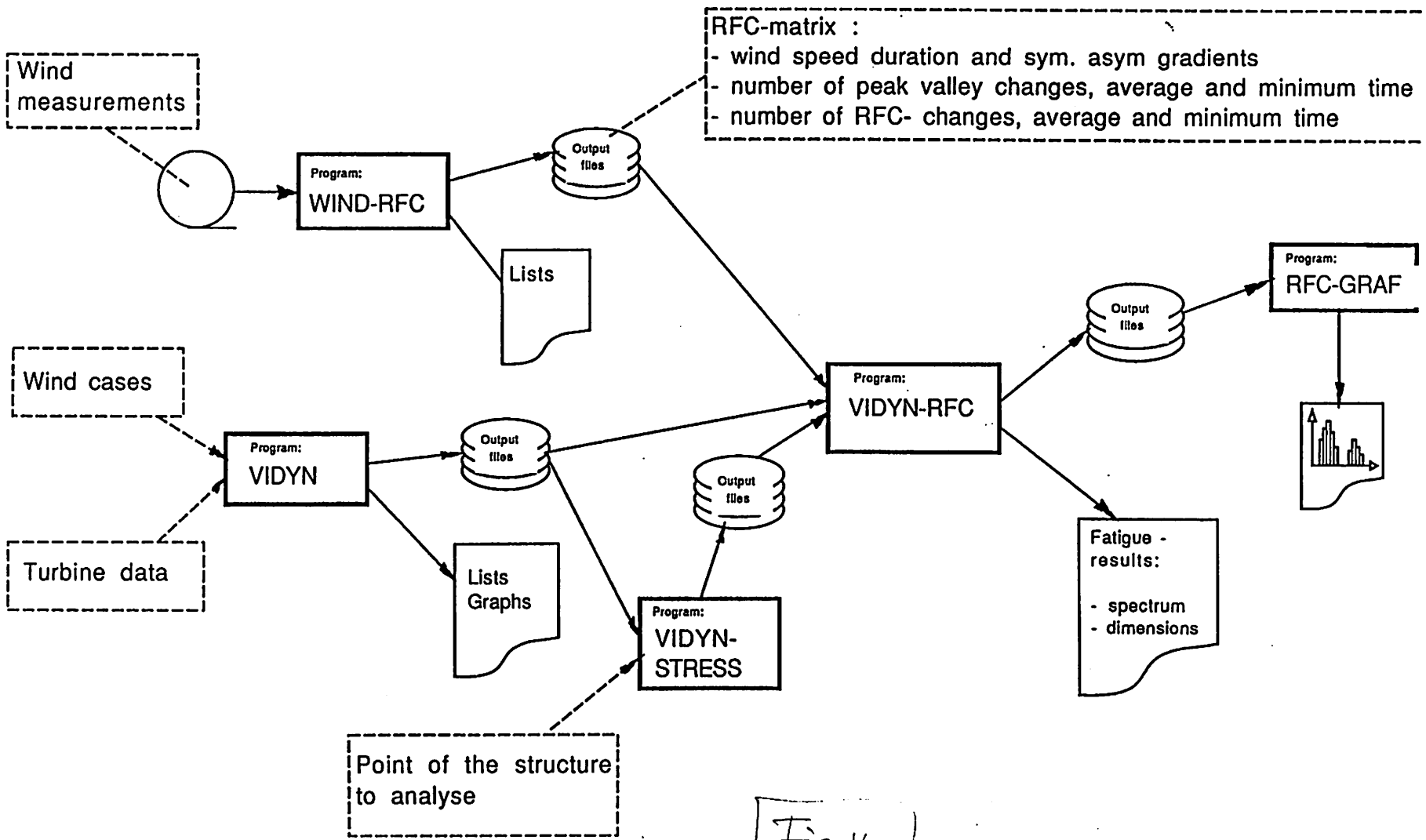

Fig 16

Wind measurements from Alsvik. Results from two 190 hours campaigns conserning gradient and wind direction.

presented at IEA R&D WECs Annex XI Meeting at FFA 7-8 of march -91, by Hans Ganander, Teknikgruppen AB, Box 21, S-19121 Sollentuna, Sweden

1. The site Alsvik

At the Alsvik site, on the island of Gotland, there are four wind turbines and two meteorological masts. One of the turbines is equipped with mechanical sensors. The meteorolgical masts are equipped with instruments measuring wind speed and wind direction at seven heights on each mast. The sampling rate is 1 hz. Measurements started in april-90 and has been going on since then, except for some minor periods.

The site is located near the shore line, which means that due to wind direction the topological conditions vary considerably. Besides that, distances between the instrumented turbine and the three turbines varies from 5 to 9 turbine diameters. Thus wakes of varied strength will occur due to wind direction. In fig 1 the site is shown.

In this presentation two 190 hour campaigns with almost opposite wind directions are analized, with regard to gradients. Two different ways of describing wind direction changes are also presented.

2. Wind gradients.

As earlier proposed space distribution of wind speed is described in terms of asymmetric and symmetric gradients, see fig 2. These two parts of the vertical wind distribution is very important for load variations on turbines. For two bladed machines they have characteristic influence on different loads, see fig 3.

The two 190 hour campaigns have wind speed and wind direction distributions as shown in fig 4. The two parts of the gradient ($\Delta V/\Delta h$ *1000 = mrad/sec) are based on 10 seconds averaged values and determined in such a way that five senors within 18 to 40 meters are used in a LQM (least squar method) procedure to calculate the asymmetric and symmetric parts. This means that at every 10:th second the parts are calculated. Fig 5 show in what way the two gradients occur together, in a kind of correlation matrix. The figures are absolute numbers of occurence in the actual campaign. It can easily be normalised, showing the statistical 2D distribution. The two curves in fig 5 indicate limits around 10 and 100 occurrances respectively.

In fig 5 distributions of asymmetric and symmetric gradients are also presented as numbers, vertically and horisontally respectively. Fig 6-9 show these distributions in diagrams for the two campaigns. There are two diagrams of each gradient. One of them with a logarithmic y-scale showing more clearly the distribution for extremes, 4-5 standard deviations away from the mean. A comparison with a normal distribution calculated with same mean and standard deviation as the measured curve is shown.

2.1. Conclusions are:

- extreme gradients (> 4 std) occur => 200-300 mrad/sec
- asymmetric gradient distributions deviate from normal distribution for negative values, as if wakes infuence the results.
- compared with normal shear these short term gradients are much larger and quite large negtive values also occur.
- symmetric gradient distributions deviate from normal distribution mainly for positive values, when wakes seem to occur.
- wakes seems to have influence on asymmetric as well as symmetric part of the gradient
- these conclusions hold for both campaigns

3. Wind direction changes

In the following two ways of describing wind direction changes are presented. In most existing wind descriptions behaviour of wind direction are very roughly described, often as extremes. An attempt to improve that is presented below.

3.1 Method 1, from-to matrix.

The first method is based on the well known from-to matrix. In case of several sensors along a mast they may be averaged not only in time but also in space. In the exemple shown five sensors within 18 - 40 m are averaged every 10 seconds. The resulting wind direction signal is then evaluated in terms of *from* what *to* what direction do every variation occur.

The whole direction range (360 degrees) is divided into 180 intervalls ($\Delta\phi$=2 degrees). The from-to matrix is quite large for presentation directly. To make it more practical, changes are refered to the diagonal (same direction as before) and represented as changes deviating from last value. In fig 10 a minor part of the resulting matrix show variations between ±28

degrees around absolute values 2-14 degrees. The fig 10 also show time duration of changes, and wind direction changes at different heights along the mast. Summing distributions of wind direction changes for all absolute directions is shown in fig 11 and plotted in fig 12.

This kind of discribtion makes it possible to judge the possiblility of assumed changes to occur. But large variations may only be of importance, conserning loads, if they are fast enough compared to yaw speed. An extended way of evaluation has therefore been developed in which the time duration distribution is introduced.

3.2 Method 2, yaw parameters simulation.

To make it even more precise a way of describing wind direction changes is proposed, in which quite general yaw parameters are taken into account. The parameters (see fig 13) are :

- yaw dead band, within misalignment does not cause yawing
- averaging time of wind direction signal of the yaw control system
- yaw speed

Behaviour of the yaw system is principally shown in fig 14. Due to wind direction variations interesting questions are:

- number of yawings
- total time of yawing
- max yaw error
- standard deviation of yaw error

Values of parameters of the yaw system which have been used are:

- yaw dead band: 3-10 degrees
- averageing time: 15-240 seconds
- yaw speed: 2 degrees/second

For one of the 190 hours campaign these different yaw systems have been used and exemples of the results can be seen in fig 15. All results are finally presented in fig 16-21, where the influnce of the yaw parameters on the behaviour of the yaw system and yaw error are shown.

3.3 Conclusions.

Major conclusions are :

- max yaw error is independen of yaw dead band but depends on averaging time

- std of yaw error seems almost independent of situation

- lots of extremes occur.

Site Alsvik.

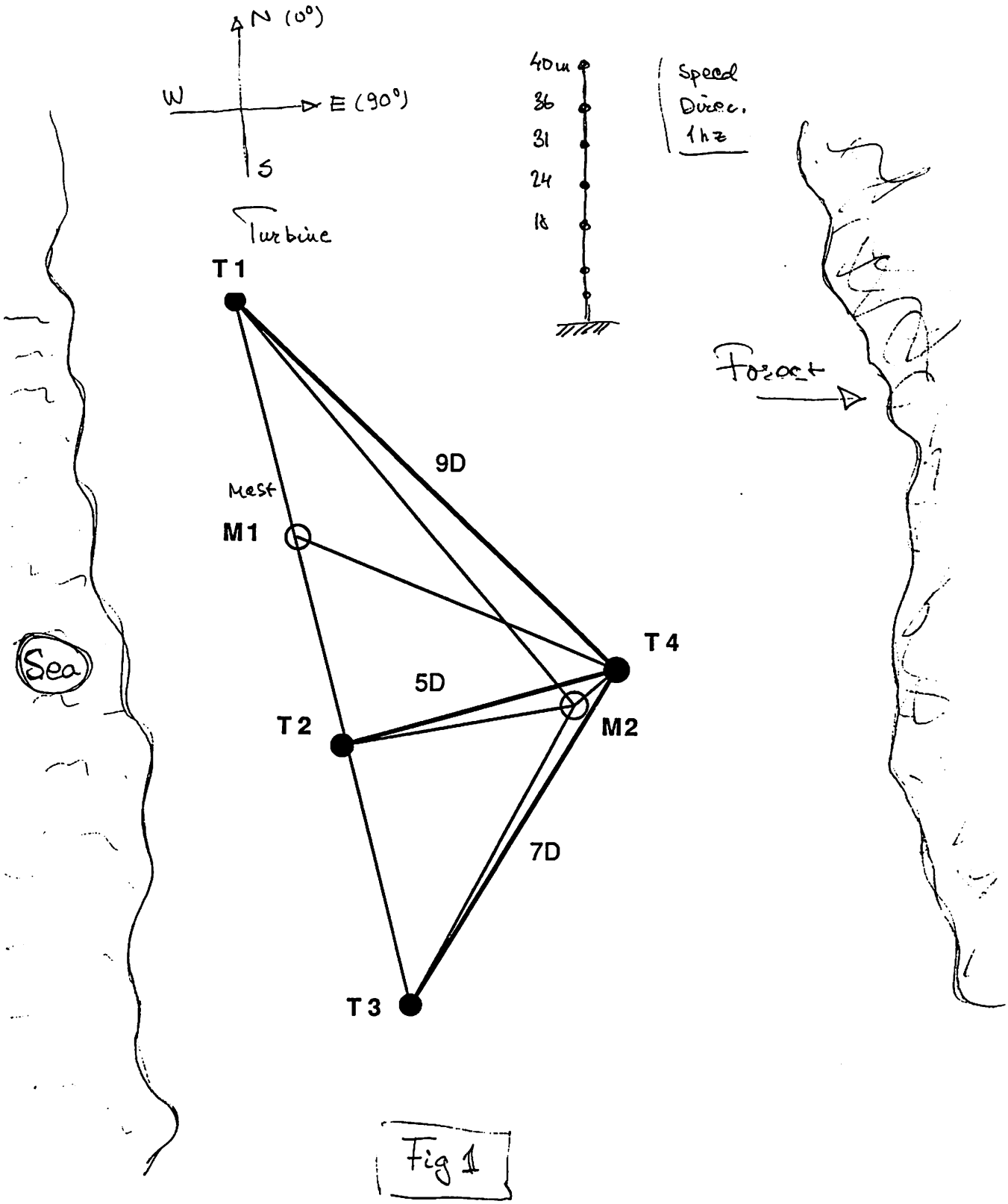

Fig 1

Symmetric and Asymmetric Gradient

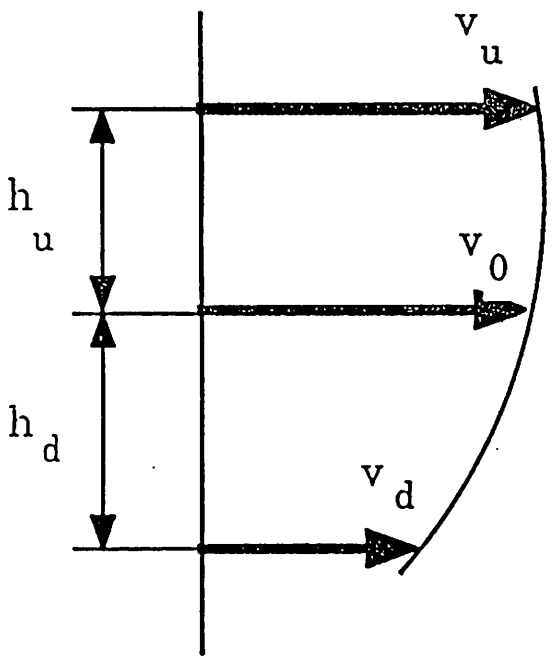

$$\gamma_s = \left(\frac{v_u - v_0}{h_u} - \frac{v_0 - v_d}{h_d} \right) * 0.5$$

$$\gamma_a = \left(\frac{v_u - v_0}{h_u} + \frac{v_0 - v_d}{h_d} \right) * 0.5$$

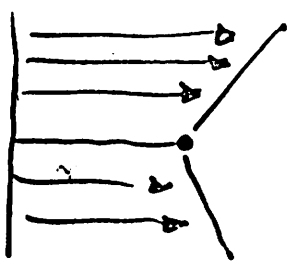

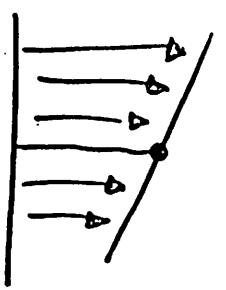

Fig 2

Load variations due to symmetric and asymmetric wind gradients

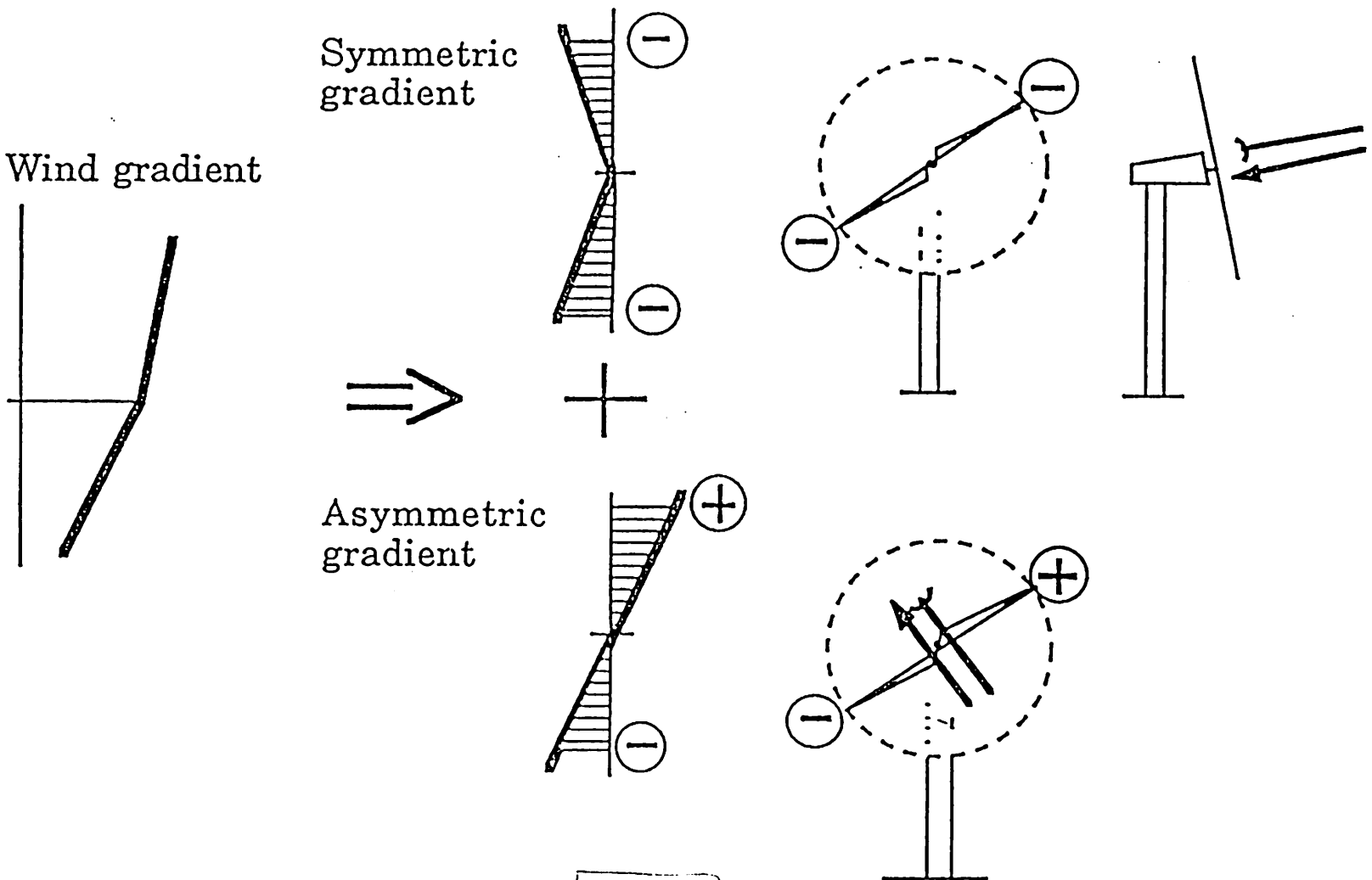

Fig 3

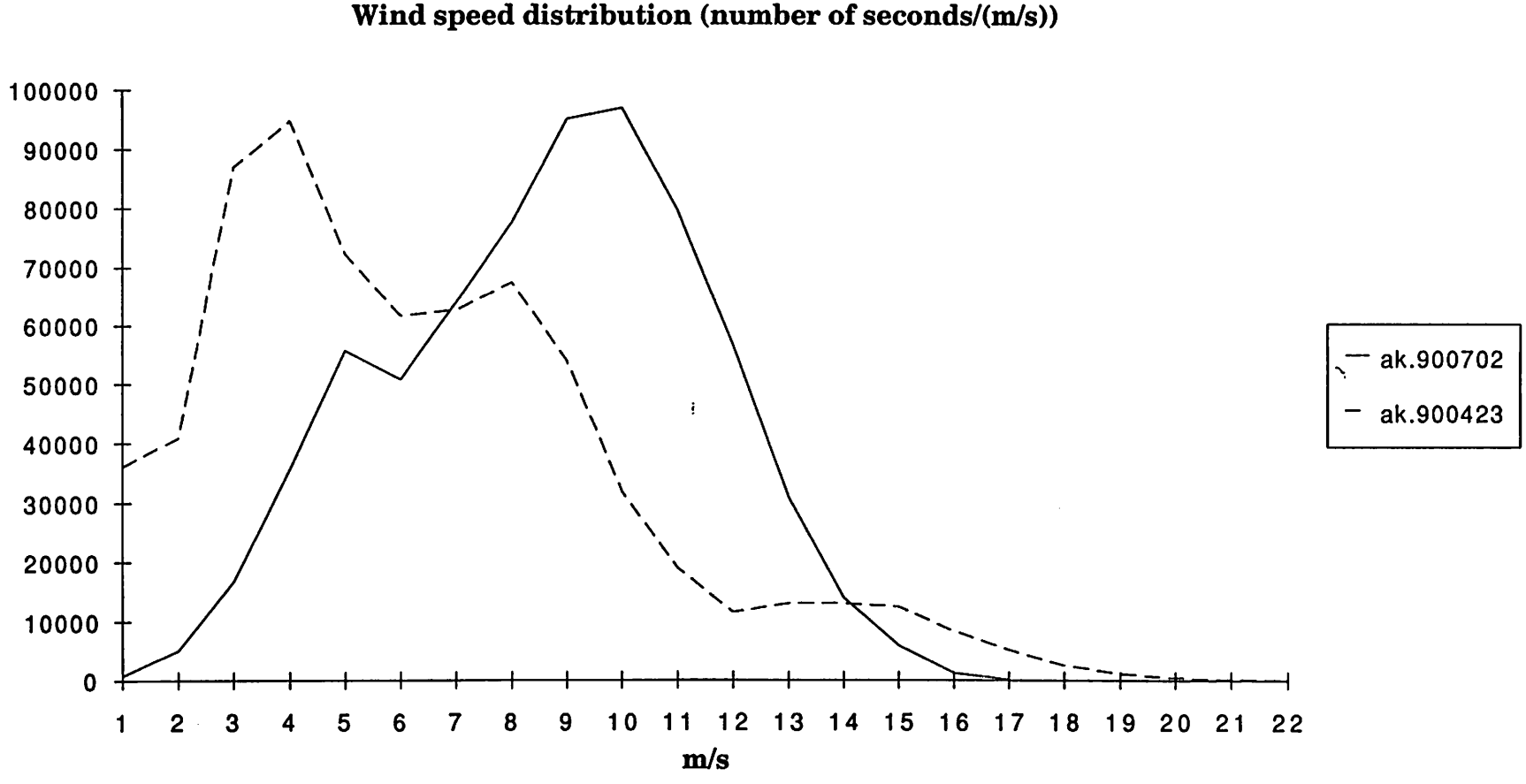
Wind speed distribution (number of seconds/(m/s))
100000
90000
80000
70000
60000
50000
40000
30000
20000
10000
0
1 2 3 4 5 6 7 8 9 10 11 12 13 14 15 16 17 18 19 20 21 22
m/s
ak.900702
ak.900423

Fig 4.1

Wind direction distribution of campaign ak900702 (190 hours)

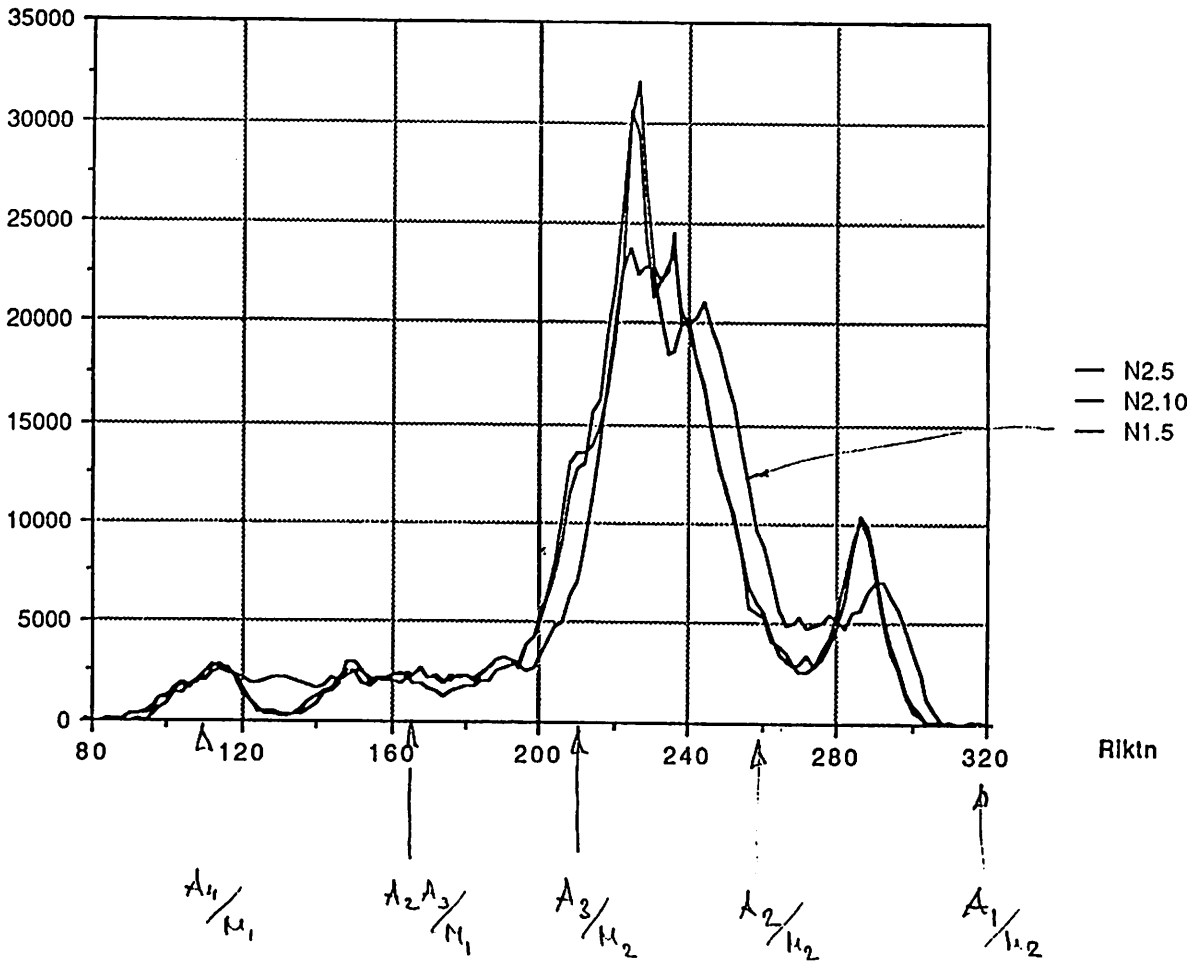

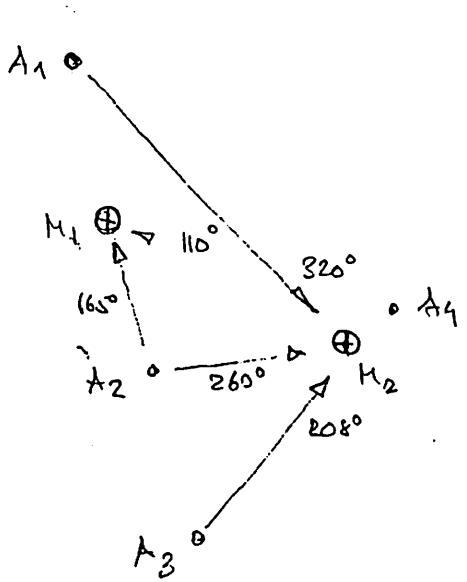

Fig 4.2

Wind direction distribution of campaign ak900423 (192 hours)

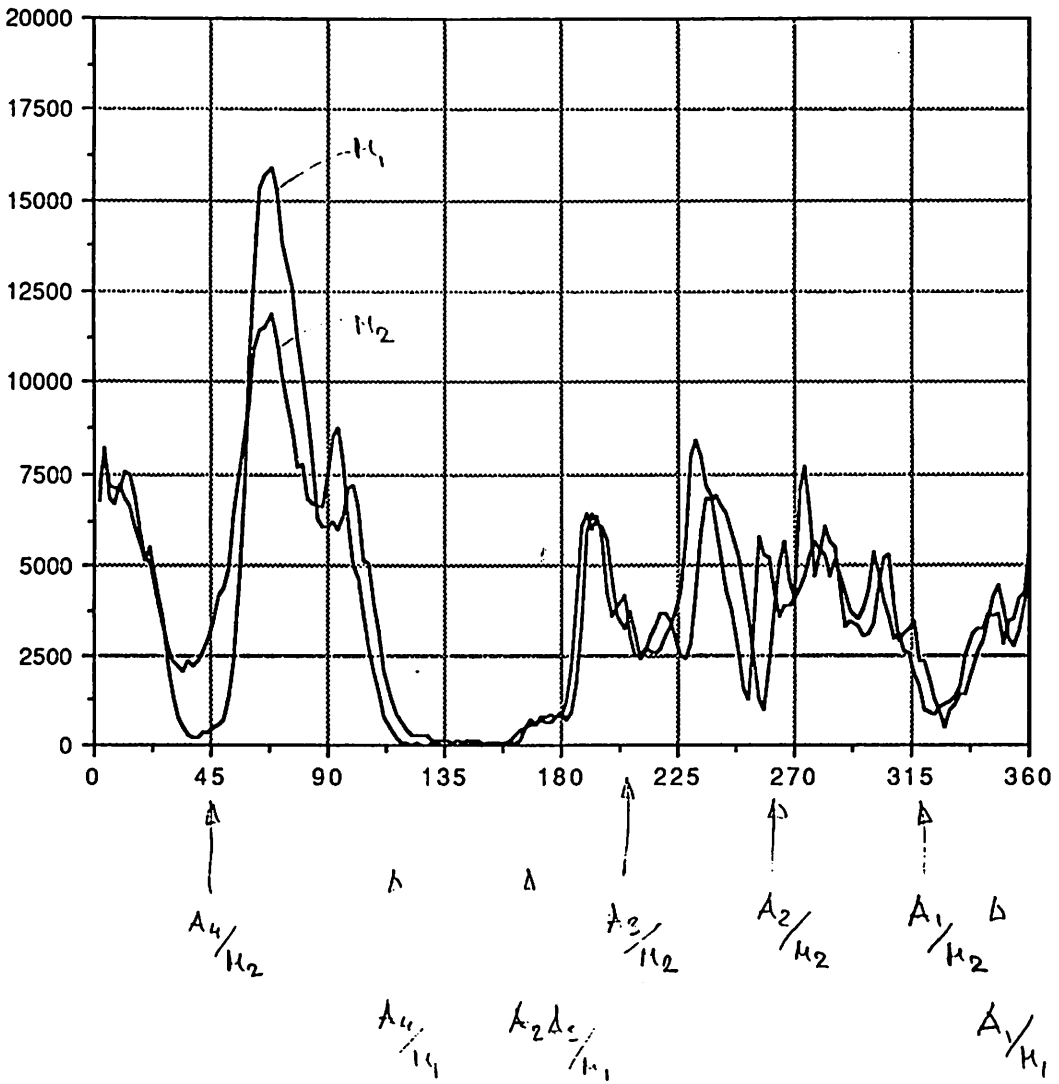

Fig 4.3

Distribution of symmetric and asymmetric gradients of campaign ak 900423

Sym skjuv:	-360	-340	-320	-300	-280	-260	-240	-220	-200	-180	-160	-140	-120	-100	-80	-60	-40	-20	0	20	40	60	80	100
Asym skjuvn	Sum	6	11	26	48	95	145	190	244	326	380	523	787	988	1025	1579	2834	6100	11162	12323	7673	4275	3121	2237	1699
-300	0	0	0	0	0	0	0	0	0	0	0	0	0	0	0	0	0	0	0	0	0	0	0	0	0
-280	2	0	0	0	0	0	0	0	0	0	0	0	0	0	0	0	0	1	0	0	0	1	0	0	0
-260	3	0	0	0	0	0	0	0	0	0	0	0	0	0	0	0	0	0	1	0	0	0	1	0	0
-240	9	0	0	0	0	0	0	0	0	0	0	0	0	0	1	0	0	0	1	0	1	0	1	0	2
-220	28	0	0	0	0	0	0	0	0	0	0	0	0	0	0	1	2	1	3	2	1	1	3	3	2
-200	46	0	0	0	0	0	0	0	0	0	0	0	0	1	0	0	1	2	3	1	1	2	3	0	2
-180	78	0	0	0	0	0	0	0	0	0	1	0	0	0	1	1	1	6	3	4	2	4	3	4	6
-160	184	0	0	0	0	0	0	0	0	0	0	1	0	0	0	3	2	6	3	12	6	7	6	28	12
-140	374	0	0	0	0	0	0	0	0	0	1	0	1	1	5	4	11	12	18	20	12	24	25	28	30
-120	678	0	0	0	0	1	1	0	0	0	3	2	2	9	7	10	17	23	36	49	43	40	36	51	53
-100	1259	0	0	0	0	3	1	3	8	6	13	10	18	19	25	31	60	57	57	68	81	94	104	86	81
-80	2132	0	0	1	2	11	9	13	22	28	34	32	49	62	61	79	82	107	101	115	149	132	148	120	107
-60	3215	2	4	5	7	14	26	35	43	58	60	76	90	87	93	129	122	156	175	191	184	218	198	174	152
-40	4680	1	3	6	14	20	35	42	51	70	85	111	127	154	146	154	205	246	351	349	378	292	291	217	210
-20	6242	1	2	6	10	22	26	43	58	69	74	117	95	132	127	177	258	526	832	632	474	466	374	299	226
0	8553	2	1	6	9	11	28	39	36	65	66	85	76	107	121	190	346	762	1342	1532	860	556	539	313	196
20	10772	0	1	2	5	8	13	11	19	24	31	37	56	121	138	205	387	1002	2219	2530	1234	577	492	345	202
40	9755	0	0	0	1	4	6	4	7	4	7	12	100	136	78	154	357	986	2083	2438	1335	544	245	191	144
60	7897	0	0	0	0	1	0	0	0	1	5	18	82	75	64	127	357	877	1589	1886	1202	506	200	132	106
80	6021	0	0	0	0	0	0	0	0	1	0	9	56	44	60	108	268	682	1268	1322	836	348	197	106	65
100	3763	0	0	0	0	0	0	0	0	0	0	11	29	18	41	107	201	405	690	688	496	251	140	82	48
120	2017	0	0	0	0	0	0	0	0	0	0	1	1	11	33	57	88	147	279	328	266	132	56	42	21
140	1001	0	0	0	0	0	0	0	0	0	0	1	3	9	11	25	34	56	78	106	72	42	34	17	11
160	491	0	0	0	0	0	0	0	0	0	0	0	1	0	6	12	20	20	21	27	15	21	11	6	4
180	291	0	0	0	0	0	0	0	0	0	0	0	0	1	2	3	12	11	6	11	17	12	10	7	10
200	104	0	0	0	0	0	0	0	0	0	0	0	1	1	5	1	2	5	1	7	5	3	3	5	2
220	28	0	0	0	0	0	0	0	0	0	0	0	0	0	0	0	0	1	1	2	2	0	1	0	1
240	11	0	0	0	0	0	0	0	0	0	0	0	0	0	0	1	1	2	0	1	1	1	0	0	1
260	4	0	0	0	0	0	0	0	0	0	0	0	0	0	0	0	0	1	0	1	0	1	0	0	0
280	1	0	0	0	0	0	0	0	0	0	0	0	0	0	0	0	0	0	1	0	0	0	0	0	0
300	1	0	0	0	0	0	0	0	0	0	0	0	0	0	0	0	0	0	0	0	0	0	0	1	0
320	0	0	0	0	0	0	0	0	0	0	0	0	0	0	0	0	0	0	0	0	0	0	0	0	0
340	1	0	0	0	0	0	0	0	0	0	0	0	0	0	0	0	0	0	0	1	0	0	0	0	0

	120	140	160	180	200	220	240	260	280	300	320	340	360	380	400	420	440	460	480	500	520	540	560	580	600
Sum	1390	1302	1105	944	844	775	704	576	532	456	440	387	411	347	292	289	290	271	213	140	81	31	18	4	1
-300	0	0	0	0	0	0	0	0	0	0	0	0	0	0	0	0	0	0	0	0	0	0	0	0	0
-280	0	0	0	0	0	0	0	0	0	0	0	0	0	0	0	0	0	0	0	0	0	0	0	0	0
-260	1	0	0	0	0	0	0	0	0	0	0	0	0	0	0	0	0	0	0	0	0	0	0	0	0
-240	1	2	0	0	0	0	0	0	0	0	0	0	0	0	0	0	0	0	0	0	0	0	0	0	0
-220	0	2	1	3	1	0	1	1	0	0	0	0	0	0	0	0	0	0	0	0	0	0	0	0	0
-200	4	6	4	2	2	4	1	5	0	0	2	0	0	0	0	0	0	0	0	0	0	0	0	0	0
-180	4	8	11	4	3	2	3	3	0	1	1	1	0	0	1	0	0	0	0	0	0	0	0	0	0
-160	16	9	13	12	14	8	6	4	6	5	1	2	2	0	0	0	0	0	0	0	0	0	0	0	0
-140	22	27	19	24	18	19	14	9	9	5	9	3	2	2	0	0	0	0	0	0	0	0	0	0	0
-120	31	43	34	31	30	27	26	18	20	11	4	6	9	1	3	0	1	0	0	0	0	0	0	0	0
-100	72	62	51	39	31	33	29	19	18	14	20	19	10	6	3	5	1	1	1	0	0	0	0	0	0
-80	98	115	89	55	61	44	48	19	21	26	24	11	16	13	11	11	4	2	0	0	0	0	0	0	0
-60	143	128	104	104	85	75	45	39	39	28	21	15	25	21	17	7	9	7	2	2	0	0	0	0	0
-40	187	154	133	112	97	78	71	47	42	30	39	28	25	20	12	10	18	6	7	3	1	2	0	0	0
-20	191	158	146	122	99	75	63	68	50	40	23	27	26	34	16	17	13	14	8	2	1	0	0	0	0
0	176	147	140	100	112	92	93	71	59	53	41	31	43	31	22	10	13	13	9	6	1	0	2	0	0
20	133	149	99	109	79	88	81	50	43	50	50	37	36	28	15	14	14	11	7	7	5	4	3	1	0
40	99	101	72	89	71	60	50	44	54	42	47	32	33	26	25	21	11	13	14	10	3	1	0	0	1
60	70	65	60	31	35	52	34	36	46	32	32	33	32	29	18	14	18	14	8	6	2	0	2	0	0
80	58	44	40	31	28	29	51	38	28	33	33	35	34	26	24	31	28	24	20	8	4	3	1	0	0
100	34	31	32	34	31	23	27	40	27	25	29	20	20	37	42	19	35	21	21	12	8	4	2	2	0
120	23	20	24	16	20	26	23	25	27	19	27	43	27	22	26	35	39	37	32	15	13	5	4	1	0
140	11	10	16	12	12	12	21	15	24	14	15	29	35	33	21	43	35	48	27	31	29	10	1	0	0
160	5	8	12	7	10	13	8	10	13	15	13	7	17	14	13	31	23	30	27	26	14	2	3	0	0
180	7	8	2	5	3	11	9	7	4	10	5	4	13	4	14	16	19	16	24	8	0	0	0	0	0
200	1	3	2	2	2	3	0	5	2	2	4	3	2	0	5	5	6	11	5	0	0	0	0	0	0
220	2	2	1	0	0	1	0	2	0	1	0	0	2	0	0	2	3	3	1	0	0	0	0	0	0
240	0	0	0	0	0	0	0	1	0	0	0	1	0	0	1	0	0	0	0	0	0	0	0	0	0

Fig 5

Asymmetric part of gradient of measurement ak900423.

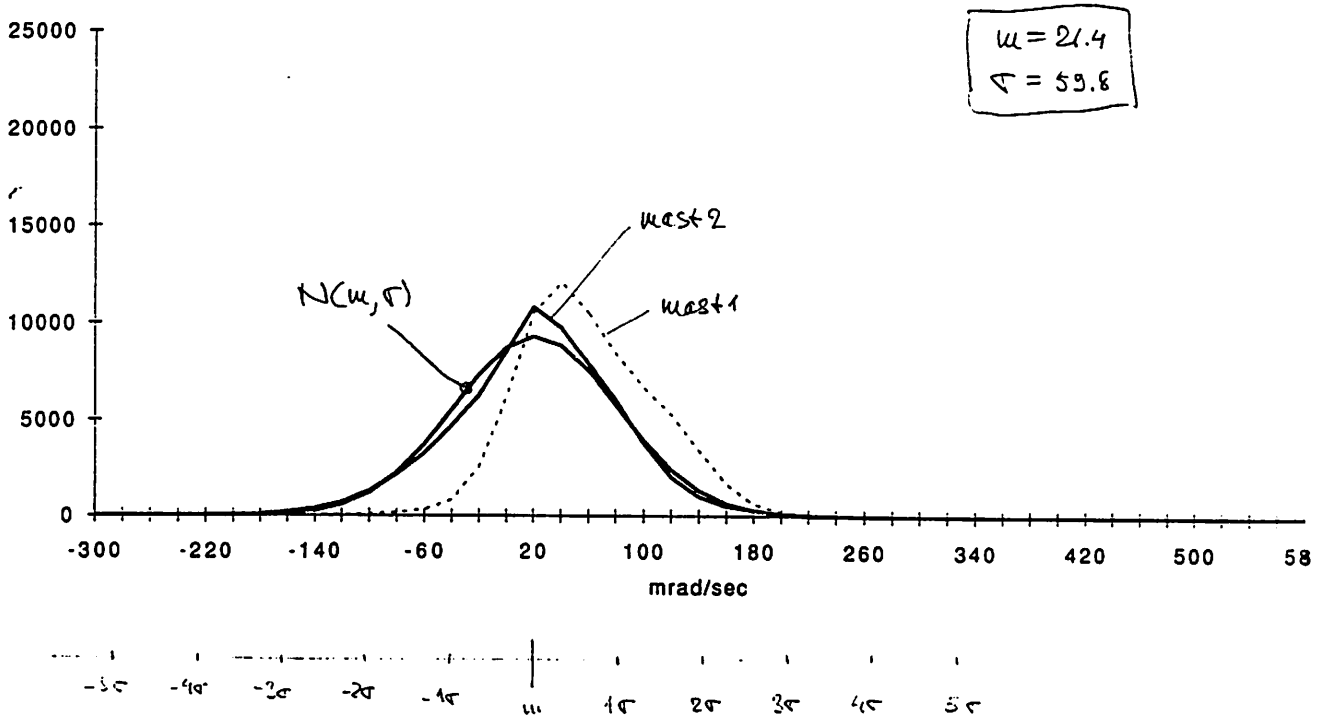

Asymmetric part of gradient of measurement ak900423.

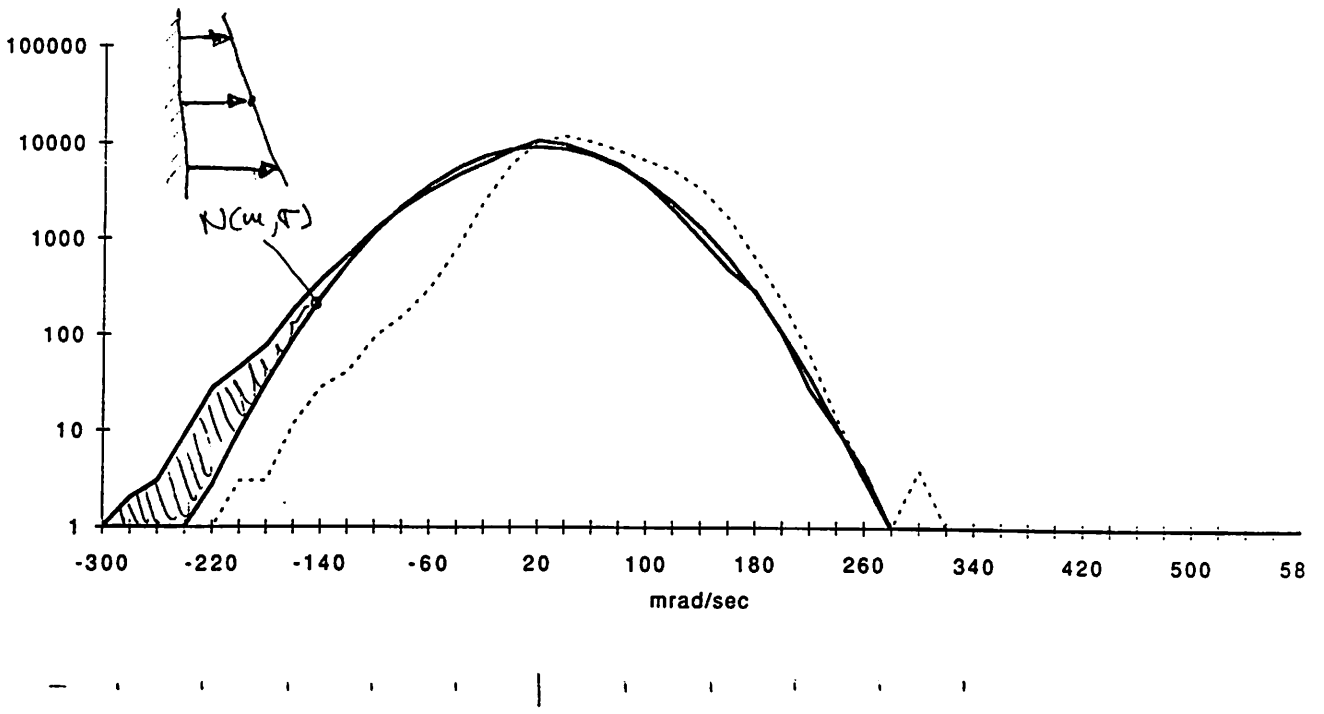

Fig 6

Symmetric part of gradient of measurement ak900423.

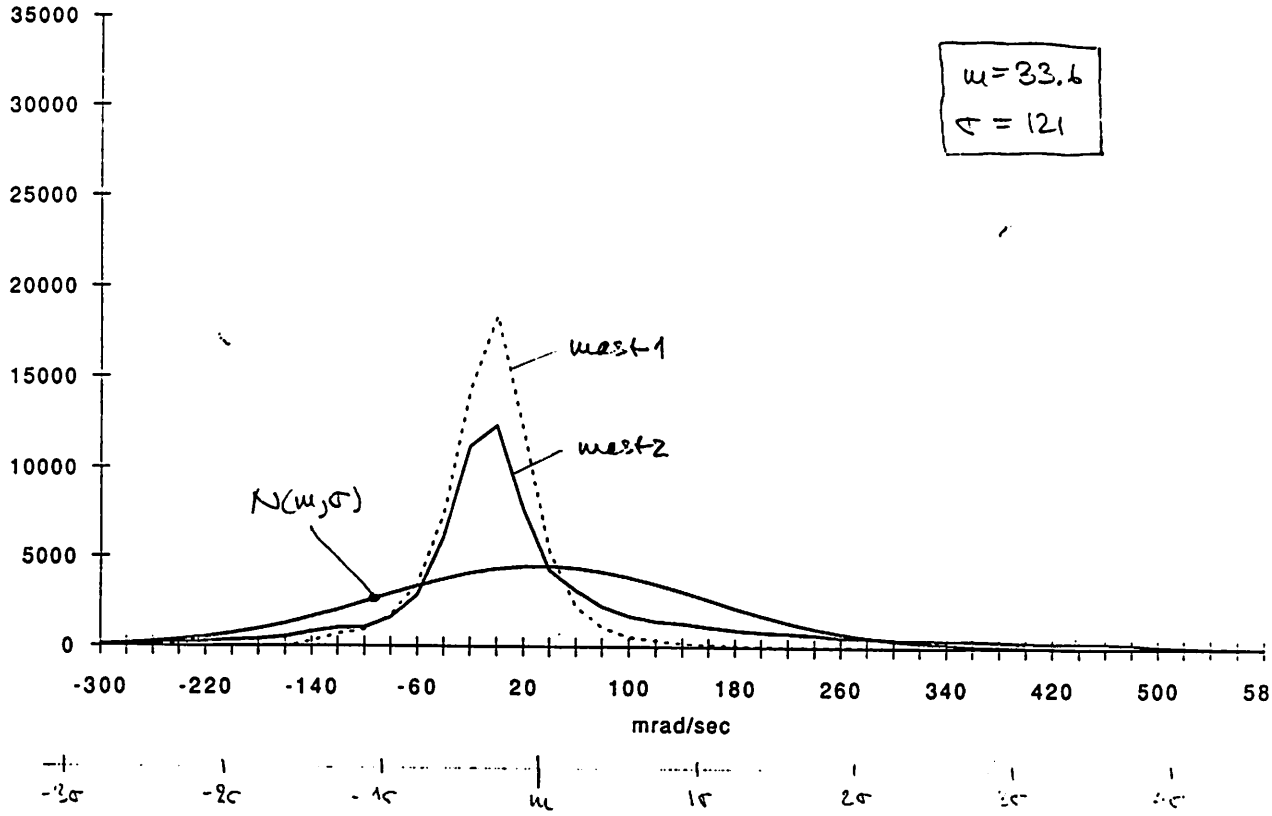

Sida 1

Symmetric part of gradient of measurement ak900423.

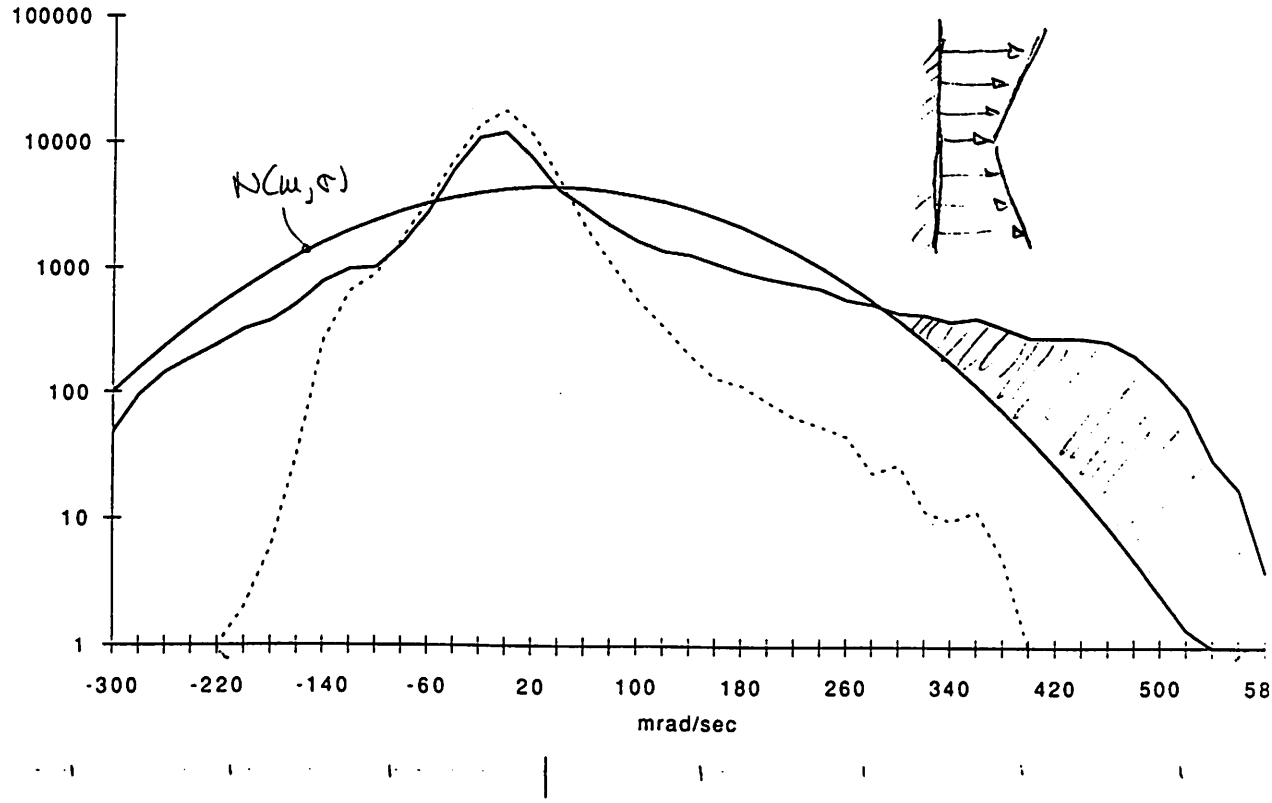

Fig 7

Asymmetric part of gradient of measurement ak.900702.

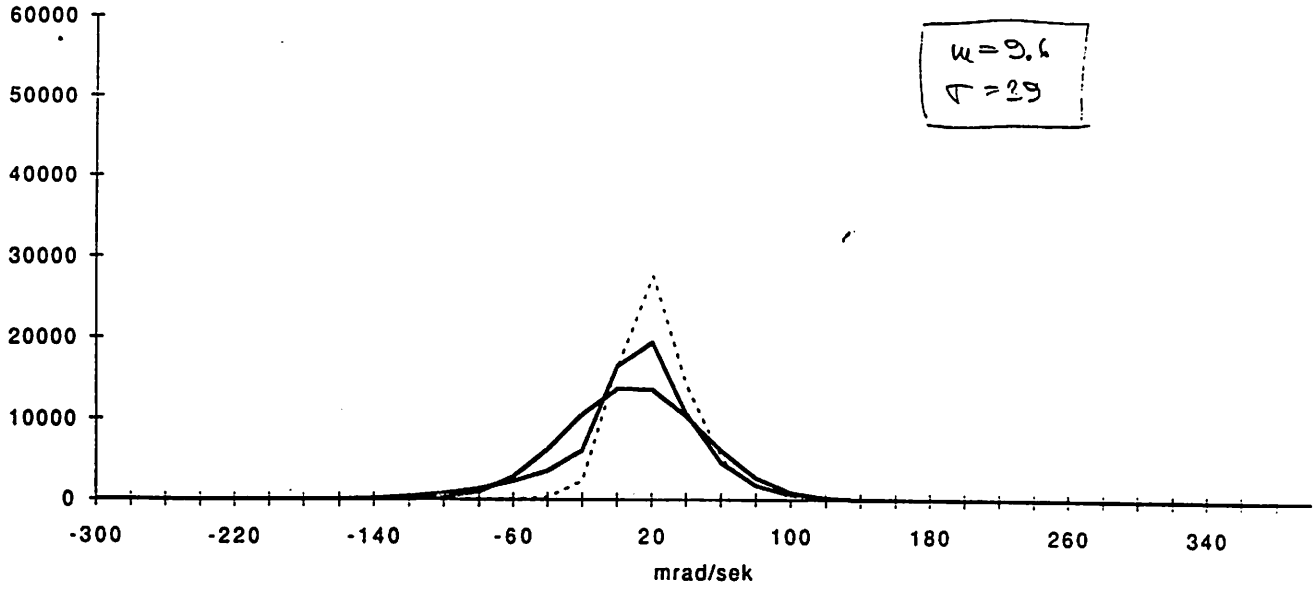

Sida 1

Asymmetric part of gradient of measurement ak.900702.

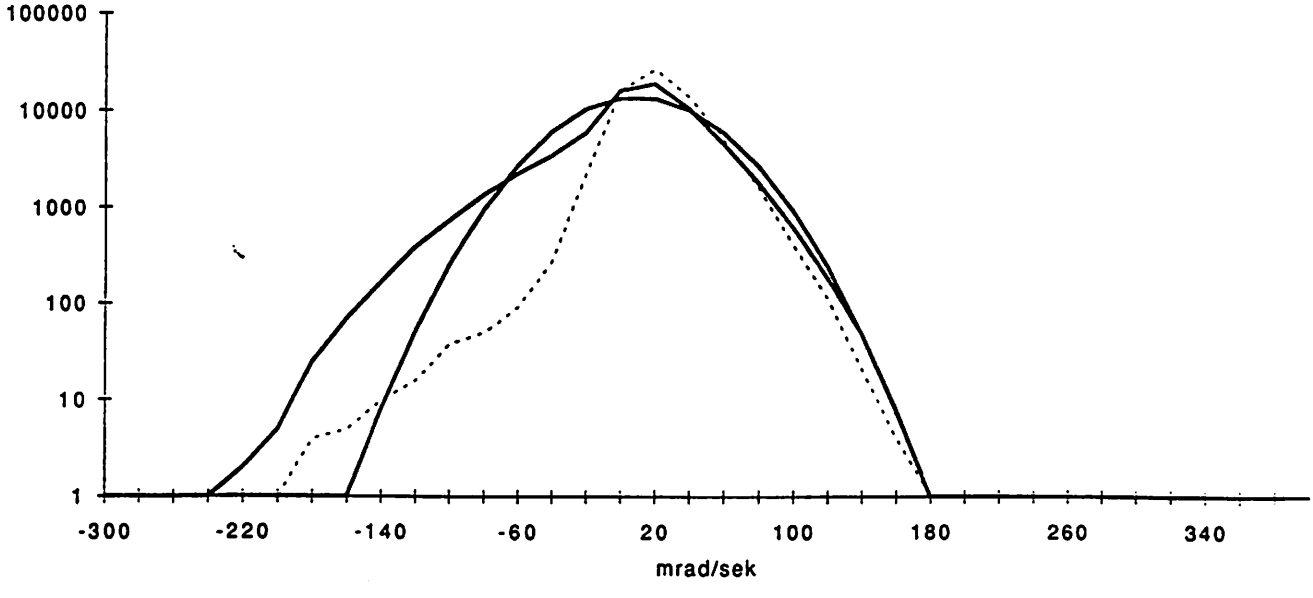

Fig 8

Symmetric part of gradient of measurement ak900702.

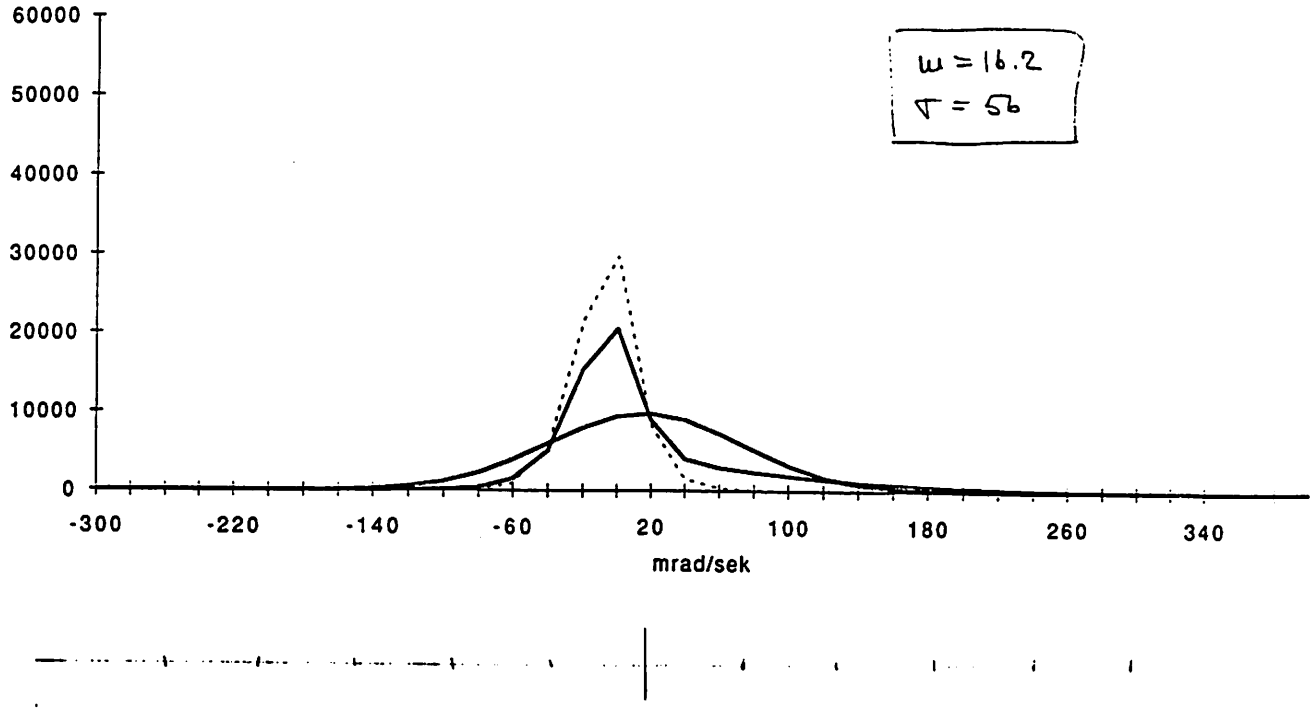

Sida 1

Symmetric part of gradient of measurement ak900702.

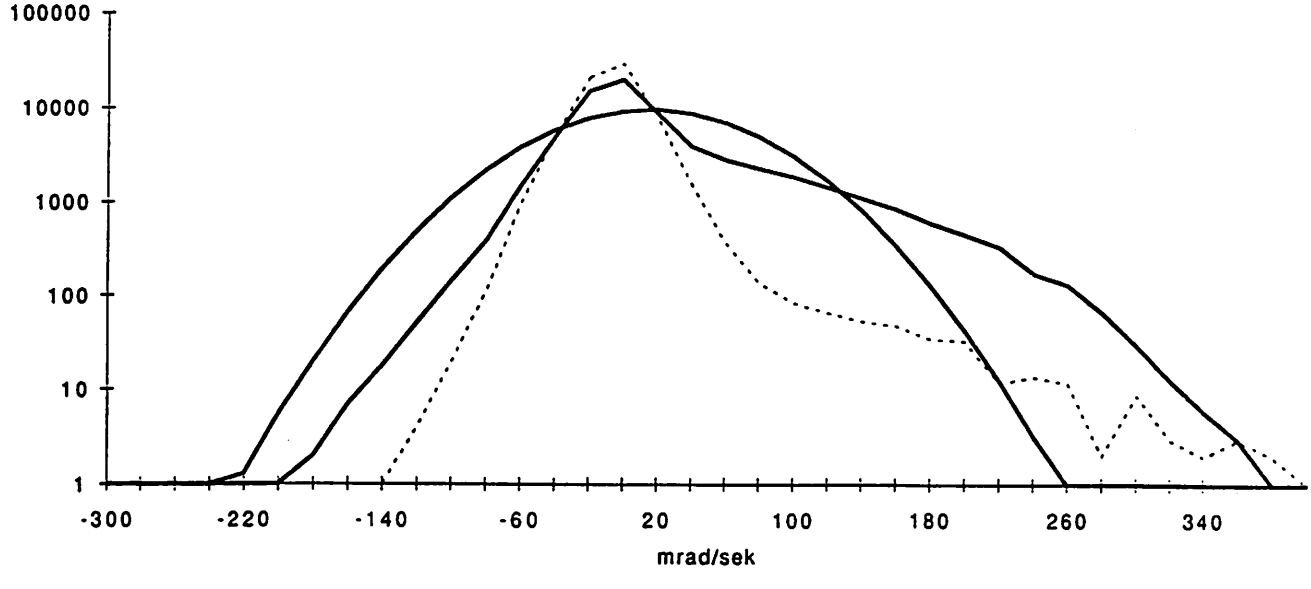

Fig 9

**** Vindriktnings-analys ***** 'Skjuvning' betecknar här vindrikt.ändring per 6 i höjdled
Älgvik vindmast T. RFC (dt = 10 s) för kvadratanpassad brytpunkt och asym. och sym.skjuvning vid nivå 30 m.
Reserat på vindmätningar från nivåerna 18.4, 24.4, 30.8, 35.6 och 40.7 m under sammanlagt 8.0606 dygn.
Indata: 'ak900423.dat' 900423 10:30 - 900501 10:35 från MIUU. Bearbetat 24/1 91.

Exp² analysis of the wake ... see fig 11

Element utanför mittkolumnen:		Mittkolumnen (0):		Kol 0 element:
	Antal byten	Vindens varaktighet (s)		Totalt = 696430
Topp-Dal	Tidsmed för byte (s)	Asym.skjuvn. (30 m) medelv (0.01gr/m)		Medelv. = 13.59
	Min.tid " " (s)	" st.avvikelse "		Medelv. = 86.28
	Antal halvcykler	" max "		Medelv. =558.69
RFC-data	Tidsmed för halvcykel (s)	Sym. skjuvn. (30 m) medelv "		Medelv. = -9.46
	Min.tid " " (s)	" st.avvikelse "		Medelv. = 82.27

Vindriktningsavvikelser i grader från rad-gruppens vindriktning, vilken avser 30 m -nivån med kvadratanpassad vinkelprofil för vindriktningen

Grader	-28	-26	-24	-22	-20	-18	-16	-14	-12	-10	-8	-6	-4	-2	0	2	4	6	8	10	12	14	16	18	20	22	24	26	28-
2	0	0	0	0	0	0	0	0	0	0	0	0	0	0	6830	32	29	22	22	22	11	7	7	2	3	1	0	1	90
2	0	0	0	0	0	0	0	0	0	0	0	0	0	0	18	41	38	20	20	32	19	37	32	35	20	10	0	10	28
2	0	0	0	0	0	0	0	0	0	0	0	0	0	0	24	10	10	10	10	10	10	10	10	30	20	10	0	10	10
2	0	0	0	0	0	0	0	0	0	0	0	0	0	0	243	0	0	0	0	0	0	0	0	0	0	0	0	0	109
2	0	0	0	0	0	0	0	0	0	0	0	0	0	0	-22	0	0	0	0	0	0	0	0	0	0	0	0	0	733
2	0	0	0	0	0	0	0	0	0	0	0	0	0	0	27	0	0	0	0	0	0	0	0	0	0	0	0	0	10
4	0	0	0	0	0	0	0	0	0	0	0	0	0	0	8000	15	26	26	25	29	25	10	5	1	4	3	1	0	80
4	0	0	0	0	0	0	0	0	0	0	0	0	0	0	19	28	18	20	23	37	32	32	24	40	27	33	20	0	32
4	0	0	0	0	0	0	0	0	0	0	0	0	0	0	75	10	10	10	10	10	10	10	10	40	10	10	20	0	10
4	0	0	0	0	0	0	0	0	0	0	0	0	0	0	1242	14	22	14	24	12	18	24	4	2	2	2	0	0	99
4	0	0	0	0	0	0	0	0	0	0	0	0	0	0	-18	44	20	42	61	60	62	282	55	89	120	220	0	0	65
4	0	0	0	0	0	0	0	0	0	0	0	0	0	0	112	10	10	10	20	10	20	80	20	80	120	220	0	0	10
6	0	0	0	0	0	0	0	0	0	0	0	0	0	0	6370	15	46	30	31	18	13	3	2	2	1	1	0	0	40
6	0	0	0	0	0	0	0	0	0	0	0	0	0	0	12	18	17	21	21	26	23	40	55	50	40	40	0	0	31
6	0	0	0	0	0	0	0	0	0	0	0	0	0	0	74	10	10	10	10	10	10	30	50	40	40	40	0	0	10
6	0	0	0	0	0	0	0	0	0	0	0	0	0	0	1398	18	62	32	20	10	10	8	4	6	4	2	2	0	50
6	0	0	0	0	0	0	0	0	0	0	0	0	0	0	-20	15	21	25	46	56	22	105	245	206	295	230	910	0	42
6	0	0	0	0	0	0	0	0	0	0	0	0	0	0	99	10	10	10	10	20	10	60	140	50	40	230	910	0	10
8	0	0	0	0	0	0	0	0	0	0	0	0	22	27	16	7190	17	48	31	29	19	17	10	7	3	1	0	0	0	31
8	0	0	0	0	0	0	0	0	0	0	0	0	22	19	15	16	16	16	17	32	27	28	33	42	40	10	0	0	0	27
8	0	0	0	0	0	0	0	0	0	0	0	0	10	-10	10	52	-10	10	10	10	10	10	10	20	10	0	0	0	-10	10
8	0	0	0	0	0	0	0	0	0	0	0	0	22	30	20	1234	22	62	28	30	12	18	4	2	12	0	0	0	2	40
8	0	0	0	0	0	0	0	0	0	0	0	0	47	22	16	-21	13	22	23	42	73	80	355	180	320	0	0	0	580	90
8	0	0	0	0	0	0	0	0	0	0	0	0	10	10	10	73	10	10	10	10	10	20	280	180	40	0	0	0	580	10
10	0	0	0	0	0	0	0	0	0	0	0	20	39	36	15	7390	21	36	23	22	16	8	9	4	3	3	1	0	0	31
10	0	0	0	0	0	0	0	0	0	0	0	32	23	15	17	6	24	18	20	25	23	30	32	25	33	34	20	0	0	39
10	0	0	0	0	0	0	0	0	0	0	0	10	10	10	10	85	10	10	10	10	10	10	10	10	20	20	20	0	0	10
10	0	0	0	0	0	0	0	0	0	0	0	32	34	42	22	190	42	44	20	10	10	10	8	0	2	6	4	2	0	32
10	0	0	0	0	0	0	0	0	0	0	0	74	26	11	20	-30	24	18	19	52	42	86	82	0	370	333	100	180	0	45
10	0	0	0	0	0	0	0	0	0	0	0	20	10	10	10	101	10	10	10	20	10	10	50	0	370	60	20	180	0	10
12	0	0	0	0	0	0	0	0	0	0	20	34	39	35	19	7690	12	37	22	17	20	11	5	3	5	2	0	1	0	21
12	0	0	0	0	0	0	0	0	0	0	26	25	21	22	21	7	11	18	16	20	24	25	44	16	22	15	0	20	0	20
12	0	0	0	0	0	0	0	0	0	0	10	10	10	10	10	97	10	10	10	10	10	10	20	10	10	10	0	20	0	10
12	0	0	0	0	0	0	0	0	0	0	34	28	24	34	19	206	12	46	16	12	14	4	10	4	0	2	2	0	4	12
12	0	0	0	0	0	0	0	0	0	0	133	42	39	24	11	-29	13	16	33	46	58	70	212	20	0	160	200	0	335	33
12	0	0	0	0	0	0	0	0	0	0	10	10	10	10	10	112	10	10	10	10	20	20	70	20	0	160	200	0	310	10
14	0	0	0	0	0	0	0	0	0	10	20	29	32	34	20	6350	22	22	21	18	19	7	7	2	11	1	0	1	0	15
14	0	0	0	0	0	0	0	0	0	31	24	24	19	18	13	13	17	15	21	20	30	47	28	25	17	10	0	50	0	32
14	0	0	0	0	0	0	0	0	0	10	10	10	10	10	10	47	10	10	10	10	10	20	10	10	10	10	0	50	0	10
14	0	0	0	0	0	0	0	0	0	22	30	26	36	32	36	173	32	30	20	14	6	4	4	6	4	2	2	0	0	16
14	0	0	0	0	0	0	0	0	0	88	56	50	27	15	13	-28	18	14	26	18	46	130	130	113	37	260	100	120	0	95
14	0	0	0	0	0	0	0	0	0	10	10	10	10	10	10	48	10	10	10	10	30	29	90	40	10	120	100	240	0	10

fig 10

Wind direction changes for ak 900423 (190 hours), mast 1.

														D			E										
-28	-26	-24	-22	-20	-18	-16	-14	-12	-10	-8	-6	-4	-2	0	2	4	6	8	10	12	14	16	18	20	22	24	26	28-
														696430														
904	70	93	111	193	231	336	450	675	1028	1494	2460	3376	1804	*****	1778	3407	2453	1555	1006	668	489	288	228	171	136	87	73	59
26	33	28	27	32	30	29	29	26	25	27	28	25	21	14	23	24	28	25	27	25	27	29	28	30	29	27	29	2
10	10	10	10	10	10	10	10	10	10	10	10	10	10	86	10	10	10	10	10	10	10	10	10	10	10	10	10	1
1032	104	106	124	196	220	303	426	594	829	1288	2202	3357	2564	559	2478	3505	2028	1290	834	603	434	290	180	154	112	95	82	102
951	318	373	110	219	243	137	133	105	66	63	47	27	22	-8	22	27	41	69	75	86	130	140	122	173	315	382	332	100
10	10	10	10	10	10	10	10	10	10	10	10	10	10	82	10	10	10	10	10	10	10	10	10	10	10	10	10	1
-28	-26	-24	-22	-20	-18	-16	-14	-12	-10	-8	-6	-4	-2	0	2	4	6	8	10	12	14	16	18	20	22	24	26	28-

D: - 0
- total time [sec]
- xxxxxx
- average of asym. grad [mrad/sec]
- standard dev. —"—
- max. of asymmetric grad [mrad/sec]
- average of sym. grad [mrad/sec]
- standard dev. —"—

E: - wind direction change
- number of changes
- average time of changes
- minimum time —"—

} peak-valley evaluation

- number of half cycles
- average time of —"—
- minimum time —"—

} RFC-evaluation

Fig 11

Wind direction changes, ak900423.

Number of changes per 2 dgr intervall

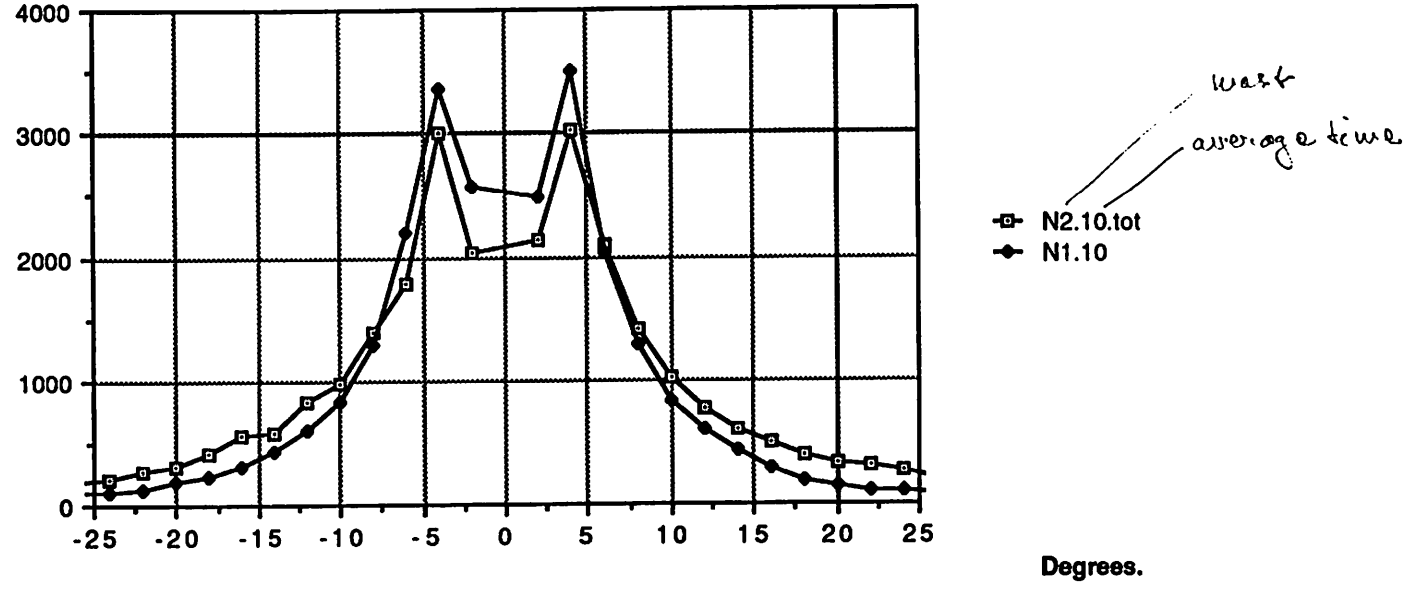

Fig 12

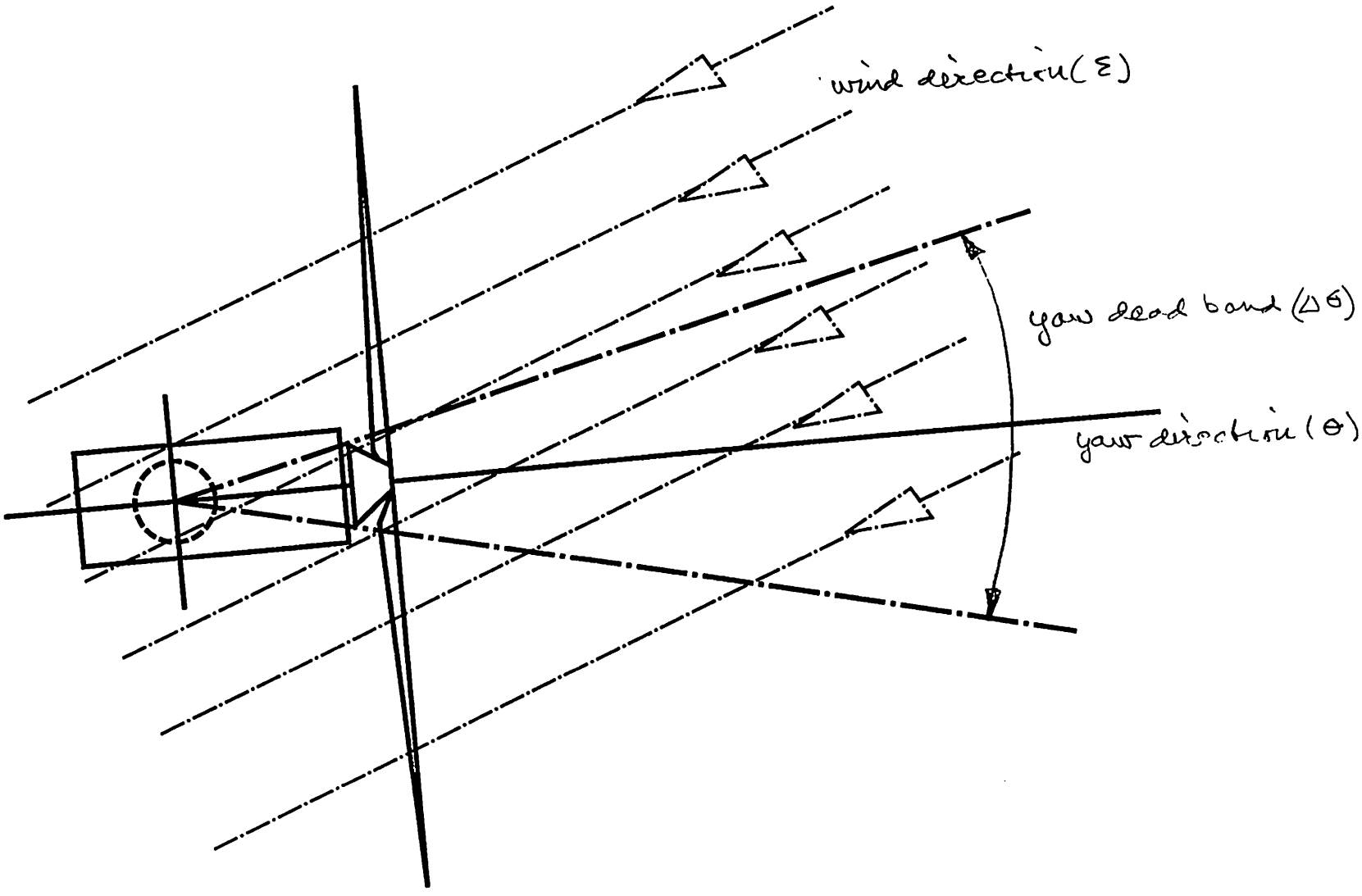

Fig 13

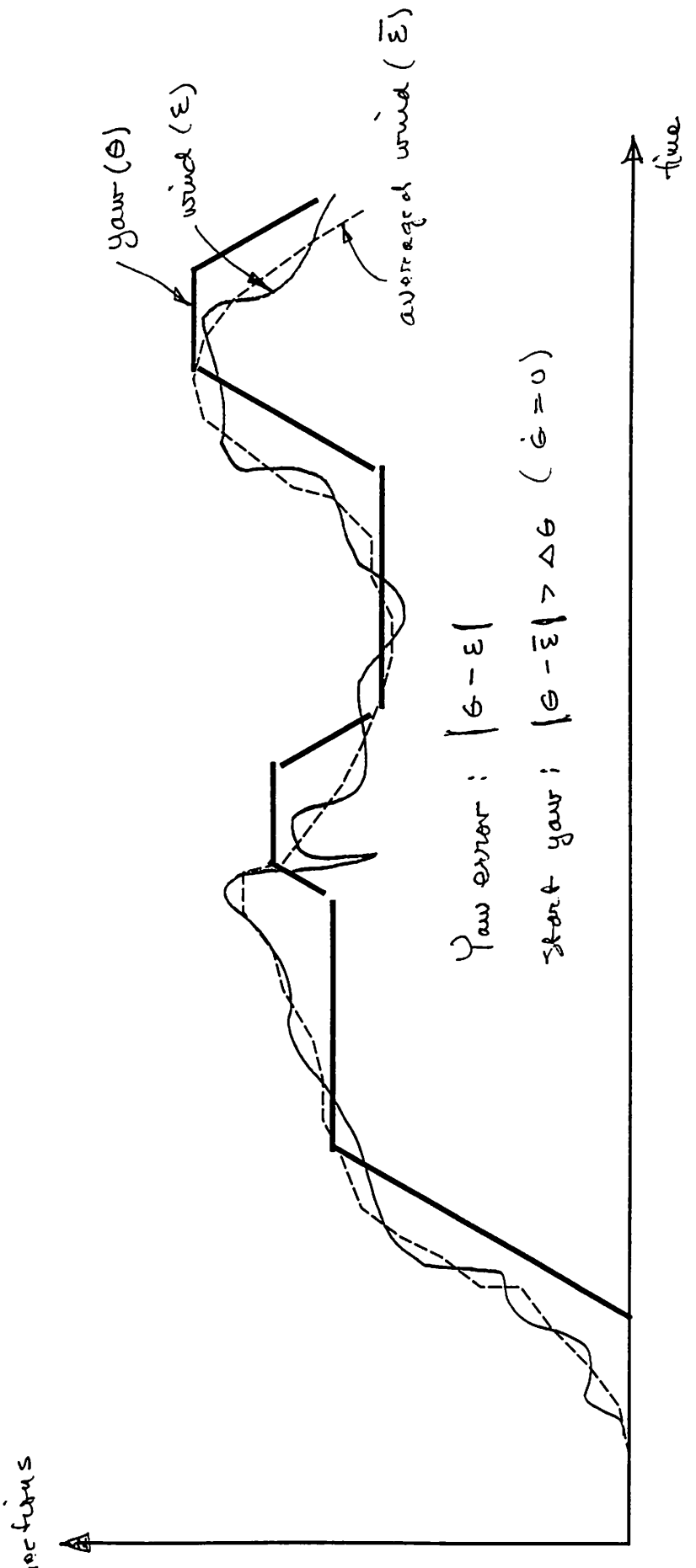
Directions
time
yaw (θ)
wind (ε)
average of wind ($\bar{\varepsilon}$)
yaw error : $|\theta - \varepsilon|$
start yaw : $|\theta - \bar{\varepsilon}| > \Delta\theta$ ($\dot{\theta} = 0$)

Fig 14

						Yaw dead band	(°)			
		Tyaw	3	4	5	6	7	8	9	
		60	(sec)							
	N of yawings		4666	3264	2115	1563	1109	877	660	
	Time of yawing		9904	9673	6866	6239	4855	4438	3623	
	Max yaw error		42,5	43,3	43,4	44,2	46,5	46,2	47,3	
	Min yaw error		-34,1	-34,3	-36	-36	-36,1	-38,1	-38,5	
	Std of yaw error		3,41	3,66	3,82	4,1	4,29	4,63	4,81	
		120	(sec)							
	N of yawings		2278	1527	996	730	541	457	337	
	Time of yawing		4604	4496	3038	2889	238	2267	1754	
	Max yaw error		68,5	69	69,5	69,9	71,8	71,9	73,5	
	Min yaw error		-32,8	-33,4	-34,8	-33,4	-34,8	-32,8	-31,2	
	Std of yaw error		3,79	4,01	4,17	4,44	4,6	4,97	5,18	

Fig 15

Std of yaw error of measurement ak 900702 (190 hours), mast 1.

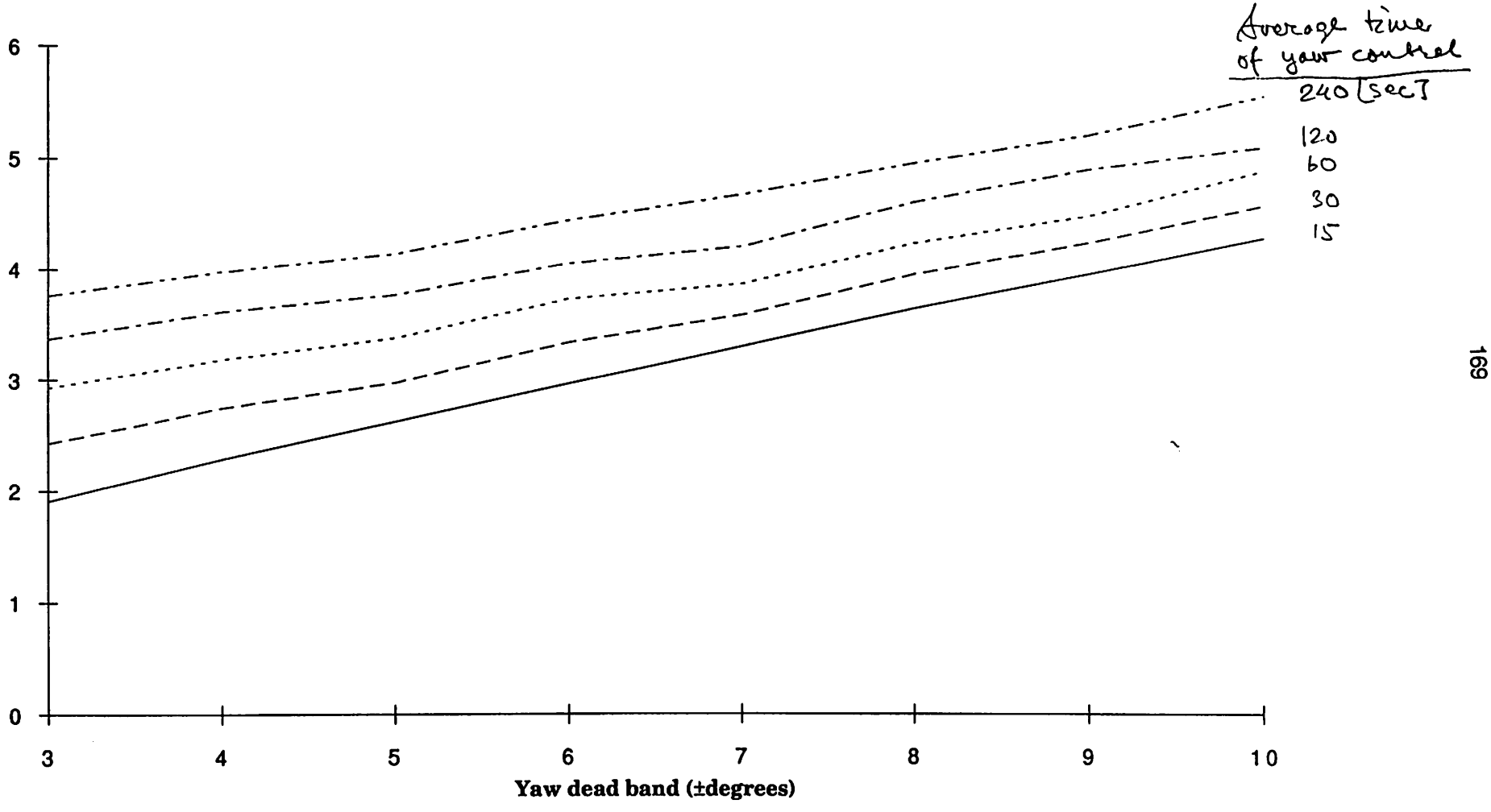

Fig 16

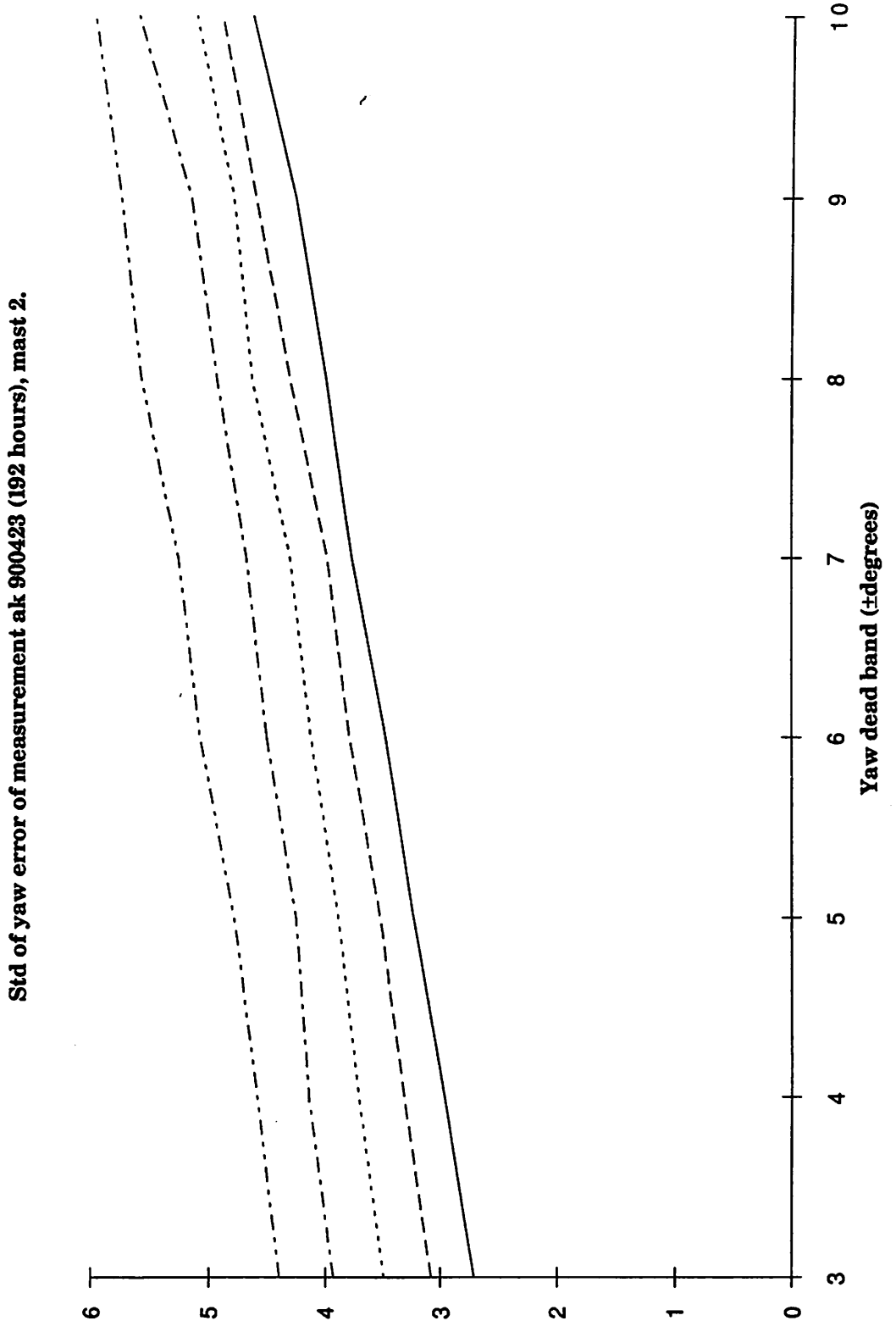
Std of yaw error of measurement ak 900423 (192 hours), mast 2.
6
5
4
3
2
1
0
3
4
5
6
7
8
9
10
Yaw dead band (±degrees)

Fig 17

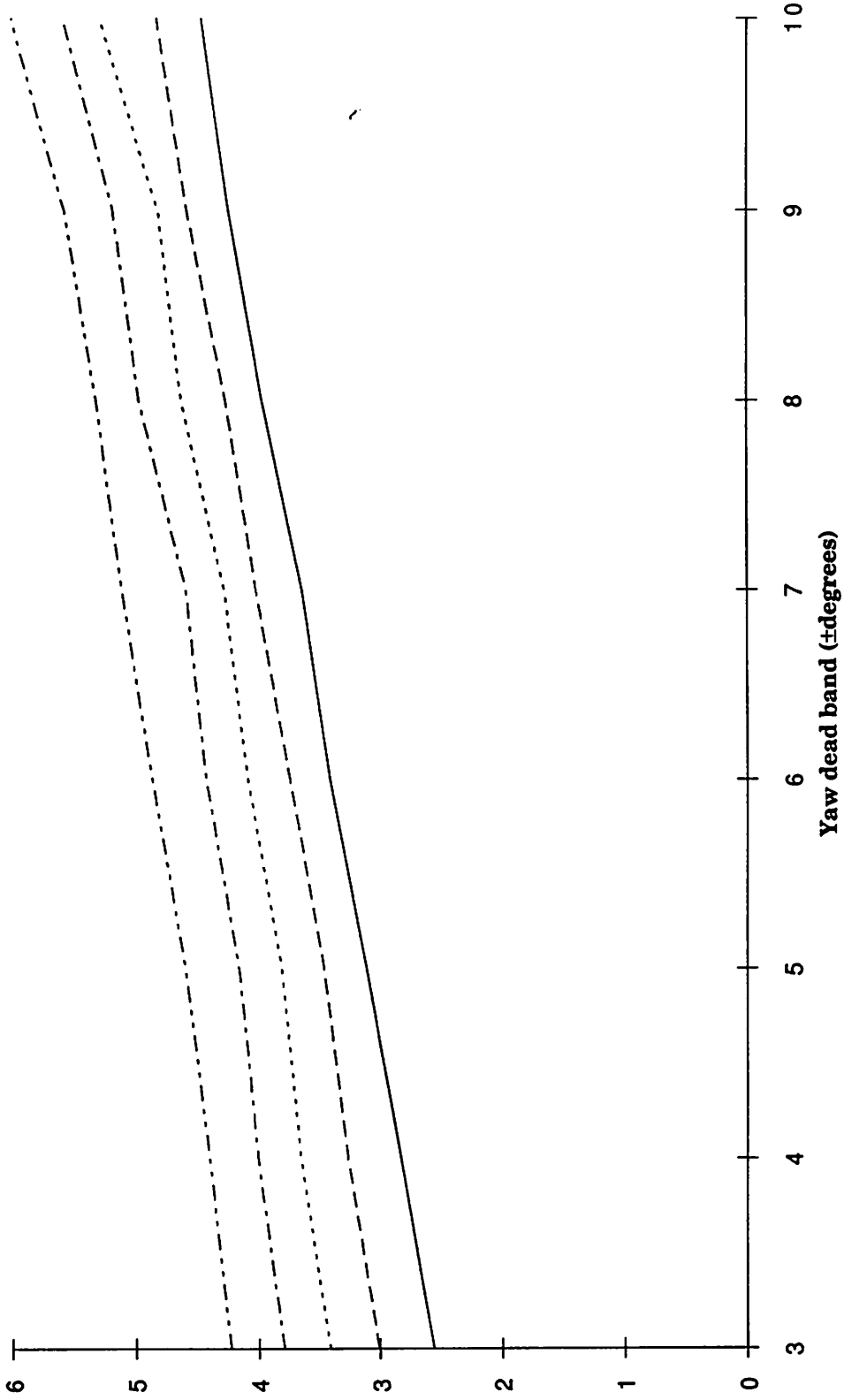
Std of yaw error of measurement ak 900423 (192 hours)
6
5
4
3
2
1
0
3
4
5
6
7
8
9
10
Yaw dead band (±degrees)

Fig 12

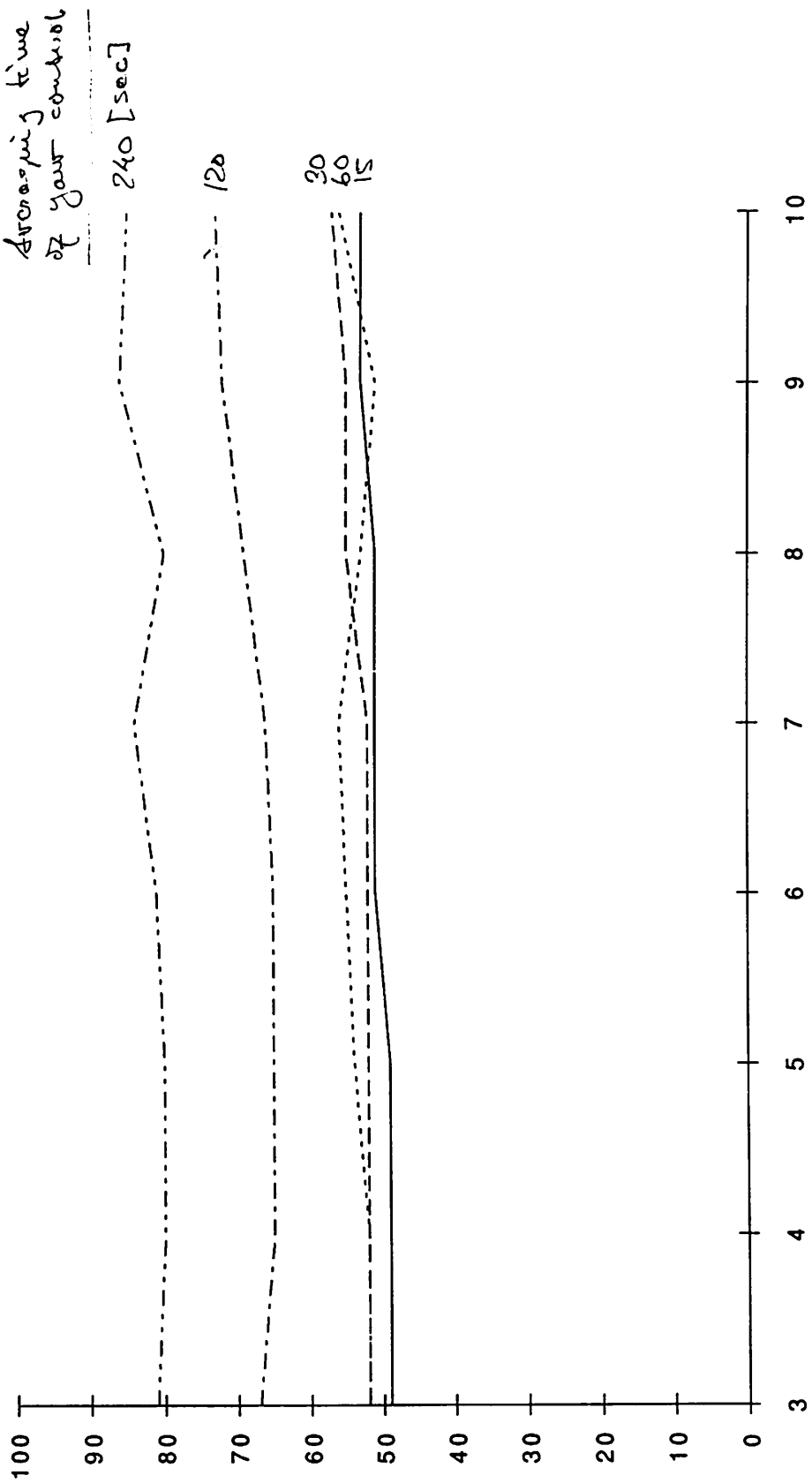

Max yaw error during measurement ak 900423 (192 hours), mast 2.

Fig 19

Time of yawing during measurement ak900423 (192 hours), mast 2.

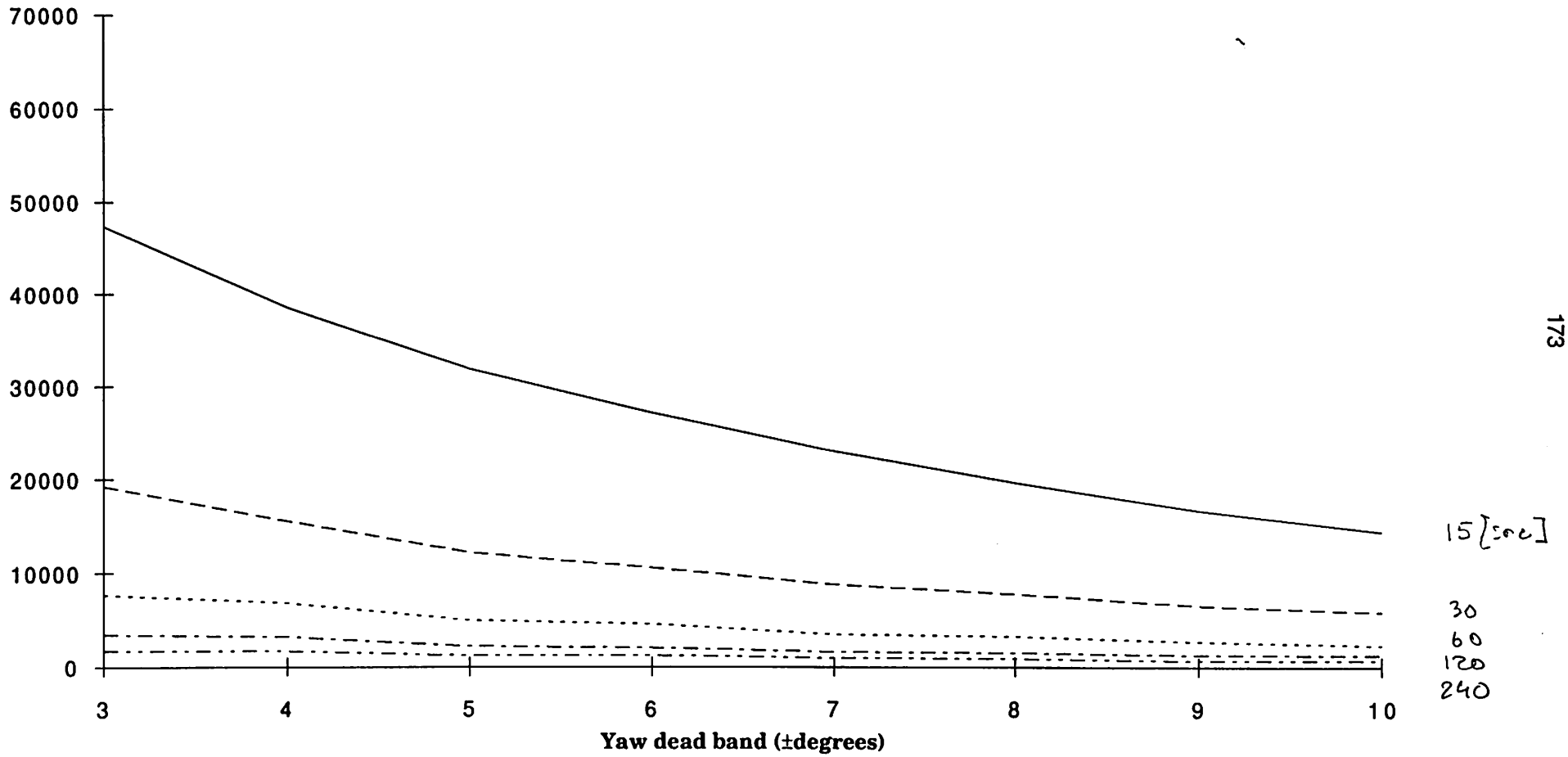

Fig 20

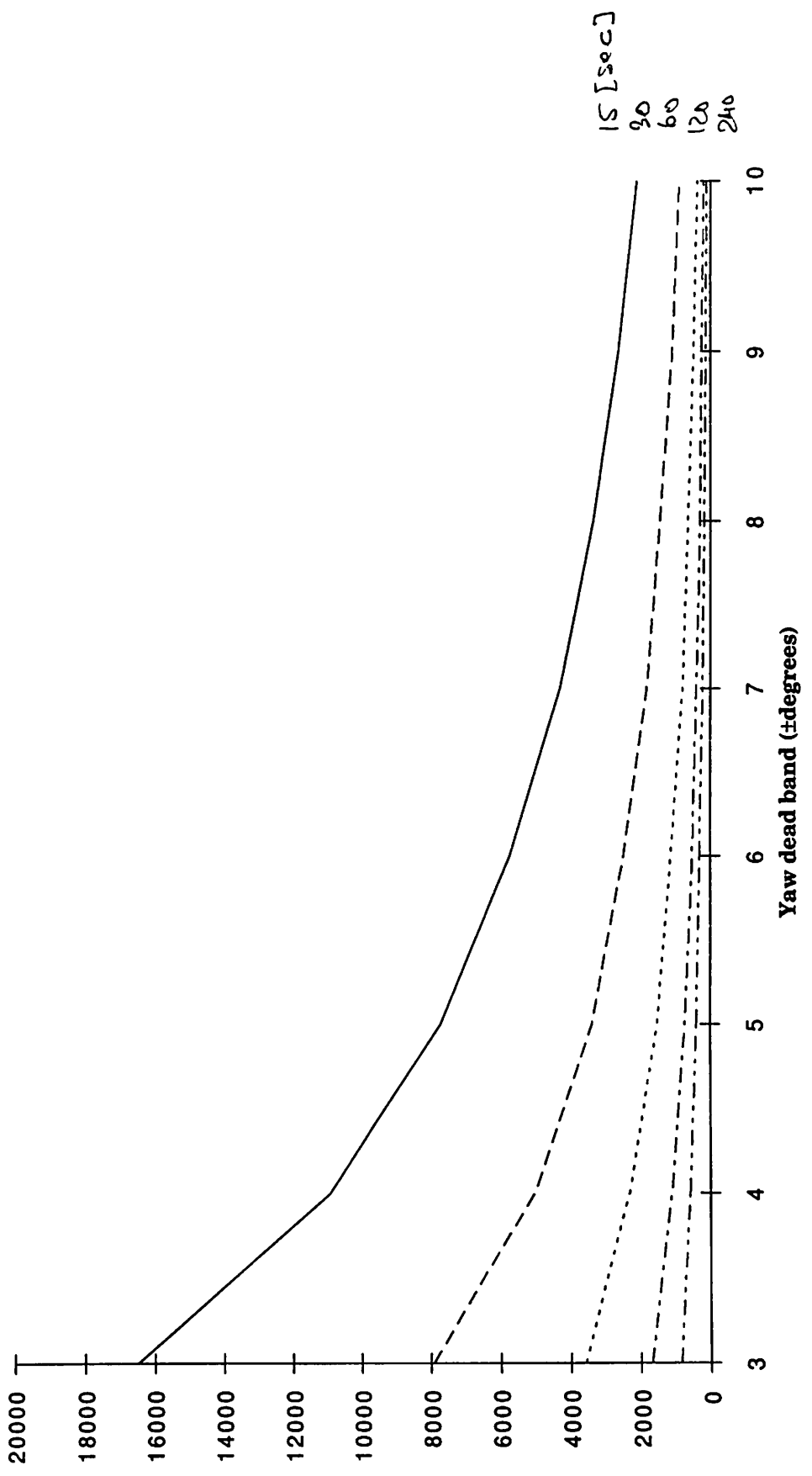
Number of yawings during measurement ak 900423 (192 hours) mast 2.
20000
18000
16000
14000
12000
10000
8000
6000
4000
2000
0
3
4
5
6
7
8
9
10
Yaw dead band (±degrees)
15 [sec]
30
60
120
240

Fig 21

SOME ASPECTS OF GUST MODELLING OF TURBULENT WINDS IN THE ATMOSPHERIC BOUNDARY LAYER

IEA Wind Meeting 7-8 March 1991, FFA, Sweden

Hans Bergström
Department of Meteorology, Uppsala University
Box 516
S-751 20 Uppsala
Sweden

1. INTRODUCTION

Variations of the wind occur over an immense range of time scales, from climate variations of periods thousands and millions of years to turbulent fluctuations with periods much less than a second, where the energy is eventually dissipated into heat.

Wind fluctuations of time scales shorter than about an hour are to a large extent turbulent, i.e. of a stocastic nature. To describe the turbulent wind field, statistical methods are therefore needed. Important information is gained by analysing the variances of the wind components, together with other second order moments.

These statistical properties do not, however, give any direct knowledge about the size distribution of the turbulent eddies. This information may be acquired using spectral analysis. By determining spectra of a time series of the turbulent wind, we will be able to tell how large portion of the turbulent energy which is found at different frequencies, i.e. the size distribution of the turbulence elements in relation to their energy content from a statistical point of view.

The spectral analysis technique has since long been used in meteorology, and methods have been developed to get generally valid, normalized, spectral curves, taking into account the effects of thermal stability, height above ground and surface roughness, which will all influence the spectral characteristics of the turbulent wind for individual situations. Thus with some knowledge of the climatological statistics of mean wind and stability, the normalized spectra may be utilized to determine the spectral characteristics at any new site.

The construction of large wind energy conversion systems (WECS) has produced an increasing demand for basic data on the turbulence properties of the atmopsheric boundary layer wind field, necessary when calculating load, fatigue and dynamic response of the systems. In order to be able to take into account

non-linear effects in these calculations, it has sometimes been argued that spectral models could not always be used for WECS modelling, especially not when dealing with two bladed turbines. Instead models using times series of the wind as input would be preferable.

But time series can for obvious practical reasons not be used directly when the calculations are meant to be representative of the whole lifetime of a turbine, say 30 years. During the last decade or so, however, several gust models have been proposed in the literature, as an alternative instrument to analyse the turbulence to get the necessary information. These gust model definitions are somewhat arbitrary, and it is not straightforward to use the results of such gust statistics as it will depend upon the choice of gust model

A technique often used in fatigue calculations is the *rain flow count* (RFC) technique. It is originally a method to evaluate varying loads and to describe load spectra for fatigue analysis. It may thus be an advantage to use the same technique when analysing the atmospheric wind field to get a statistical description of the turbulence. One reason for this is that the RFC statistics will include long period cycles with large amplitudes which other gust model formulations will filter out, and which may be of importance when estimating the lifetime of the turbines.

Which type of turbulent wind description is best to use then? The spectral representation is to be prefered from a pure meteorlogical point of view, as it very elegantly compress detailed information on the scales of the turbulent wind and their relative importance to the total turbulent kinetic energy. Also the knowledge about atmospheric boundary layer wind spectra is large today, as they have been studied intensively for several decades.

On the other hand, the wind turbine designer may sometimes prefer to use gust model statistics. To determine the type of wind descriptions which is really best to use in this context, comparisons with direct measurements on wind turbines of e.g. forces and thrusts should be done. The choice of wind description may also be dependent upon the type and size of the wind turbine. The lack of a theoretical and physical foundation for the gust models does, however, speak in favour of the spectral description.

The aim here is not to answer the question about the choice of wind description, but to shed some light upon problems connected to the use of gust models when analysing atmospheric wind data. Especially the use of the rain flow count method will be treated in somewhat more detail.

2. GUST MODEL COMPARISONS AND SENSITIVITY TESTS

Three types of gust models are commonly quoted in the literature: 1) *the zero-passage model*, 2) *the top-valley model*, 3) *the velocity difference model* (Powell and Connell, 1980; Bergström, 1987). To these models we may also add: 4) *the rain flow count model*. Models of type 1, 2 and 4 have been compared in Bergström (1990), where also a detailed description of the models may be found.

One major difference between the rain flow count model and the other two models is that in the others each part of the wind time series may only enter into one gust, while the RFC definition allows the gusts to be nested into each other so that one large cycle may contain many medium size cycles, and a lot of small size cycles. In this particular point the RFC model has some resemblance with the spectral analysis, as it is capable of decomposing the time series into variations of different time scales.

All gust models give as output jumps in the wind velocity over some time intervals according to the model definitions. Alternatively we may say that the turbulent wind time series will be decomposed into a series of gusts with given *amplitudes*, A, and *durations*, T. The statistical distributions of these amplitudes and durations may then be studied to estimate the occurrence of gusts of different sizes.

A comparison between these distributions reveal that, as could be expected, the result will depend upon the choice of model. As could be expected from the gust model definitions, the RFC gust description results in a much higher probability of large amplitude gusts as compared with the two other models, who both give quite similar results (cf. Bergström, 1990).

Of course the gust statistics, as well as the spectral characteristics, of the turbulent wind field will also depend both upon the atmospheric conditions, such as mean wind speed and thermal stability, and upon the boundary conditions at the surface, especially then the roughness but also topographical features. This clearly illustrates the need to carefully pick out representative data when making gust statistics or, which should be preferable, generalize the statistics e.g. by non-dimensionalizing with relevant physical parameters in analogy with what is done when generalizing the results from a spectral analysis of the tubulent boundary layer wind field.

One such parameter is the standard deviation of the wind speed, σ_u, which is also affected by both the atmospheric conditions and by the surface properties.

It is easy to determine and we may get more generally valid amplitude statistics by first dividing the amplitudes with σ_u. Examples of normalization with σ_u are shown in Section 4.

When making the gust statistics it is not obvious how the prefiltering of the measured turbulent wind signal should be made. The choice of filter may depend both upon the type of wind turbine the statistics should be applied to, and the size of the turbine. Some sensitivity tests have therefore been carried out to illustrate how the gust statistics are affected by prefiltering of the data. These tests were also presented in Bergström (1990).

It is also important to be aware of the frequency response of the anemometer used to measure the turbulent wind, as various types of cup- and propeller anemometers may have quite different time constants, and of course hot-film and sonic anemometer data need to be low-pass filtered if the gust statistics are to be directly compared with data from instruments with less good frequency response.

The effect of low-pass filtering is most dramatic when the gust duration distribution is studied. This is shown in Figure 1 for the RFC model, and in Figure 2 for the zero-passage model. The probability for some given gust duration differs about an order of magnitude between the statistics using non-filtered data and when applying a 10 s mean value low-pass filter before the gust analysis is made.

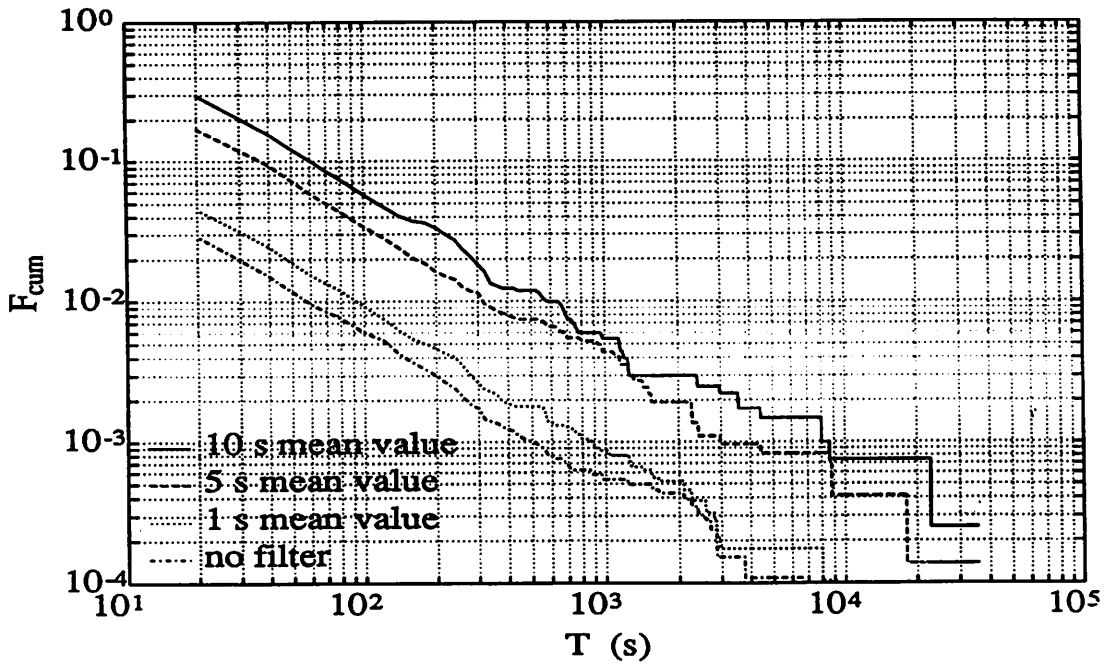

Figure 1. Cumulative distribution for the gust periods of the RFC model. Shown is also the influence of low-pass filtering the data.

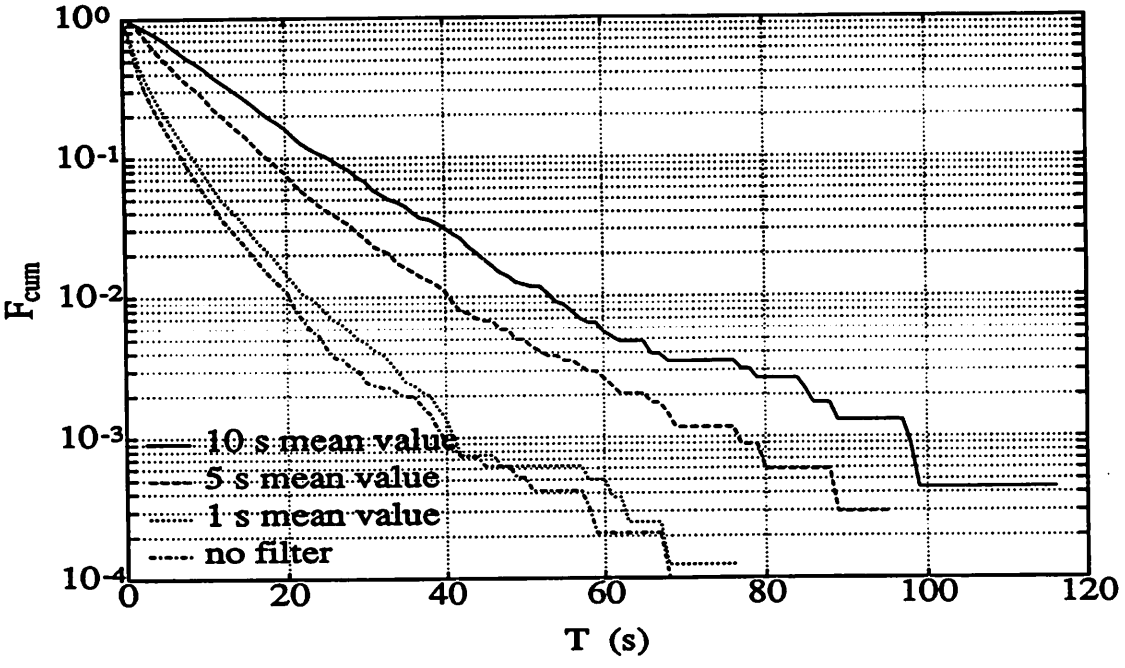

Figure 2. As Figure 7 but for the zero-passage model.

The difference between the two models is also striking. The capability of the RFC model to catch very large cycles is manifested by the fact that the maximum periods are of the order several hours, while the zero-passage model gusts are no more than a couple of minutes long. Of course one could maintain that the longest RFC cycles are to be associated with variations of the mean wind speed, but as we shall see in the next section, the correlation between large amplitudes and long duration is not overwhelming. In fact the correlation coefficient is just 0.16 when the whole population of RFC cycles for the run shown in Figure 1 is considered, but is increased to 0.35 when just gusts with periods greater than 100 s are included, and to 0.42 including only gusts longer than 500 s.

We have thus demonstrated that the statistics arrived at using different types of gust models may vary quite a lot, and one should keep this in mind when using such statistics. Also prefiltering of the data, made either by the anemometer itself or later on by applying mathematical filters, highly influences the results, both as regards the gust amplitude and duration distributions.

The actual choice of gust model is therefore of importance to the wind turbine designer who will not or can not use a spectral description of the turbulent wind field. The RFC model then looks somewhat more promising, comparing the gust mo-

dels, as it is capable of catching cycles in the wind signal which are nested into each other, and not just partition the time series into consecutive gusts. The problem then remains to try to understand the behaviour of the RFC cycles and to seek for methods to make the RFC statistics generally valid and possible to the wind turbine designer to include in his load and fatigue calculations.

3. A COMPARISON BETWEEN RFC AND SPECTRA

Due to the capability of the RFC model to allow cycles to be nested into each other, the RFC statistics and the spectral representation of a turbulent wind signal may just be two methods of getting similar information about the frequency distribution of the wind fluctuations. To test this two sine waves with the periods 60 s and 20 s, and with the phase shifts $\pi/3$ and $\pi/8$ respectively, were put together into a time series, given by

$$u = \sin(t+\pi/3) + \sin(3t+\pi/8)$$

as illustrated in Figure 3.

This 'two periodic' time series were used as input to the RFC model and its spectral characteristics were determined using the usual FFT technique. The

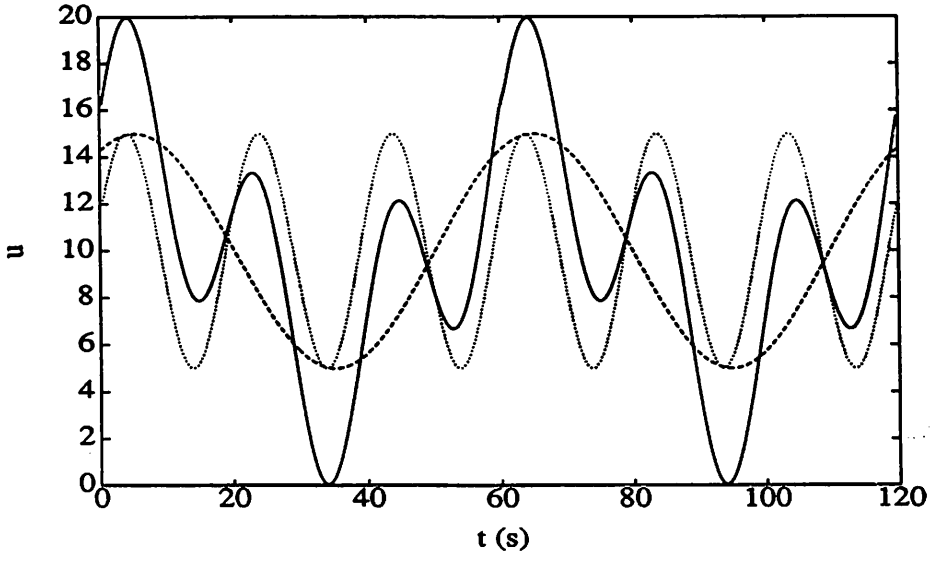

Figure 3. Composite time series (full line) made up from two sine waves with periods 60 s and 20 s, and with phase shifts $\pi/3$ and $\pi/8$, given by the dashed and dotted lines respectively.

spectral curve shows just two distinct peaks corresponding to the periods of the two sine waves. This clearly illustrates the capability of the spectral technique to resolve the time series into its two parts.

The RFC model analysis could be presented in frequency distributions of the cycle amplitudes and periods. Two amplitudes of 6 and 20 units are found corresponding to the cycles seen in Figure 3. The period or length of these half-cycles turns out to be *8 s* and *30 s*, which is *not* in accordance with the periods of the original two sine waves. But if we study Figure 3 carefully, we see that the period of the smaller amplitude cycle is indeed 8 s, while the time between minimum and maximum values is 30 s, just as is the period of one of the sine waves.

This simplified test thus shows that the spectral calculations reproduce the two periods included in the time series, while this is not true for the RFC model. This does not, however, say that the RFC technique is in error of any kind, only that it will partition the time series into cycles whos periods may not agree with the two original periods. But as can be seen from Figure 3 the period 8 s is indeed a *true* period of the composite time series.

The RFC model might in this sense be prefered to the spectral model, as the 8 s cycle in the resulting time series is the one a wind turbine should feel, and not the period 10 s of the 'hidden' original sine wave. On the other hand this is a very simplified situation with only two periods included. When it comes to 'the real thing', i.e. the turbulent atmospheric boundary layer wind, it is composed of fluctuations within a wide frequency band, and not of a few distinct frequencies, so that the above difference may be of inferior importance to the actual choice of model.

4. RFC STATISTICS

In this section we will look into some detail regarding the statistical distribution of rain flow count cycles. We will also look into the problem of how it may be possible to generalize the statistics to make the results independent of atmospheric and surface conditions.

The RFC cycles may be studied using two methods. In the first one only the magnitudes of the cycle *amplitudes* and their distributions are considered, together with the *period* or *duration* of the cycles. These two parameters may be stu-

died separately or together in a two-dimensional distribution. In doing this we loose, however, the information about the level at which the RFC cycles occur, i.e. we will only keep the knowledge that e.g. a cycle of amplitude 5 m/s and period 20 s has occurred, not knowing if the cycle was observed between 5 and 10 m/s or between 10 and 15 m/s.

If we want to keep information about the level at which the cycles occur, we have to make a kind of three-dimensional distribution. A matrix may be formed where on the x-axis is the wind speed from which the RFC cycle starts, and on the y-axis the speed at which the cycle ends (cf. Ganander and Johansson, 1988). Dividing both axes into classes of width 1 m/s we get a number of boxes, or elements in the matrix, which may contain statistical information about the actual cycle it corresponds to. This could be e.g. number of cycles, mean period of the cycles or the minimum period.

The data used in this section is from the WECS site Alsvik on the island of Gotland in the Baltic Sea, where two 42 m high meteorological towers are equipped with fast response cup-anemometers and wind vanes at 7 levels in both towers, measuring both wind speed and direction at a sampling rate of 1 Hz.

The towers were primarily located for the purpose to take measurements in the wakes behind the four 180 kW wind turbines at the site. In order not to complicate the RFC analysis with the influence from wakes, the tower where an undisturbed flow is measured has been chosen according to the current wind direction.

The analysis has been restricted to data from the 30 m level. Data from 7 weeks in April and May 1990 has been used, during which the mean wind speed varied between 1 and 17 m/s. The site is located right at the coast line, so that winds from the western sector come from the sea, while easterly winds come from the interior of the island. Both these sectors are present in the data set, which thus represents a rather wide range both as ragards mean wind speed, stability and surface roughness.

4.1 Amplitude and period statistics

Let us start by looking at the amplitude statistics. The cumulative distributions from the 7 runs are shown in Figure 4. The great diversity in the atmospheric conditions during which these runs were taken is clearly manifested in this plot. The amplitude corresponding to the probability 10^{-4} varies for these runs between 7 and 14 m/s.

To generalize the amplitude distribution we now simply divide the amplitudes with σ_u, the standard deviation of the wind speed. This has been accomplished by first determining σ_u for consecutive 1 hour periods during each run, whereafter a smooth curve has been fitted to the data.

The result is shown in Figure 5. The distributions from the 7 runs now fall close together into one general curve. Using standard meteorological relations between mean wind, stability and surface roughness, it is then possible to determine the amplitude distribution for any desired atmospheric and surface condition.

Looking at the distribution of the lengths in time of the RFC cycles, shown in Figure 6, they seem to be independant of the conditions during which the measurements have been taken. That is the size of the cycles as regards the variation in wind speed is highly affected by the atmospheric conditions, while the distribution of the duration of the cycles is not. It is also almost linear in a log-log representation, at least for cycles longer than 10 s.

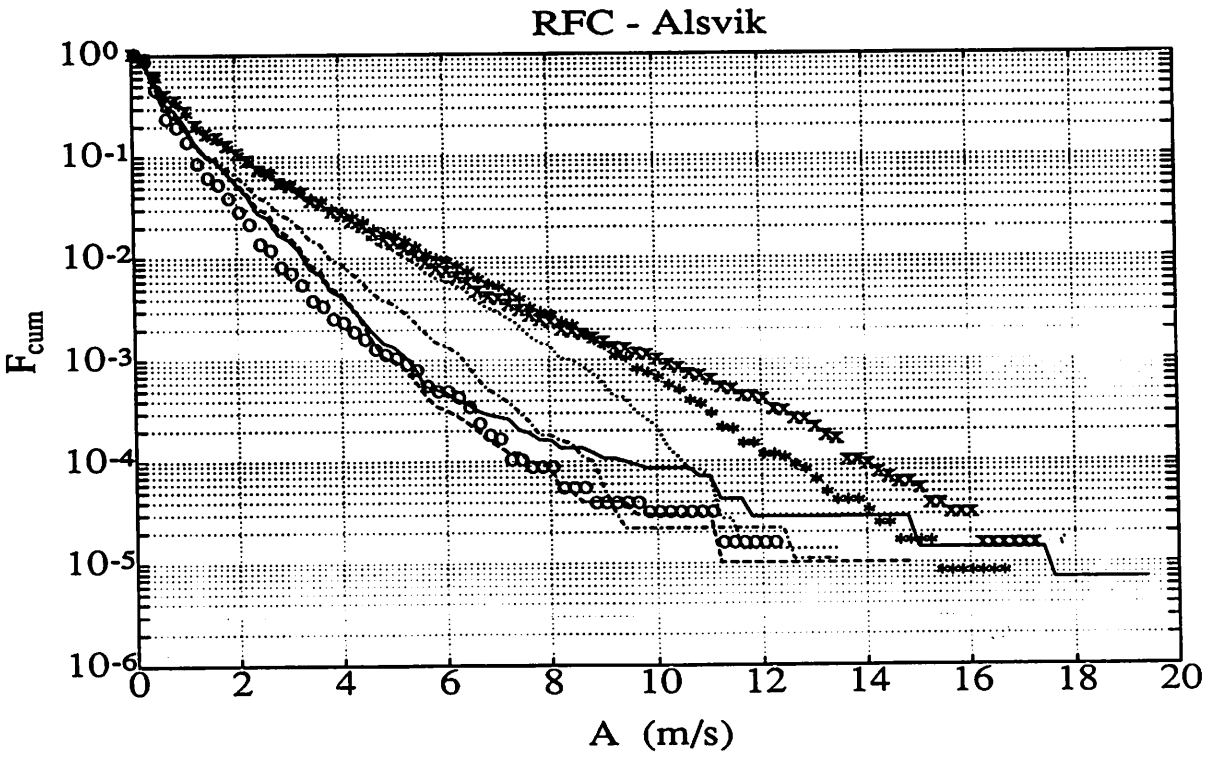

Figure 4. Cumulative distribution of RFC cycle amplitudes at Alsvik for 7 runs during April and May 1990, each about one week long.

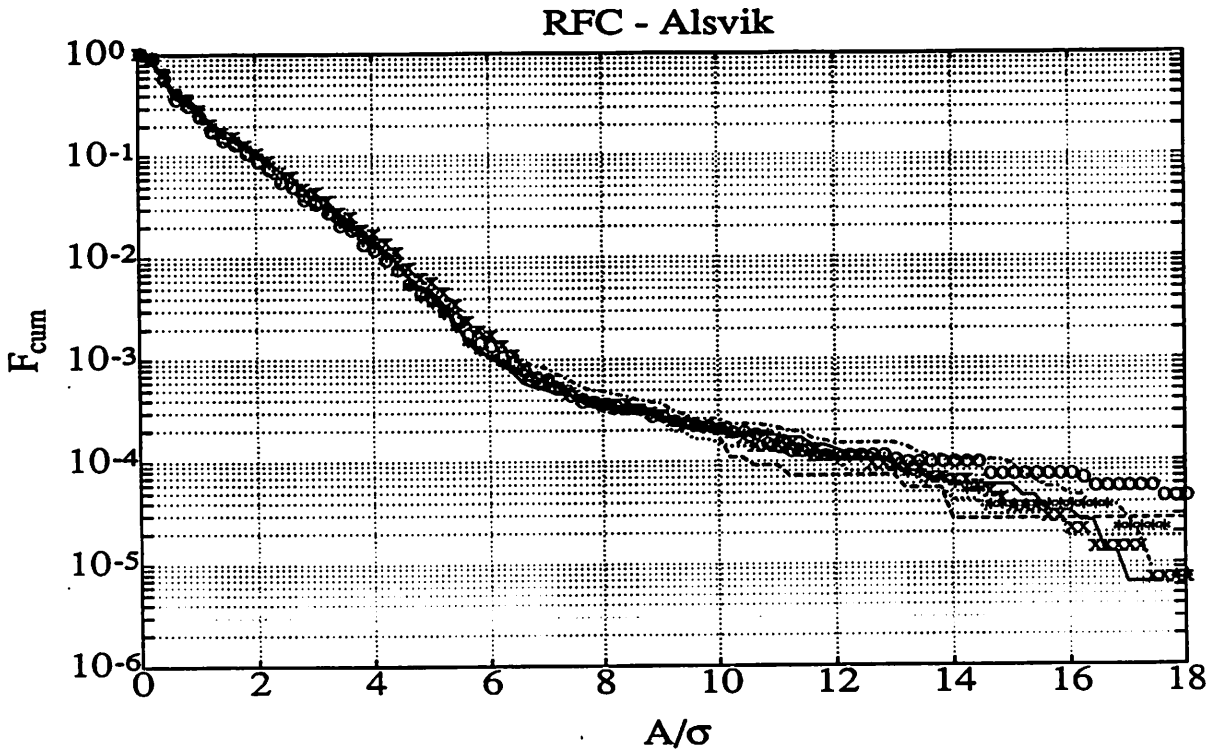

Figure 5. As Figure 4 but the amplitudes normalized with σ_u.

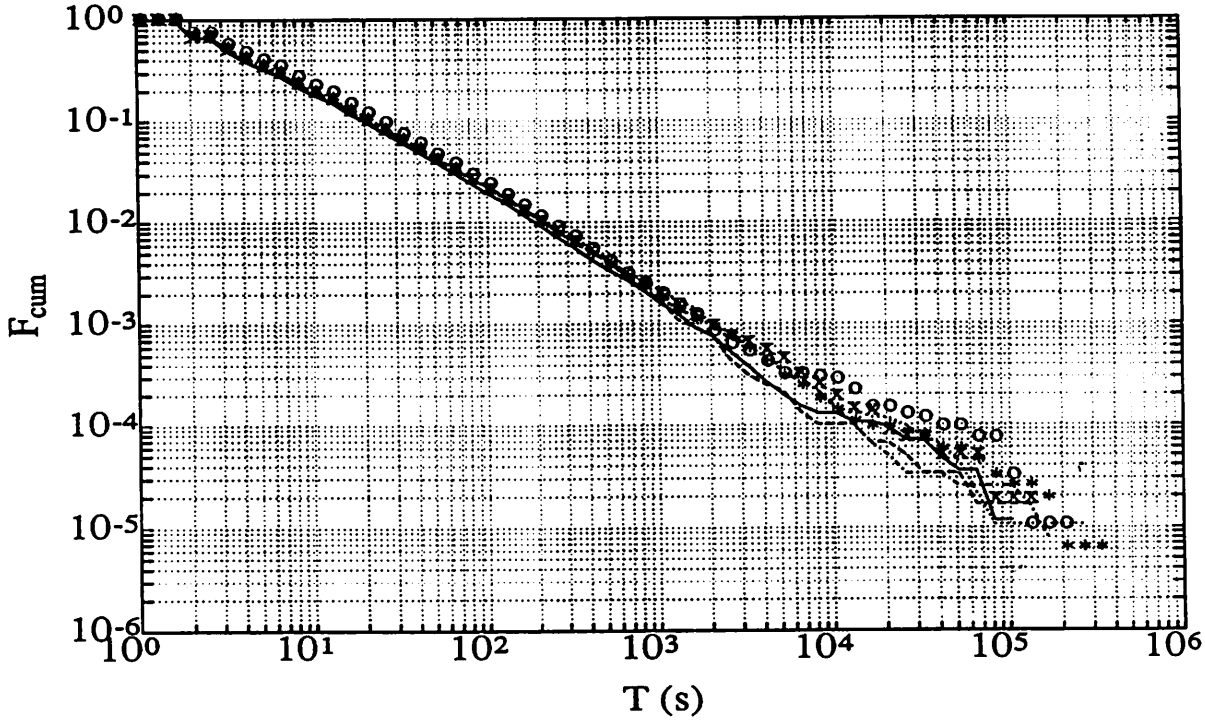

Figure 6. As Figure 4 but for the RFC cycle periods.

4.2 Two-dimensional amplitude/duration statistics

In search for a relation between RFC cycle amplitudes and durations, it seems plausible to assume that the large amplitude gusts should be the ones with the longest periods. This is to some extent true as may be seen from Figure 7, showing a plot of amplitude versus duration of the RFC cycles from one of the runs. The tendency is clearly towards the expected increase in period with growing amplitude, but large amplitudes are found also for rather short periods and vice versa, resulting in a small correlation coefficient between the two, only 0.16 for this particular run.

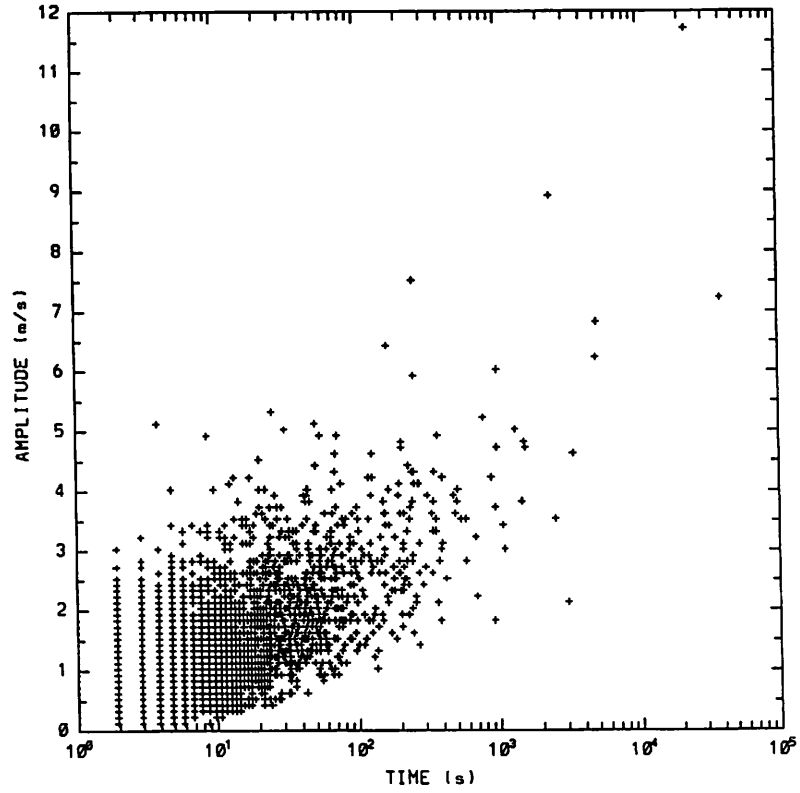

Figure 7. Example of a scatter diagram between RFC cycle amplitude and period using data from 1 week of measurements at Alsvik, 30 m level.

But the correlation coefficient is sometimes a poor judge of a relationship. Instead we determine the conditional cumulative distributions of the amplitudes, i.e. we divide the data into 7 intervals according to the period of the cycles, choosing an approximately logarithmic separation. The result is shown in Figure 8, from which it is obvious that the probability for large amplitude gusts increase dramatically with increasing gust duration. The median amplitude varies

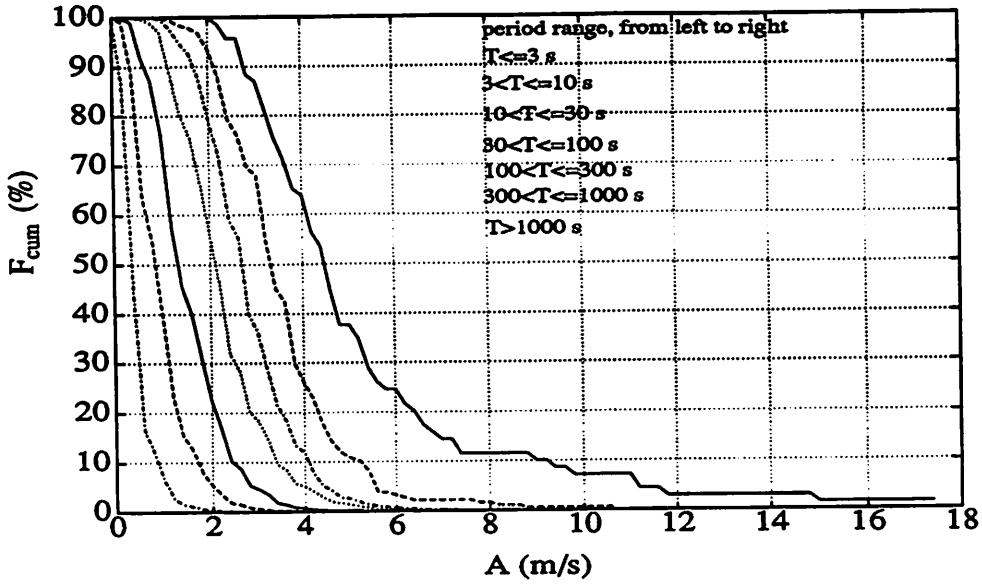

Figure 8. Conditional cumulative distributionss of RFC cycle amplitudes using data from 1 week of measurements at Alsvik, 30 m level.

between 0.3 m/s for gusts shorter than 3 s, to 4.5 m/s for durations larger than 1000 s. At the 10% level the corresponding figures are 0.8 m/s and 9 m/s for this particular run.

Two examples of the complete two-dimensional RFC amplitude-duration distribution is shown in Figures 9-10, where the amplitudes have been normalized with σ_u. Contour lines are drawn for approximately logarithmically spaced percentages from 0.001% to 30%.

As above, concerning the cumulative amplitude distribution (cf. Figure 4), the difference between these two runs was originally very large. After normalizing the amplitudes with σ_u, the two-dimensional distributions from these two runs agree quite well. Of course there are differences in the details, and between the individual runs, but as a whole the normalization with σ_u works quite well.

Putting the data from all 7 runs together, we get the normalized two-dimensional amplitude-duration distribution of the RFC cycles shown in Figure 11, which compared to the ones from the individual runs gives a smoother appearance, especially at the smaller percentages. Of course one must be careful when judging the lowest probabilities, but the shape of the distribution ought to be rather correct, and the axis of centre do imply the increased probability for large amplitude gusts with increasing duration.

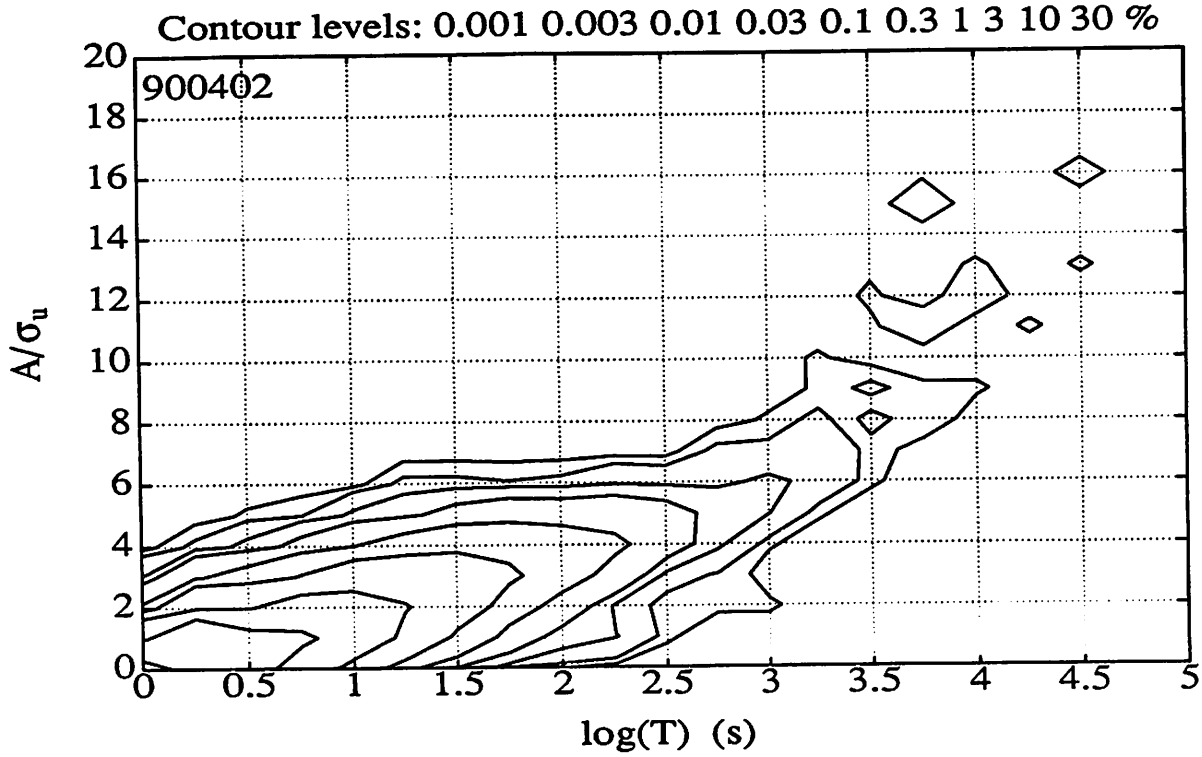

Figure 9. Two-dimensional amplitude-duration probability for the RFC cycles from run 900402, 30 m level. Amplitude normalized with σ_u.

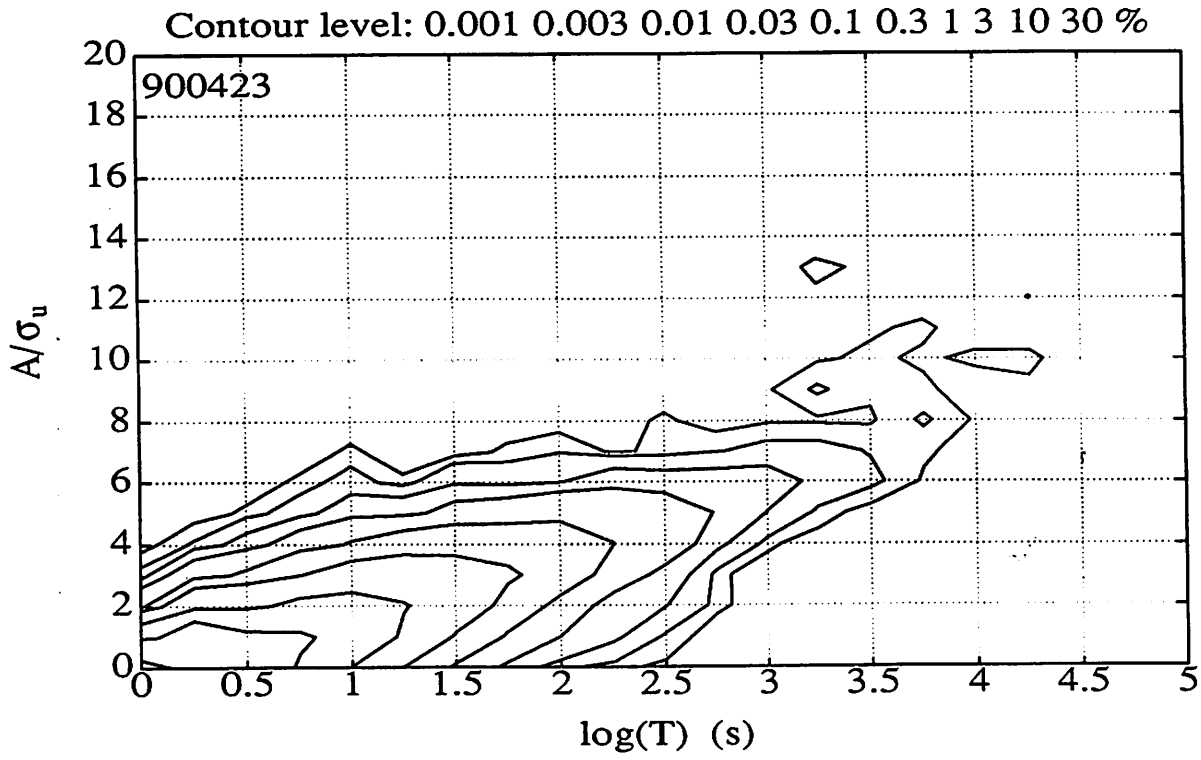

Figure 10. As Figure 9 but for run 900423.

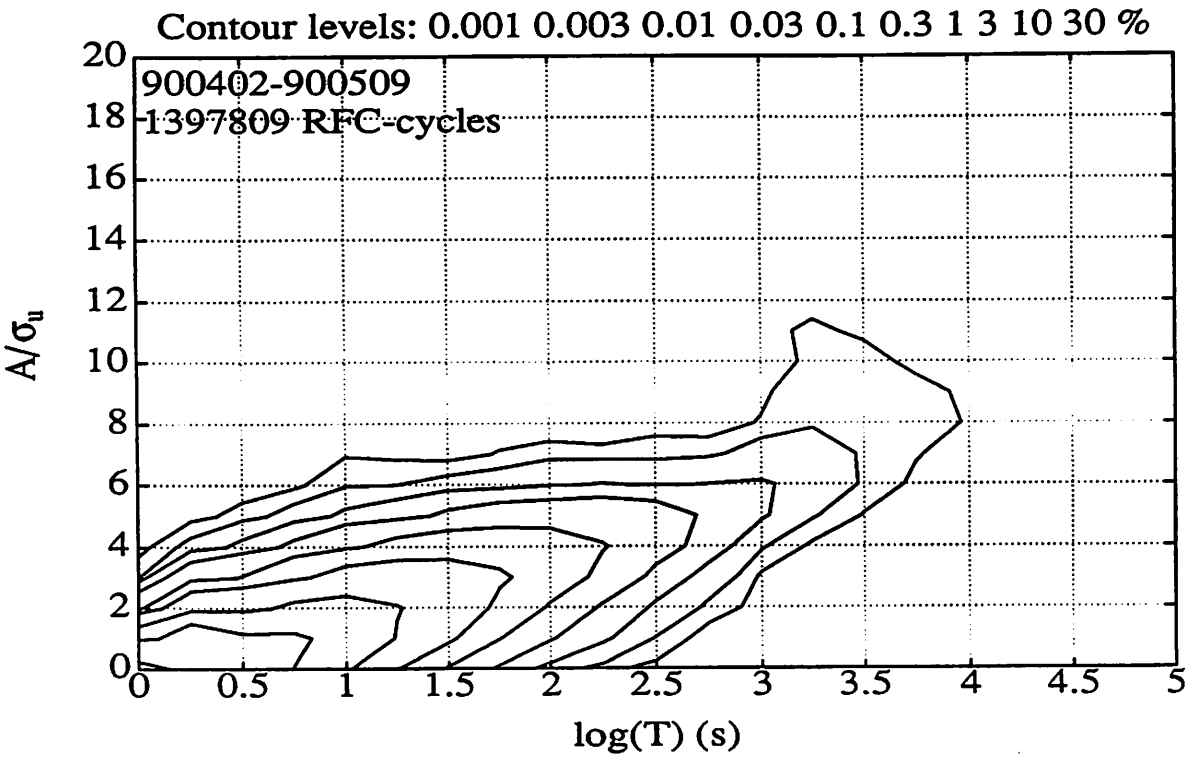

Figure 11. Mean normalized two-dimensional amplitude-duration RFC cycle distribution from 7 runs, each about one week long.

4.3 Matrix statistics

A second method to study the RFC cycle distribution and also keep the information about at which level in wind speed the cycles occur, consists of forming a 'wind from-wind to' matrix. The elements of the matrix may then be e.g. the number of cycles, or more generally the percentage of the total number of RFC cycles, ocurring between the different wind speeds. This gain of information about the wind speed level of the cycles will be at the expense of a direct relation between amplitude and duration.

Let us compare the resulting matrices from the same two runs compared above. They are shown in Figures 12-13, where lines of logarithmically spaced percentages are drawn. As for the amplitude-duration distribution, the difference between the two is large. The main reasons for this are the higher mean wind speed during run 900402, and that during this run the wind direction was from the sea, while during run 900423 the wind direction was from the land sector a large part of the time.

This has as a consequence that the centre of the distribution is found at higher wind speeds for run 900402 due to the difference in mean wind speed, and that the

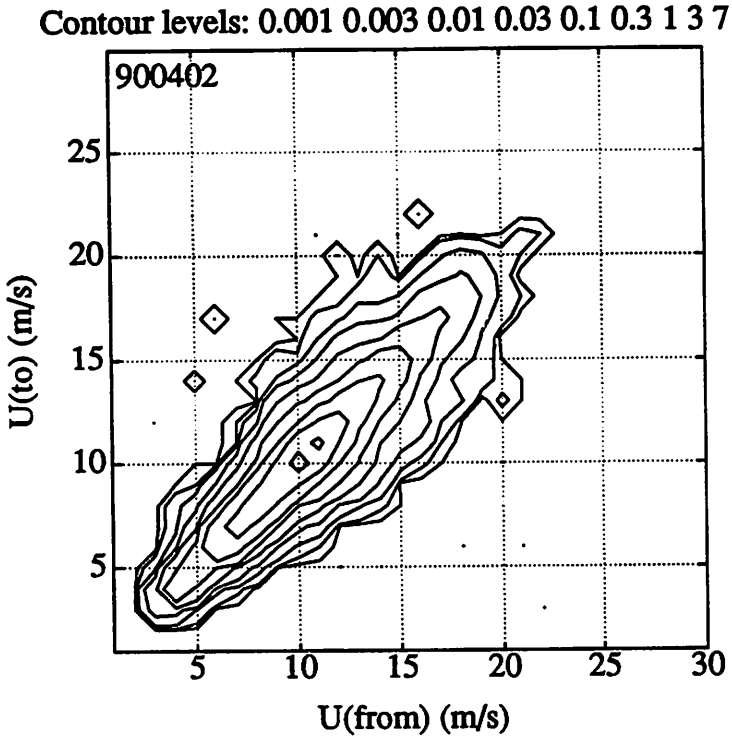

Figure 12. RFC cycle matrix from run 900402.

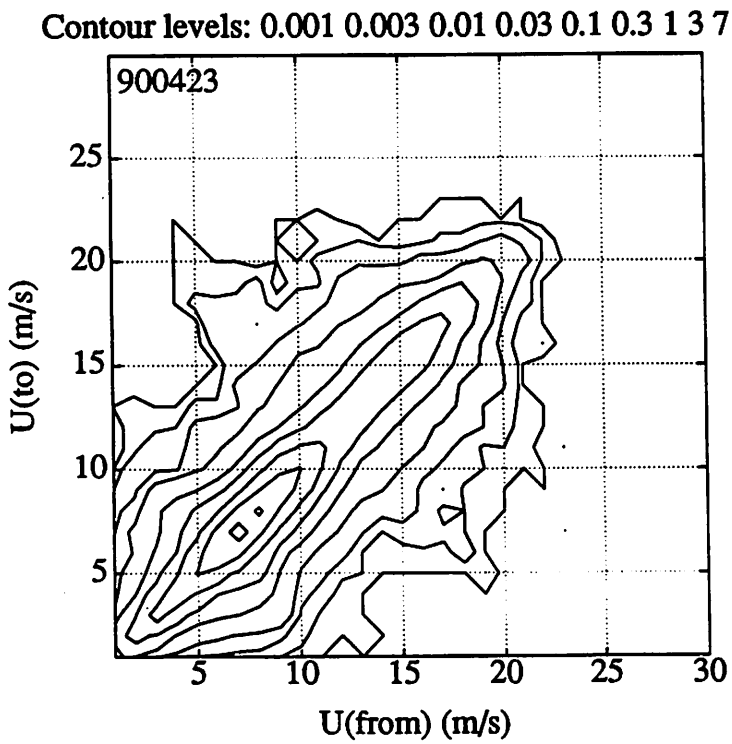

Figure 13. RFC cycle matrix from run 900423.

distribution of run 900423 is wider due to the larger roughness length with winds from land, and maybe also a larger influence from the thermal stratification.

Attempting to generalize these matrices, we normalize as above with σ_u, the standard deviation of the wind speed. The result is shown in Figures 14-15. Compared to the original matrices, the normalized ones are much more similar. But the locations of the centres of the distributions are still affected by the different mean wind speed during the two runs, while the widening effect of the higher surface roughness with easterly winds in run 900423 is coped with by non-dimensionalizing with σ_u.

In Figure 16 the mean matrix from all 7 runs are plotted. The mean wind speed for these runs is 6.4 m/s, which is not far from the expected long term mean value at 30 m, but as the mean wind seams to influence the appearence of the distribution, at least as regards its centre, one should be careful to check that the mean wind distribution is close to its climatological mean if such a mean matrix is to be used as a climatological mean.

Thus during this period of about seven weeks, although the mean wind speed is

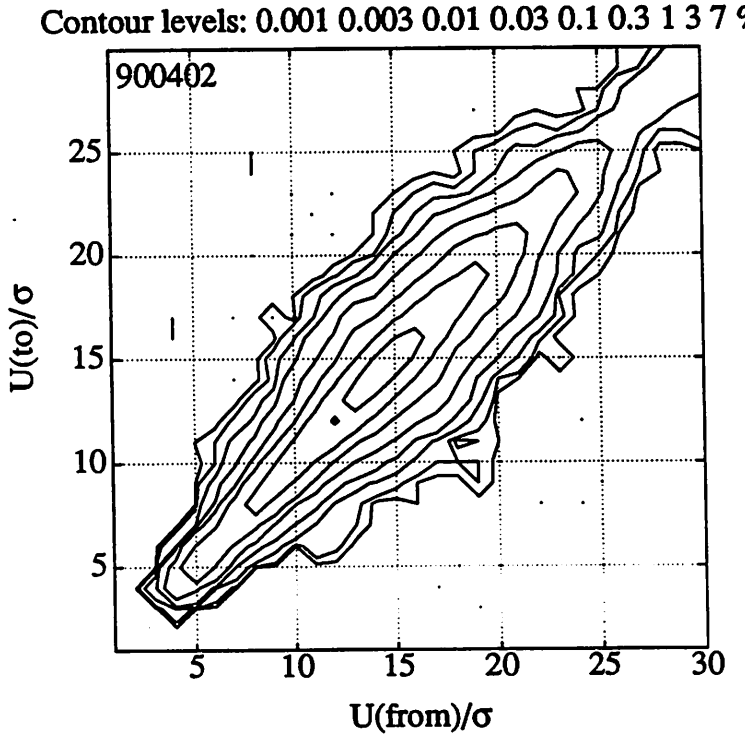

Figure 14. RFC cycle matrix from run 900402, wind speed normalized with σ_u.

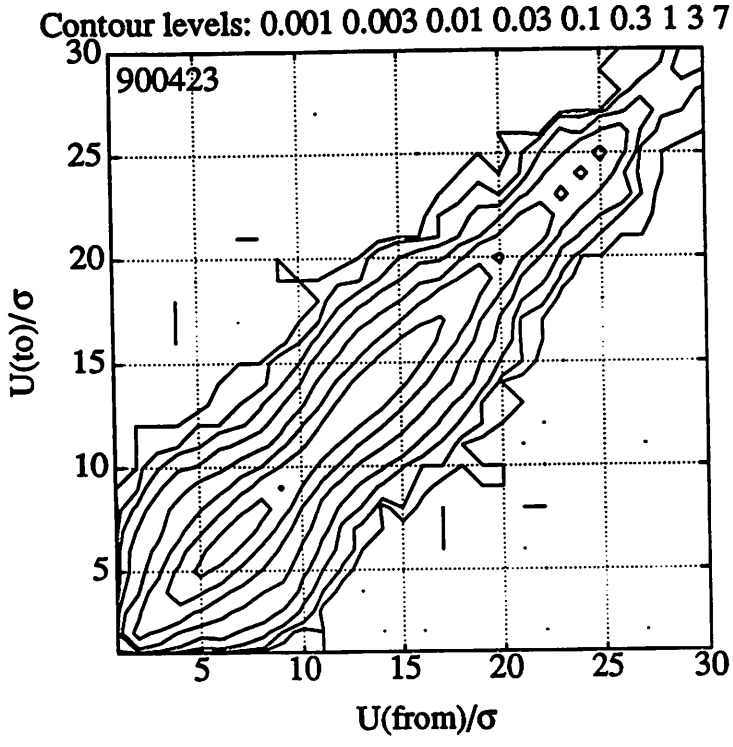

Figure 15. RFC cycle matrix from run 900423, wind speed normalized with σ_u.

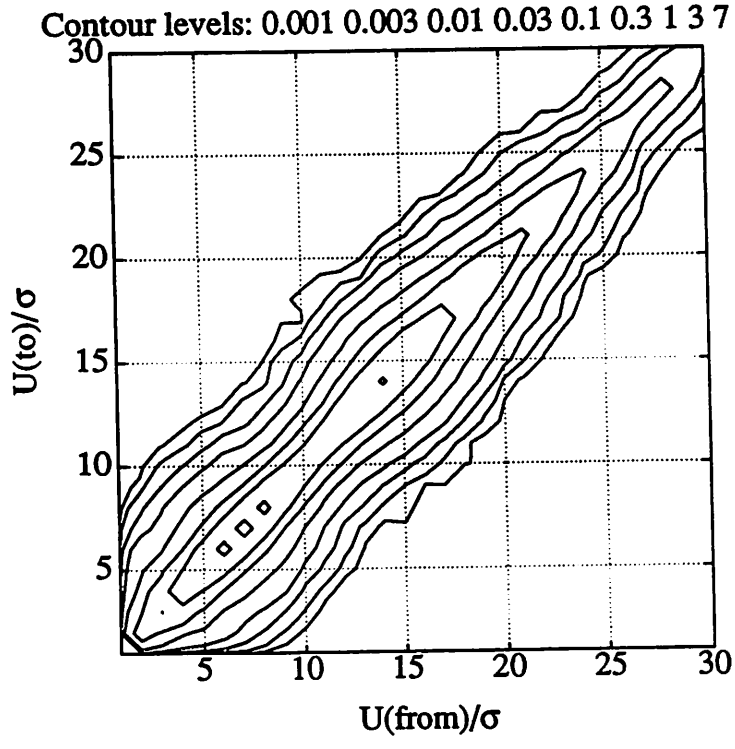

Figure 16. Mean RFC cycle matrix from 7 runs. Wind speed normalized with σ_u.

close to its climatological mean, the distribution is not, as periods with either high or low winds tend to be too frequent compared to medium wind conditions. This is also seen in the mean matrix, where two broader regions in the distribution are found, one for values of U/σ_u around 7, one for values around 14.

5. SUMMARY AND CONCLUSIONS

The need for a statistical description of the turbulent atmospheric wind field not using the spectral concept, has brought forward several ideas concerning gust models. We have seen, however, that this concept does not give general results, as the gust model definitons are somewhat arbitrary.

The results are also affected by eventual filtering of the data before the models are applied. This could be either pure instrumental filters, caused by the time constants of the anemometers, or mathematical filters applied to the measured time series.

The choice of filters is also arbitrary to some extent, and they may have to be chosen according to the type and size of the wind turbine. Some gust models need a high pass filtering of the data in order to be able to identify the gusts. All models should be fed with low pass filtered data, mathematically and/or instrumentally. Especially the choice of low pass filter will affect the gust duration statistics.

Most gust models will divide the measured time series into consecutive gusts, having some amplitude and length in time. The rain flow count model, however, is capable of nesting the gusts (or cycles) so that a cycle with a long period may contain a number of shorter cycles, which in turn may contain even shorter cycles, and so on, which seems somewhat more appealing.

In that sence the RFC model also has some resemblance with the spectral technique. But a comparison between the two, using a simple time signal composed of two sine waves differing a factor of three in period, reveal that while the spectral analysis bring back the frequencies of the sine wave components, the RFC model does not. Instead it picks out cycles with periods actually observed in the composite time series, which somehow seems more in accordance with what a wind turbine will 'feel'.

The gust models do, however, lack the theoretical foundation which the spectral analysis rests upon. Although many details regarding the spectral

characteristics of the turbulent wind flow are still missing, e.g. regarding the conditions in complex and hilly terrain, the knowledge is far greater than as regards the gust amplitude and duration statistics. If possible, the spectral description should therefore be preferable to use, directly or as the basis for further analyses.

REFERENCES

Bergström, H., 1987. A statistical analysis of gust characteristics. Boundary-Layer Meteorol., 39, 153-173.

Bergström, H., 1990. Gust statistics using the rainflow count technique. Proceedings of European Community Wind Energy Conference, Madrid, 10-14 September 1990, pp. 150-153.

Ganander, H., and Johansson, H., 1988. Fatigue design by using a modified RFC description of the wind. Proceedings of AWEA National Conference, 18-22 September 1988, Honolulu, Hawaii.

Powell, D. C., and Connell, J. R., 1980. Definition of gust model concepts and review of gust models. Battelle Pacific Northwest Laboratory, PNL-3138, 95 pp.

DESCRIPTION OF WIND AND TURBULENCE AS INPUT TO LOAD CALCULATION MODELS.

by

Ann - Sofi Smedman
Department of Meteorology, University of Uppsala
S-751 20 Uppsala, Sweden

Presented at IEA meeting 7-8 Mars 1991 in Stockholm.

ABSTRACT.

The Näsudden wind turbine is a 2 MW machine with two blades and a hub height of 77 m. The turbine is situated 1500 m from the coast line in smooth level terrain. However, after five years of operation a large crack on one of the blades suddenly appeared. It was probably caused by fatigue.

Analysis of meteorological data reveal the importance of the influence of atmospheric thermal stability on the wind and turbulence structure and thus on the loads on the turbine. For example very stable stratification over the sea during spring and early summer created strong low level jets which increase the wind shear dramatically and also the cyclic loading on the blades.

A very simple method has been constructed, which relates the variation in bending moment at the blade root in the flap wise direction to two meteorological parameters; turbulence intensity and wind shear. A time simulation model (VIDYN) has been used to separate the effect on loading from the two factors. The bending moment can thus be calculated from measurements of σ_u/U and $\Delta U/U$ which often are available from routine wind speed measurements on towers.

The model can so far only be used for wind turbines of the same kind as the Näsudden turbine i.e. large two bladed stiff machines. We believe that similar results (with different numerical constants) are likely to be valid for any conceivable turbine design after proper 'calibration' with a time simulation model like VIDYN.

LIST OF SYMBOLS.

This paper is a joint effort of research in two fields, meteorology and mechanics. Thus the symbols sometimes denote two different variables which both are common notation in each field.

A = coordinate transformation matrix

c = blade cord

c_d = drag coefficient

c_t = thrust coefficient

c_l = lift coefficient

dv/dh = vertical wind shear

dD = blade segment drag force

dL = blade segment lift force

D = rotor diameter

$EI(r)$ = blade stiffness at radial position r

f_0 = external loads in the fixed system (o)

F = frequency distribution

F_{q_i} = generalized force of the i-th degree of freedom

h = vertical coordinate

h = hub height

I_{jk} = mass inertia property along principal axis k of rigid body j

k = von Karman constant = 0.40

L = turbulent length scale

m = variation from the mean of bending moment in flap direction

m_j = mass element

M = mean bending moment in flap direction

M_j = generalized mass of mode j

n = frequency

q_i = i:th degree of freedom

r = radial position of the blade element

r_0 = position of regarded mass point in an inertial coordinate system (o).

r_b = blade element position in blade coordinate system

R = rotor radius

$S(n)$ = power spectrum

T = total kinetic energy

u = longitudinal wind component

u = deflection of the blade in flap direction

u_* = friction velocity

U = mean wind speed

U = total kinetic energy due to deflections

v = lateral wind component

v = deflection of the blades in edge direction

v_0 = wind speed in an inertial coordinate system (o)

vn = wind speed at hub height

V = total potential energy

w = vertical wind component

w_0 = inflow speed relative blade element

w_b = inflow speed in blade coordinate system

z = height above ground

z_0 = roughness parameter

z_0 = vertical component of r_0

α = teetering movement of hub relative main shaft

α = D/2L

β = cone angle

δ_3 = angle between blade and teater hinge

φ = angle of rotation

Φ_{u_j} = shape of j th mode in flap direction

Φ = inflow angle

ω_j = frequency (rad/s) of j th block deflection mode

Θ = yaw angle of the nacelle

ρ = density of air

σ = standard deviation

τ = tilt angle relative a horizontal plane

1 INTRODUCTION.

For large scale exploitation of wind energy it will be necessary to site wind turbines not only in flat coastal areas but also in rough inhomogeneous terrain. In order to maximize the use of costly land with a suitable wind resource wind turbines will also be put together in wind parks, where they will interact with each other.

Atmospheric turbulence and wind shear are recognized as the primary cause for cyclic loading of horizontal axis wind turbines. The level of turbulence as well as the wind shear are often increased in rough terrain and wind turbines operating in the wake of another will experience additional fluctuating loads also due to additional turbulence and wind shear.

In the future when performing meteorological site investigations it will not be sufficient only to map down mean wind condition. Turbulence structure and wind speed variation with height will probably be equally important. Variation of blade loads must thus be described as functions of simple meteorological parameters which can easily be measured or calculated from routine observations.

An attempt is now made to relate the variation of flap wise bending moment of one blade of the 2 MW wind turbine at Näsudden in Sweden to statistical parameters such as turbulence intensity and mean wind shear.

2. THE NÄSUDDEN WIND TURBINE AND THE SITE.

The wind turbine is a 2 MW upwind machine. It has two steel blades rotating with 25 rpm and the diameter of the rotor is 75 m. The hub is rigid with the primary shaft tilting 10° and the rotor has no cone angle. The height of the tower is 77 m and it is made of concrete. Cut-in wind speed is 7 m/s and at rated wind speed which is 12.5 m/s pitch control of the blades starts.

The Näsudden wind turbine is situated on a peninsula at the southwest coast of the island of Gotland in the Baltic, Figure 1. The ground is quite flat, with

scattered juniper bushes. The distance from the machine to the shore line is 1500-2000 m for a wide sector from south over to northwest, with long unobstructed fetch over the open sea.

Judging from the topography one should expect the meteorological conditions at Näsudden to be 'ideal' with steady winds coming from the sea most of the times, indicating low turbulence intensity and small wind speed gradients. Nevertheless after five years of operation, in the summer of 1988, a two meter long crack near the root of one blade in practice ended the life of the turbine. The crack could be diagnosed as appearing suddenly but the cause was fatigue. This severe damage had been preceded by several minor cracks earlier. The true cause of these fatigue damages is not clear yet but one possibility is that loading due to wind shear and turbulence was much stronger than anticipated. Also power fluctuations and yaw moment variations often exceeded calculated values.

Turbulence measurements have been taken on the 145 m meteorological tower at the site (Figure 1) during several field experiments. It can be shown [1] that the influence of the cross wind components (v,w) is small for a horizontal axis wind turbine during normal operational conditions. Thus the necessary information on the approach flow is usually assumed to be the variation in the longitudinal wind component (u). Turbulence statistics of the u component have been thoroughly investigated [2,3] and power spectra, variances as well as coherence functions have been compared with results found for ideal sites [4]. Measurements from those experiments generally indicate a decreased level of turbulence at Näsudden with winds coming from the sea.

However, meteorological measurements recently performed at Näsudden show that deviations from 'standard atmospheric condition' are more than exception to the rule. Two meteorological situations, one with increased level of turbulence (horizontal roll circulations) and the other with strong wind shear (low level jets), which are likely to substantially increase load variations are discussed in Section 5.

3. CYCLIC BLADE LOADING.

As stated in the Introduction the fluctuations in the approach wind field are the main cause for blade loading of a horizontal axis wind turbine. The cyclic blade loads can be divided into a deterministic part and a stocastic part. For a turbine with constant rotation angular velocity loads which depend on the azimutal position of the rotor become periodic while the turbine rotates. These deterministic loads are due to wind shear, tower interference, gravity and to the rotation such as centrifugal forces. The stocastic loads on the other hand depend on the turbulent fluctuations in the longitudinal wind component.

3.1 Wind shear.

Most so far published investigations concerning blade and rotor loading are dealing with three bladed turbines with hub heights around 20-40 m [6,7,8,9 and 10]. For those rather small turbines the influence of the wind shear seems to be negligible [5]. However, for large two bladed machines the wind shear can be as important as the turbulence for the cyclic loads [11,12]

In wind energy applications only meteorological situations with fairly high wind speeds are of importance. During such events the atmosphere is usually assumed to be neutrally stratified and near the ground the variation of wind speed with height can be expressed by the logarithmic wind law

$$U(z) = u_* / k \ln(z/z_0) \qquad (1)$$

The difference in wind speed over a turbine rotor $(z_2 - z_1)$ is according to (1)

$$\Delta U = \text{Const} \ln(z_2 / z_1) \qquad (2)$$

and as the ratio of rotor diameter D and hub height h for different turbine sizes is approximately equal to one in most cases, we have

$$D/h = (z_2 - z_1)/[(z_1+z_2)]/ 2 = 1$$

$$z_2/z_1 = 3$$

and from (2)

$$\Delta U = \text{Const. } \ln(z_2 / z_1) \sim \text{Const.}$$

This means that the effect of the difference in wind speed over the rotor area should be the same for large and small machines.

However, as will be shown below, stratification can totally change the result. The effect of stratification on the wind profile also increases with height. The existence of internal boundary layers, which emerge from terrain discontinuities, can also affect the wind shear. Again a large wind turbine is more likely 'to see' different terrain than a small.

3.2 Turbulence.

Loads and structural responses of a wind turbine rotor are described in a rotating reference system and it is thus desirable to describe turbulence in the same system. Due to rotation of the wind turbine in the turbulent wind field, the turbulence seen from a point on a moving blade is altered. This is called 'rotational sampling'.

The effect of 'rotational sampling' on the spectrum of the longitudinal wind component is to redistribute energy from lower frequencies to the rotational frequency and its harmonics. There are several investigations, both theoretical [5,13,14] and experimental [15] dealing with this problem. The most commonly used method to calculate excitation of energy by rotation was first described in [5] and is built on expressions for the spectrum curve and the coherence function between different points on the rotor. As spectra and coherence depend on the scale of turbulence (L) and thus on stability and height above ground, the effect of 'rotational sampling' will also vary with those two parameters. Figure 2 taken from [5] shows the effect of α on the power spectrum , where $\alpha = D/2L$. The 'rotational sampling effect' increases with increasing α up to α=0.5. In the layer near the ground (the surface layer) L scales with height z but higher up in the transition layer the large eddies scale with the boundary layer height. It can thus be assumed that the 'rotational sampling effect' will be less pronounced for large turbines with hub height above 50 m.

Figure 3 shows an example of spectrum of the longitudinal wind component measured at hub height at Näsudden together with the spectrum of flap moment

at the blade root. From n ~ 0.03 the redistribution of energy because of rotation is evident.

3.3 Variation of flap moment of the blade.

A basic assumption for analyzing and modeling turbulence loads during stationary operation is that the loads from turbulence are random and independent of the cyclic deterministic loads and that superposition applies.

The variation of flap moment of a blade can be expressed

$$\sigma_m^2 = (\sigma_m^2)_{turb} + (\sigma_m^2)_{shear} + (\sigma_m^2)_{mean} \qquad (3)$$

where

turb = part of the variance depending on turbulence
shear = " wind shear
mean = " mean wind, gravity etc

To be able to separate the influence of the three different parts in (3) a simulation model has been run. The model VIDYN, which is described in the next Section, has been developed by Teknikgruppen AB and has been used during the evaluation of the two large wind turbine prototypes in Sweden situated in Maglarp and Näsudden.

4. THE VIDYN MODEL.

Up to now there exists a number of models which can be used to provide reliable estimates of the structural loads and fatigue damage experienced by wind turbines. Some of the models work in the frequency domain [6,9,10,12]. The input turbulence field can thus be expressed in spectral form and a 'rotational sampling' model like the one described in [5] can be used. However, to use spectral models one has to linearise the dynamic response of the turbine. This approximation is probably not important when dealing with fairly small three-bladed turbines as most investigators have done so far. However, for large two-bladed machines it is necessary to take all

nonlinearities into account.

The VIDYN model is developed as a time simulation model and has proved to be a useful tool for the designer of the overall mechanical system and also of the control system. The model is capable of treating all kinds of turbines and nonlinearities such as variable rotational speed and aerodynamic stall behavior.

A brief description of the principles used in the time simulation program will be given below.

4.1 Basic dynamic equations.

Derivation of the dynamic equation is based on Lagrange general formulation of dynamic system

$$\frac{d}{dt}\left(\frac{\partial T}{\partial \dot{q}_i}\right) - \left(\frac{\partial T}{\partial q_i}\right) + \left(\frac{\partial V}{\partial q_i}\right) = F_{q_i} \qquad (4)$$

In the following subsections these quantities will be described in some more detail.

4.2 Geometry.

All horizontal wind turbines consist of three main parts: rotor, nacelle and tower. The properties of these and the connections between them are characteristic for each wind turbine type. In the present model all the different parts are described as masses and stiffnesses (and aerodynamic data of blade profile), but the way of combining the main parts can be chosen rather freely. For example the rotor may consist of one, two or three blades and can be located up or down wind the tower. The connection between the primary shaft and the rotor can be a hinge, described as a spring and/or a damper. The yaw system, which primary aligns the nacelle to the wind direction may also be regarded as a hinge with spring and/or damping properties.

The geometry of the whole turbine system is shown in Figure 4a.

4.3 Degrees of freedom.

In order to describe the kinetic energy as well as the potential energy of the system, coordinates which describe the position of each part of the masses are introduced. These coordinates (q_i) are usually called degrees of freedom of the system. Normally they are distances or angles. Figure 4b shows the degrees of freedom used in VIDYN to describe the turbine system.

The deflection of the blades are described in the following way:

$$u = \sum_{j=1}^{m} q_{uj}(t)\Phi_{uj}(r)$$

$$v = \sum_{j=1}^{m} q_{vj}(t)\Phi_{vj}(r)$$

This model description of the blade (rotor) deflection is based on FEM calculations of the blade, which requires distributions of mass and stiffness along the blade. When regarding the whole of the rotor the flexibility of the primary shaft is taken into account. Each mode (j) is not only characterized by its shape ($\Phi_{uj}(r)$), but also by the generalized mass (M_j) and the frequency ω_j.
Figure 5 shows typical shapes of the three first blade modes.

4.4 Kinetic energy.

The kinetic energy of the whole system is the sum of kinetic energy of its parts:

$$T = \sum_{i}^{n} T_i$$

For rigid bodies the general expression of kinetic energy is calculated according to

$$T_j = \frac{1}{2}\left[m_j \dot{r}_{0j} \dot{r}_{0j} + \sum_{k=1}^{3} I_{jk} \omega_k^2\right]$$

The kinetic energy of the rotor is calculated as the integral along the rotor

$$T_r = \frac{1}{2}\int_{-R}^{R} \dot{r}_0 \dot{r}_0 dm \qquad (5)$$

where

$$r_0 = Ar_b \quad \text{and} \quad r_b = \begin{pmatrix} u \\ v \\ r \end{pmatrix} \qquad (6)$$

and thus

$$\dot{r}_0 = \dot{A}r_b + A\dot{r}_b$$

For simplicity in this case r_b is regarded as being fixed in rotor center which coincides with the inertial system (o).
The matrix A is a transformation matrix which contains all angles, time dependent as well as constant.

4.5 *Potential energy.*

Besides kinetic energy of different parts of the turbine system motions in vertical direction represent variation in potential energy.

Deflections of the system may also be treated as potential energy of the system. For one blade the potential energy due to deflection is

$$U = \frac{1}{2}\sum_{j=1}^{m}\int_{0}^{R} EI(r)(\Phi_{uj}''(r))^2\, dr = \frac{1}{2}\sum_{j=1}^{m}\left(q_{uj}(t)^2\, \omega_j^2\, M_j\right)$$

4.4 Generalized force.

The generalized force F_{q_i} will be calculated as the scalar vector expression

$$F_{q_i} = f_0 \frac{\partial r_0}{\partial q_i} \qquad (7)$$

where f_0 represents different external loads in the fixed system (o). The influence of aerodynamic loads is calculated in this way.

4.6 Aerodynamic loads.

The basic principle to calculate aerodynanical loads is to derive the total relative velocity felt by each blade element and express this velocity in the blade element coordinate system. This requires calculation not only of wind speed but also the velocity of the blade element.
The blade element at point r_0 has the velocity $\dot{r}_0$ according to (6). Assuming wind speed in mean wind direction together with wind shear, the wind speed at this point is

$$v_0 = \begin{pmatrix} vn \frac{dv}{dh} z_0 \\ 0 \\ 0 \end{pmatrix}$$

The inflow speed relative to the blade element is

$$w_0 = v_0 - \dot{r}_0$$

which is transformed to the blade element system by the matrix A^T, the transpose of A. Notice that $A^{-1} = A^T$ in this case. Thus

$$w_b = \begin{pmatrix} wxb \\ wyb \\ wzb \end{pmatrix} = A^T w_0$$

Knowing these inflow conditions makes it possible to calculate aerodynamic loads on a blade element dr by definitions of loads on an aerodynamic profile,

$$dL = \frac{1}{2} \rho \, c \, w^2 c_l(\Phi) \, dr \qquad (8)$$

$$dD = \frac{1}{2} \rho \, c \, w^2 c_d(\Phi) \, dr \qquad (9)$$

where

$$w^2 = wxb^2 + wyb^2$$

$$\Phi = \arctan\left(\frac{wxb}{wyb}\right)$$

and wxb and wyb represent the inflow conditions in velocities relative to the blade element coordinate system. This is shown in Figure 6.

The aerodynamic coefficients c_l and c_d are taken from experimentally determined values. The VIDYN model also takes influence factors into account according to [16].

4.7 Wind description.

As stated before, a realistic description of the fluctuating wind field as input to the model should be time series (real or simulated) from several heights within the rotor area. This requirement can not always be met and simplifications have to be made. For example in the runs analyzed in this investigation measured time series of the three wind components for three levels, representing the top, bottom and center of the rotor respectively, have been used.

4.8 Solution method.

The total system of differential equations are nonlinear in the q_i variables. But knowing q_i and $\dot{q}_i$ makes the system linear in $\ddot{q}_i$. This property of the system makes it possible to integrate numerically. From given values of $q_i(t)$ and $\dot{q}_i(t)$ the value of $q_i(t+\Delta t)$ can be found as the solution to the linear equation system.

Thus it is possible to find the solution without linearizing trigonometric functions or products and squares of variables.

4.9 Verification.

The model has been used extensively in the Swedish Wind Energy Program, especially for evaluating the measurements taken at the two Swedish prototypes (Näsudden and Maglarp). Comparison between measured and calculated values are given in [11]. Figure 7 shows one example of measured and calculated parameters from the Näsudden turbine. The comparison is displayed in polar plots and comprises three variables; power (a), lateral force (b) and blade root flap moment (c). All three curves very well reproduce the variation with phase angle.

5. MODEL SIMULATIONS.

The VIDYN model has been run for three meteorological situations which we have found to be typical for the Näsudden site. For all three cases the wind is coming from the sea.

5.1 The 'common simple case'.

The first case represent meteorological conditions which one would expect to find at a flat coastal site during summer when the thermal stratification is slightly unstable. The wind and temperature profiles are shown in Figure 8. The turbulence intensity σ_u/U is 0.07 at hub height and variances of wind components as well as fluxes of momentum and heat decrease smoothly with height.

Five simulations of a duration of one minute each have been performed. The meteorological input to the model is real time series of the three wind components at three heights (11, 77 and 135 m) which represent the lower and upper heights of the rotor and the hub height. The sampling rate of the measurements is 20 Hz and in the model a linear interpolation between the measuring heights is made.

5.2 Two special meteorological cases.

During spring and early summer when the sea surface is colder than the air, a strong inversion will form next to the surface over the sea. The air coming from the sea often has a low level wind speed maximum (*low level jet*) at heights between 50 to 150 m, which is in the height range of the rotor [17]. In Figure 9 the profiles of wind and potential temperature are given for the the modeled case. The stratification in the layer below ca. 40 m is unstable (the internal boundary layer over the land surface) whereas the stratification is very stable aloft. In this stable layer the turbulent motion is suppressed and the turbulence intensity at hub height is often as low as 0.02-0.03. However, the vertical wind shear is large and positive below the wind speed maximum and negative above. It is believed that the low level jet situation is very frequently occurring during the period of the year when the air is warmer than the sea surface.

Also for this case five simulations are run for one minute long time series measured at three heights.

When stratification is slightly unstable and wind speed is moderately high (>5 m/s) *horizontal roll circulation* is often observed at Näsudden [18]. Those rolls are aligned almost parallel to the mean wind and may occur in clear air or be revealed by the presence of cloud streets. They are believed to be caused by a combination of convective and dynamic instability. During roll conditions there is an increase in turbulent energy especially in the vertical component.

For this case one simulation has been performed. Again the measurements at three levels covering the passage of one roll (3 minutes) have been used as in- data to the model.

5.4 Simulations.

To be able to separate the influence of the three different parts in expression (3) of the total variation of bending flap moment, the VIDYN model has been run for the three meteorological cases described above. For

each case first a simulation with a constant mean wind speed as input was performed. The second group of simulations were run with a constant wind shear and finally simulations were made with real time series.

In addition 32 runs with different mean wind shear have been carried out for the 'common simple case'.
All simulations are made for wind speeds in the range 6 - 13 m/s i.e. with the turbine working without pitch control

6. RESULTS.

6.1 Simulations.

To be able to interpret the results from the model runs power spectra have been calculated with a FFT (Fast Fourier Transform) routine of the simulated time series of the blade root bending moment in the flap wise direction.

Figure 10 shows the contribution to the cyclic variation of flap moment from the three parts in expression (3) for one specific run. From the Figure it is clear that the variation caused by effects such as gravity and tower shadow when the turbine is working in a constant mean wind field (Figure 10c) can be neglected in comparison with turbulence and wind shear.

The contribution caused by the vertical variation of wind speed can be calculated by using the 32 runs with different constant wind shear. The mean wind shear over the rotor expressed as ΔU (difference in wind speed over the rotor) should be the relevant parameter rather than the shear itself. The normalized velocity difference $\Delta U/U$ has been plotted against the normalized variation of flap moment σ_m / M in Figure 11. The data are well represented by the following expression:

$$(\sigma_m / M)_{shear} = 0.7\ \Delta U / U \qquad (10)$$

The first term in expression (3) represents the variation due to turbulence.

The flap moment at the blade root can be written [19]

$M = \text{Const.}\ U^2\ c_t$ and for the Näsudden turbine c_t can approximately be said to vary as ~ 1/ U.

Thus

$$M \sim \text{Const. } U \qquad (11)$$

Differentiating yields

$$\delta M/M = \delta U/U \qquad (12)$$

and approximately

$$(\sigma_m / M)_{turb} \sim \sigma_u / U \qquad (13)$$

Expression (3) can then be written

$$(\sigma_m / M)^2 = (\sigma_u / U)^2 + (0.7\ \Delta U/U)^2 \qquad (14)$$

The first term on the right hand side of (14) gives the variation of bending moment caused by turbulence. As stated above turbulence at lower frequencies will exitate energy at higher frequencies because of rotation of the turbine. The discussion in Section 3 gives some support to the idea that the effect of 'rotational sampling' is less pronounced for large machines. To find a simple way to handle it, we just suppose that the areas denoted 1 and 2 in Figure 12 are equal. The Figure shows simulated curves for the longitudinal wind component and bending moment, when the variation caused by wind shear has been subtracted.

The turbulence intensity in expression (14) will thus represent the total σ_u measured for that specific time period, in this case one minute.

In the boundary layer the turbulence intensity can be as low as 0.02 during very stable stratification over the sea and perhaps more than 0.5 over a forest in unstable air. The variation of $\Delta U/U$ lies in the same range of values, so depending on atmospheric conditions the relative importance of the two terms in (14) will change. However, neither of them can be omitted at least for the Näsudden turbine.

To verify expression (14) the five simulations for the first meteorological case have been used. For each run the normalized variation of flap moment has been calculated according to (14) and compared with the simulated one. The result, which is given in Table I, is very promising. The correlation coefficient between calculated and simulated values is as high as 0.99.

6.2 Measurements.

An extensive measuring program has been carried out at Näsudden. Measurements comprise meteorological variables such as wind speed, direction and temperature but also values from sensors mounted on the turbine and the tower for example strain gauges and accelerometers.

During one period from October 1983 to February 1985 (478 days) meteorological parameters were recorded as one minute averages. Wind speed was measured at six levels on the 145 m tower (Figure 1) together with fast response Gill anemometers at three heights. The sensors on the turbine were not sampled continuously but in short (60 s) campaigns.

From the measurements comprising bending moment 24 campaigns have been selected. The criteria for chosing the data were that the turbine should be working without pitch regulation, there should be no start or stop procedure and no specific tests should be performed during the campaign. In Figure 13 the measured normalized bending moments are plotted against values calculated with expression (14). The mean value of measurements is 0.133 to be compared with 0.140 for the calculations. The correlation coefficient is 0.75. In view of the rather crude model and all simplifications the result in Figure 13 is encouraging.

6.3 The two special meteorological cases.

From the meteorological data frequency distributions of $\Delta U/U$ and σ_u/U have been calculated. The median values of the two distributions are 0.25 and 0.07 respectively. The former is surprisingly high for a flat coastal site like Näsudden and can entirely be associated with the frequent occurrence of low level jets (see above).

On the other hand the turbulence intensity is in agreement with other measurements over homogeneous terrain. The highest values, around 0.20, are measured in horizontal roll circulation.

In Figure 13 four cases with a low level jet at heights within the rotorrotor diameter have been included ( ) together with one case with a roll circulation (Δ). Those calculations fall within the scatter of the data points.

6.4 Extreme values.

An attempt has been made to represent the frequency distribution of calculated σ_m/M values with a Weibull distribution given by

$$F(>v) = e^{-(v/c)^k} \qquad (15)$$

where F(>v) is the cumulative frequency and denotes the probability of a value greater than v. c and k are constants.

An indirect way to justify the use of a Weibull distribution is to study the double logarithmic transformation of (15).

$$1/k(\ \ln(-\ln F(>v))) = \ln(v) - \ln c \qquad (16)$$

The linearity of the distribution is evident from Figure14a. The exponent k = 2.3 i.e. rather close to 2 valid for a Weibull distribution. Figure 14b shows the cumulative frequency distribution of σ_M/M with a median value of 0.18.

From extreme value theory [20] it is straightforward to derive the exact distribution for the highest value of n independent observations from a Weibull population.

$$F_n(> v_n) = 1 - e^{-e^{-\alpha_n(v_n-\beta_n)}} \qquad (17)$$

where $1/\alpha_n = c/k\ (\ln n)^{1/k-1}$ = dispersion factor

$\beta_n = c(\ln n)^{1/k}$ = modal value

A difficulty found in adopting this approach is that extreme value theory assumes that the n sample values are independent of one another. The effective number of uncorrected sample periods is, therefore, somewhat smaller than the total number. For time series of wind speed the effective number of observations can be calculated from spectra [21,22]. As the bending moment is a function of the wind and turbulence field we made the assumption that approximately the same correlation between values in time series exist. For an averaging time of one minute the number of observation should be multiplied with 1/20 [22].

Figure 15 shows three cumulative frequency distributions of extreme values of normalized standard deviation of bending flap moment for three different time periods 1, 5 and 20 year. The corresponding median values are 0.58, 0.62 and 0.65 respectively, which means that with 50 % probability the highest one-minute- value of σ_m/M will exceed 0.65 during 20 year.

7. CONCLUSIONS.

From a combination of meteorological and aerodynamic measurements and model simulations it has been possible to construct a very simple method to calculate normalized standard deviations of bending moment at the blade root in the flap wise direction of a wind turbine.

It has been shown that variation of flap moment σ_m/M depends mainly on two meteorological parameters; turbulence intensity and wind shear. The relative importance of the two varies with the meteorological situation as well as with the site. Both factors should, however, always be considered when performing load and fatigue calculations. The bending moment at the blade root can thus be calculated from measurements of σ_u/U and $\Delta U/U$ which often are available from routine wind speed measurements on towers.

Generally speaking this simple calculation model can so far only be used for wind turbines of the same kind as the Näsudden machine i. e. large two bladed stiff turbines. But we believe that similar results (with different numerical constants) are likely to be valid for any conceivable wind turbine design after proper 'calibration' with a time simulation model like VIDYN.

Long term meteorological measurements at the Näsudden site also show the influence of thermal stratification on both wind shear and turbulence intensity. To make the assumption that the atmosphere is neutrally stratified as soon as the wind speed is stronger than 7-8 m/s can lead to severe underestimation of loads and fatigue. At Näsudden very stable stratification over the sea during spring and early summer created strong low level jets with wind speeds between 10 and 20 m/s and extremely large wind shear.

ACKNOWLEDGEMENTS.

The authors would like to thank Mr H. Johansson at Teknikgruppen AB for running the model simulations. Many thanks also to Mr J-Å Dahlberg at the Aeronautical Research Institute of Sweden who carried out the evaluation of the meteorological tower data at Näsudden and to the wind energy group at MIUU for performing the turbulence measurements. We also appreciate several fruitful discussions with Prof. U. Högström.

The work has been sponsored by the National Energy Administration Sweden.

REFERENCES.

1 N.O. Jensen and S. Frandsen, Atmospheric turbulence structure in relation to wind generator design, Proc. 2nd Int. Symp. Wind Energy System, Amsterdam, Oct. 3-6 (1978) C1:1-9.

2 U. Högström, Analysis of turbulence and wind measurements at the Näsudden peninsula during two periods with near neutral stratification,

Department of Meteorology, Univ. of Uppsala, Sweden, Report 75 (1984) 20 pp

3 A. Smedman and U. Högström, Turbulence characteristics of a shallow convective internal boundary layer, **Boundary-Layer Meteorol.,30** (1983) 351-373.

4 A. Smedman, Some additional data of coherence in the inertial subrange, **J. Clim. Appl. Meteor.,26** (1987) 1770-1773.

5 L. Kristensen and S. Frandsen, Model for power spectra of the blade of a wind turbine measured from the moving frame of reference, **Journ. Wind Eng. Ind. Aerod.,19** (1982) 249-262.

6 P.H. Madsen, S. Frandsen, W.E. Holley and J.C. Hansen, Dynamics and fatigue damage of wind turbine rotors during steady operation, Risö National Lab., Report Risö-R-512 (1984) 167 pp

7 P.H. Madsen and F. Rasmussen, Rotor loading on a three-bladed wind turbine, Proc. European Wind Energy Conf. and Exhibition, Glasgow, July 10-13 (1989) 488-493.

8 F. Rasmussen and P.H. Madsen, Rotor loading - the influence of dynamics, European Community Wind Energy Conf. and Exhibition, Madrid, Sept. 10-14 (1990).

9 A.D. Garrard and U. Hassan, The dynamic response of wind turbines for fatigue life and extreme load predications, Proc. European Wind Energy Association Conf. and Exhibition, Rome Oct. 7-9 (1986) 401-406.

10 K.S. Hansen, J. Höjstrup, P.H. Madsen and P. Nielsen, Evaluation of test results from the two Danish Nibe turbines, Proc. European Wind Energy Association Conf. and Exhibition, Rome Oct. 7-9 (1986) 347-353.

11 H. Ganander, Importance of yaw system of two bladed HAWT, practical and theoretical results,Proc. European Wind Energy Conf. and Exhibition, Glasgow july 10-13 (1989) 779-782.

12 J.B. Dragt, T.D. Oei, H.C. Rieffe and J.W.M. Dekker, Experimental

verifications of a model for rotor loads by turbulence, Proc. European Wind Energy Association Conf. and Exhibition, Rome Oct. 7-9 (1986) 375-380.

13 J.B. Dragt, Load fluctuations and response of rotor system in turbulent wind fields, Netherlands Energy Research Foundation, Report ECN-172 (1985) 33 pp.

14 M.L. Bovarnick and R.D. Miller, Goodnoe Hills MOD-2 cluster test program vol 3: Rotational wind-sampling. Tests and Analysis, Electric Power Research Institute, Seattle, Washington, Report EPRI AP: 4060 (1985) 60pp.

15 M.G. Verholek, Preliminary results of a field experiment to characterized wind flow through a vertical plane, Pacific Northwest Lab., Richland, Washington, Report Pln-2518 (1978) 31 pp.

16 R.E. Wilson, P.B.S. Lissaman and S.N. Walker, Areodynamic performance of wind turbines, Oregon State University (1976) 25 pp.

17 U. Högström and A. Smedman, The wind regime in coastal areas with special reference to results obtained from the Swedish wind energy program, **Boundary-Layer Meteorol.,33,** (1984) 351-373.

18 A. Smedman, Occurrence of roll circulation in a shallow boundary layer. Submitted to Boundary-Layer Meteorol. (1990)

19 D.M. Eggleston and F.S. Stoddard, Wind turbine engineering design, Van Nostrand Reinhold Company, New York, (1987).

20 A.E. Bury, Statistical models in applied science, Wiley, New York, (1975).

21 A.G. Davenport, The dependence of wind loads on meteorological parameters, Proc. Int. Research Seminar, Ottawa Sept. 11-15 (1967) 63 pp.

22 H. Alexandersson, A statistical analysis of wind, wind profiles and gust ratios at Gränby, Uppsala, Department of Meteorology, Univ. of Uppsala, Sweden,Report 55 (1979) 71 pp.

TABLE I.

Results from 5 simulations of the 'common simple case' with real time series as in-put. Turbulence intensity σ_u/U and $\Delta U/U$ are calculated from measurements. Both simulated and calculated (exp. 14) values of σ_m/M are given.

Run	σ_u/U	$\Delta U/U$	$(\sigma_m/M)_{sim.}$	$(\Delta U/U)_{cal.}$
AB1	0.11	0.07	0.12	0.10
AB2	0.30	0.14	0.21	0.24
AB3	0.15	0.14	0.17	0.17
AB4	0.14	0.05	0.12	0.11
AB5	0.05	0.06	0.08	0.07
MEAN			0.140	0.138

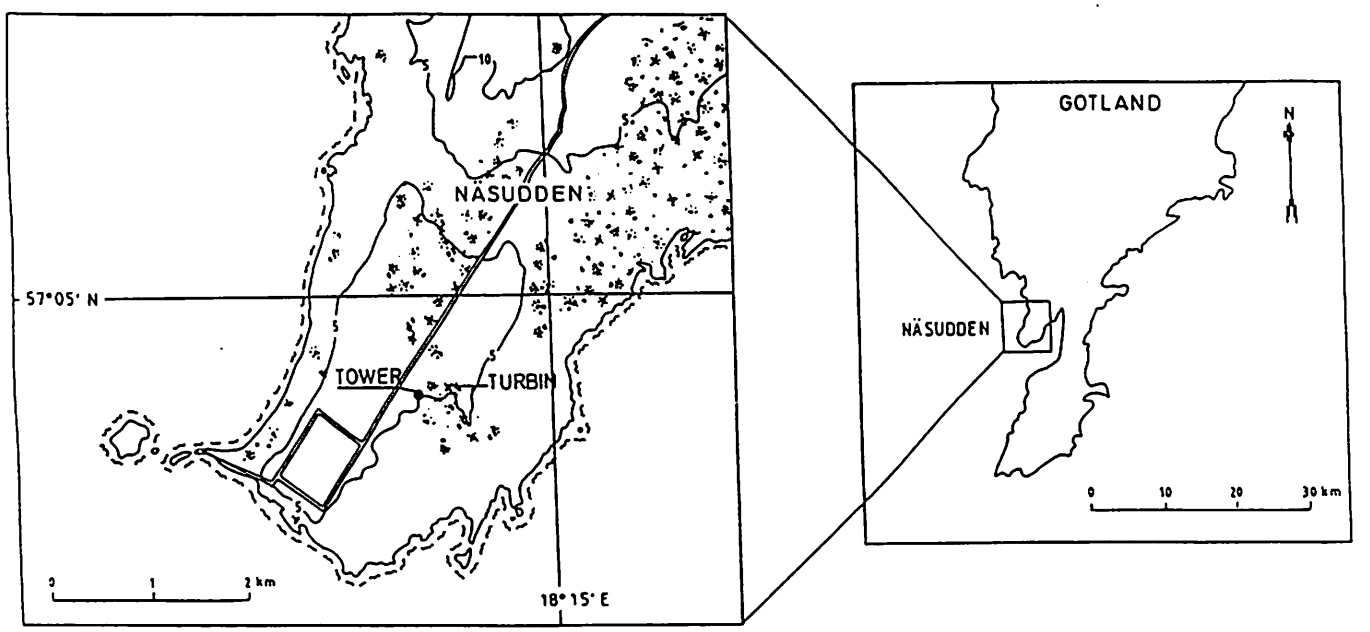

FIGURE 1. Map of southern Gotland with a close-up of the Näsudden site.

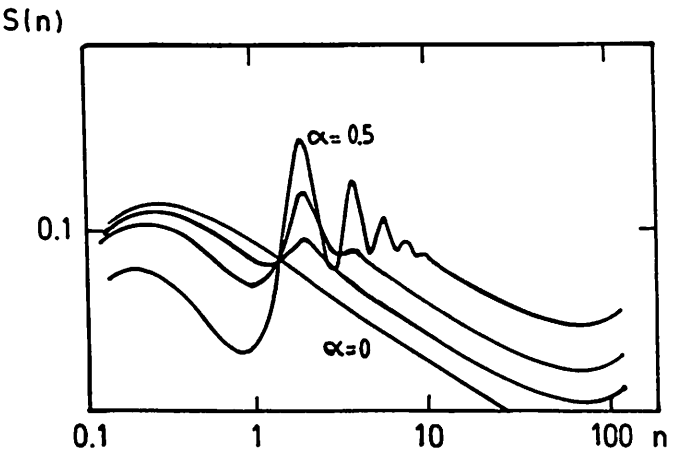

Figure 2. Effect of 'rotational sampling' as a function of α = D/2L where D = turbine diameter and L = turbulence length scale. After [5].

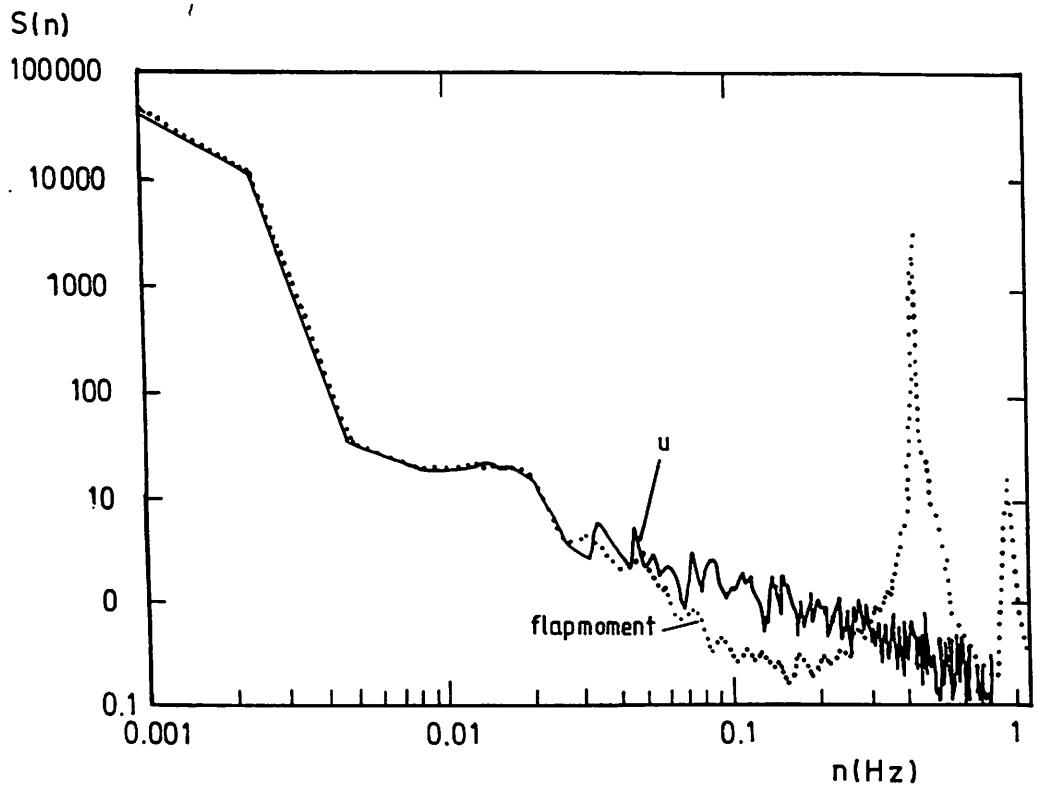

FIGURE 3. Power spectra of longitudinal wind component (--) and bending moment (...).

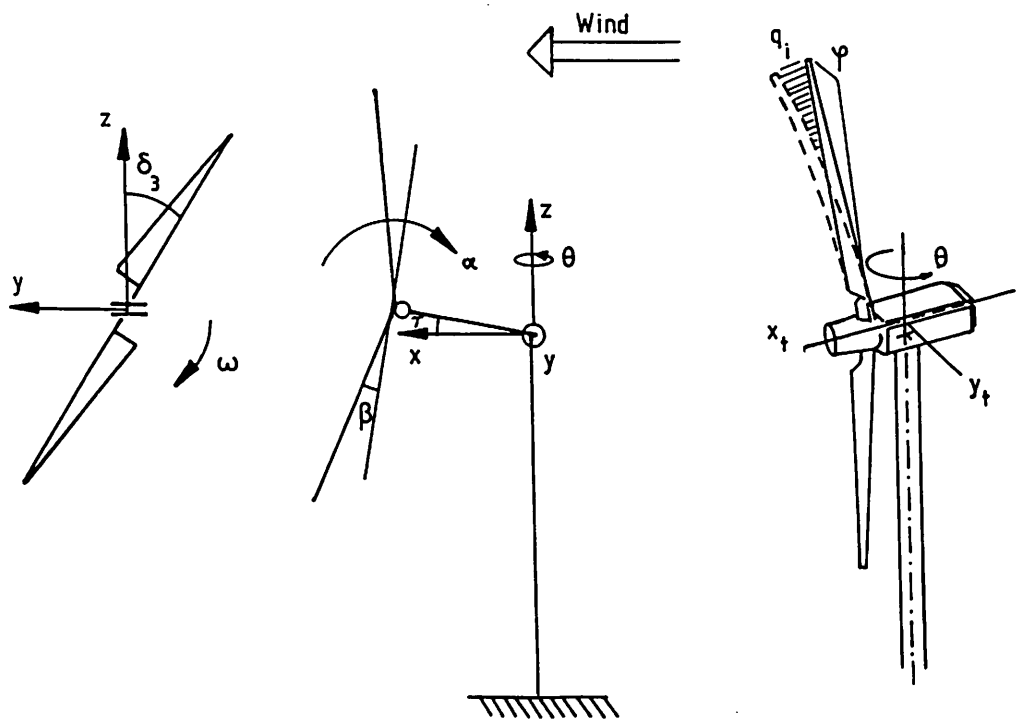

FIGURE 4 a and b. Geometry of the turbine system. The degrees of freedom used in Widyn are : Horizontal translatory movment of the tower top in two directions (x_t, y_t), vertical movement of the rotor centre of gravity (z_r not shown in the Figure), teetering movement of hub relative to main shaft (α), yaw motion of the nacelle (Θ), pitch angle of blade number i (not shown in the Figure), rotor angle of rotation (φ), generator angle of rotation (not shown in the Figure), rotor flapwise deflection (q_{ui}) and rotor edgewise deflection (q_{vi}).

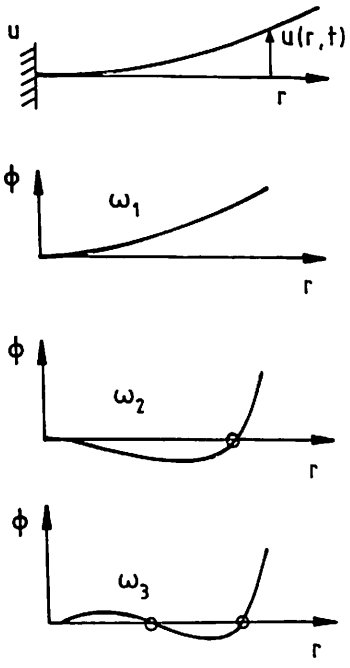

FIGURE 5. Shape of the blade modes.

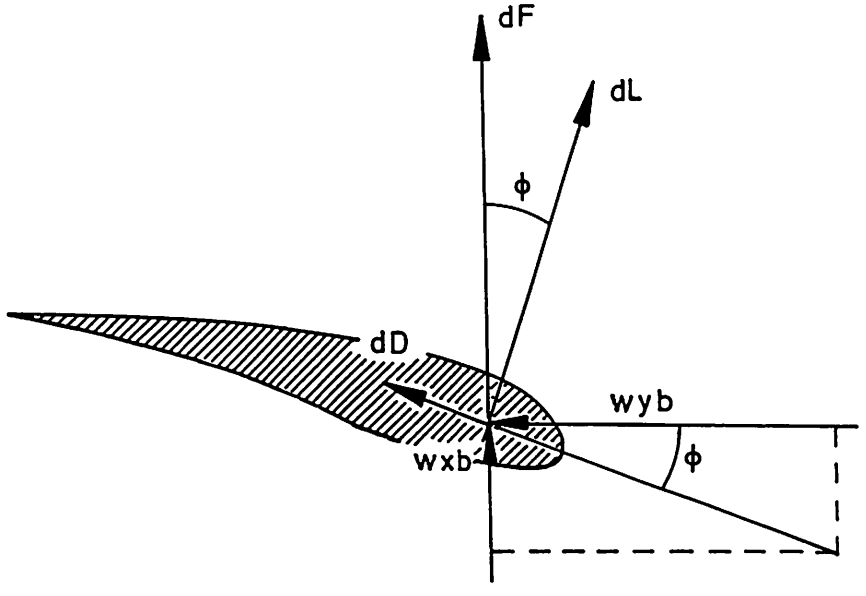

FIGURE 6. Inflow conditions and aerodynamic loads.

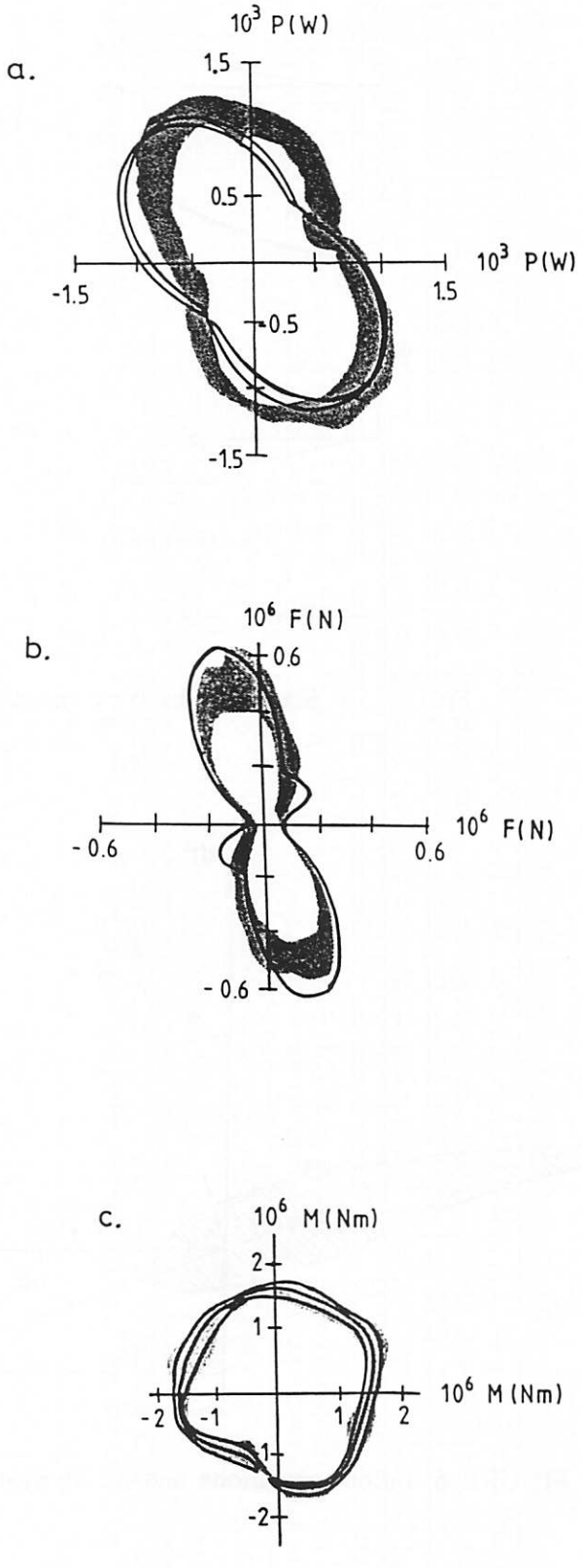

FIGURE 7. Comparison, in polar plots, between measured and simulated values of a) power b) lateral force c) bending moment in the flap wise direction. Measurements are indicated with the shaded areas and simulations with full lines.

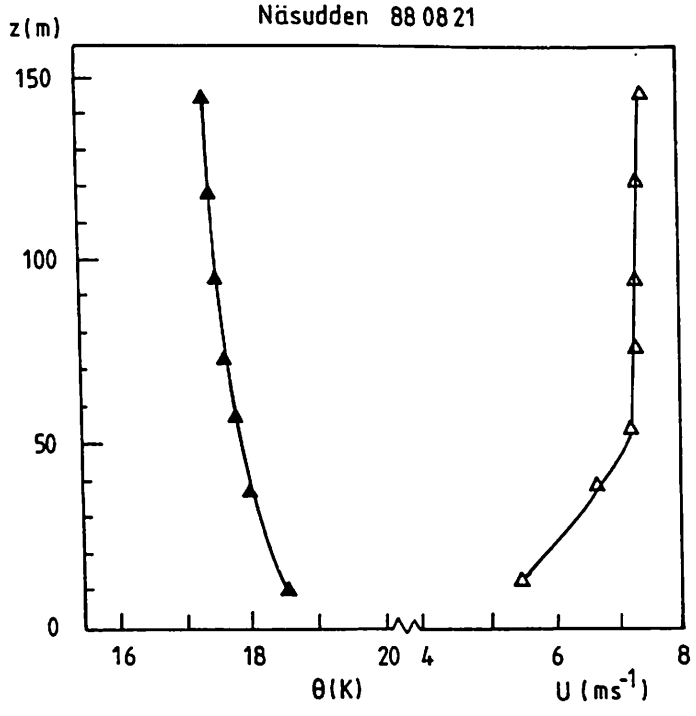

FIGURE 8. Profiles of potential temperature and wind speed at Näsudden during the 'common simple case' (see text for explanation).

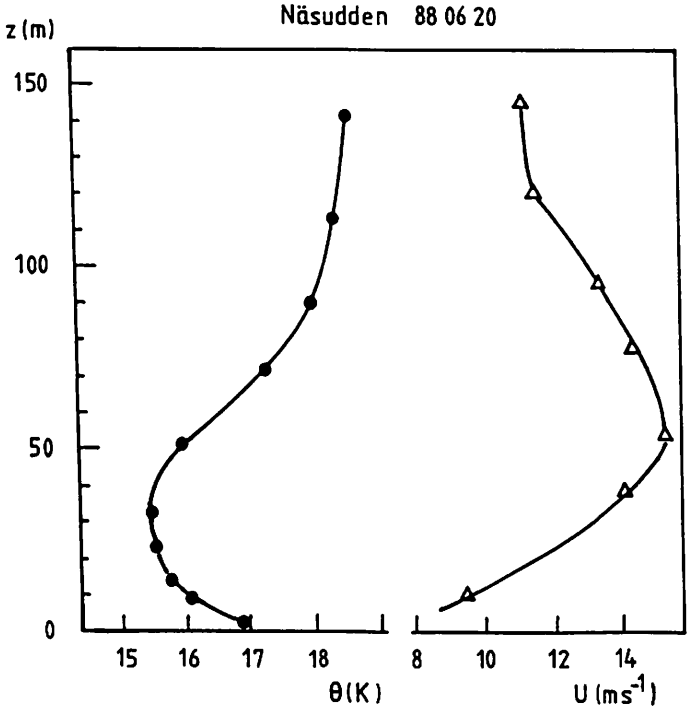

FIGURE 9. Profiles of potential temperature and wind speed during a situation with low level jet.

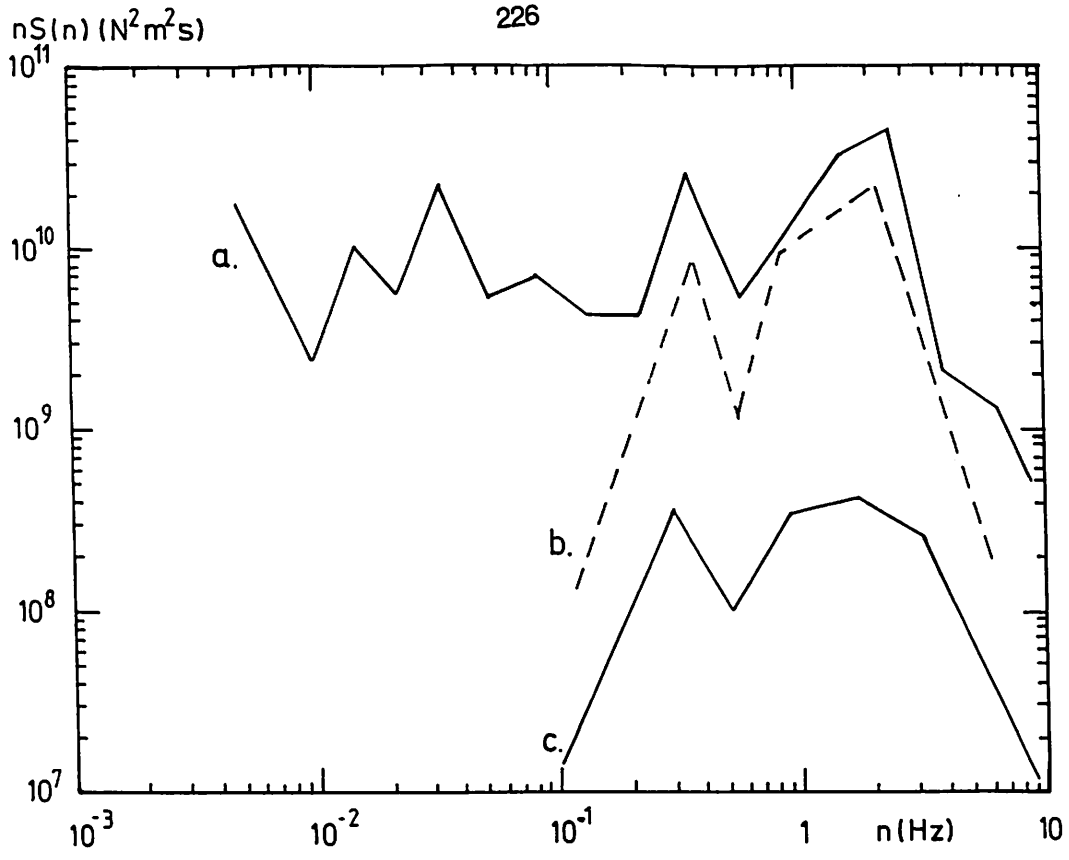

FIGURE 10. Power spectra of simulated bending moment. The three curves represent a) total variation of bending moment b) variation depending on wind shear and c) variation depending on tower, gravity, mean wind etc.

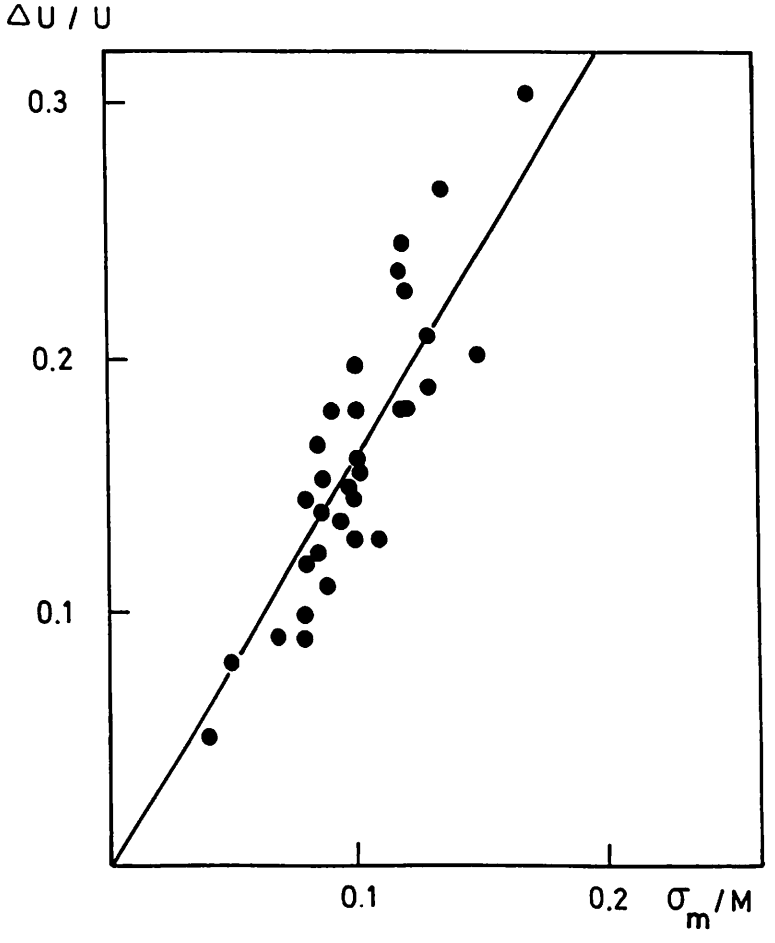

FIGURE 11. Simulated σ_m/M - values as a function of $\Delta U/U$ for 32 runs.

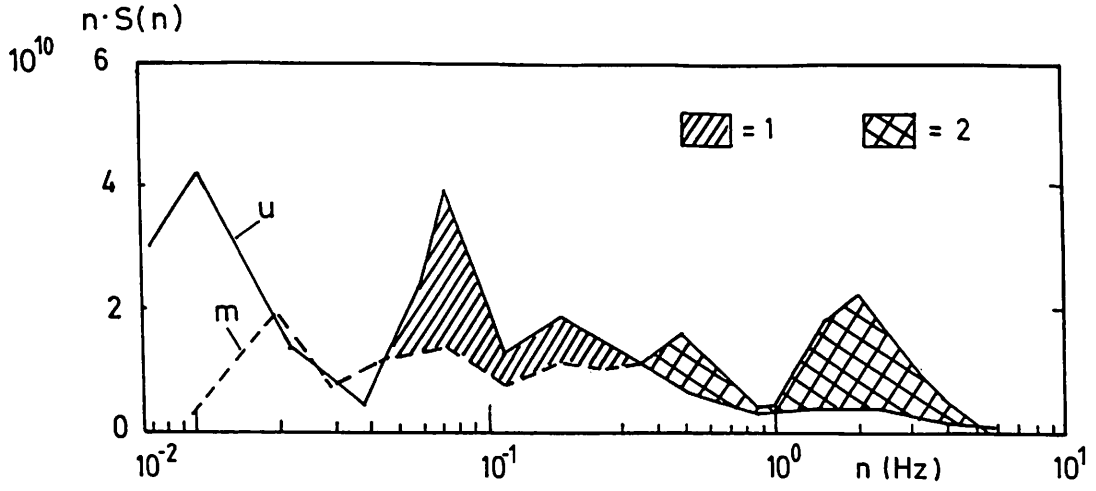

FIGURE 12. Simulated spectral curves of bendingmoment (m) and longitudinal wind component (u). The cyclic variation due to wind shear has been removed. As a first approximation area 1 ~ area 2 (see text for further explanation).

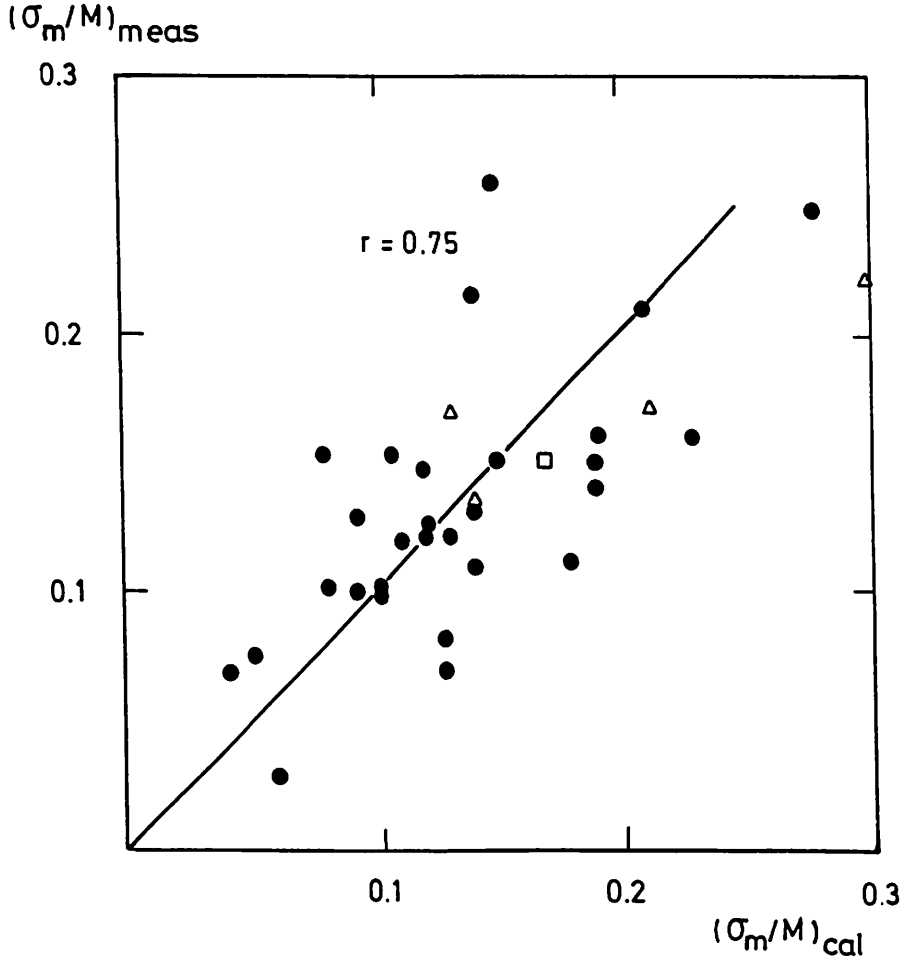

FIGURE 13. Measured values of σ_m/M as a function of simulated ones.
o = 'common simple case'
= 'low level jet case'
Δ = 'horizontal roll case'

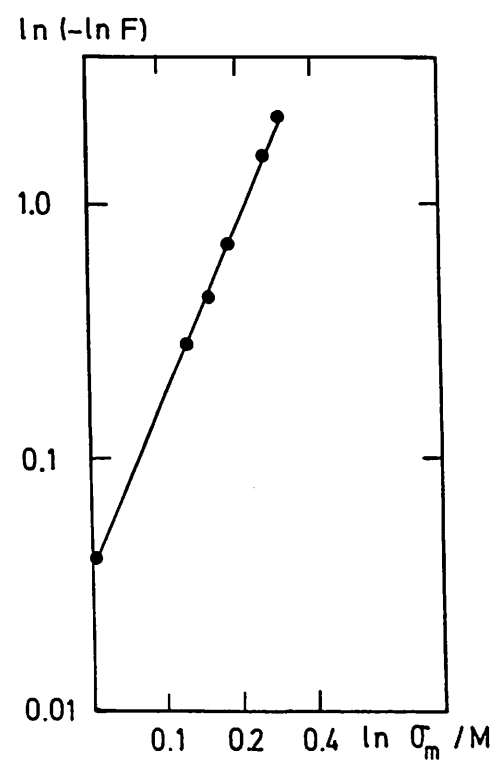

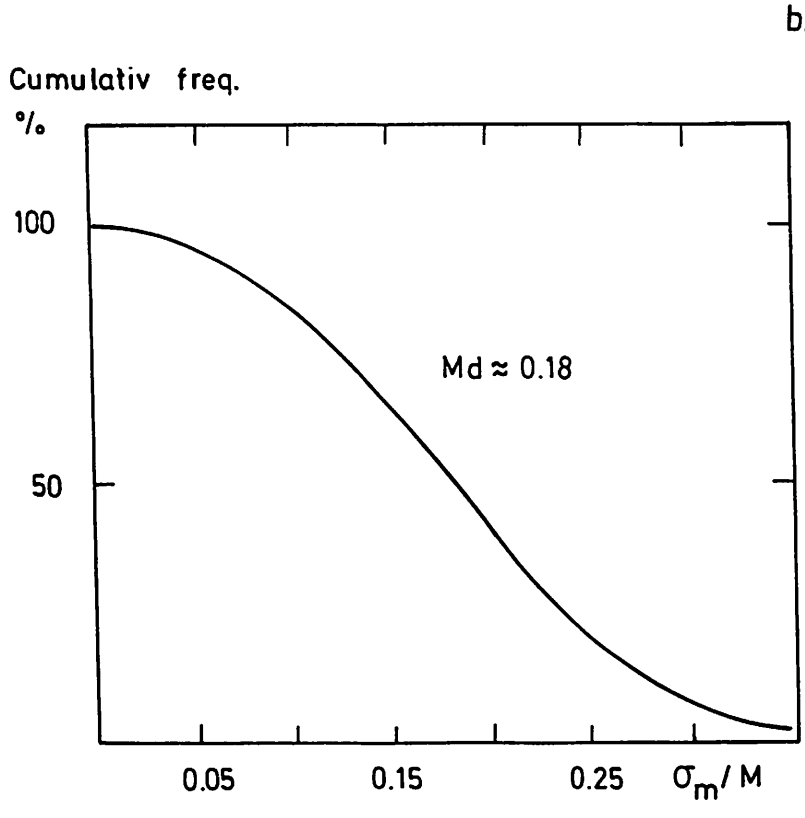

Figure 14. Weibul distribution of σ_m/M in two representations:(b) cumulative distribution and (a) double logarithmic curve with the constants c = 2.3 and k = 0.21.

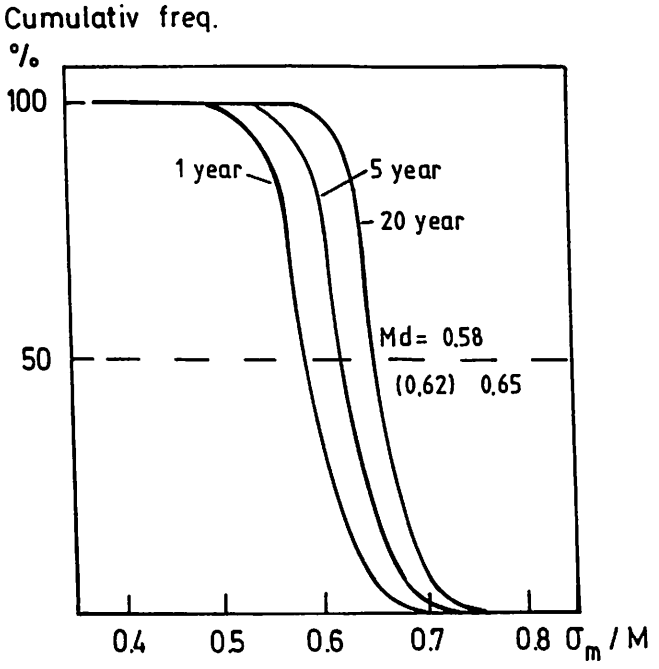

Figure 15. Cumulative distributions of extreme values of σ_m/M. The three curves show the distributions for 1, 5 and 20 year respectively.

FULL DISK GUST DIVIDING FREQUENCY

B. Montgomerie, WEST, Taranto, Italy

WEST

WIND ENERGY SYSTEMS TARANTO S. p. A.
VIA ARCHIMEDE, ZONA INDUSTRIALE
741 00 TARANTO
ITALIA
PHONE (099) 476 91
FAX (099) 471 85 64

Note: At the conference the title of this topic was as it appears on this page. The underlying report that already existed had another title, however. That title appears on the next page. - The author appologizes for this potential reason for confusion.

WIND COHERENCE FOR HORIZONTAL AXIS WIND TURBINES

By Bjorn Montgomerie, Consultant engineer to WEST
Wind Energy Systems Taranto, Italy
February 1991

SUMMARY

In the design of horizontal axis wind turbines the influence of the variable wind must be taken into account for assessing the size of different load carrying components. In the case of an existing turbine measurements of the wind and signals from strain gages are used to predict the life time of the turbine. Under both circumstances the wind gust frequency range is divided into a low frequncy and a high frequency band. The significance of finding the frequency that divides the total range is that the low frequency wind variation leads to steady force response in the turbine whereas the high frequency gusting causes dynamic response in the turbine. It is advantageous to make this distinction because of the convenience of being able to disregard dynamics in the low frequency case. In the treatment of high frequency winds the more complicated dynamic response calculations are reduced to a lower number of cases because of the reduction of the frequency range.

It is of great importance to be able to assess the location of the border frequency between these two intervals. To do this a coherence function is used. The standard coherence is a function, in the science of meteorology, that uses measurements from two points in three-dimensional space. These measurements can be longitudinal, lateral or vertical wind components of which the longitudinal one should be of major importance in this context. When the coherence function is 1.0, the agreement between the measurements from the two points is perfect, meaning that when the wind undulates in a certain pattern in the one measuring point so does the wind in the other measuring point. When the points are moved more apart the agreement between the point measurements declines to approach zero for large distances. In a crude way it can be said that when the coherence is above .5 there is agreement. When the coherence is below .5, there is no agreement. Since the coherence is a function of the independent variable Fourier frequency of the wind, the border frequency is found where the coherence is .5.

One difficulty in the past has been to select the correct distance between the two points to represent the turbine size. The question has been raised how adequate is the coherence function for this purpose.

This paper contributes to the simplification of this discussion by introducing new concepts into the coherence function. Instead of using the standard two-point coherence a different approach is taken. Coherence can be found between one wind measuring point, e.g. on the nacelle, and the thrust or torque of the turbine. To approximate this coherence the concepts of area coherence and moment coherence are introduced. The area coherence can be thought of as the coherence between the nacelle point wind and the average wind over a disk perpendicular to the wind like the turbine disk. The moment coherence is slightly more complicated. The area coherence is believed to be close to the coherence between the measured wind at the hub ant the turbine thrust. Instead of going through the trouble of creating the coherence function from measurements of both the wind and the turbine, only the wind needs to measured or an empirical expression can be used.

WIND COHERENCE FOR HORIZONTAL AXIS WIND TUBINES

1. INTRODUCTION

A wind turbine is subjected to the variable wind. The variation can be divided into two ranges. One range is signified by having a frequency of change such that all structural response stress changes happen slowly. This is to say that the structural dynamics contributes no additional stress. Contrary to this range is the frequency range in which the structural dynamic response creates a significant contribution to the total response. It is important to separate the two regimes for reasons of convenience in the context of analytical evaluation. Previously the concept of two-point coherence has been discussed to help find the dividing frequency. It is, howerver, not totally adequate.

An alternate coherence function is sought which corresponds to the coherence between the hub located wind anemometer and the rotor response. This response can be expressed as thrust or torque. The technique below circumvents the method of first converting the wind to forces in the structure and then perform the coherence calculation. In stead the full disk average wind is used with a one point wind measuring location to generate a coherence function. It is believed that this constitutes a good approximation for the one-point/forces coherence calculation below a certain gust frequency. This certain frequency is sought in wind turbine design and analysis of material fatigue considerations. More thorough descriptions of this activity does not appear in this text. Instead such documentation makes reference to the present paper as a reference on useful coherence.

2. TWO-POINT GENERAL WIND DIRECTION COHERENCE

In meteorology the concept of coherence is applied to measurements in two points in space. The coherence function, based on the wind component fluctuations in these two points in the same direction, is a measure of the similarity of the winds in the two points. If the coherence is 1.0 the similarity is perfect. If the coherence is a very small fraction approaching zero there is no similarity. The coherence function is constructed never to assume values below zero. Gusts with a relatively large extent engulf both measuring points giving very similar signals in the two points. This also gives a high value of coherence between the points. Small gusts may pass one measuring point but not the other. This results in a low value of the coherence.

The laterally large gust also has a large measure in the longitudinal, i.e. in the general wind direction. These gusts therefore rise and decline slowly as seen in the points where the measurements are taken. In a Fourier expansion of the one point measurement of a large gust the frequency is low. Vice versa the small gust frequency is high. We anticipate that the coherence plotted in a diagram vs frequency is a falling curve as frequency increases.

3. SEPARATION OF GUSTS IN TWO FREQUENCY REGIMES

For a horizontal axis wind turbine the concept of the two-point coherence is favorably extended to somehow encompass the whole disk area, not just any two odd points. The wind turbine engineer asks the question - how does the wind turbine behave in relation to a singular point wind. He has no direct need for the coherence between two points. How should the wind data be treated in order to be made most useful? - A new hypothesis to further this end is presented here.

In wind turbine design and in analysis of measured wind turbine characteristics it is of importance to be able to separate the spectral gusting. One part can be thought of as consisting of gusts that include the whole disk. These gusts will be referred to as "large gusts". The other part consists of gusts whose extents are smaller than some significant distance such as the disk diameter or perhaps a large fraction of it ("small gusts"). In fatigue calculation the large gusts affect the turbine as a static load whereas the small gusts induce eigenfrequencies. The response in the turbine from these small gusts must therefore be calculated considering the turbine as a dynamic "filter". It is desirable to be able to make the distinction between these two classes of gusts although, admittedly, there is no principle difference when viewing the wind alone. Also the effects in the turbine structure, from the two, float together without a sharp border line in between. But the approximation of treating small gust wind separate from large gust wind is believed to be good if each part is treated correctly and if the separation between the two is well chosen. How to utilise the separation of the wind, once it has been found, is not treated in this text. It is the aim of this text to make the frequency separation, i.e. finding the border line frequency, using the concepts of area coherence and moment coherence.

4. AREA COHERENCE and MOMENT COHERENCE

Just as in the case of the two-point coherence it is possible to formulate the coherence between the wind, as measured in front of the hub, and the rotor thrust. The rotor thrust, however, derives its characteristics from the sum of all contributions over the disk area. As the rotor blades sweep the disk, they sample winds that have their respective coherence with the hub wind. This lead the author to the idea that a better measure than two-point coherence must exist, at least for wind turbine purposes.

To better explain the idea Fig. 1 will be helpful. In Fig. 1a two lateral points are used to form the wind coherence. If the atmosphere has the same horizontal coherence as vertical then it does not matter where in the lateral plane point B is located. The coherence between A and B will be the same as long as the distance between them is the same. In Fig. 1b the point B has been given several such alternative locations. Then it can be stated that wherever point B is located in the plane, it represents all other points on the same circle around A.

Now we will take the step from point coherence to ***area coherence*** by assuming that each point B is "responsible" for the coherence in its ring. Its ring has a radius of r and a ring width of dr. The area of the ring is $2\pi r dr$. The average coherence between the point A and the disk with radius R therefore becomes

$$cohA = \frac{1}{\pi R^2}\int_0^R 2\pi r \cdot coh(r)dr \qquad (1)$$

where the function coh(r) is the standard two-point coherence in the lateral plane. This function has been studied intensively and different curve fit expressions exist. We will be using the following expression.

$$coh(r) = e^{-\gamma\frac{nr}{\overline{U}}} \qquad (2)$$

where

$\overline{U}$ = the mean wind speed

n = Fourier gust frequency

γ = Curve fit constant - example: 14

The coefficient γ is different in different circumstances and with different authors. If (2) is inserted in (1) it is possible to evaluate the integral analytically. We obtain

$$cohA = \frac{2}{\rho^2}\left\{1-(1+\rho)e^{-\rho}\right\} \qquad (3)$$

where

$$\rho = \frac{\gamma R n}{\overline{U}} \qquad (4)$$

where

R = The upstream stream tube radius (power level dependent)

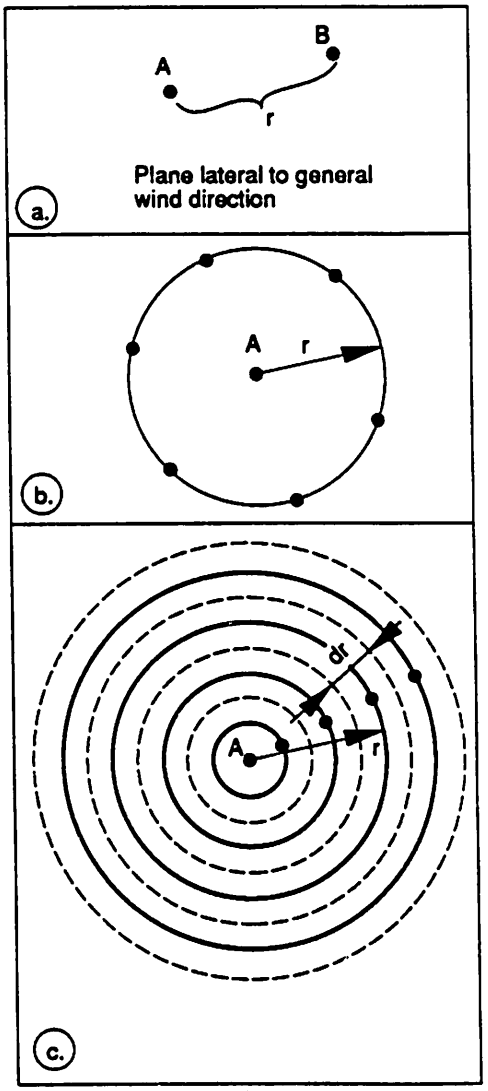

Fig. 1

This defines the area coherence. Next the ***moment coherence*** will be defined. The bending moment on a turbine blade in the lead-lag direction constitutes the sum from the individual part forces multiplied by the moment arm length to the point of evaluation. Each part force is assumed to be produced by some division of the blade into, so called, blade elements. Each blade element sweeps a ring area.

It is suggested that the coherence between the hub wind measuring point and the moment is similar to a coherence that has been weighted not only with its area ring but also with the moment arm. The basic similarity with the area coherence is also seen in the formulae that follow.

$$cohM = \frac{\int_0^R coh \cdot 2\pi r^2 dr}{\int_0^R 2\pi r^2 dr} \qquad (5)$$

This expression can also be evaluated analytically

$$cohM = \frac{3}{\rho^3}\left\{2 - e^{-\rho}\left(\rho^2 + 2\rho + 2\right)\right\} \qquad (6)$$

A comparison of the three types of coherence is seen in Fig. 2. As should be expected, for any given value of the independent variable, the area and moment coherences are larger than the two-point coherence. This reflects the integration which functions as a damper on function fluctuations. Another way of understanding the difference is to think about the two-point coherence being based on a certain distance R. If the very same distance is used, for say the area coherence, then the latter even includes two-point coherence on the way out to R. On the way the two-point coherence is on the average higher than at R.

5. COMPARISON WITH MEASURED RESULTS

Ref. 1 contains a graph which represents the coherence between the nacelle anemometer wind reading and a blade root moment sensor. This coherence is most favorably compared to the ***moment coherence*** (cohM) described above and seen as the mid-curve in Fig. 2. In order to make a comparison between the coherence of the measurements in Ref. 1 and the cohM function, the independent variable must first be converted to the same kind as that in the reference.

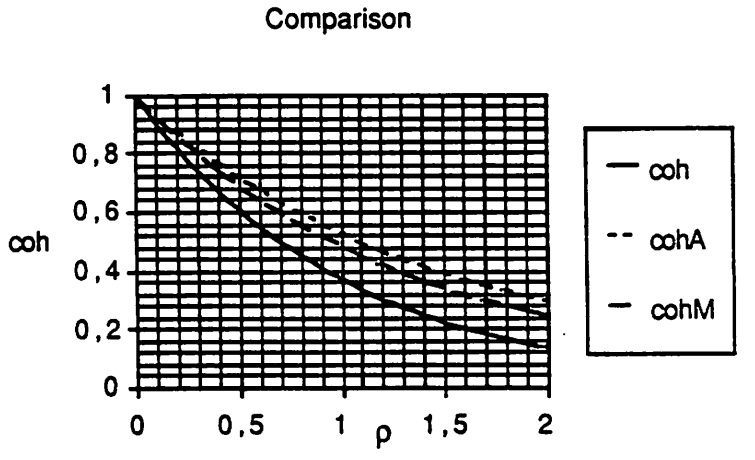

Fig. 2

Eq. (4) is used to calculate the absolute frequency n from ρ using γ = 14, Ubar = 8.7 m/s and the radius was taken to be the nominal rotor disk radius of 37.5 m. The plot was obtained by first calculating cohM as a function of the dimensionless frequency ρ both put in one column each. With ρ multiplied by the factor Ubar/(γR) the frequency is obtained in column 5 (See table!). Then the cohM values were plotted against the frequency (Hz) in the diagram of the reference, see Fig. 4. All that can be said about the quality of the similarity between the measured and the calculated curves is that it looks promising. Too little data in the measurements did not allow a thorough comparison under different measuring conditions.

The diagram from the reference and the tabled data for the three coherence functions appear on the two last pages of this report.

6. HOW TO USE THE RESULT

It is suggested that the user of this method first decides the coherence level at which the dividing frequency is to be found. (At the time of writing no better information than coh = .5 is available.) The table values for respectively area coherence or moment coherence (3) and (6) are used. Then the knowledge of the average wind (10 min filtered) and the turbine radius allows a curve similar to that seen in Fig. 4 to be plotted. At the chosen coherence value the frequency is the dividing frequency sought. Unfortunately both (3) and (6) are too complex to find the analytical inverse from. Otherwise a direct expression for the dividing frequency could have been found. Therefore, under the circumstances, plotting of the curve seems to be the simplest way to find the dividing frequency.

If, however, the reader is satisfied with the suggested level of coh = .5 as being he guide value then a straight forward and simple algorithm can be devised accordingly. The coherence curves seen in the figure above were replotted with higher resolution. For cohA = cohM = .5 respectively the following values of ρ are found:

$$\rho A = 1.09 \quad \text{and} \quad \rho M = .95 \qquad (7)$$

Then the following simple algebraic steps lead to the dividing frequency:

From (4) we have

$$f_A = 1.09\frac{\bar{u}}{\gamma R} \qquad (8)$$

Similarly

$$f_M = .95\frac{\bar{u}}{\gamma R} \qquad (9)$$

As an approximation the coefficients $1.09 \approx .95 \approx 1.0$. We simplyfy by ignoring the difference between the area frequency and the moment frequency setting

$$f = \frac{\bar{u}}{\gamma R} \qquad (10)$$

To get the cycle time (10) is inverted giving

$$T = \frac{\gamma R}{\bar{u}} \qquad (11)$$

The distance traveled during the cycle time is

$$x = T\bar{u} = \gamma R \qquad (12)$$

We have found a physical interpretation of the mathematical quantity γ.

The ratio between the distance traveled and the radius is = γ which is recorded in the literature to be from 14 to 17. Say that the figure 16 can be used then x = 16radii = 8 diameters. We conclude the following:

For a gust to cover an essential part of the turbine disk (essential enough to give a coherence value of .5) its length is 8 diameters. This leads to the visualisation of geometric coherence of gust structures. It appears that gusts have an oblong shape, at least 8 times as long as wide. The background material for coherence measurements is statistical with a statistical spread. Our conclusion must be that, on the average, the gust structure is shaped like an ellipsoid traveling with the major axis aligned with the general wind direction. If this is the truth it is perhaps amazing that the longitudinal extent is so much greater than the lateral one. The author takes the liberty to make reference to these shapes using the expression "gust cigars"!

If the reader has accepted the concept of the "gust cigar" then a very simple rule how to obtain the dividing frequency can be formulated: Take the 10 min average wind speed and divide it by the cigar length (8 turbine diameters).

$$f_{Div} = \frac{\bar{u}}{8D} \qquad (13)$$

Finally we need to discuss a few elements of the theory put forth here. What inate significance does the coherence value of 0.5 have? - The answer is that there is no such special physical significance in the choice of this value. A rather heuristic discussion must be employed accordingly.

It is associative and simple to think about the coherence (no matter which one) as being approximated as = 1 for all values exceeding 0.5. Vice versa, a coherence below .5 can be approximated by saying that there is no coherence at all, i.e. the coherence is zero. With such loose guidance for the selection of the dividing frequency, is this text worth reading? - The author proposes a definite YES to be the answer. The reader can always manipulate the dividing frequency up or down to see the sensitivity in the change of number of cycles that results for fatigue consideration. Moreover, the cycles are taken care of in one of the two methods used for the fatigue assessment. One method is necessary for the low frequency gusting, another for the high frequency. To change the dividing frequency a little only changes the heading under which some of the frequencies are "booked". They are not lost but are taken care of by the good methods that the reader possesses. Such methods, for fatigue estimation, are not treated in this report, however.

7. SUGGESTIONS FOR CONTINUATION OF THIS WORK

A note on the definition of the parameter R appearing in expression (4) is that the stream tube upstream diameter is unknown. It could be estimated if the power extraction was known. However, considering the large data scatter in that plot

the added effort to find a slightly smaller value of R was not ventured into. Instead the turbine radius was used directly as an approximation. The idea to use the stream tube diameter in place of the rotor radius emanates from the knowledge that only the wind which is inside the stream tube will ever go through the disk. All air outside is irrelevant from a forces as well as from a coherence standpoint. In future verification of the coherence effects, a corrected value for R should be used utilising the equation of continuity and other wind turbine technology calculational techniques.

More measurements of the type described in Ref. 1 are needed to assess the usefulness of the coherence concepts put forth in this report. This would include data at different atmospheric conditions, longer measuring times and measuring of thrust so that the area coherence function also be put to the test.

8. REFERENCE

"UTVARDERING AV SAMBAND (KOHERENS) MELLAN VINDHASTIGHET OCH OLIKA AGGREGATPARAMETRAR VID VINDKRAFTVERKET PA NASUDDEN"
Rep. nr: TR S88.163 (Available from FFA, box 11021, 16111 Bromma, Sweden)
By: S-E Thor and K. Ahlin, 1988

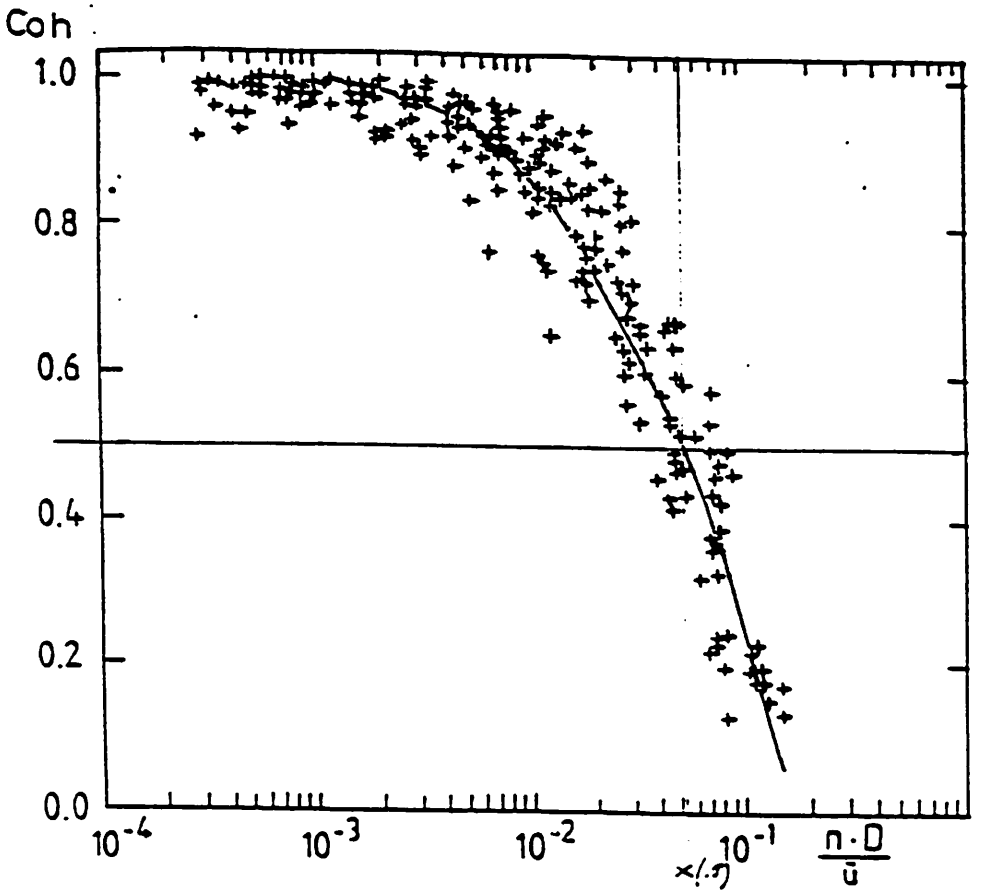

Fig. 3

Lateral coherence for the u-component as a function of $n \cdot D/\bar{u}$ for near neutral condition. The curve is exp (-14 $n \cdot D/\bar{u}$).

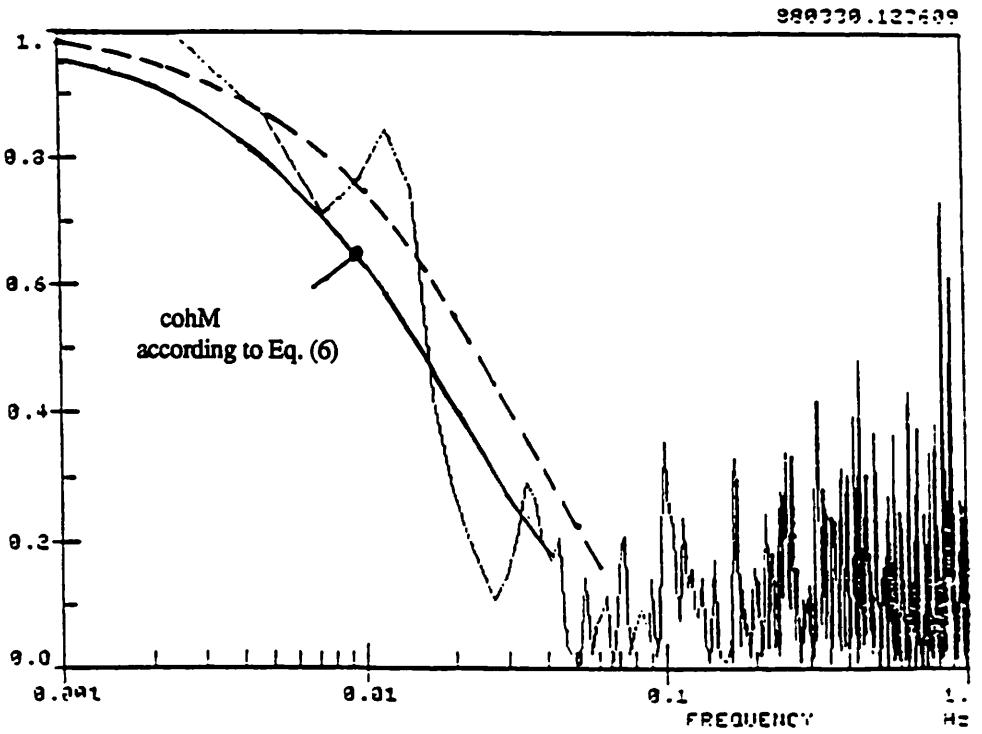

Fig. 4

Coherence between wind speed and lead-lag blade root moment.
and
- - - - - - Coherence between two points in space at a distance of 1/2 blade radius from each other.

gam=14 R=37.5 Umean =8.7 m/s

ro	coh	cohA	cohM	frequency
1.000000E-04	.999900	.000000	.000000	1.657275E-06
5.000000E-02	.951229	.967312	.961304	8.286377E-04
.100000	.904837	.935769	.927687	1.657275E-03
.150000	.860708	.905408	.893911	2.485913E-03
.200000	.818731	.876153	.861347	3.314551E-03
.250000	.778801	.847969	.830017	4.143189E-03
.300000	.740818	.820809	.799894	4.971826E-03
.350000	.704688	.794631	.770933	5.800464E-03
.400000	.670320	.769399	.743095	6.629102E-03
.450000	.637628	.745078	.716331	7.457740E-03
.500000	.606531	.721632	.690605	8.286378E-03
.550000	.576950	.699027	.665874	9.115016E-03
.600000	.548812	.677230	.642092	9.943654E-03
.650000	.522046	.656210	.619222	1.077229E-02
.700000	.496585	.635939	.597229	1.160093E-02
.750000	.472367	.616386	.576077	1.242957E-02
.800000	.449329	.597524	.555733	1.325821E-02
.850000	.427415	.579328	.536165	1.408684E-02
.900000	.406570	.561772	.517341	1.491548E-02
.950000	.386741	.544831	.499232	1.574412E-02
1.00000	.367879	.528482	.481809	1.657276E-02
1.05000	.349938	.512703	.465044	1.740139E-02
1.10000	.332871	.497472	.448912	1.823003E-02
1.15000	.316637	.482769	.433388	1.905867E-02
1.20000	.301194	.468573	.418447	1.988730E-02
1.25000	.286505	.454866	.404067	2.071594E-02
1.30000	.272532	.441630	.390226	2.154458E-02
1.35000	.259240	.428845	.376900	2.237321E-02
1.40000	.246597	.416497	.364072	2.320185E-02
1.45000	.234570	.404569	.351721	2.403049E-02
1.50000	.223130	.393044	.339828	2.485912E-02
1.55000	.212248	.381909	.328376	2.568776E-02
1.60000	.201897	.371148	.317346	2.651640E-02
1.65000	.192050	.360748	.306723	2.734504E-02
1.70000	.182684	.350695	.296491	2.817367E-02
1.75000	.173774	.340978	.286635	2.900231E-02
1.80000	.165299	.331582	.277139	2.983095E-02
1.85000	.157237	.322498	.267990	3.065958E-02
1.90000	.149569	.313713	.259175	3.148822E-02
1.95000	.142274	.305216	.250680	3.231686E-02
2.00000	.135335	.296997	.242493	3.314549E-02

$\rho = \frac{\gamma \cdot R \cdot n}{\bar{u}}$ ... $\gamma = 14$

R = STREAM TUBE UPSTREAM RADIUS
(... ALTHOUGH TURBINE RADIUS WAS USED IN COHERENCE VS FREQUENCY PLOT COMPARISON SEE FIG. 4)

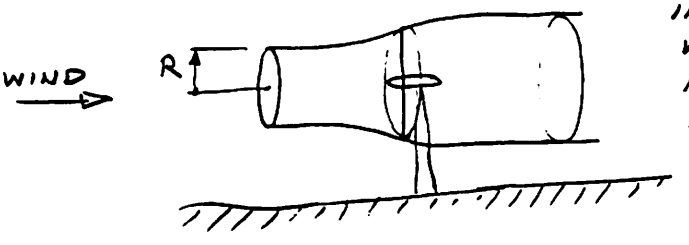

Fig. 5

RIVA CALZONI

IEA WECS R/D ANNEX XI - Topical Experts Meeting
"Wind Characteristics o Relevance or Wind Turbine Design"
Stokholm, 7th March 1991

A THEORETICAL METHOD FOR THE PROBABILITY ASSESSMENT OF A DESIGN EXTREME GUST ON A WTG

E.Dalpane, D.Niccolai
RIVA CALZONI S.p.A.
Via Emilia Ponente 72
40133 Bologna (Italy)

1 - Introduction

An appropriate wind model is the basic input for any WTG aerodynamical calculation.
Beside the need of considering three dimensional turbulence effects of the wind velocity over the rotor disk, to evaluate fatigue loading, some deterministic gust can be necessary to check the control system behaviour in extreme conditions.
A strong longitudinal gust against a pitch controlled WT, working at the rated speed, can be simultaneous with a grid loss.
The transient behaviour of the WTGS in this case leads sometime to a very severe loading which affects the whole design of the WTG.
The gust to be considered in this case is a pure theoretical assumption, therefore no direct probability calculation is possible. Anyway some consideration to estimate a proper gust model can be done on a quantitative base, if some assumptions are accepted:

a) The theoretical gust is a linear or sinusoidal increase of the longitudinal wind velocity, uniform over the rotor disk, from V1 to V2 in a time tau (see fig.1); before and after the wind speed change the wind velocity is constant and uniform.

b) The probability of this gust is assumed to be equal to the probability of a wind speed change "uniform" over the rotor disk such that $V(t) \leq V1$ and $V(t + tau) \geq V2$.

The probability calculation adopted is based on Gaussian distributions and on the power spectral density function $Sy(\Omega)$, derived by Holley and Thresher [1], of the longitudinal wind velocity component "uniform" over the rotor disk.

The mathematical method is equivalent to measure, with a scanning time tau, the longitudinal wind velocity "uniform" over the rotor disk, for a sufficiently long time, and to count all the couples of samples (Vi, Vi_{+1}), which satisfy the condition $Vi \leq V1$ and $Vi_{+1} \geq V2$.
The number of the events counted devided by the whole measuring time expressed in years is Ny: R is simply given by 1/Ny.

2 - Mathematical methodology

Since the velocity change Du is defined as:

$$Du = u(t + tau) - u(t) \tag{1}$$

the standard deviation of Du is:

$$sDu(tau) = \{\frac{1}{T} \int_0^T [u(t + tau) - u(t)]^2 \, dt\}^{1/2} \tag{2}$$

According to [2] the standard deviation sDu (tau) can be expressed in terms of the radian frequency Ω as:

$$sDu(tau) = 2 \left[\int_{-\infty}^{+\infty} \pi \, Sy(\Omega) \, (1 - \cos(\Omega \, tau)) \, d\Omega\right]^{1/2} \tag{3}$$

where $Sy(\Omega)$ is, according to [1]:

$$Sy(\Omega) = \frac{(b^* \frac{U}{L})^2 \, su^2 \, \frac{L}{U}}{(a^* \frac{U}{L})^2 + \Omega^2} \tag{4}$$

The analytical integration of the right term of (3) is possible, thanks to the relatively simple expression of $Sy(\Omega)$, therefore sDu(tau) can be expressed in a closed form as:

$$sDu(tau) = su \, \frac{b^*}{a^*} \, [1 - \exp(- tau \, a^* \, U/L)]^{1/2} \tag{5}$$

If a Gaussian distribution is assumed for Du, the probability density function is completely known.
Anyway to know the probability density function of Du is not sufficient for the purposes of the present calculation, because the velocity changes Du are to be selected on the base of their actual position with respect to V1 and V2.
The problem can be solved by considering also the probability density function of the middle position of the wind speed change:

$$um = 1/2 \, [u(t + tau) + u(t)] \tag{6}$$

With a procedure similar to the one described from (2) to (5), the standard deviation of um can be obtained:

$$sum(tau) = 1/2\ su\ \frac{b^*}{a^*}\ [1 + exp(-\ tau\ a^*\ U/L)]^* \qquad (7)$$

In the assumption that p(Du, sDu) and p(um, sum) are statistically independent, the joint probability density function of Du and um is simply given by the product of the two.
A numerical integration of the joint probability density function can be performed in a way similar to the one described by [2], introducing also an integration over the U values to account for a Weibull frequency distribution.
The extremes of this integration are the cut in (Vi) and cut out (Vo) wind speeds of the concerned WT.
Some results of this calculation for a given site of installation and for the WTG of Riva Calzoni M30, are reported in fig.2, where the value of the gust size DV is showed versus the duration tau, in the assumption of a given recurrence time R.
This method can be improved by considering that the su measured values are always very inconstant; furthermore, the average turbulence intensity I is also depending on U.
A very simple law to link I to U can be assumed as shown in fig.3; while the distribution of the measured values of i around I is roughly assumed to be Gaussian with a standard deviation si.

3 - Sensibility analysis

According to the methodology adopted, the probability of a gust is dependent upon many parameters referred to the following models:

- gust (Vl, DV, tau)
- annual frequency distribution of U (Vav, K)
- turbulence (I10, Ir, Ii, L)
- WT (Vi, Vo, D)

For every parameter of site and WT, the range of possible variation was separately defined such as to represent all possible existing conditions. As a reference value for the sensibility analysis, the center of the range is selected for each parameter. The ranges of the parameters defining the gust, were selected in order to consider extreme conditions with respect to gust amplitude and wind acceleration.
The range assumed for the gust initial value Vl represents the possible variation of WTGs rated wind speed.

The sensibility analysis showed in fig.4 therefore, is to be understood as an evaluation of the relative importance of the above mentioned parameters in the probability assessment of an extreme gust on a WT, running at its rated wind speed.

4 - Conclusions

Beside a few parameters (Ir, Vi, Vl), which are not very significant, the analysis shows that both site and WT characteristics can have big influences over the likelyhood of a given extreme gust condition.
The biggest effects are deriving, of course, from the turbulence conditions, with a special remark for the Ii parameter, which takes into account the fluctuations of the actual turbulence intensities measured.

5 - References

[1] W.E. Holley, R.W. Thresher and S-R Lin, 1984
"Atmospheric Turbulence inputs for horizontal axis wind turbines"
Proc. EWEC, Hamburg, FRG.

[2] W.C. Cliff, G.H. Fichtl, 1978
"Wind velocity-change (gust rise) criteria for wind turbine design"
DOE-Report EY-76-C-06-1830 by PNLR, Washington, USA.

Index of notations (All wind speeds are referred to the hub height)

SYMBOL DESCRIPTION

a*	Shape parameter for Sy(Ω) function (dependent from D/L)
b*	Shape parameter for Sy(Ω) function (dependent from D/L)
D	Diameter of the concerned horizontal axis WT
Du	Wind speed change during the time interval tau defined as u(t + tau) - u(t)
DV	Gust size defined as V2 - V1
i	Actual turbulence intensity at the wind speed U defined as 100 $\frac{su}{U}$
IU	Average turbulence intensity at the wind speed U defined as the average of i
I5	Average turbulence intensity at U = 5 m/s
I10	Average turbulence intensity at U = 10 m/s
Ii	Index of turbulence intensities distribution defined as 100 $\frac{si}{I}$
Ir	Turbulence intensity ratio defined as I5/I10
K	Nondimensional shape parameter of the Weibull distribution
L	Integral scale length parameter of turbulence
Ny	Number of events per year
p(x,s)	Gaussian probability density function of the parameter x, having a standard deviation s
R	Recurrence time (years) defined as $\frac{1}{Ny}$
sDu	Standard deviation of Du
si	Standard deviation of i
su	Standard deviation of u
sum	Standard deviation of um
Sy	Power spectral density function for the longitudinal component of the wind velocity "uniform" over the rotor disk
t	actual time
T	Time period for defining turbulence (ten minutes)
tau	Gust duration (time over which the wind speed change takes place)
u	Instantaneous wind speed deviation from U
U	Absolute ten minutes average wind speed
um	Middle position of the wind speed change defined as ½(u(t + tau) + u(t))
V	Absolute instantaneous wind speed defined as U + u
V1	Reference wind speed for gust initial value
V2	Reference wind speed for gust final value
Vav	Annual average wind speed
Vi	Cut in wind speed of the concerned WT
Vo	Cut out wind speed of the concerned WT
Ω	Radian frequency of the wind fluctuations

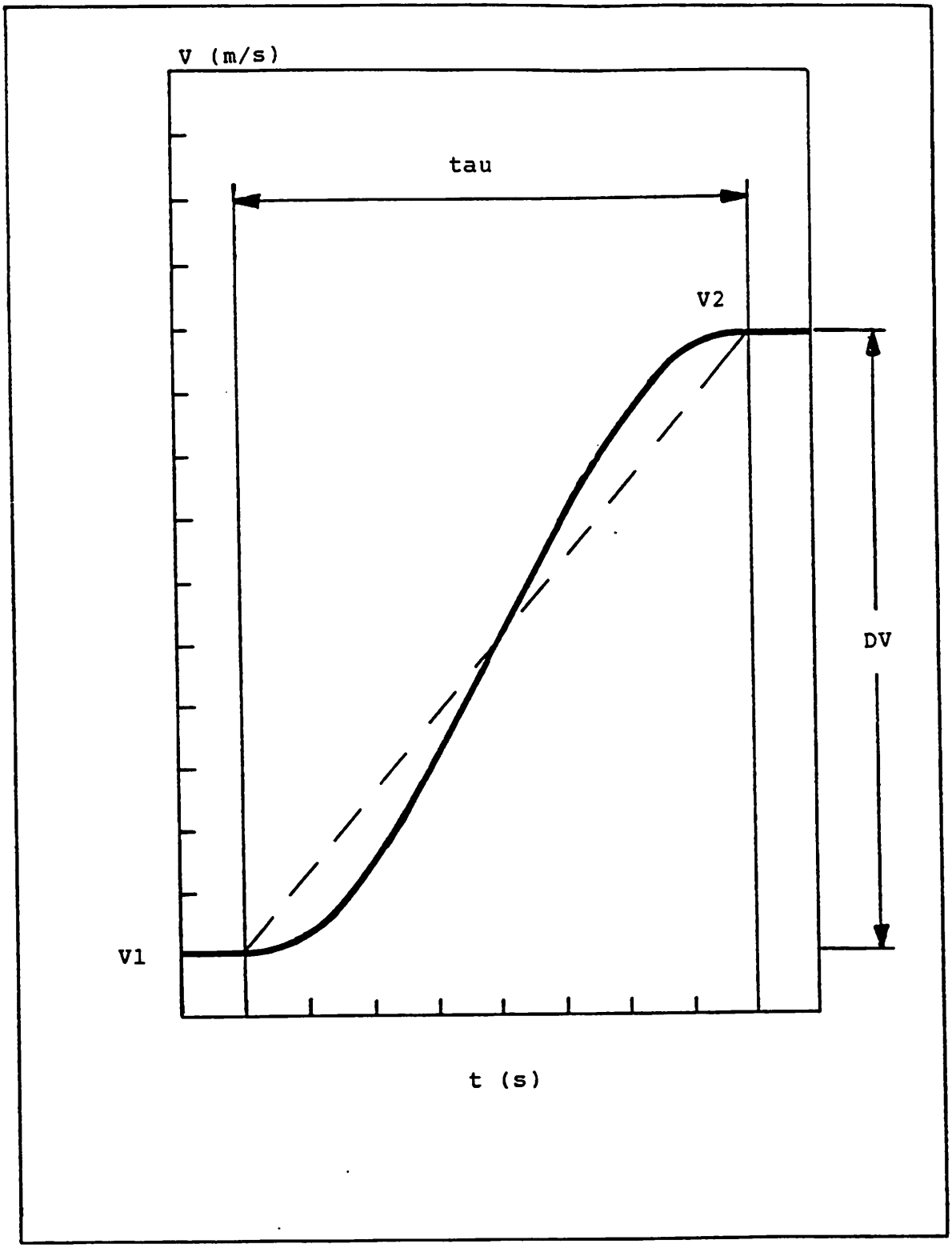

Fig. 1 - Possible shapes of the theoretical gust: rectilinear or sinusoidal.

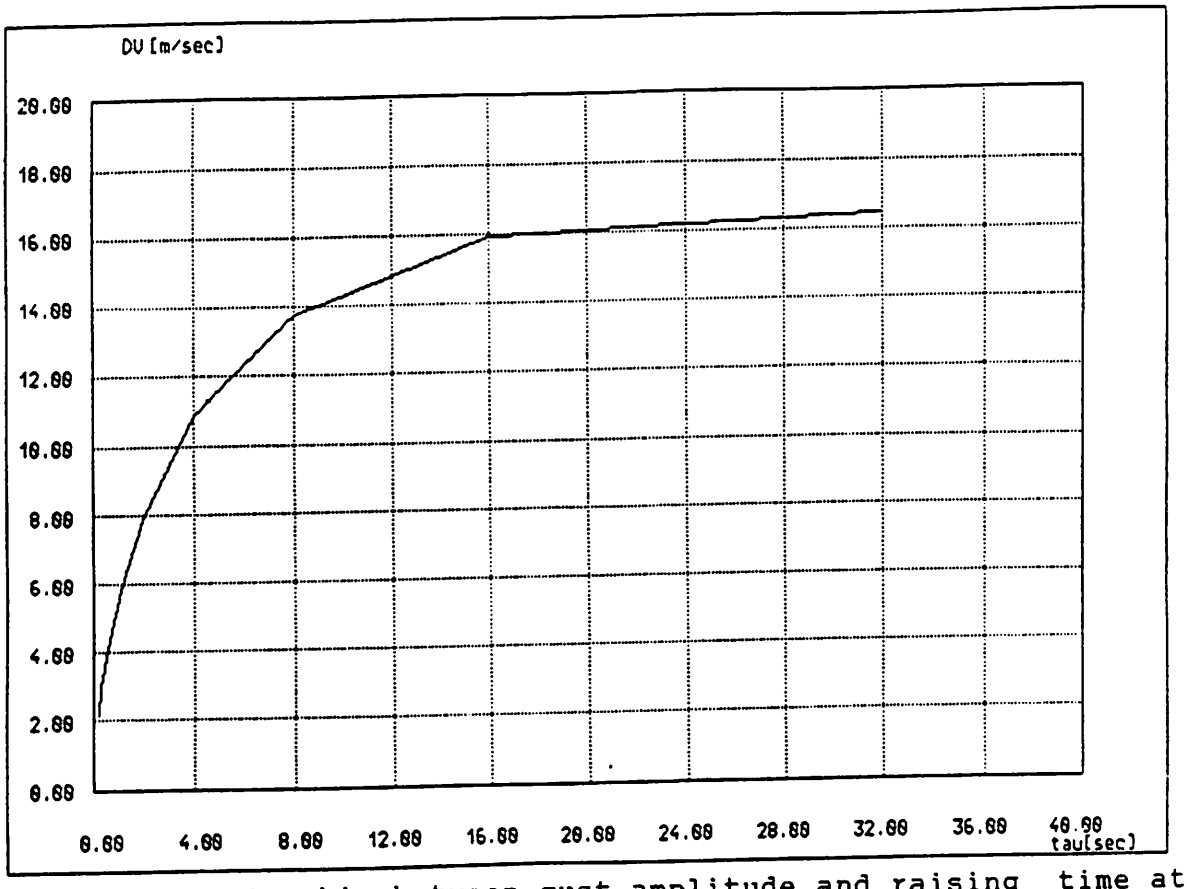

Fig. 2 - Relationship between gust amplitude and raising time at constant recurrence time (30 years) for the WTG M30 in a given site of installation

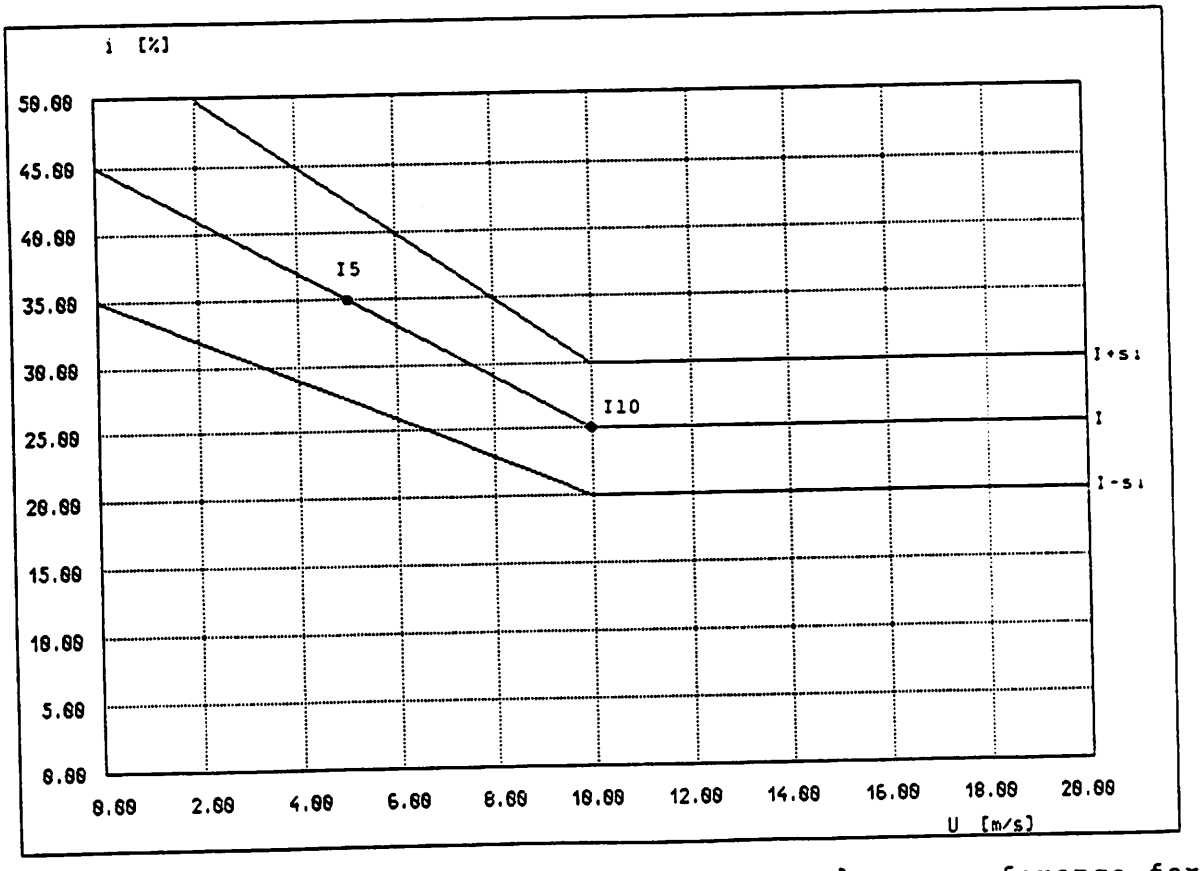

Fig. 3 - Turbulence distribution model assumed as a reference for the sensibility analysis

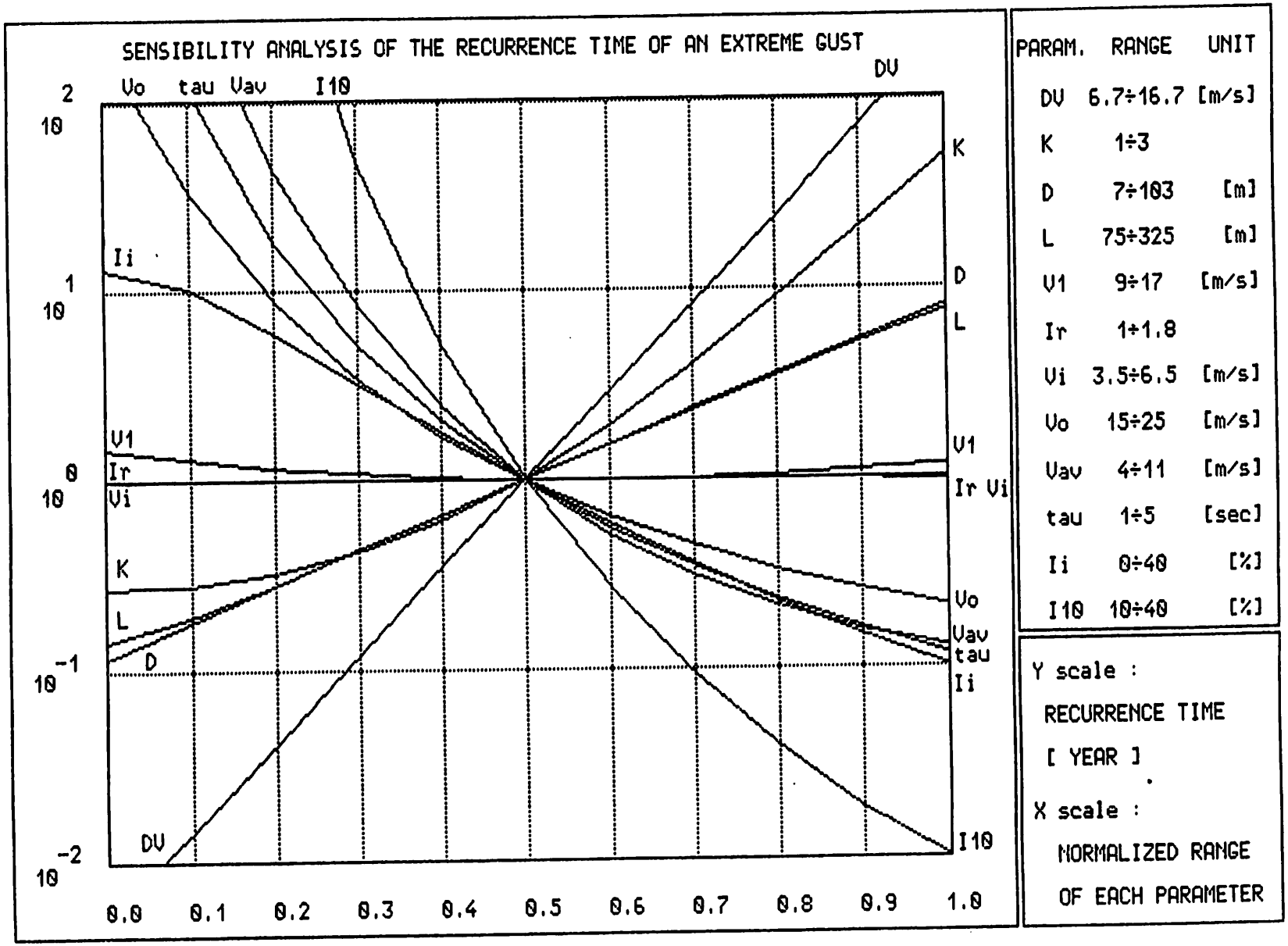

Fig. 4 - Results obtained with the pure theoretical model for the probability assessment of an extreme gust on a WT.

GUST MODELLING FOR THE DUTCH HANDBOOK ON WIND LOADS

F.J. Verheij
TNO - Environmental and Energy Research
P.O. Box 342
7300 AH Apeldoorn
The Netherlands

SUMMARY

In this paper the TNO gust analysis method and the resulting TNO gust model are described. The method has been applied to a set of 700 hours of stationary wind speed time series measured at the meteorological mast at Cabauw, The Netherlands. The results are discussed in this paper.

The TNO gust model has been developed for the calculation of wind turbine loads, especially fatigue loads. To model gusts an analysis method has been developed to statistically analyze full-scale wind speed data and translate these to discrete gusts.

The main result of the TNO gust model is that finally, all gust amplitudes are described by one single expression being a function of the height, the mean wind speed, the turbulence intensity, the gust duration and the probability exceedance level within an error band of less than 5%.
The model also gives a relation between the gust duration and the frequency of occurrence of the gusts.

The TNO gust model has been incorporated in the Dutch Handbook Wind Data for Wind Turbine Design.
Verification of this handbook has been performed by comparing the flap and lag loads on the blade root of three different wind turbines by means of the Handbook with the loads measured. The comparison showed very good agreement especially in the range 10^2 to 10^8 load fluctuations per year.

1. INTRODUCTION

Turbulent wind makes an important, if not the most important, contribution to the load of a wind turbine. This applies both to fatigue wind loads as to loads under extreme wind conditions. In order to arrive at reliable and cost-effective machines a profound knowledge of the atmospheric turbulence is essential.
TNO - Environmental and Energy Research has developed a method which enables the derivation of discrete model gusts from measured wind data (Luken and Verheij '89, Verheij '91). Results of the discrete wind gust analysis on wind data supplied by the Royal Dutch Meteorological Office (KNMI) have been used as a solid basis for the Dutch Handbook 'Wind Data for Wind Turbine Design' (Föllings et al. '89, Verheij et al. '91),

which wind turbine designers frequently use. Making use of the discrete gusts wind load calculations in the time domain can be performed straightforward.

In the near future the TNO gust analysis method will be used for the analysis of wind speed time series measured during extreme wind conditions. Application of the method to wind turbine wake data are planned in 1992.

2. TNO GUST ANALYSIS METHOD

The TNO gust analysis method has been developed to reduce measured wind speed data statistically and translate these data into discrete gusts. The gusts are applied to calculate wind turbine fatigue loads.
One of the aims of the method is to describe the wind experienced by the wind turbine. The rotation of the turbine blades is therefore taken into account.
The method consists of the following steps, see also figure 1.

- The measured wind signal is split into a 10 minute running average value (mean wind speed) and wind speed fluctuations (turbulence) superposed on it. Based on these signals the running rms value (turbulence intensity) is known.
- The resulting time series consists of a series of gusts, separated by zero-crossings which has been defined as the crossing of the instantaneous value with the running average value (figure 1a). The location of each zero-crossing is determined by interpolation between the two nearest data points. The period between a positive and a negative zero-crossing has been defined as the gust duration T (half a period!). The value of the mean wind speed and the turbulence intensity at the beginning of a gust and the gust duration are of importance for further analysis of the gusts.
- The gusts are translated into non-dimensional gusts, the non-dimensional gust amplitude being a function of the non-dimensional gust duration (figure 1b). The non-dimensional gust duration is derived dividing the time t by the gust duration T. The non-dimensional gust amplitude is derived dividing the wind speed fluctuation u by the running average value U and multiply this by a function of T (see Chapter Gust Analysis).

- Gust analysis matrices have been created divided into 10 columns (time intervals i) and 35 rows (amplitude intervals j). The combination of wind speed increment Δu and time step Δt after the zero-crossing forms a pair of coordinates (figure 1c). All pairs of coordinates within a measured gust are transferred into non-dimensional coordinates denoting matrix elements. Each time the same pair of non-dimensional coordinates is found for another gust the value of the matrix element is increased by one.
- The number of points N(i,j) in element (i,j) divided by the sum of the number of points N(i,0) up to N(i,j) inclusive defines the probability exceedance level P(i,j) of the gust amplitude at element (i,j).
- The gusts are binned according to several external conditions, such as (rotor hub) height, mean wind speed and turbulence intensity and recorded in a gust analysis matrix. Meanwhile the number of gusts, divided into several gust duration intervals, is recorded in a separate matrix. For each combination of conditions a matrix is created.
- Under the condition that a suficiently large number of gusts exists discrete model gusts are derived statistically. The discrete gust is described by its amplitude, duration, shape and probability exceedance level.

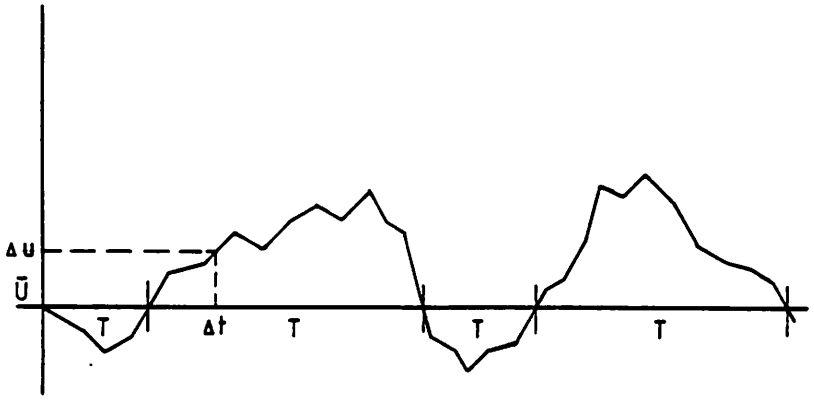

a. Measured wind speed time series divided into mean wind speed and superposed gusts with duration T. The denoted point is found Δt seconds after a zero-crossing and Δu m/s above the mean wind speed.

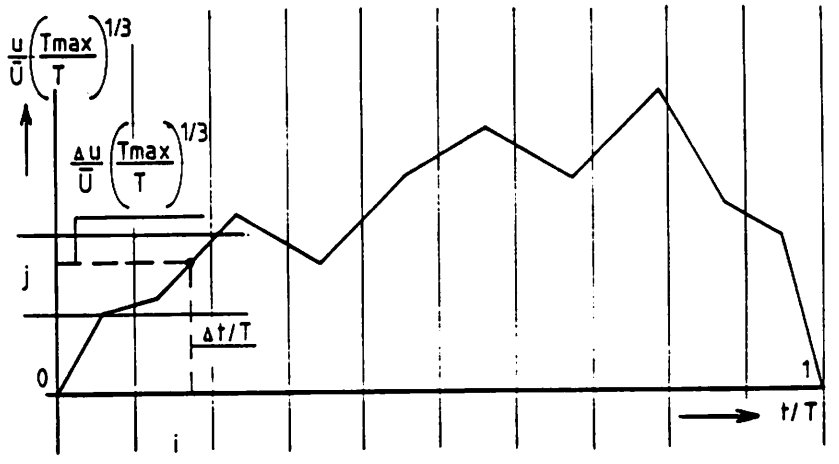

b. Transferring a gust into a non-dimensional gust. The denoted point is found in matrix element (i,j) (column i on the non-dimensional time axis and row j on the non-dimensional wind speed axis).

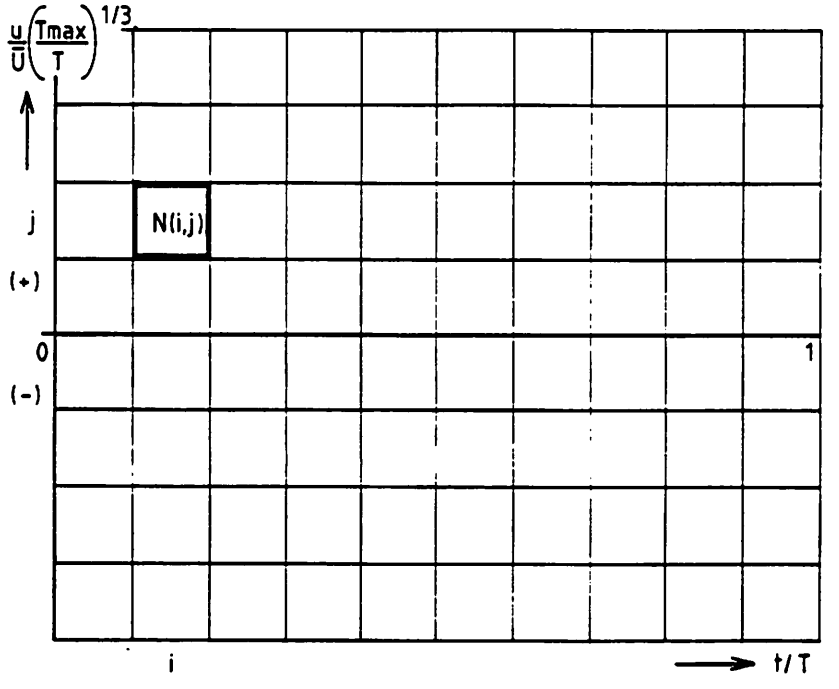

c. Gust analysis matrix. The number of points N(i,j) in matrix element (i,j) divided by the sum of the number of points N(i,0) up to N(i,j) inclusive defines the probability exceedance level P(i,j) at this element.

Figure 1. Processing of wind speed time series according to the TNO gust analysis method

The TNO gust analysis method has been applied to a set of 700 hours of wind speed time series measured at the meteorologistical mast at Cabauw, The Netherlands.

3. SITE DESCRIPTION CABAUW

The 213 m meteorological tower of the Royal Dutch Meteorological Institute which has been used to collect the wind speed data is located in the centre of The Netherlands, near the village of Cabauw. The local topography is very suitable for boundary layer measurements. The surrounding area is flat within a radius of at least 20 km. The area includes meadows and ditches, with scattered villages, orchards and lines of trees. The surface roughness length depends on wind direction and season and varies between 0.05 m and 0.35 m.

The tower is constructed as a closed cylinder of 2 m diameter. From 20 m upwards horizontal booms are installed at 20 m intervals. At each level there are three booms, extending 9.4 m beyond the cylinder, located at wind directions of 10°, 130° and 250°. In this investigation only the 10° and 250° booms at 20 m, 40 m and 80 m have been used.
An additional mast, located South-East of the main mast, has been used to measure wind speeds at 10 m.

The wind speed measurements have been carried out with a sample frequency of 2 Hz during times when high wind speeds were expected. In this way a data set was obtained specifically focused on high wind speeds and instationary situations associated with passing weather fronts generating high winds.
A set of approximately 700 hrs of wind speed data was collected during a 1.5 year measuring period.

4. INITIAL ANALYSIS OF THE CABAUW WIND SPEED DATA

As the relationship between gust amplitude, gust duration and gust shape is expected to be dependant on the mean (or running average) wind speed, the turbulence level, the gust duration and the measuring height, these parameters are used to bin the data into specific intervals. The various intervals are described in table 1. The applicability for wind turbine

design purposes combined with the site conditions defines the limits of the intervals.

4. INITIAL ANALYSIS OF THE CABAUW WIND SPEED DATA

As the relationship between gust amplitude, gust duration and gust shape is expected to be dependant on the mean (or running average) wind speed, the turbulence level, the gust duration and the measuring height, these parameters are used to bin the data into specific intervals. The various intervals are described in table 1. The applicability for wind turbine design purposes combined with the site conditions defines the limits of the intervals.

Table 1 Bin intervals for gust analysis

1.	Height H	:	10, 20, 40, 80 m.
2.	Running average wind speed U	:	10 equidistant classes of 2 m/s from 0 to 20 m/s and others > 20 m/s.
3.	Gust duration	:	7 classes i.e.: [0,2 s]; [2,4 s]; [4,8 s]; [8,12 s]; [12,18 s]; [18,26 s] and others > 26 s
4.	Turbulence level	:	7 classes i.e.: [0,8%]; [8,11%]; [11,14%]; [14,16%]; [16,18%]; [18,22%] and others >22%
5.	Gust sign	:	positive and negative gusts with respect to running average wind speed

The gust analysis method aims at establishing a relationship between amplitude, duration and shape of a gust. Before applying this method to the Cabauw data pre-analysis of the data has been performed to define whether the data is reliable and whether the data fulfils the known statistical description of the wind data in the Netherlands. To this end among others spectra (APSD) and probability density functions have been produced for several wind speed classes measured at the abovementioned heights.

From the results the following can be stated:

- The distribution of the 10 minute averages can be described using customary Weibull probability density functions;
- The distribution of the wind speed fluctuations within these 10 minute periods is in agreement with the Gaussian probability density functions;

- The range of turbulence intensities is in accordance with the existing terrain roughnesses in the surroundings of the met mast;
- The spectra fits with the Kaimal spectra also used in ESDU '75.

Initial gust analysis of only 40 hours out of the available 700 hours of data has been carried out. These 40 hours consist of 13 wind speed time series with a length of about 3 hours each. All series fulfil the strict stationarity criterium of:

$$U_{max} - U_{min} < 0.2 * (U_{max} + U_{min})/2 \qquad (1)$$

U_{max} and U_{min} being the maximum and the minimum 10 minutes average wind speed within the 3 hours respectively.

The time series of the selected hours has been processed as outlined in the previous chapter.
To start with similarity of the gusts within a gust duration interval has been assumed. The normalised gust amplitude then can be created by multiplying the non-dimensional amplitude u/U by T_{max}/T, T_{max} being the upper limit of the gust duration interval.
Plots of the filled gust analysis matrices have been made for several combinations of intervals. Analysis of these plots achieves the following results:

- The gusts generally are symmetrical. Their maximum value therefore is reached halfway the gust duration. This maximum value, the gust amplitude (u_{max} or A) is the key parameter in wind turbine fatigue calculation.
- The difference between gusts with positive and negative sign as compared to size and shape of the gust is negligible.
- For the chosen intervals the following relation between gust amplitude and gust duration holds:

$$A = f(other) \times T^{(1/3)} \qquad (2)$$

f(other) being a function of other parameters, but independent of the duration T.
By theoretical analysis it can be shown that the gust amplitude should indeed be inversely proportional to the gust duration cubed. Taking the energy content of the wind speed fluctuations according to the atmospheric energy spectrum in the high frequency range to be:

$$E \div n^{(-2/3)} \tag{3}$$

and the energy content of a gust to be proportional to the gust amplitude squared (u^2 or A^2) it can be shown that:

$$A \div n^{(-1/3)} = T^{(1/3)} \tag{4}$$

The agreement between analysis and theory supports the application of the TNO gust analysis method to gust modelling for wind turbine design.

- The distribution of the gust amplitudes is not Gaussian but tends to be more like a Weibull type of distribution. For exceedance probability levels in the 1 - 10% range the difference between the two distributions however appears to be small.
- The function f(other) appears to be clearly dependent on the measuring height. This function is also supposed to be dependent of the average wind speed and the turbulence intensity. However, the 40 hours of data mainly consist of data within a small range of both parameters mentioned.
- The 40 hours contain too little data to describe gusts with a probability exceedance level smaller than 1%. It is therefore impossible to model the wind loads in the low frequency range of the load spectra well.

5. FINAL ANALYSIS OF THE CABAUW WIND SPEED DATA

5.1 Amplitude

The final objective of the gust analysis method is to arrive at a relation between the gust amplitude and duration as a function of the height, wind speed and turbulence as well as the exceedance probability level.

As shown above the non-dimensional gust amplitude A' now can be written as

$$A' = u/U * (T_{max}/T)^{1/3} \tag{5}$$

T_{max} being 26 seconds, the maximum gust duration to be investigated.

As far as the gust amplitude is concerned this means that no distinction

between gust duration intervals has to be made. This way the number of gust analysis matrices is reduced and the number of gusts per matrix is increased hence the amount of statistical information.
The amount of statistical information is also increased by applying 700 hours of data instead of 40. More than 80 matrices each representing a unique combination of intervals existing of hundreds of gusts have been used for detailed analysis. This way sufficient statistical information on the gusts is available to model gusts with probability exceedance levels down to 0.1%.
An example of such a result is given in figure 2 at the end of this paper. The presented gusts represent the amplitude probability levels of 25, 10, 1% and 0.1%. It should be noted that the gusts are the result of a statistical analysis and therefore do not necessarily represent a physically occurring gust.

The following results has been achieved:

- The probability density of the non-dimensional gust amplitudes seems to be in accordance with a Weibull probability density function using the shape parameter k = 1.8. This function holds for almost the full range of intervals. For the lowest and for the highest wind speed intervals the shape parameter should be slightly lower and higher respectively.
- The shape of the gusts agree with the sine function

$$\sin^{0.3}(\pi t/T) \tag{6}$$

- An empirical relationship has been established between the gust amplitude and the measuring height, the average wind speed and the turbulence intensity.
- The main result is that finally, all gust amplitudes are described by one single expression being a function of the height, the mean wind speed, the turbulence intensity, the gust duration and the probability exceedance level within an error band of less than 5%.

$$A = 0.052\, C_A\, H^{-0.19}\, (1 + 5.6\, \sigma_{u,eff}/U)\, T^{1/3}\, (1 + 0.34\, U^{1/3})U \tag{7}$$

C_A being a constant dependent on the probability exceedance level, $\sigma_{u,eff}/U$ being the rotor averaged turbulence intensity.

5.2 Number of gusts

The number of gusts are counted for each gust duration interval as mentioned in the foregoing chapter. From these statistics an expression has been derived in which the number of occurrence of the gusts is described as a function of the gust duration.

$$N = 1.09\ T^{-1.57} \tag{8}$$

The constant has been chosen in such a way that the total number of gusts with gust duration between 2 and 30 seconds, an important range for operating wind turbines, and a duration interval of 1 second equals one.

This expression too fits for the full range of intervals.

6. TNO GUST MODEL

Expressions 6 and 8 mould the basis of the TNO gust model. Derived from this intervals of the mean wind speed U, the gust duration T and the probability exceedance level P are recommended.
The TNO gust model has been incorporated in the Dutch Handbook Wind Data for Wind Turbine Design. The Handbook enables designers to calculate gust amplitudes for 72 combinations of intervals: 8 wind speed classes times 3 gust duration intervals times 3 probability exceedance levels.

6.1 Wind speed classes

There are 8 classes of mean wind speeds with a width of 2 m/s between 4 and 20 m/s. The probability density of each class is calculated using the yearly mean wind speed at hub height and the Weibull probability density function with the belonging parameters.

6.2 Gust duration intervals

There are 3 gust duration intervals which has been chosen in such a way that each interval occurs 20 minutes per hour. The weighted average gust duration T_d defines the number of gusts occurring per hour N_{hr}. The intervals are:

	interval	T_d	N_{hr}
1	2 - 7 s	4 s	150
2	7 - 16 s	10 s	60
3	16 - 30 s	20 s	30

6.3 Probability exceedance level

Within each gust duration interval the gusts are divided into 3 discrete gusts which amplitude is dependent of the probability exceedance level defined by the Weibull parameters. This is represented by the constant C_A in equation 7. All gust amplitudes are normalised with the 10%-gust. The number of gusts occurring is also based upon the probability exceedance level:

probability exc. level	constant C_A	number of gusts occurring
10 %	1.00	80%
1 %	1.64	18%
0.01%	2.52	2%

7. WIND TURBINE LOADS

Verification of this handbook has been performed by comparing the flap and lag loads on the blade root of three different wind turbines in the range of 250 to 1000 kW by means of the Handbook with the loads measured. The comparison showed very good agreement especially in the range 10^2 to 10^8 load fluctuations per year.
Extensive presentation and discussion of these results will be given in papers of Berkelmans '91 and Rademakers et al. '91.

8. FUTURE PURPOSES

At present the method has only been applied to the calculation of fatigue loads of wind turbines. In the near future the analysis of gust shape, amplitude and duration will be extended to situations of extreme wind conditions in order to calculate extreme wind turbine loads.

At the moment TNO is involved in a CEC JOULE project in which application of the TNO gust analysis method to wind turbine wake data is planned in 1992.

9. CONCLUSIONS

The TNO gust analysis method to statistically analyze measured wind speed data has proven to be a very useful tool to derive gust parameters.
Application of this method to the Cabauw data set resulted in the TNO gust model. The main result is that finally, all gust amplitudes are described by one single expression being a function of the height, the mean wind speed, the turbulence intensity, the gust duration and the probability exceedance level within an error band of less than 5%. The model also gives a relation between the gust duration and the frequency of occurrence of the gusts.

The results provide an important basis for the TNO gust model applied in the Dutch Handbook Wind Data for Wind Turbine Design.
The gust amplitudes are used as input data for wind turbine fatigue load calculations. Comparison of calculated loads with measured wind turbine loads showed very good agreement especially in the range 10^2 to 10^8 load fluctuations per year. We believe therefore that the model gives a reliable discrete description of the atmospheric wind as far as wind turbine loads are concerned.

10. REFERENCES

[1] Berkelmans, M. (to be published);
The relevance of different gust components for the load spectrum;
IEA Workshop Wind characteristics of relevance for wind turbine design, Stockholm, March 7-8 1991.

[2] Föllings, F.J., et al.;
Gust Modelling for Windturbines: development of a handbook for wind turbine design;
Proc. of European Wind Energy Conference EWEC'89, Glasgow, Scotland (1989), pp. 513-517.

[3] Luken, E. and Verheij, F.J.;
Multi-Parameter Statistics for Gust Analysis. A Statistical Method to Derive Discrete Fatigue Gusts from Full-Scale Wind Speed Data;
Wind Engineering, Vol. 13 No. 5 1998, pp. 252-258.

[4] Rademakers, L.W.M.M. et al. (to be published);
Verification of the Dutch handbook wind data for wind turbine design;
European Wind Energy Conference EWEC'91, Amsterdam, The Netherlands (1991).

[5] Verheij, F.J. and Pleune, R.;
Modelling of extreme wind conditions for wind turbine design;
Proc. of European Commently Wind Energy Conference ECWEC'90, Madrid, Spain (1990), pp. 374-378.

[6] Verheij, F.J., Föllings, F.J. and Curvers, A.P.W.M.;
Handbook Wind Data for Wind Turbine Design - Version 3;
TNO - Environmental and Energy Research, Apeldoorn, January 1991.

[7] Verheij, F.J. (to be published);
TNO Gust Model;
TNO - Environmental and Energy Research, Apeldoorn, June 1991.

[8] Engineering Sciences Data Units;
Characteristics of atmospheric turbulence near the ground.
Part III: variations in space and time for strong winds (neutral atmosphere);
ESDU 75001, London, UK, 1975.

Figure 2 Example of statistical gusts at 20 m and 80 m. The gusts presented refer to two different wind speed and two different turbulence intensities intervals as mentioned in the headings.
The horizontal axis refers to time as a fraction of the gust duration, the vertical axis represents the normalised gustamplitude.
The gusts presented refer to probability exceedance levels of 25, 10, 1 and 0.1% respectively.

H=20m, U=14−16m/s, turb.=14−16%

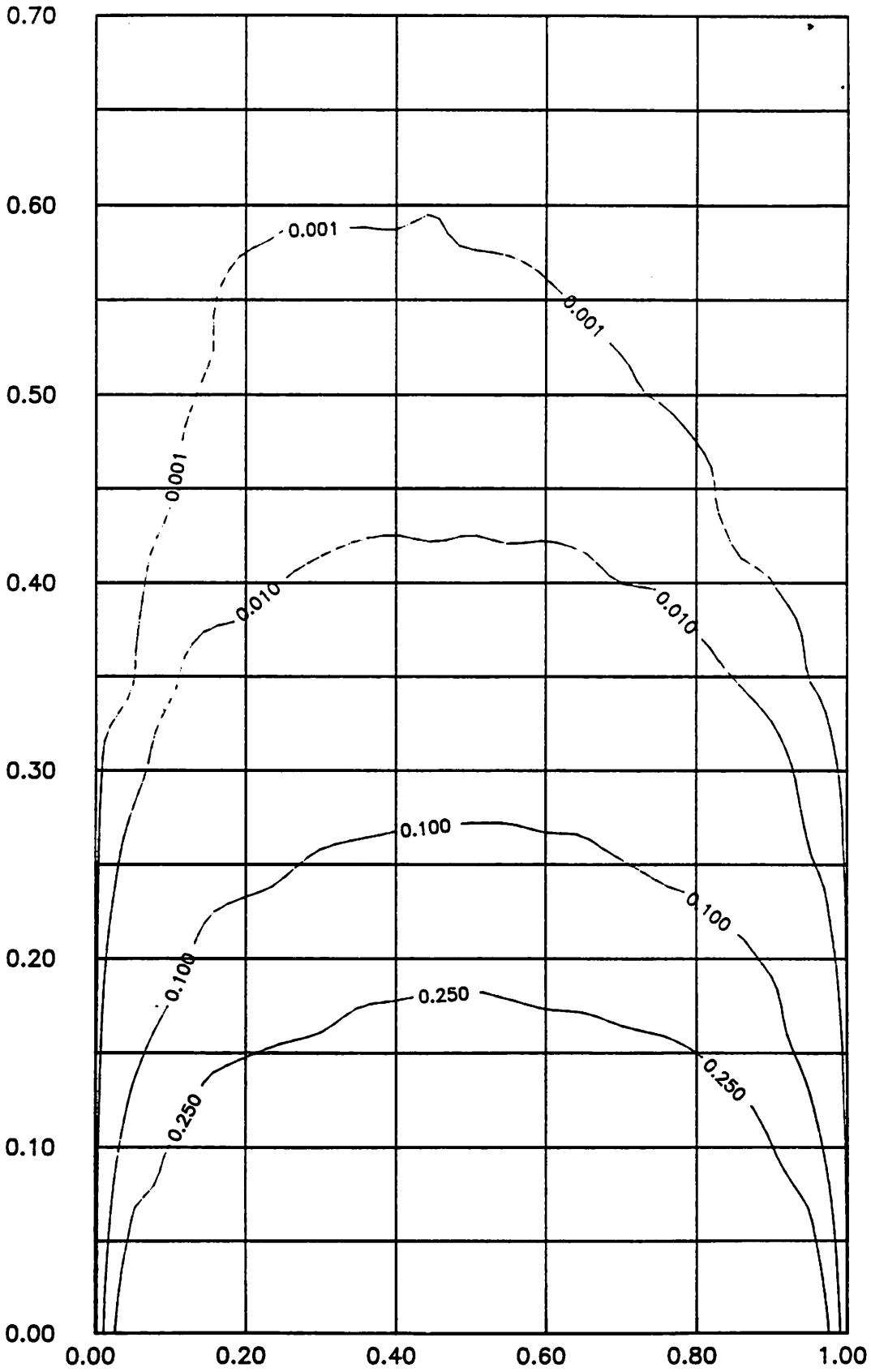

H=20m, U=8−10m/s, turb.=14−16%

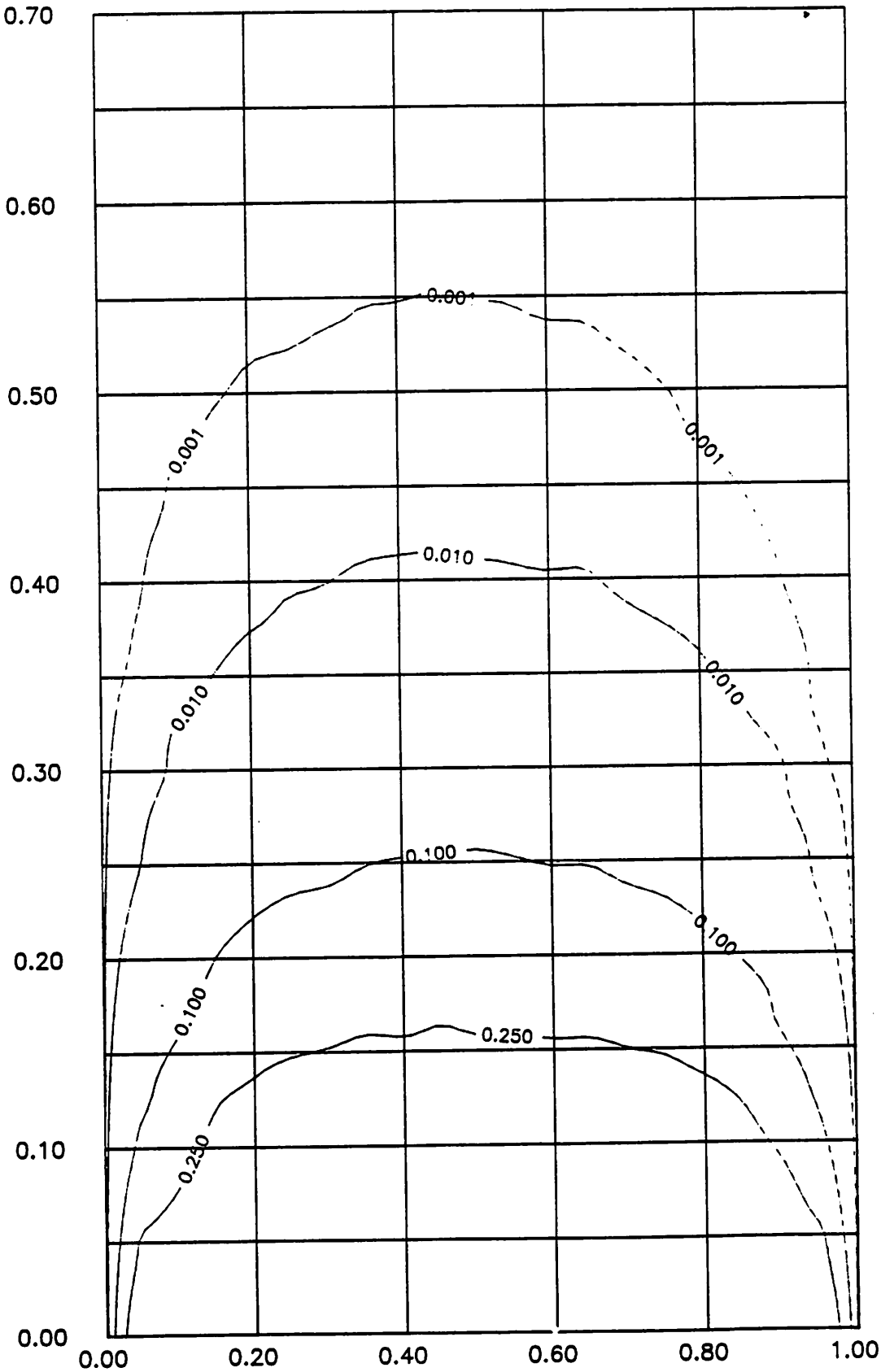

H=20m, U=8−10m/s, turb.=11−14%

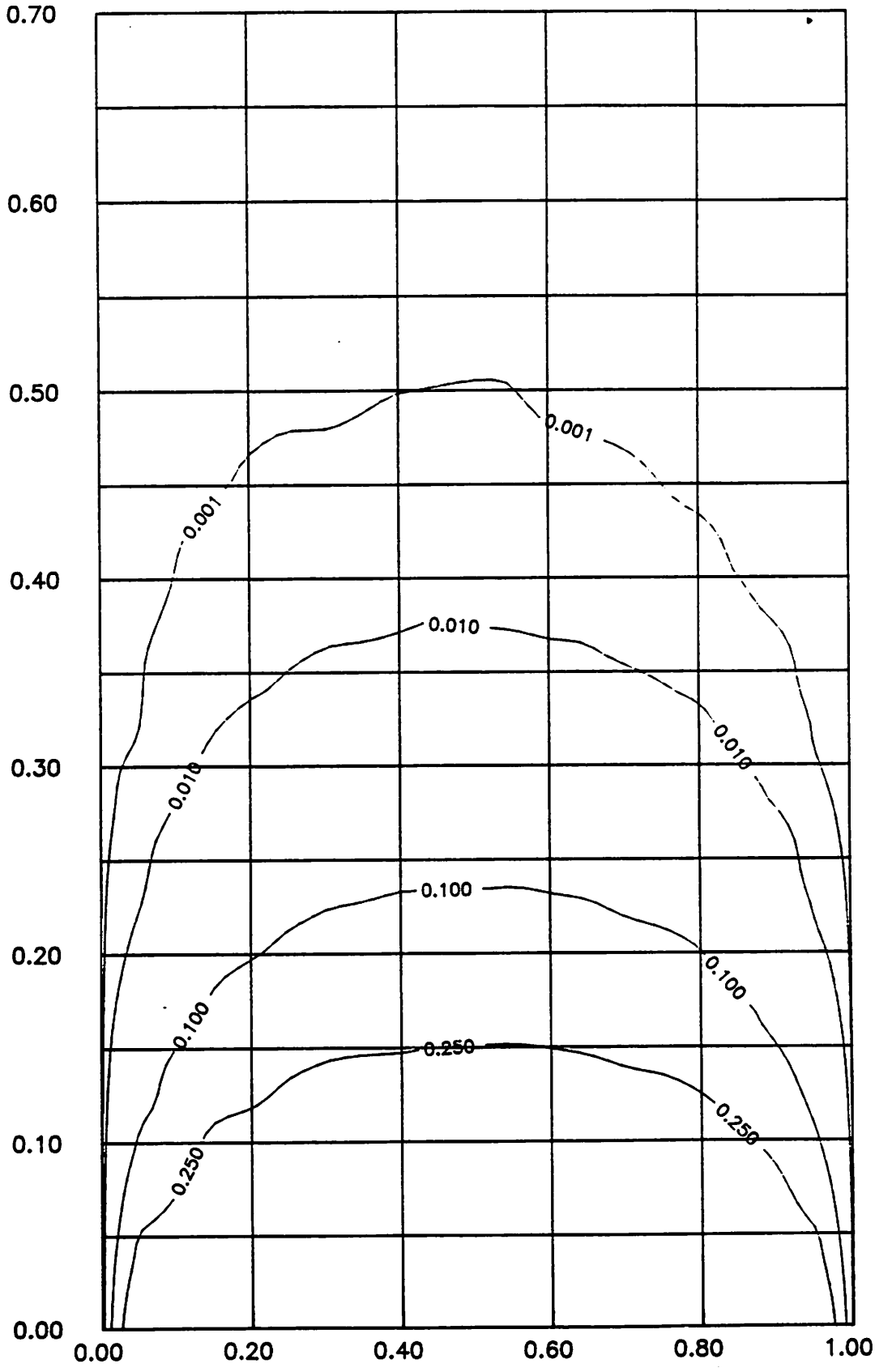

H=80m, U=8−10m/s, turb.=11−14%

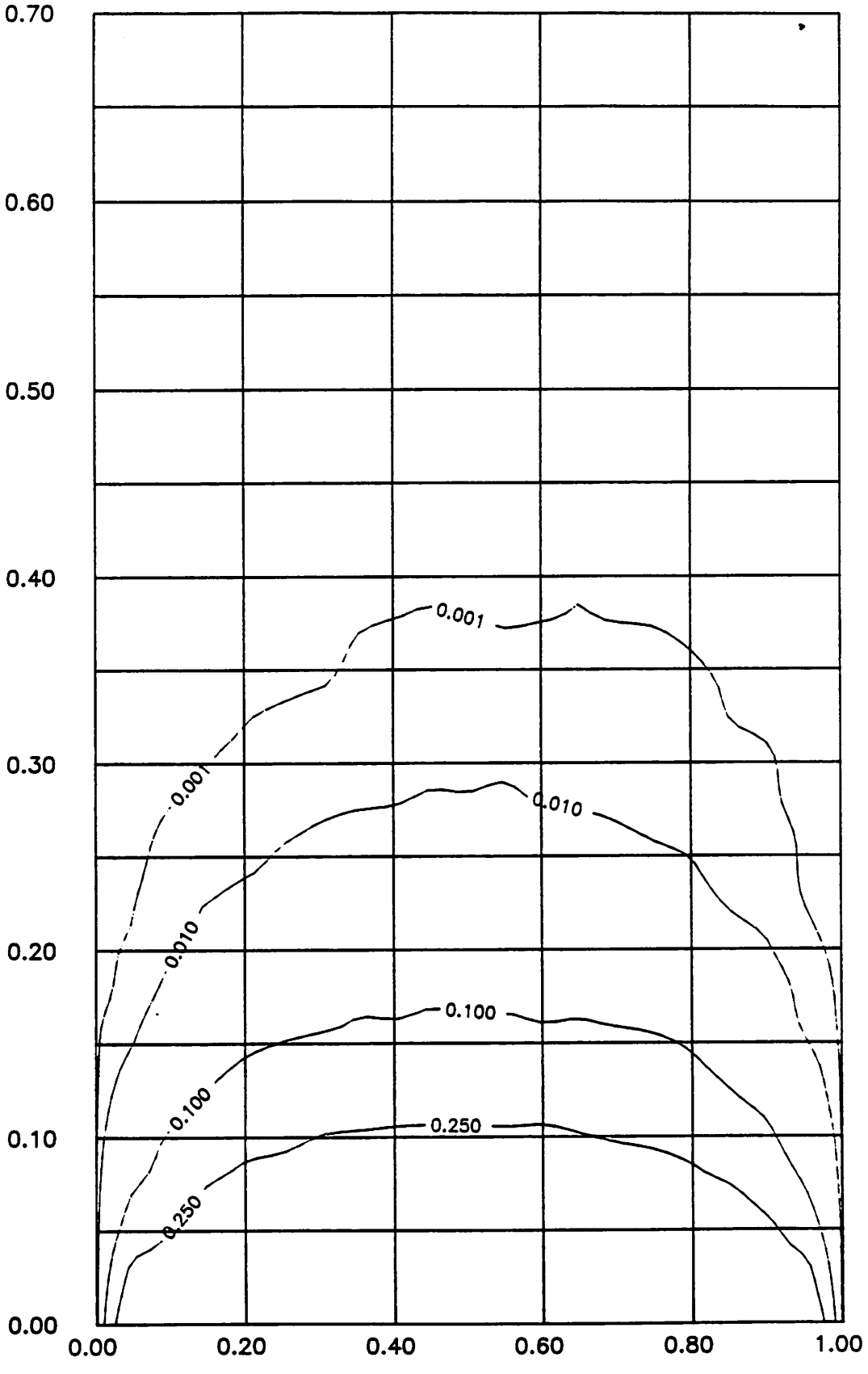

Wind Characterization Research for Wind Turbine Design

IEA R&D WECS Annex XI
March 7-8, 1991
Stockholm, Sweden

Pacific Northwest Laboratory
Richland, WA 99352 USA

Dennis L. Elliott
Senior Research Scientist
Atmospheric Dynamics
ATMOSPHERIC SCIENCES DEPARTMENT

TURBULENCE CHARACTERIZATION PROJECT

OBJECTIVES

- To determine the criteria for wind measurements to characterize turbulence in a standard form for wind turbine design and siting considerations.

- To make the appropriate measurements of turbulence in a variety of terrain types typical of good wind energy sites.

- To establish representative turbulence characteristics for use by designers and developers for specific site types.

TURBULENCE CHARACTERIZATION PROJECT

TECHNICAL APPROACH

- Work with the wind energy community to establish the parameters required, measurements needed, and measurement system requirements.
- Assemble several turbulence measurement systems for loan to the wind energy community for cooperative measurement efforts.
- Deploy the systems in the wind energy community on a rotating basis.
- Apply a standardized analysis package for consistency.

TURBULENCE CHARACTERIZATION

OUTPUT:

- Reports on turbulence conditions encountered in specific terrain and climatic types.
- A summary report on appropriate bounds for turbulence and shear conditions for different types of wind turbine sites.
- Documentation of standardized turbulence analysis package for wind energy applications.
- Recommendations for types of turbulence measurements required to characterize a prospective wind turbine site.

STATUS:

- Assembled and tested a prototype system at PNL.
- Selected six proposals for sites and placed six cooperative agreements.
- Installed three systems in Tehachapi Pass and one in San Gorgonio Pass.
- Initiated analyses of data from first installation.

CANDIDATE ANEMOMETERS

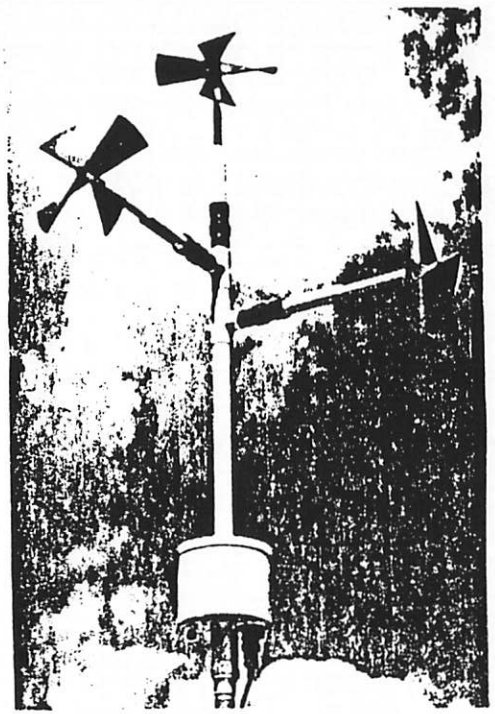

GILL UVW ANEMOMETER

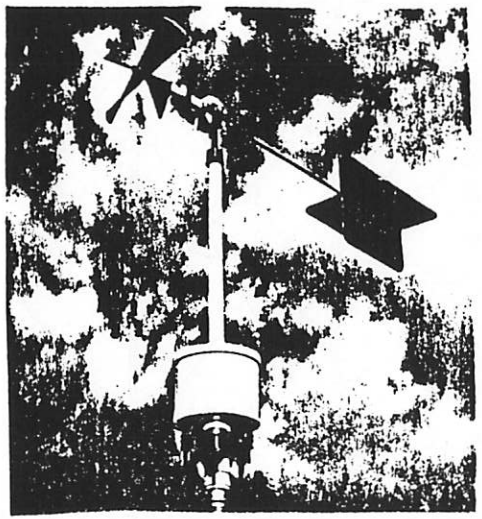

ANEMOMETER BIVANE

WIND MONITOR

TURBULENCE CHARACTERIZATION SYSTEM CONFIGURATION

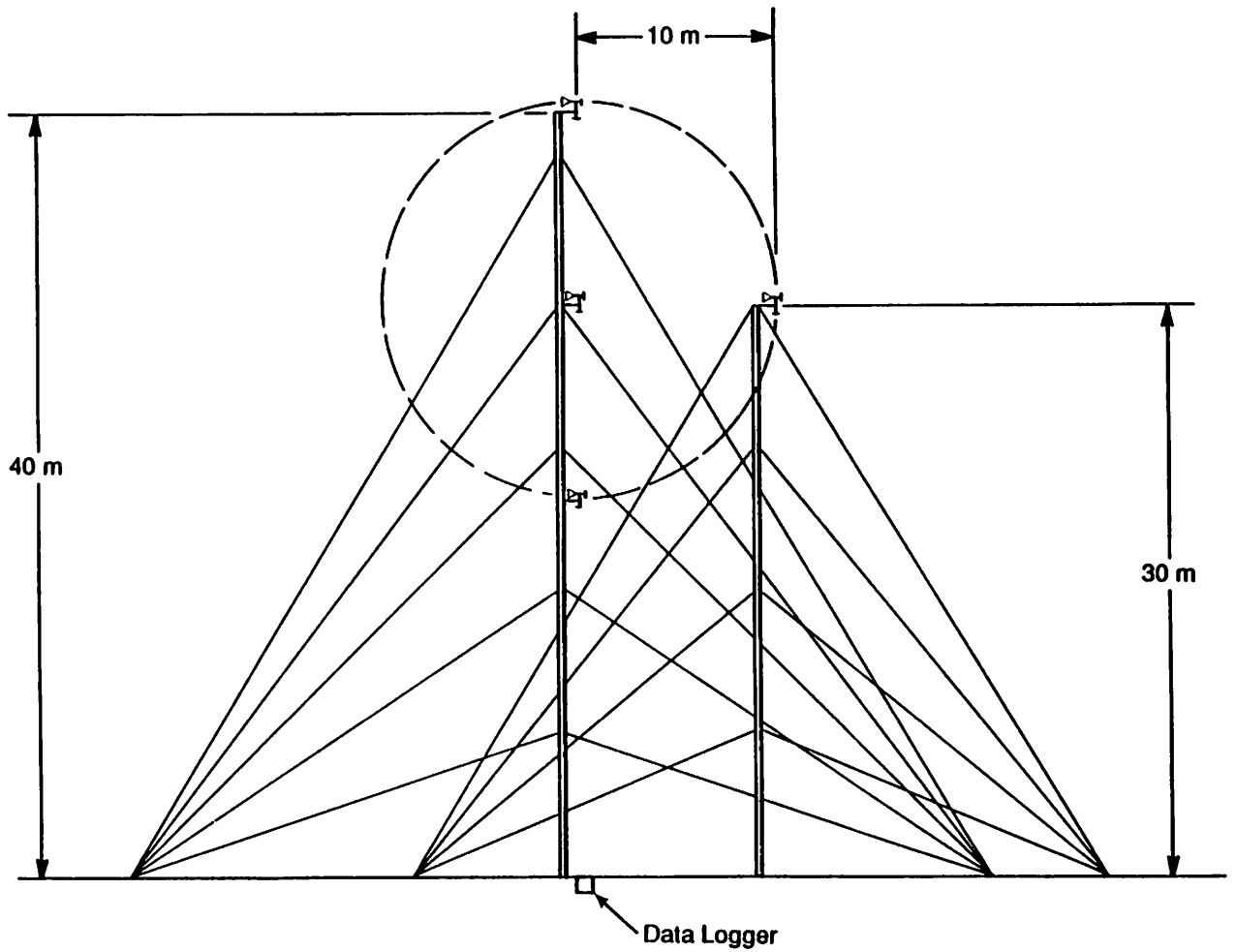

DETAILED SCHEMATIC DRAWING OF SENSOR LAYOUT

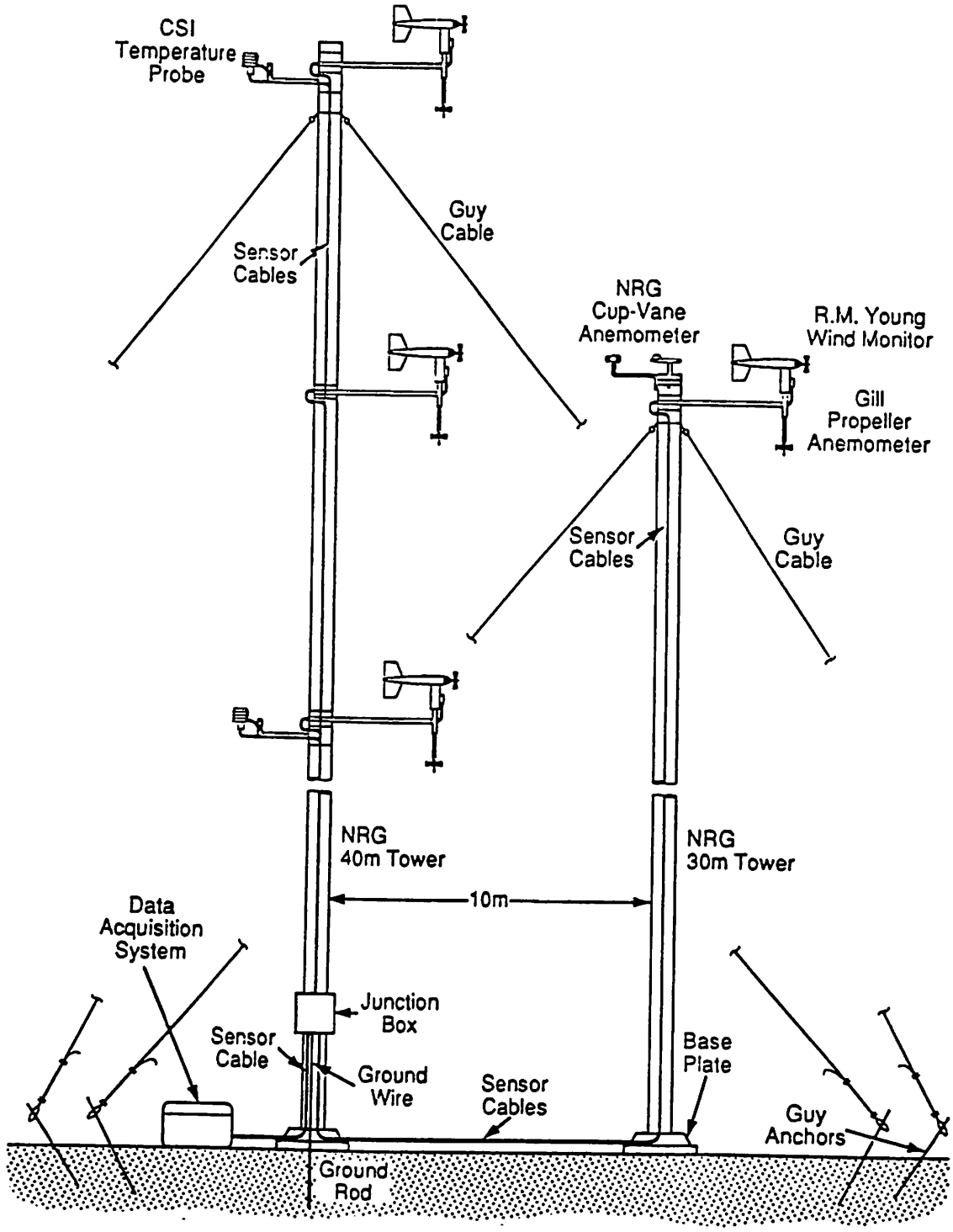

TURBULENCE MEASUREMENT SYSTEM COMPONENTS

TOWERS	$ 4,540
- NRG 40-m tall tower (1)	
- NRG 30-m tall tower (1)	
- NRG sidemount booms (4)	
WIND SENSORS	4,650
- R. M. Young wind monitors (4)	
- Gill propeller anemometers (4)	
- Signal cable	
TEMPERATURE SENSORS	250
- CSI temperature probe (2)	
- Gill radiation shield (2)	
DATA ACQUISITION SYSTEM	7,000
- CSI CR21X micrologger (1)	
- Chaplet 286 laptop computer (1)	
- Tecmar high-capacity tape drive (1)	
- Software	
- Enclosure	
TOTAL	$16,440

DATA COLLECTION SCENARIO

- The CR-21X data logger is programmed to continuously monitor the winds from the four wind sensors measuring 3-D winds and 20- and 40-m temperature sensors at a 5-Hz sampling rate.

- The program causes the laptop computer to
  - record the 5-Hz data on its hard disk when the "hub-height" wind has exceeded 5 m/s for 5 minutes
  - stop recording the 5-Hz data when the winds have been below the 5-m/s threshold for 5 minutes and simply monitor the data ready to resume the recording when the threshold is exceeded.

- The data on the hard disk of the laptop computer are automatically transferred to the high-capacity tape drive.

- A separate system consisting of an NRG data logger and a cup and vane sensor are used to keep a continuous record of 10-min average wind speed and direction at hub height.

DATA ANALYSES CONSIDERATIONS

MEAN AND FREQUENCY DISTRIBUTIONS FOR:

- Turbulence Intensity (speed and direction)
- Gust Characteristics (single point and "enveloping")
- Vertical and Horizontal Shear
- Direction Fluctuations (single point and "enveloping")

PARAMETERS FOR TURBULENCE SIMULATION MODELS:

- Power Spectral Analyses
- Coherence and Coherence Decay Factor
- Longitudinal and Lateral Length Scales
- Surface Roughness Length

COMPARISON OF PROP. VANE AND GILL UVW
(ALONG-WIND COMPONENT - U)

TIME SERIES

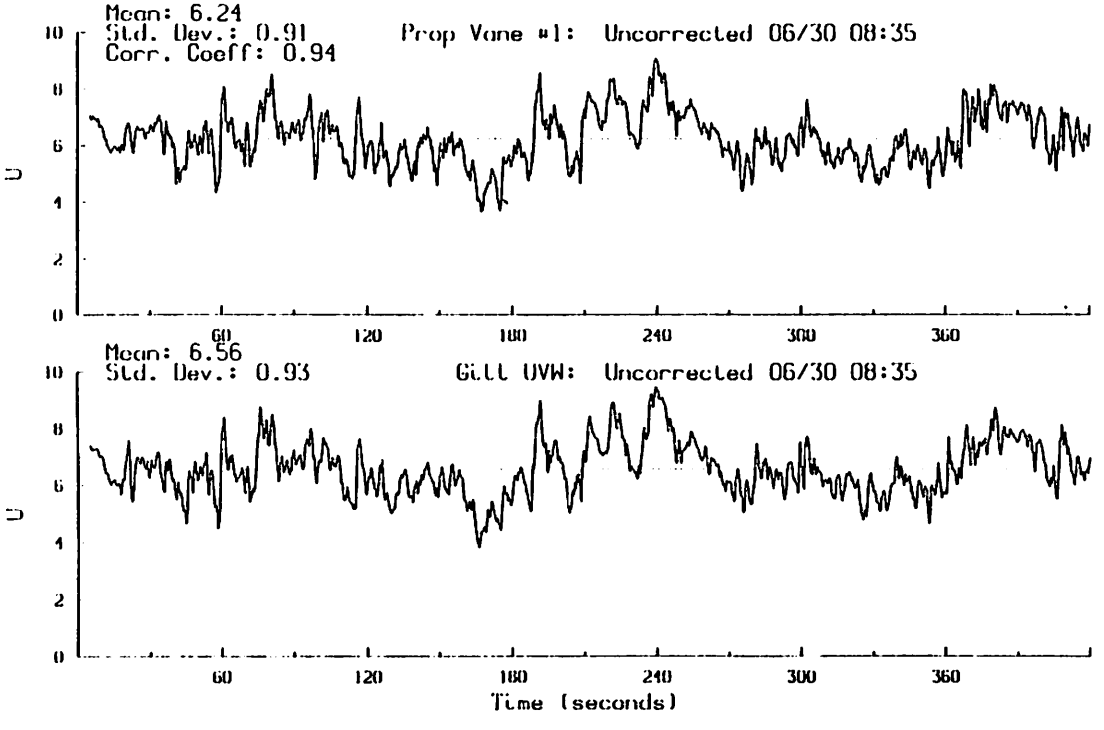

POWER SPECTRA

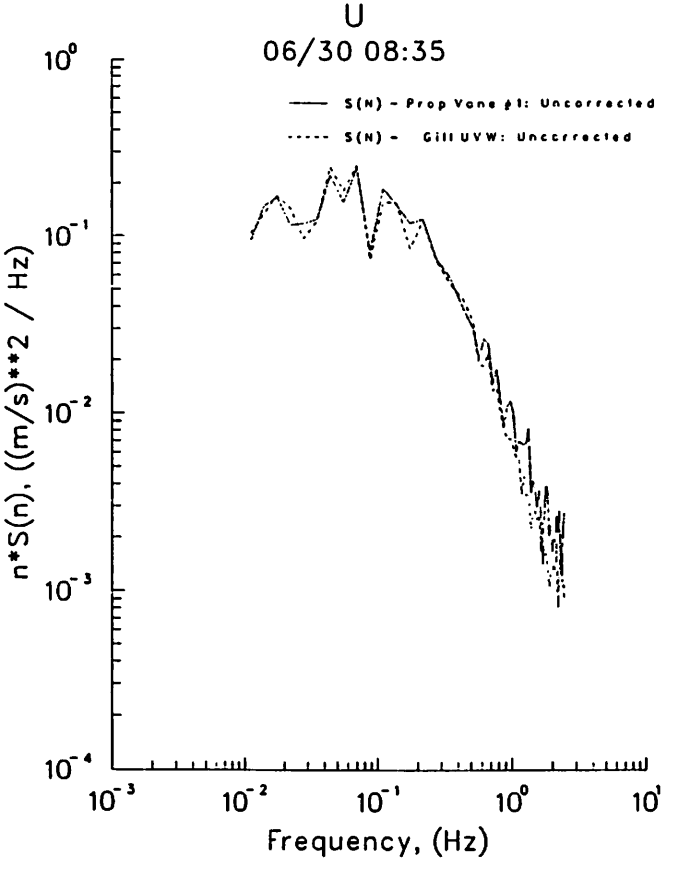

COMPARISON OF PROP. VANE AND GILL UVW
(CROSS-WIND COMPONENT - V)

TIME SERIES

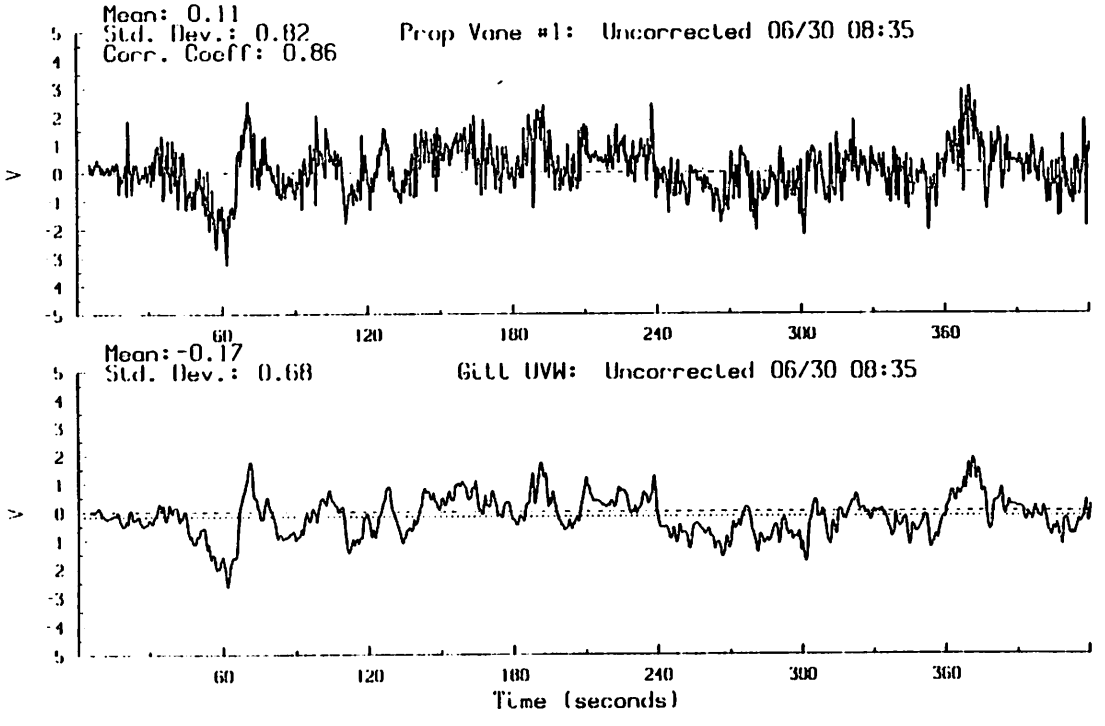

POWER SPECTRA

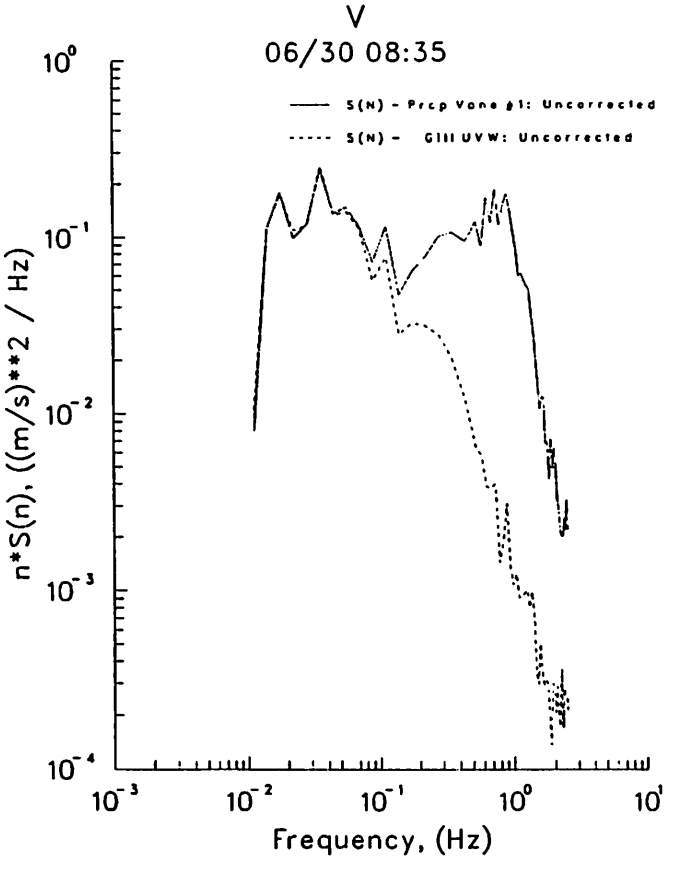

COMPARISON OF PROP. VANE AND GILL UVW
(CROSS-WIND COMPONENT - V)

TIME SERIES

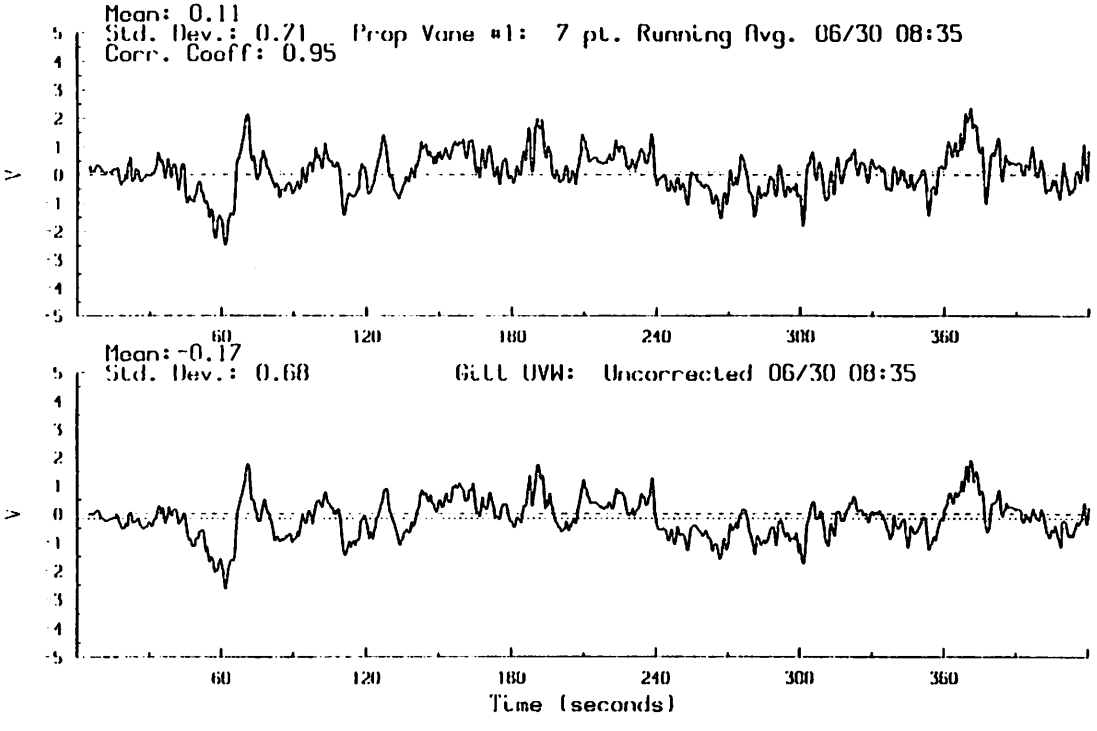

POWER SPECTRA

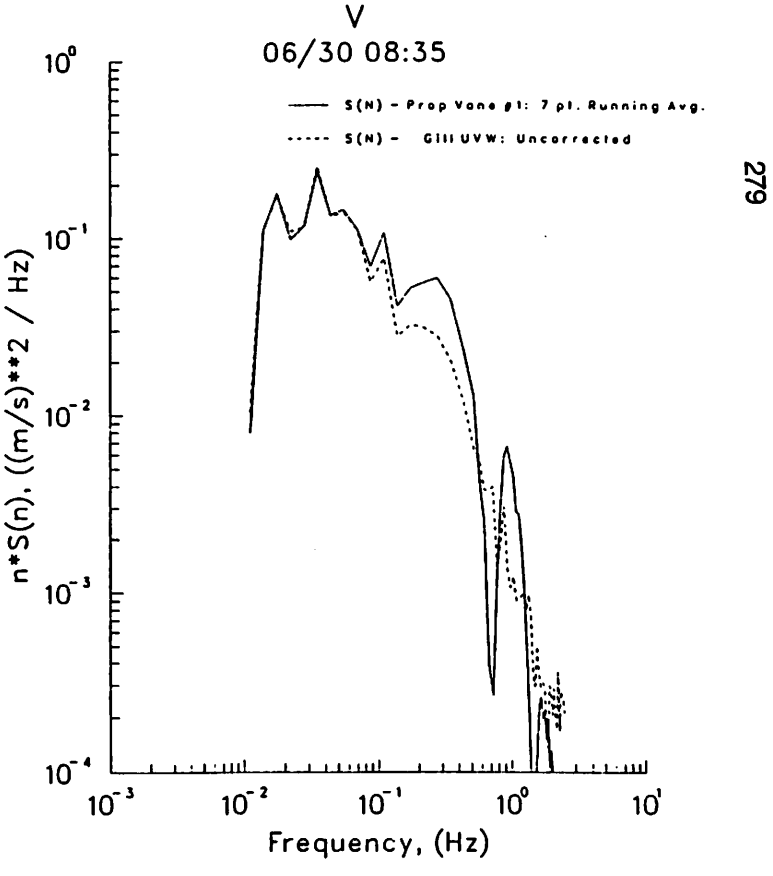

COMPARISON OF PROP. VANE AND GILL UVW
(VERTICAL COMPONENT -W)

TIME SERIES

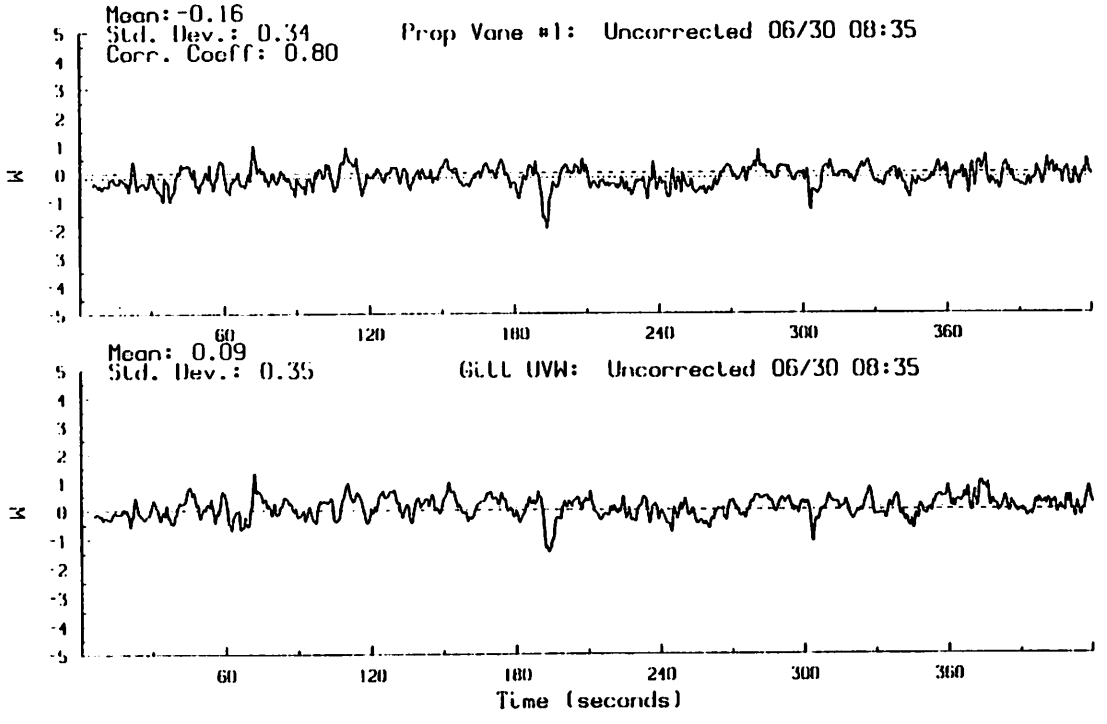

POWER SPECTRA

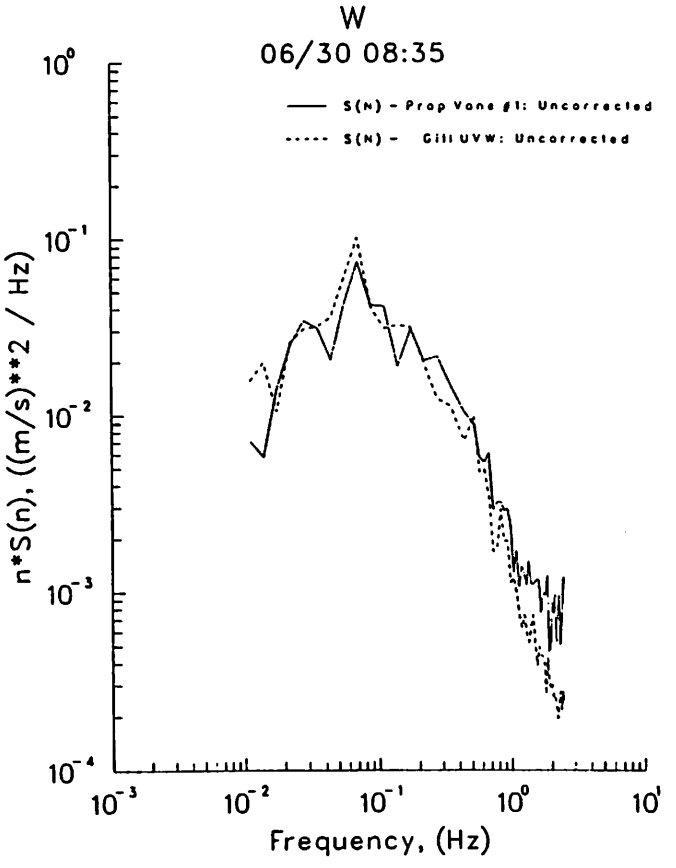

EXAMPLE OF SINGLE PROP. CORRECTION EFFECTS
(VERTICAL COMPONENT - W; U &V FROM PROP. VANE #1)

TIME SERIES

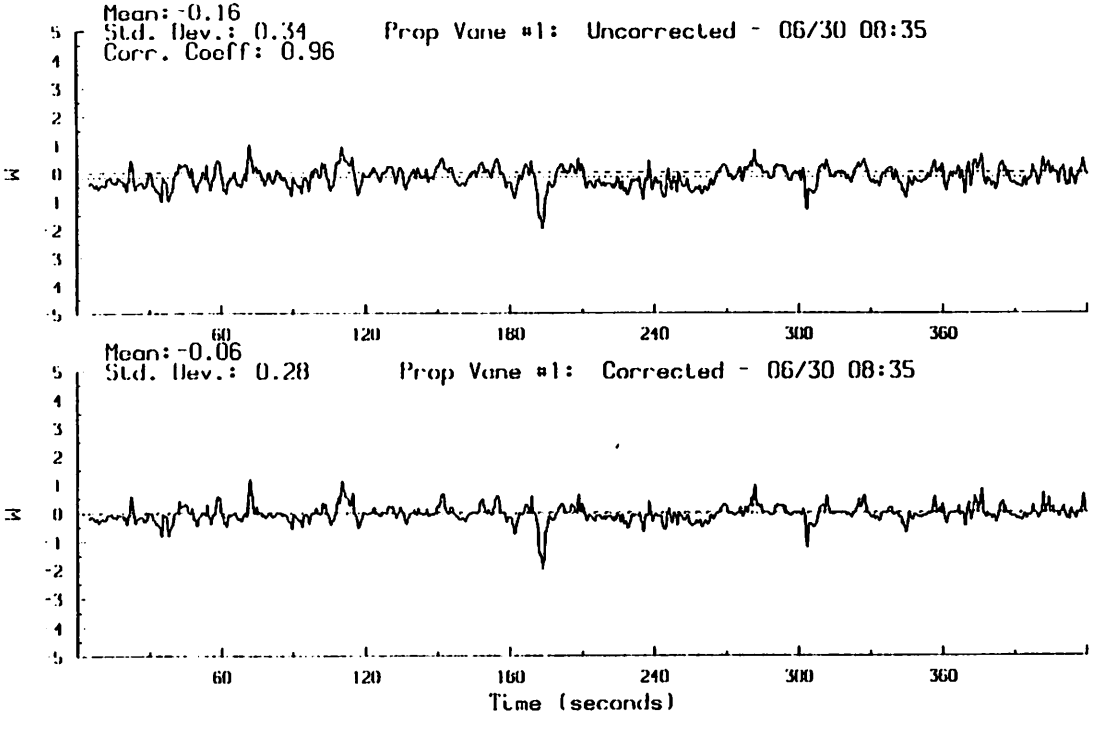

POWER SPECTRA

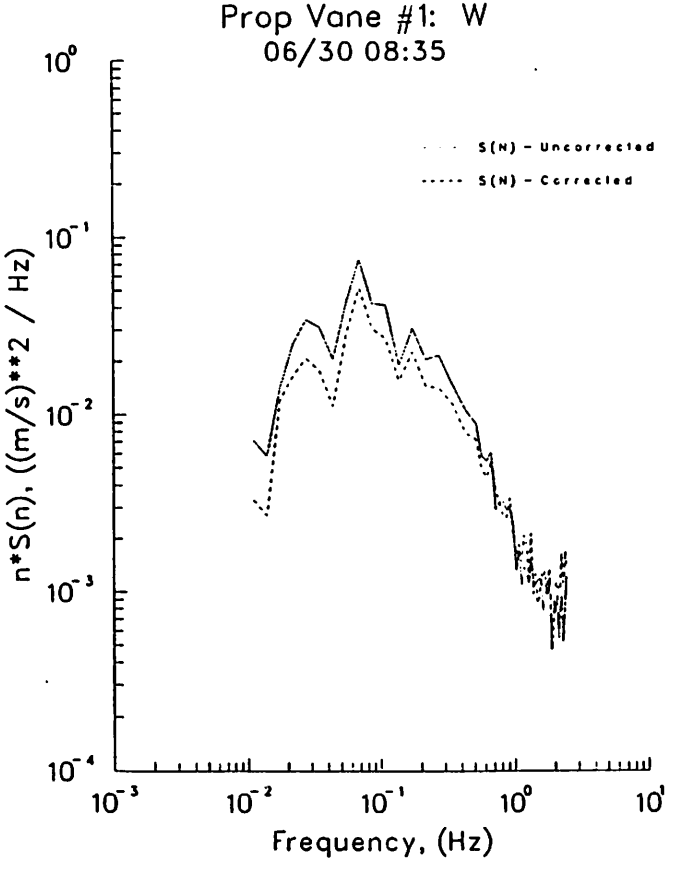

TURBULENCE CHARACTERIZATION

FUTURE PLANS:

- Rotate the turbulence measurement systems through enough cooperative participants to cover a representative number of conditions likely to be encountered at wind turbine sites.

The Outlook of Wind Observation in Japan and Development of a Statistical Method for Vertical Wind Profile

==== Abstracts ====

Stockholm, 7. -8. March, 1991

Chiyoda Dames and Moore Co.,Ltd

Masanori Higashino

Company: Chiyoda Dames & Moore
Adress : 5-38-3 Kamata, Ota-Ku
Tokyo, 144 Japan

1. Title : The outlook of wind observation in Japan and development of a statistical method for a vertical wind profile

2. Objective : Plain area in Japan islands only amounts to 25% of the total, and the most of plains are used for residential, industrial and agricultural purposes. The rest of the area(75%) are mountains and hills covered by forest and woods, and have complex topographical features.

In consideration of these, Japanese Government has been planning the development of mega watt-class and middle-class wind turbine to be installed in narrow plain space, rather than the development of small size wind turbines.

The project of a wind energy development in Japan has been promoted by the government as a part of Sun-Shine Project and consists of two parts; one is the development of mechanical elements of a wind turbine and the other is a survey and an analysis of wind conditions in upper atmosphere(layers).

The latter development has been conducted since FY1983 and the primary purposes of a survey and an analysis are (1) to evaluate wind characteristics in Japan and (2) to estimate wind energy potentials in Japan and (3) to find suitable sites for a wind energy development .

The development works, however, will require more fund and time to achieve the targets if they are based only on wind observations of prospective sites. Then an approach by statistical model was undertaken for vertical wind profile (characteristics) from which the wind condition is easily estimated for upper layers.

3. Summary

The general description of the present survey is shown in Fig.1 . Two types of wind observation have been conducted in this study. The one is the upper layer wind observation which measures wind conditions from ten meters to 140 meters above the ground level. The other is the lower layer wind observation which consists of a measurement at 10 meter and 20 meter height. The upper layer observations have been conducted for ten sites since 1983. The more wind observations will be planned for seven or eight sites in the near future. The lower layer observation at 13 sites just started this fiscal year and more observations at 50 to 60 sites are under plan, throughout Japan, in the near future.

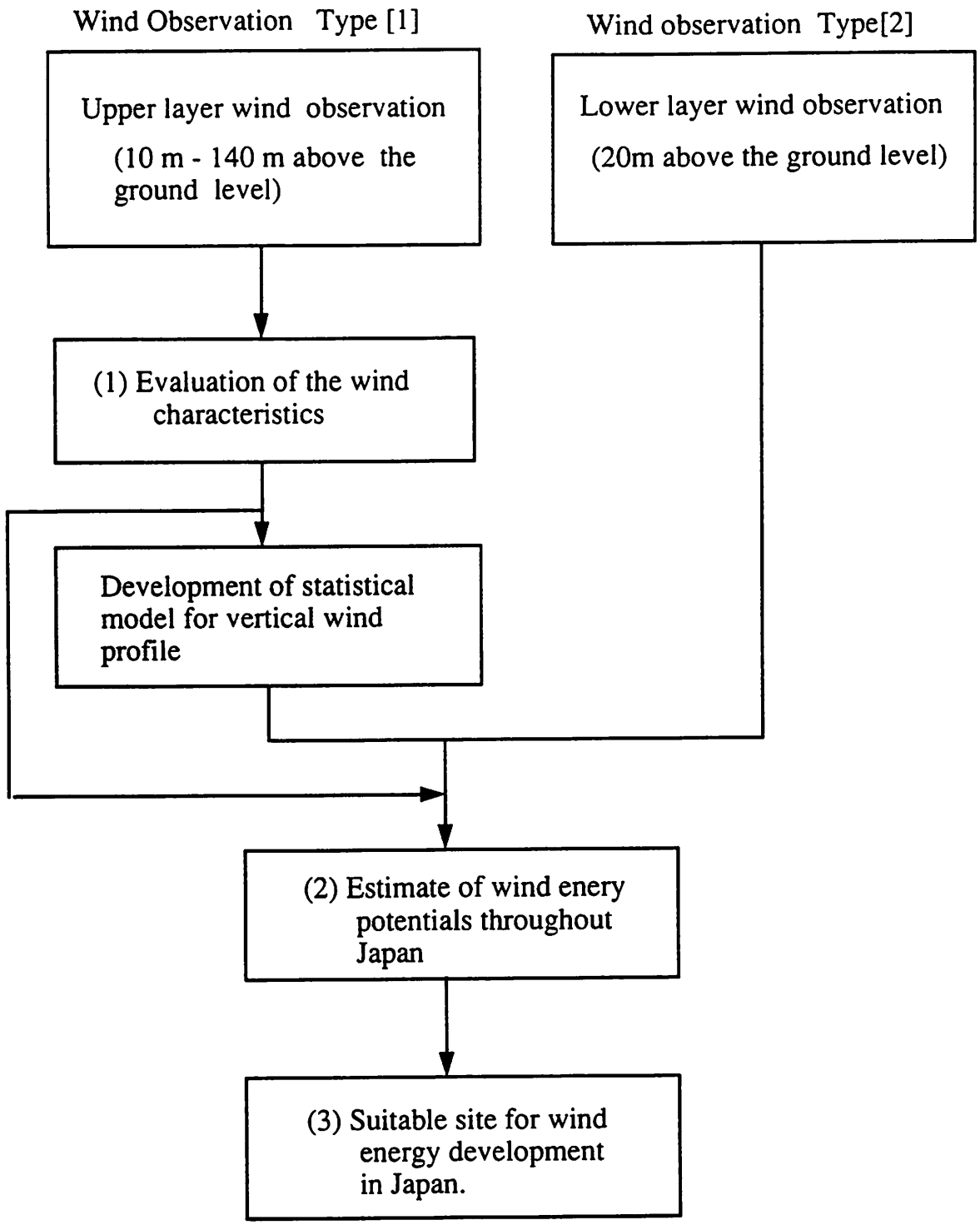

Fig. 1 General Description of the Survey

(1) The method of the wind observation

A Doppler-Acoustic Remote Wind Sensor and an wind mill anemometer with wind vane are used for the observation. Altitudes of the observation for each apparatus are as follows;

Doppler-Acoustic Remote Wind Sensor(XONDAR):
for upper layer at 42m,65m,88m,111m and 134m
Wind mill anemometer with wind vane(Aero vane):
for lower layer at 10m and 20m

The system and block diagram of each equipment were shown in Fig. 5 to 6.

(2) Observation Sites

Wind observation sites are shown in Fig. 6. In the figure, square symbols indicate the upper layer observation sites and circle symbols the lower layer observation sites.

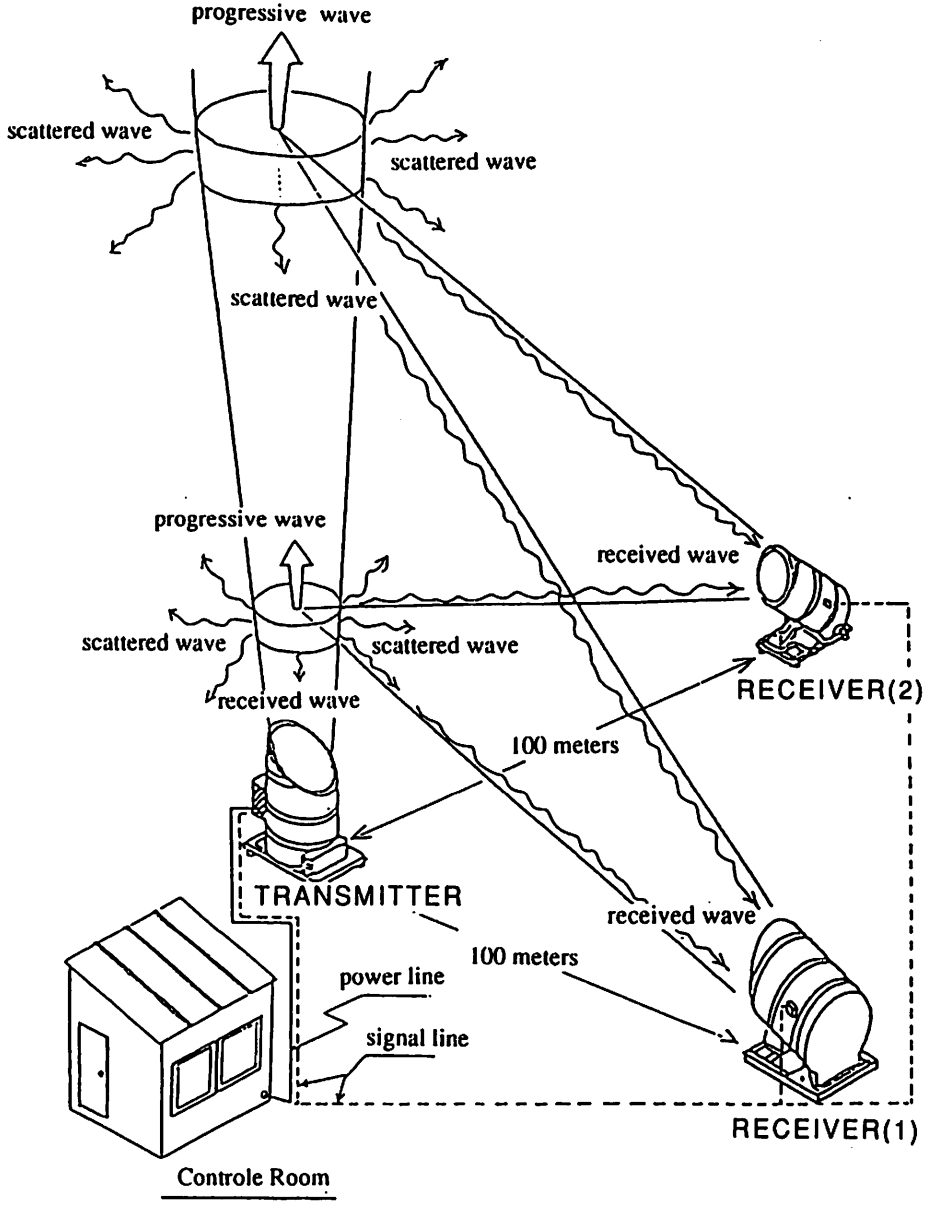

Fig. 2 Wind Observation System of Doppler Acoustic Remote Wind Sensor(XONDAR)

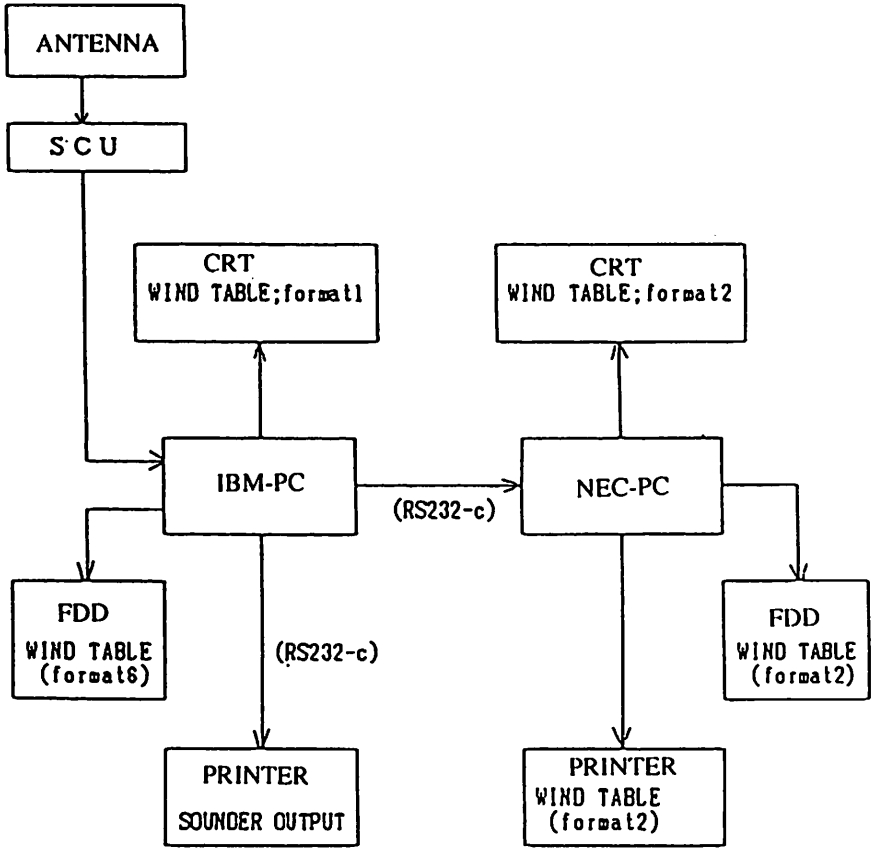

Fig. 3 Block Diagram of XONDAR

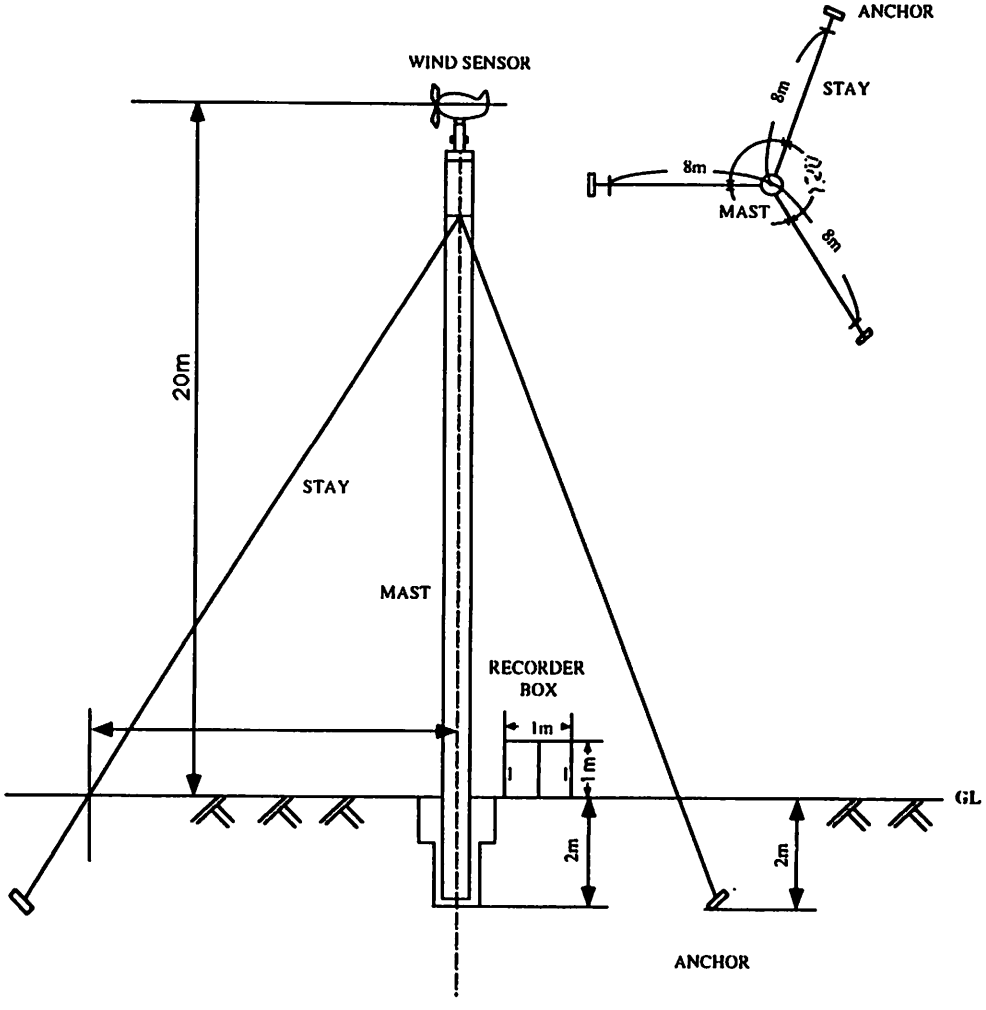

Fig. 4 Wind Observation System of Aero-Vane

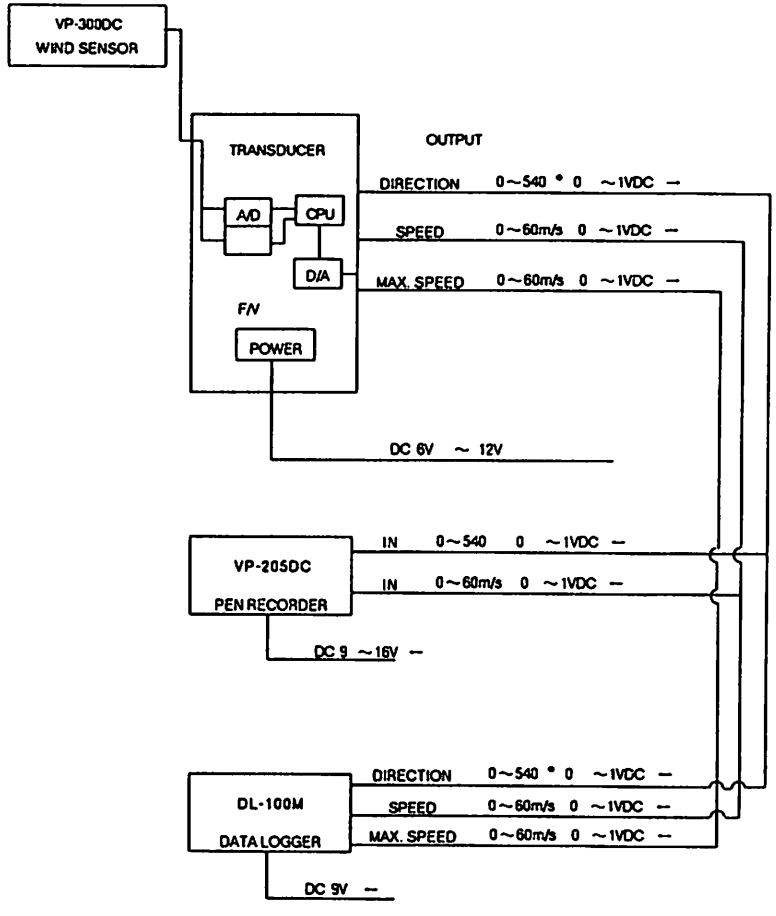

Fig. 5 Block Diagram of Aero Vane System

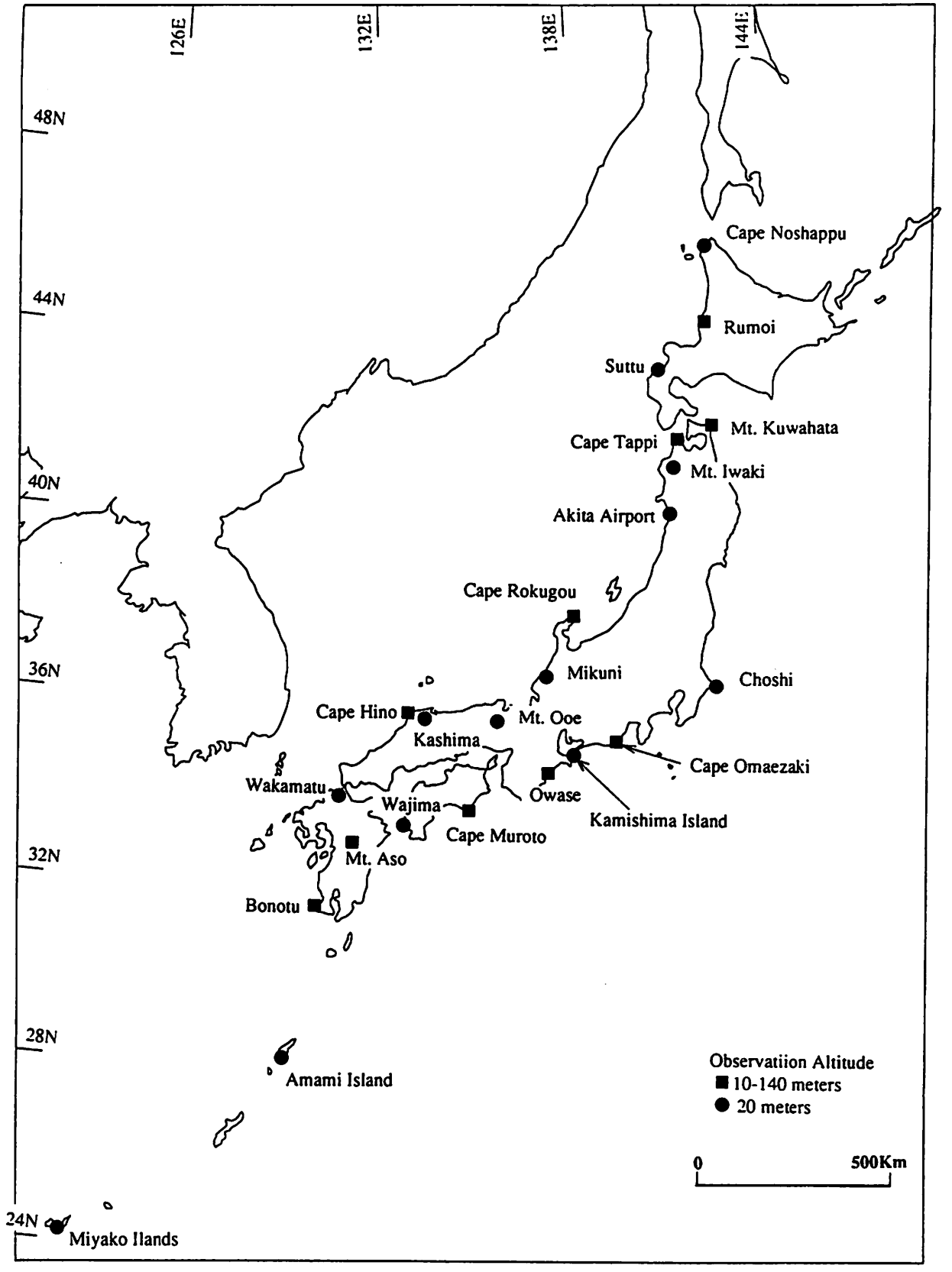

Fig. 6 Wind Observation Sites for a MW-class Wind Turbine since 1983

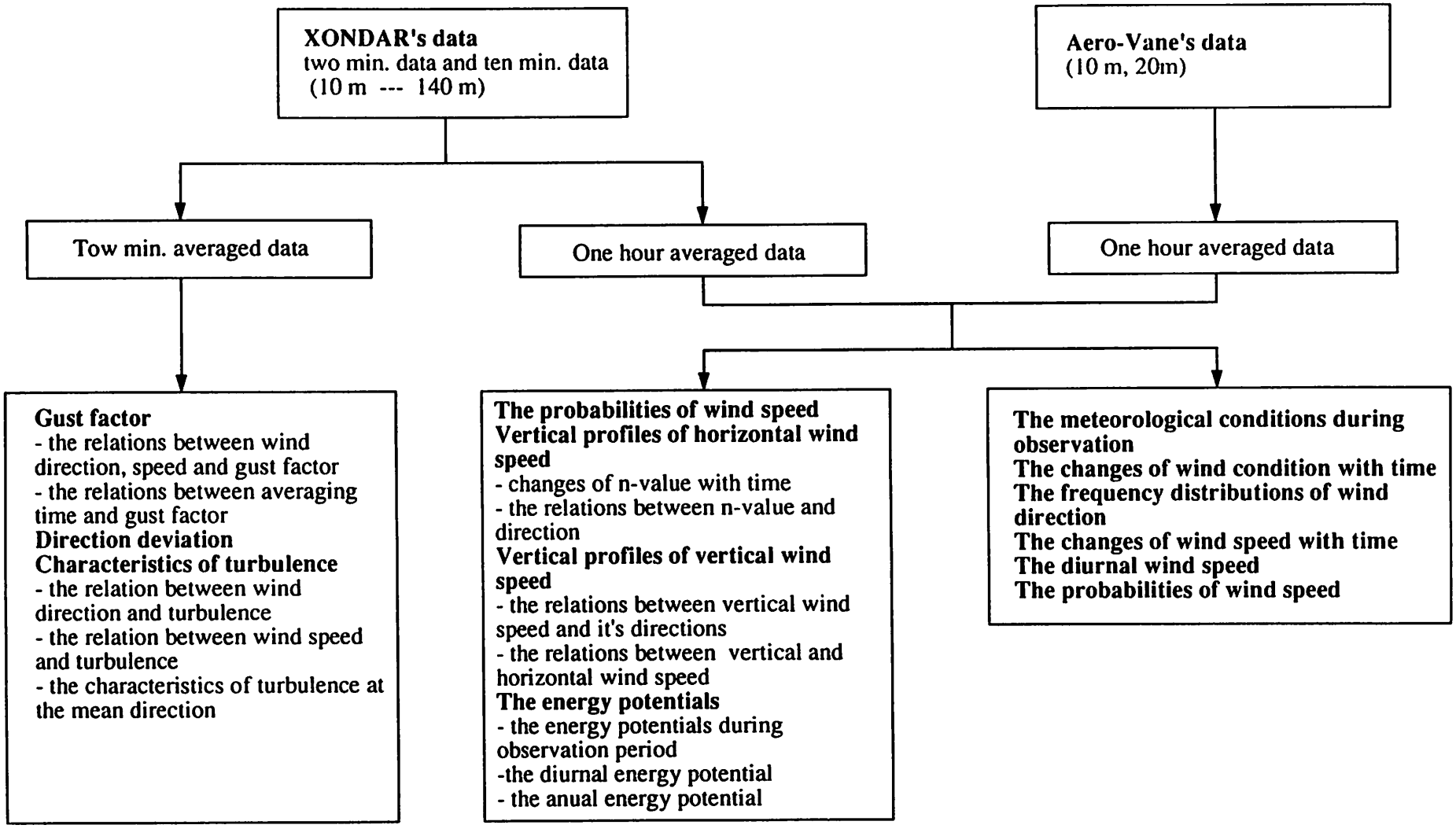

Fig. 7 Flow Scheme for Wind Data Analysis

(3) Data handling procedure and analysis

A wind data analysis is carried out based on the flow scheme in Fig. 7. One hour averaged data are employed for the analysis. In the case of gust factors, wind direction's deviations and turbulence analyses, two minute averaged data are used.

(4) Primary results up-to-date

(a) Outlook of suitable sites for MW-class wind turbines in Japan

Japan Meteorological Bureau has about 1,300 meteorological stations named AMeDAS(Automated Meteorological Data Acquisition System) for a weather forecasting throughout Japan. Among these AMeDAS's stations, there are about 840 stations that carry out a wind observation. The wind observation altitude at the AMeDAS's station is basically 6.5 meters high in order to forecast a wind condition of living atmosphere. Review of topographic conditions around the all AMeDAS's stations unveiled that about 50% of AMeDAS's stations were undesirable for a wind energy evaluation because of obstacles around them, such as house, trees, mountains and so on.

There were many problems to apply such a wind data of AMeDAS's stations for a wind energy development . However, as the first step of the survey, distribution maps of wind speed were prepared at 40 meter and 100 meter height by using AMeDAS's data in order to know the outlook of suitable sites for wind turbines in Japan. The power law (wind shear) of a vertical wind profile(n=4.7) was applied to calculate a wind speed at 40 meters and 100 meters heights. The n-value(n=4.7) is the average value of observed data at three cape sites and one coastal site in the past

The suitable areas for a MW-class wind turbine are shown in Fig. 8. On this map, suitable sites for MW-class wind turbines were defined by the area where the wind speed exceeds 6.0 m/s.

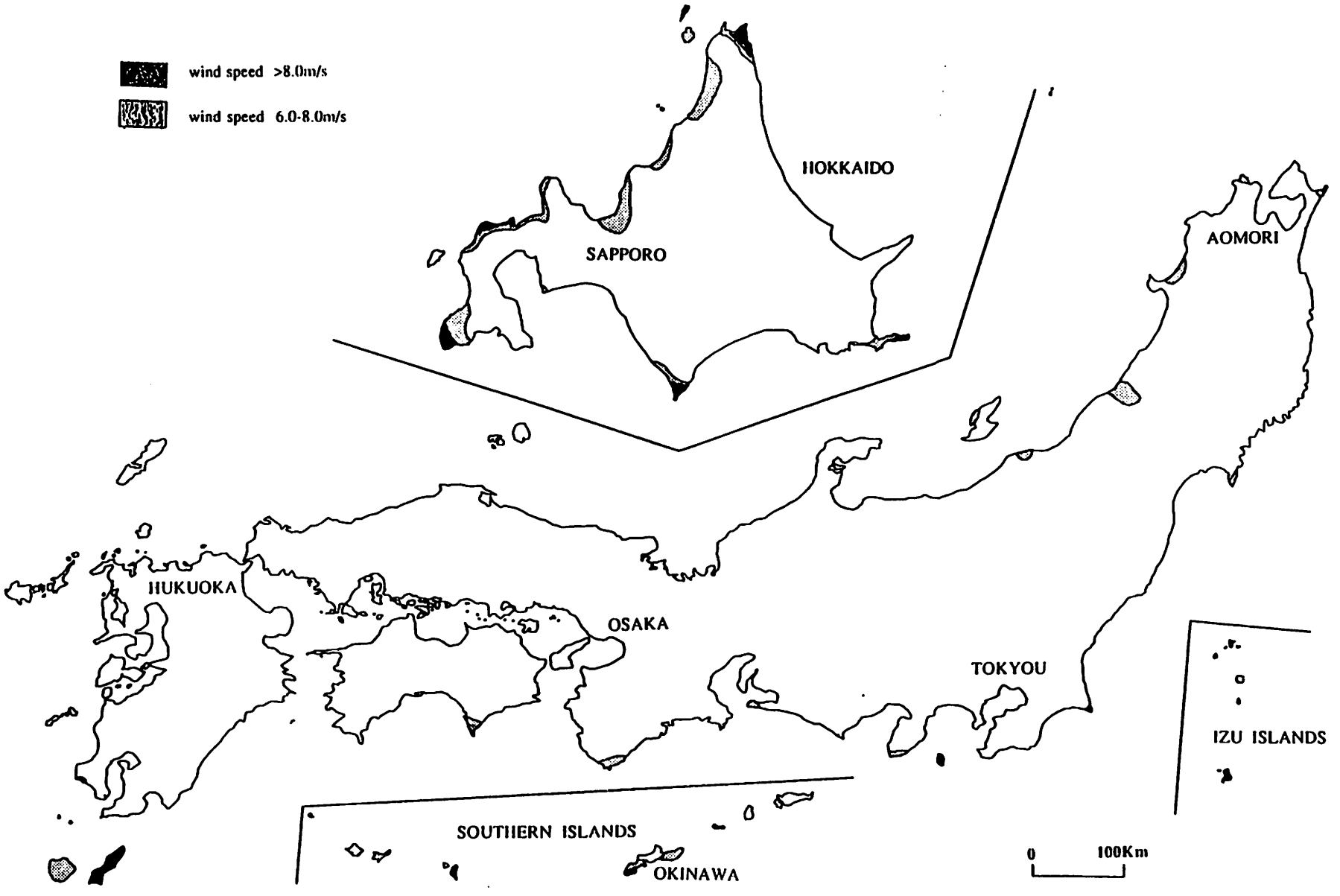

Fig. 8 Suitable Sites for a Wind Turbine in Japan(Wind Speed at 100 meter Height)

Table 1 shows the summary for a potential wind energy development area throughout Japan. The suitable area for a wind energy development was estimated at 2,552 square kilometers at a wind speed of 40 meter height and 5,058 square kilometers at a wind speed of 100 meter height. These areas correspond to 0.69% and 1.36% of the total area of Japan, respectively.

Table 1 Suitable area for a MW-class wind turbine in Japan

(unit: square kilometer)

wind speed at;	site	6-8m/s	8.0m/s<	6.0m/s<
40 meters	Main Land	1296.9	155.8	1452.7
	Island	505.4	593.4	1098.8
	Total	2395.7	155.8	2551.5
100 meters	Main Land	2589.8	795.0	3384.8
	Island	770.4	902.4	1672.8
	Total	3360.2	1697.4	5057.6

(b) Energy Potentials of Wind Turbines

Considering the size of the existing MW-class wind turbines in foreign countries and the wind turbine designed in Japan, general specifications of a MW-class wind turbine were decided as follows;

Rotor diameter : 50 meters and 80 meters

Tower height : 40 meters and 100 meters

Taking specifications of the MW-class wind turbine mentioned above, a layout of wind turbines, and social and natural environmental conditions into consideration, the potential number of MW-class wind turbines which could be installed throughout Japan was sought(Refer to Table 2).

By setting the rotor diameter at 50 meters and the tower height at 40 meters, the potential number of a wind turbine was calculated to be 5,500 throughout Japan. It became clear that most of wind turbines could be installed in Hokkaido Prefecture(Northern island of Japan).

The generating capacity of these wind turbines was estimated to be about 3,200 MW and it correspond to 2.2% of total power generated throughout Japan.

Table 2 Potential Number of a MW-class Wind Turbine in Japan

Tower Height (m)	Rotor Diameter (m)	Wind Speed (m/s)	Generating Capacity (KW)	Number of Wind Turbine						
				Hokkaido	Tohhoku	Kantou, Tohkai	Shikoku, Kinki	Kyushu	Islans	Total
40m	50m	exc. 6.0m/s	500-600	4919	143	89	20	298	14	5483
		exc. 8.0m/s	900-1000	348	143	0	0	19	0	510
100m	50m	exc. 6.0m/s	500-600	15706	546	103	44	298	24	16721
		exc. 8.0m/s	900-1000	3192	143	0	18	298	7	3658
	80m	exc. 6.0m/s	1000-1400	4872	194	44	25	81	12	5228
		exc. 8.0m/s	2100-2600	1014	46	0	10	81	3	1154

(c) Statistical Model

(i) n-values

Wind shear is affected by the roughness of the earth's surface in a given location, i.e., whether it contains buildings, trees, wind machine, or other obstacles. In general, a vertical profile of a wind speed follows logarithmic function or power law(exponential function) and the wind speed increases with the altitude.

In Japan, an empirical power law of wind speed profile is usually utilized for a design stage of buildings and bridges.

$$Vz=Vh(z/h)\exp(1/n)$$

In the above equation, typical n-values are available from existing standard and literatures for various topographical features, but most of n-values calculated from observed data do not conform to typical n-values because of complexities in topography for the observation sites in Japan.

n-values of power law calculated by wind observation are shown in Fig. 9 to 11.

By using wind speed data at six altitudes, Least-Square Method was applied in order to calculate n-values. Furthermore, it is considered that n-values would be affected by stabilities of atmospheric conditions. Six different conditions such as "daytime"/"night", "all wind speed data"/"wind speed exceed 4.0m/s" were taken into consideration.as follows;

(a). applied for all wind speed data

(b). applied for all wind speed data during daytime(8am-5pm)

(c). applied for all wind data during night(6pm-7am)

(d). applied for wind speed exceeding 4.0m/s

(e). applied for wind speed exceeding 4.0m/s during daytime (8am-5pm)

(f). applied for wind speed exceeding 4.0m/s during night(6pm-7am)

Fig. 9 to 11 indicate that most n-values are ranging from zero to 15 and tend to differ at each wind direction. These differences of n-values are strongly related to topographic features at each wind direction. Six cases conditions did not show remarkable difference on n-values and they showed the same changes by the wind directions. Fig. 9 to 11 also show relations of n-values between condition (a) and (d), (b) and (c), (e) and (f) mentioned above. Since comparisons of n-values of these three sets indicate linear relation each other, it is suggested that n-value was not strongly affected by stabilities conditions of the atmosphere.

Fig. 12 to 14 show the topographic profile around the observation point and n-values of 16 sites. Some n-values indicate large number when the wind come from sea side, and also indicate small number when the wind come from land side. But the rest of n-values can not explain only by topographic profiles.

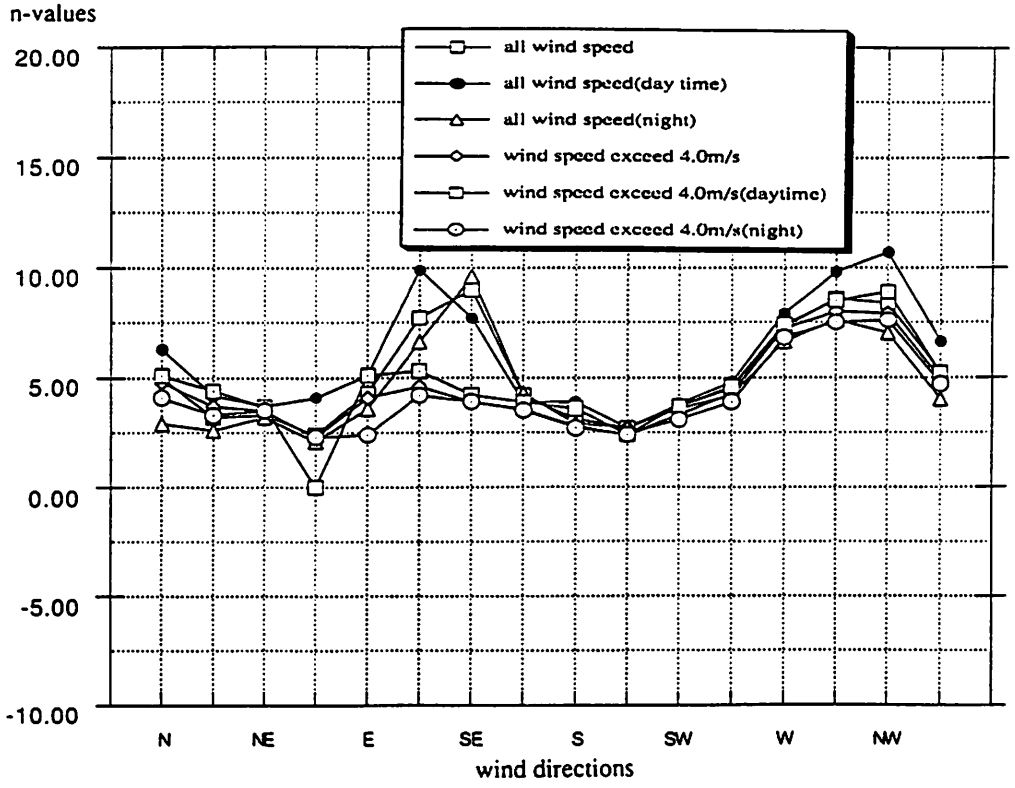

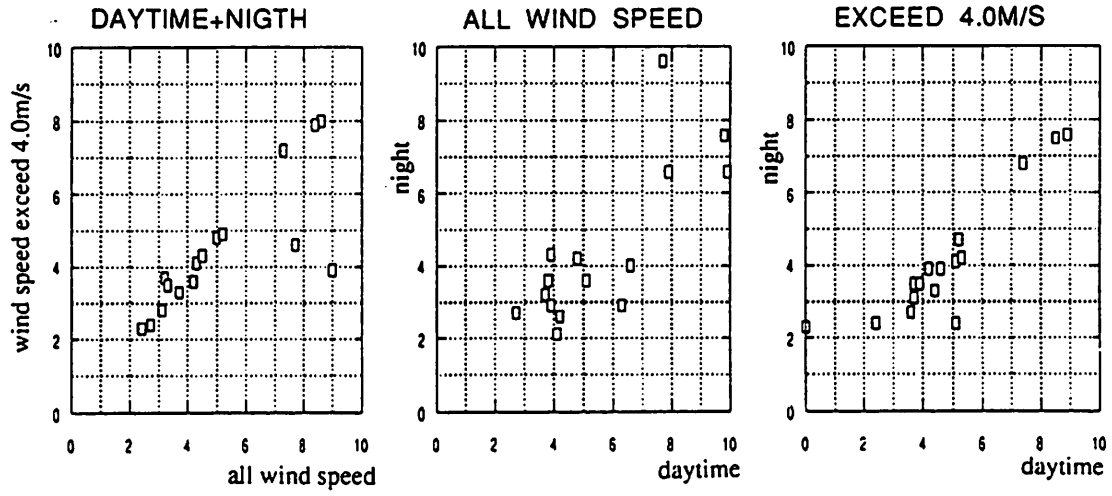

Fig. 9 n-values at different conditions(site:Rumoi,Warm season)

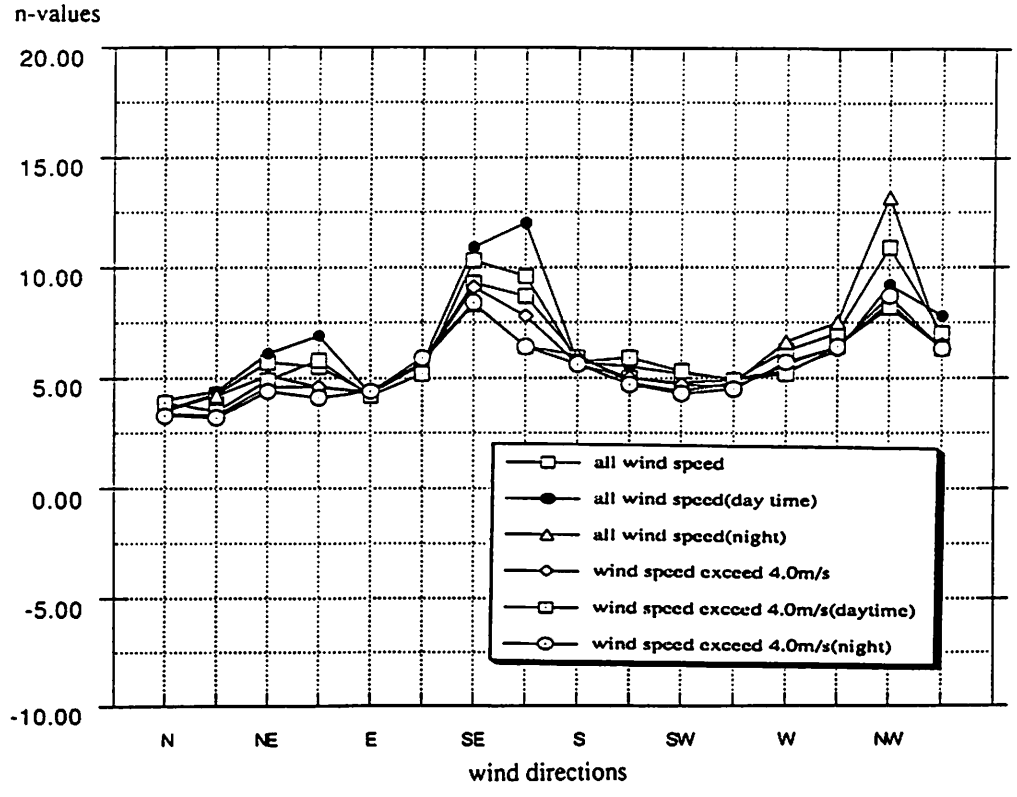

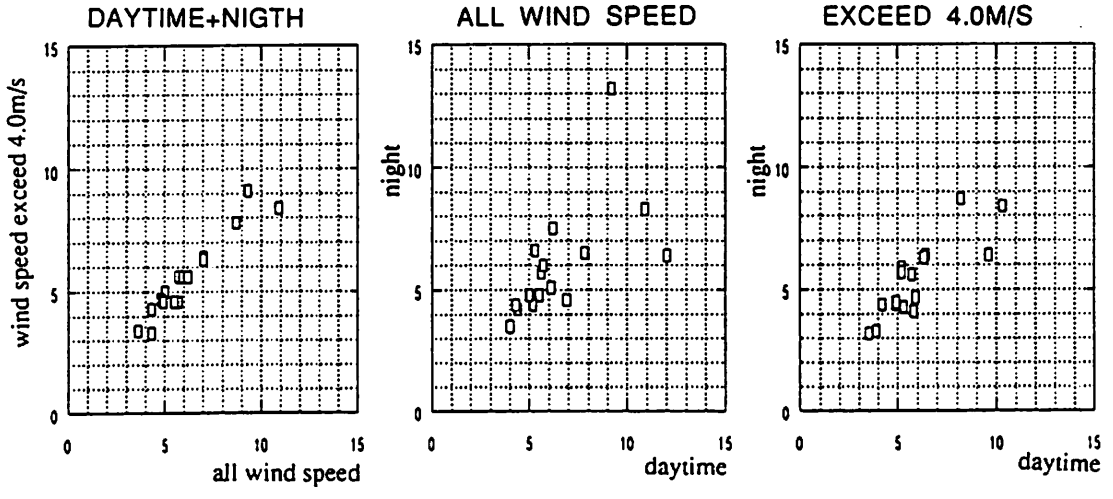

Fig. 10 n-values at different conditions(site:Mt. Kuwahata, Warm season)

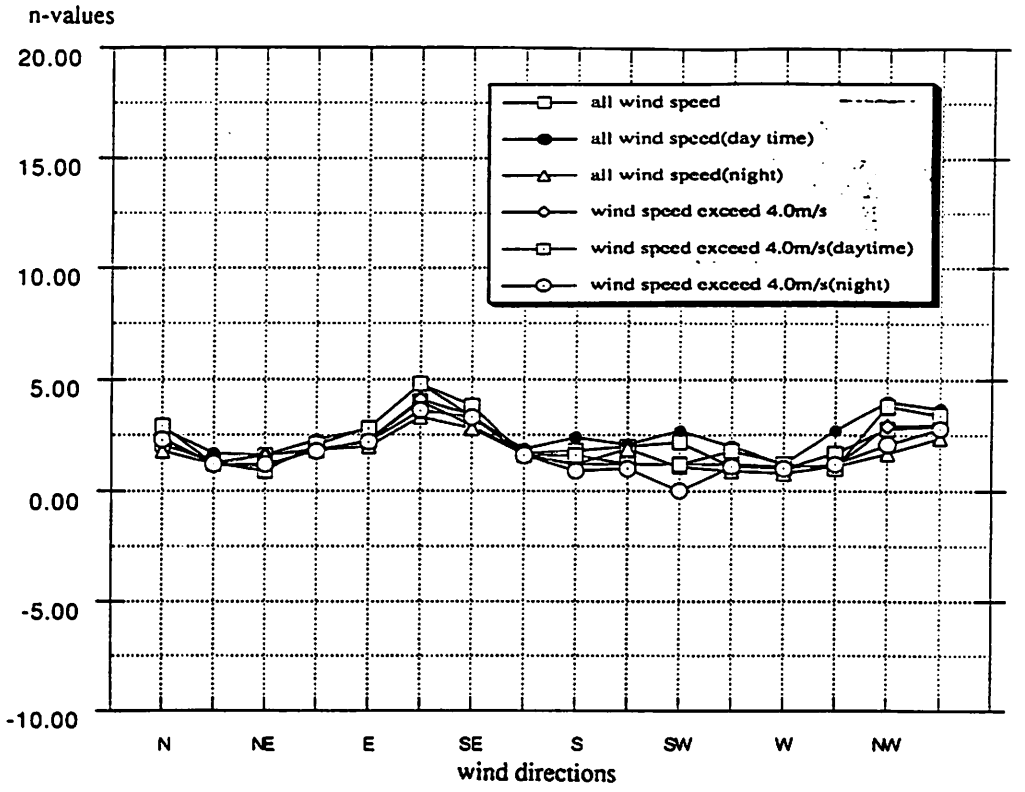

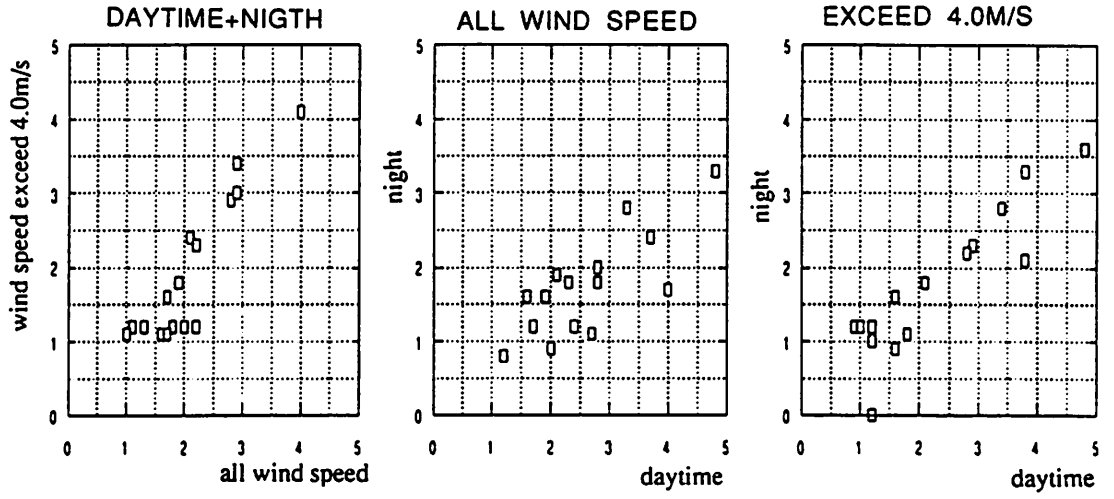

Fig. 11 n-values at different conditions(site:Bonotu,Warm season)

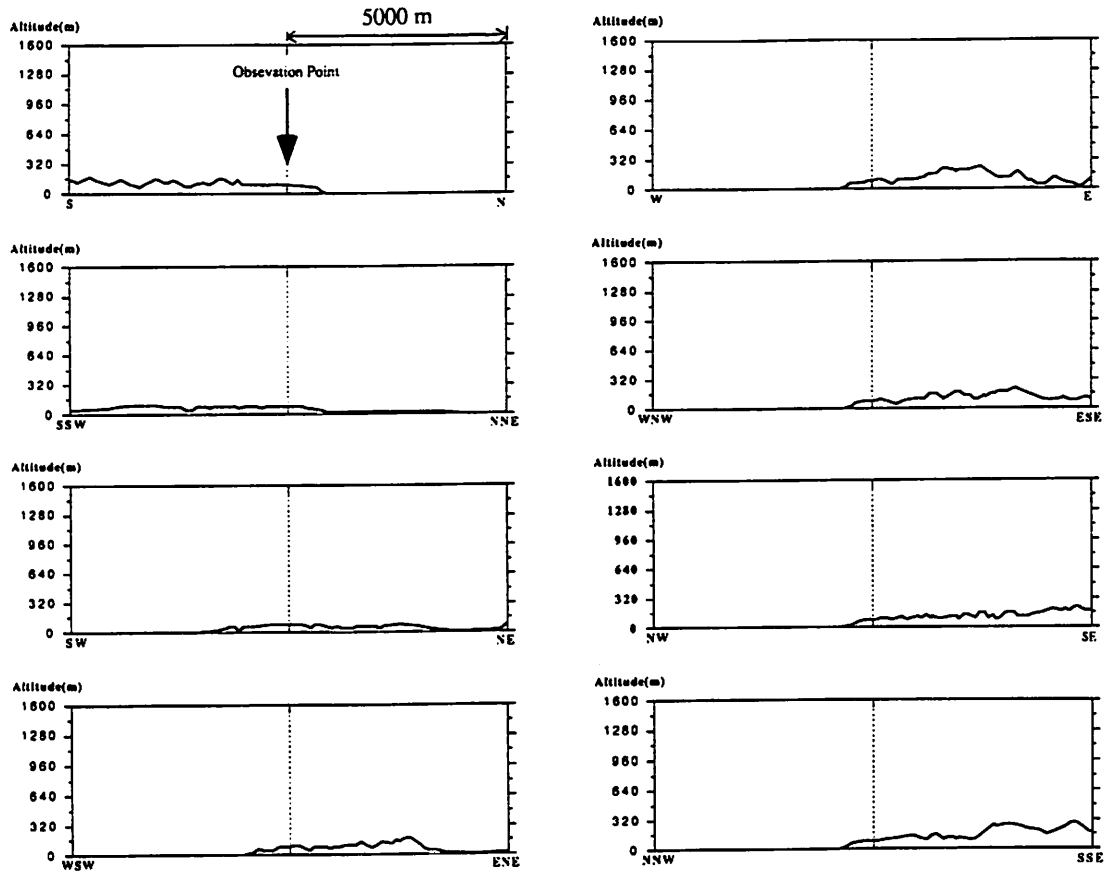

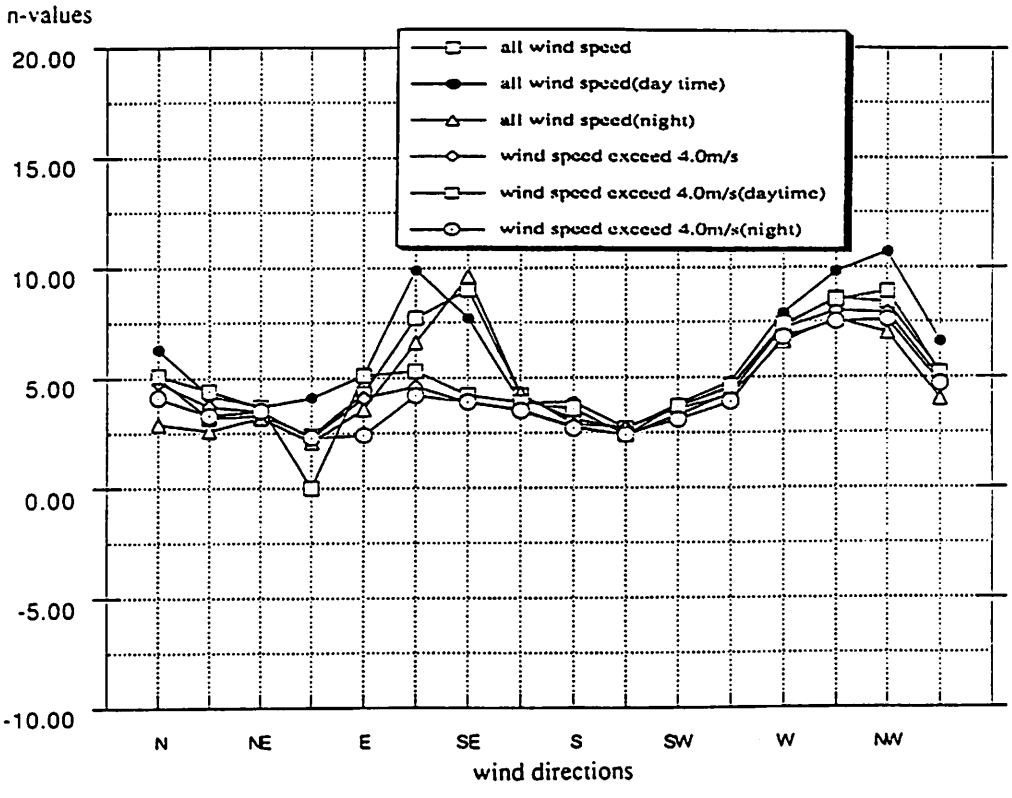

Fig.12 Topographic profiles and n-values(site:Rumoi)

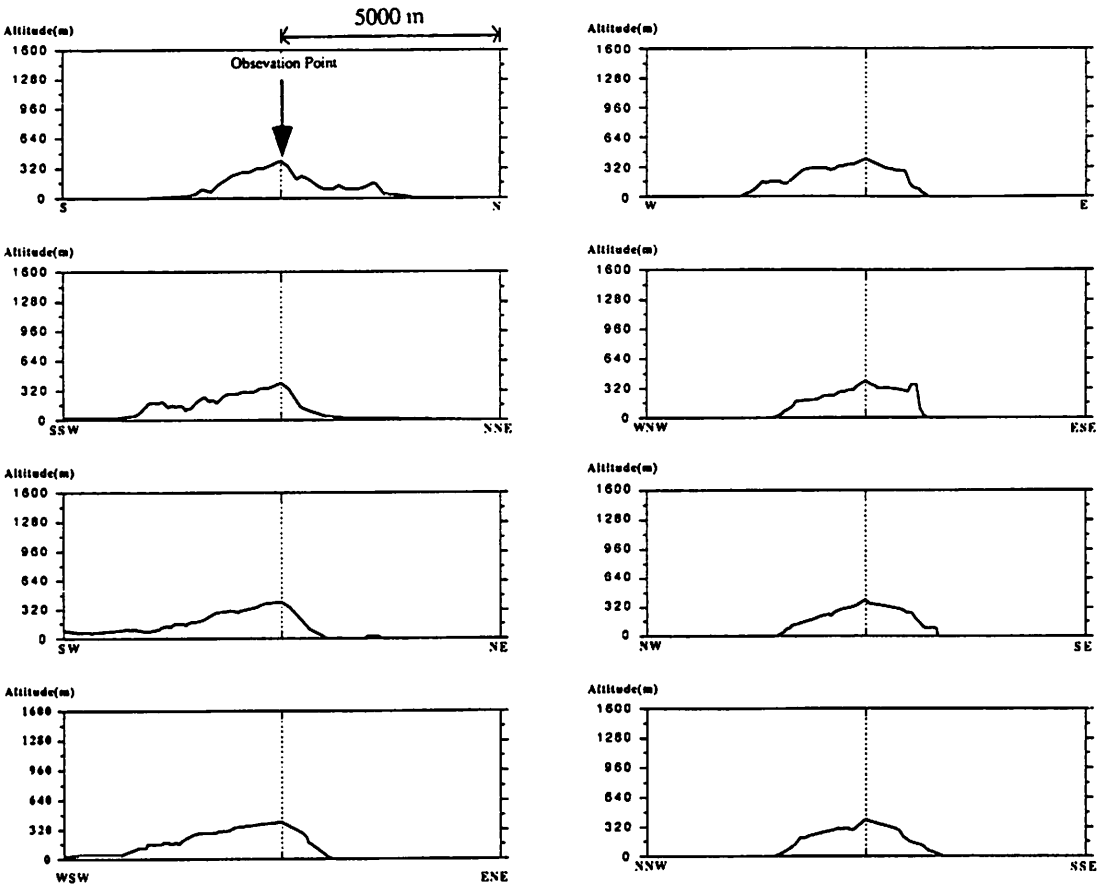

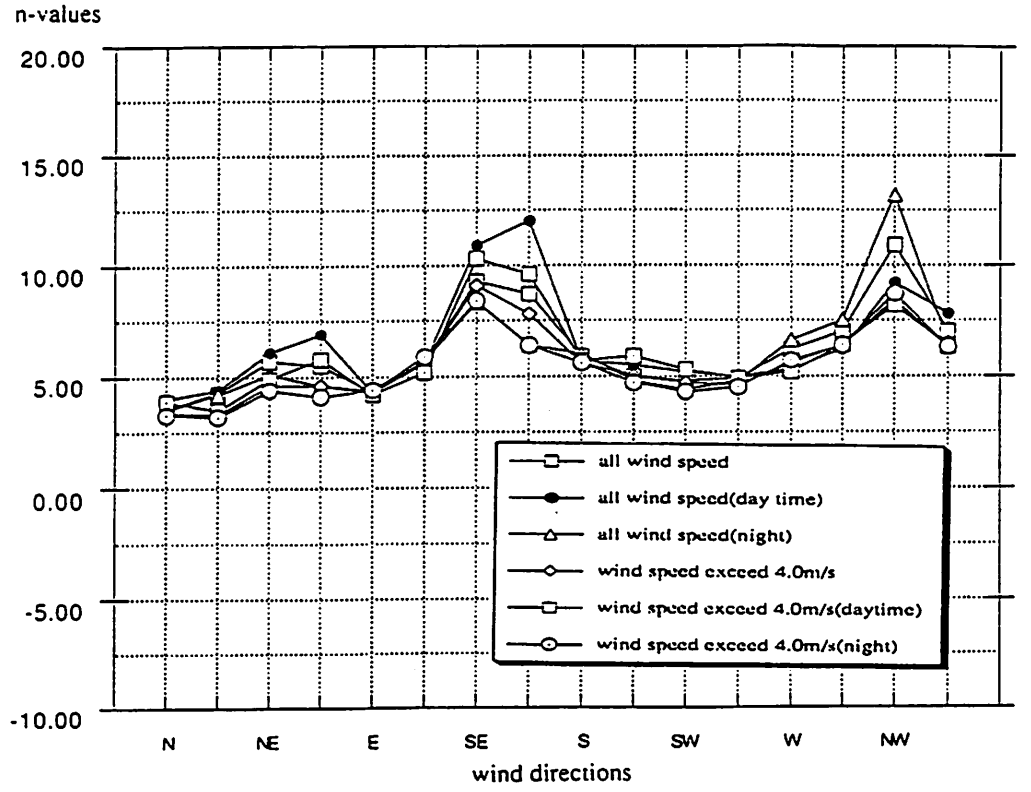

Fig.13 Topographic profiles and n-values(site:Mt.Kuwahata)

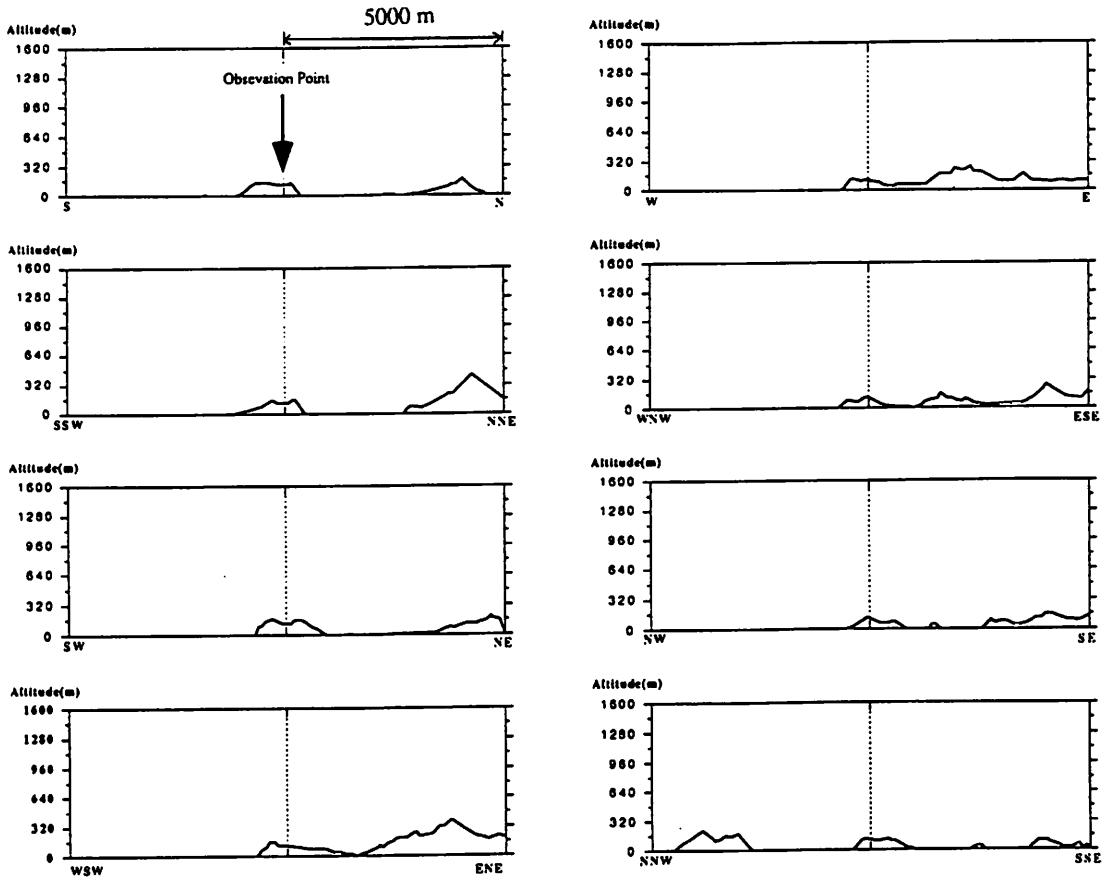

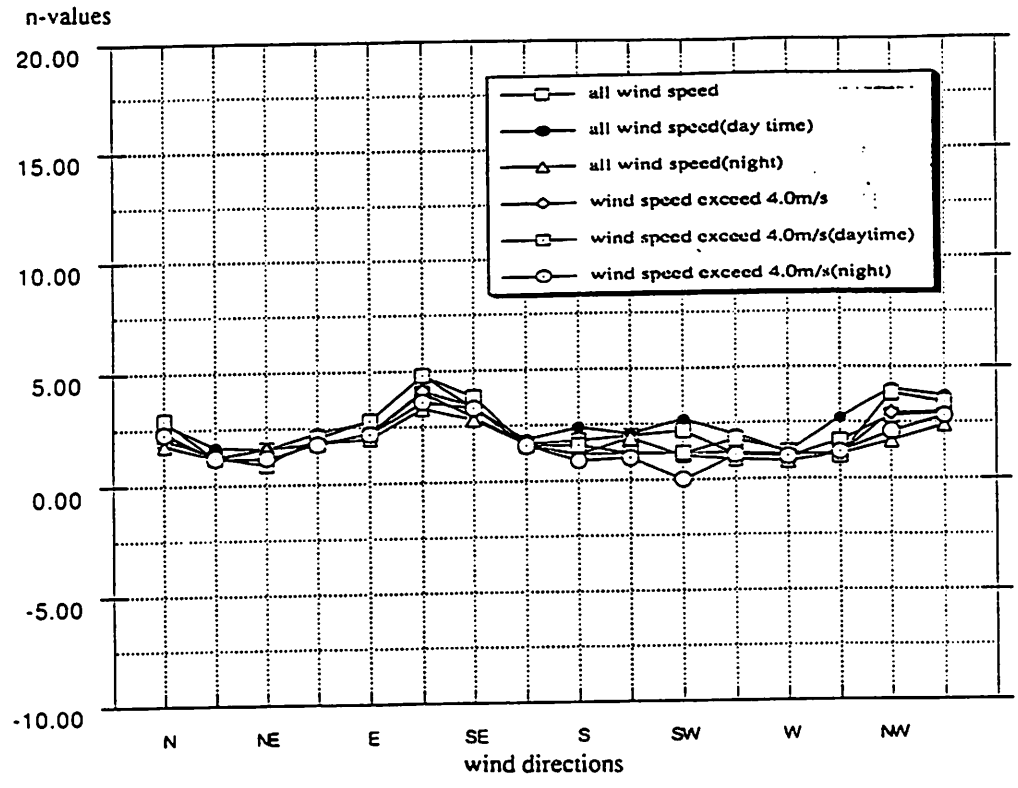

Fig.14 Topographic profiles and n-values(site:Bounotsu)

(ii) The method of analysis

In order to estimate a vertical profile of wind speed of at a certain point, a correlation between n-values of power law which calculated by observations and topographic features of each wind direction at the observation site was evaluated.

The statistical method of Multiple Regression Analysis was applied for this study. Multiple Regression Analysis describes the linear relationship between one dependent variable, Y, and several predictor variables. The word "linear" means the predictors are combined in simple sums and contain no other functions such as exponentials or squares. In general, the model for linear regression is:

$$Y=b0+b1X1+b2X2+b3X3+-----+bnXn+e$$

where Xn is a predictor(independent) variable; bn is regression coefficient. In this analysis, n-values calculated from observation data be dependent variables and topographic features be independent variables.

Numerical values of topographic features which indicate, for example, the altitude or gradient of a certain point were prepared by topographic map of 1/25000. Fifty five independent variables with 15 kinds of topographic features were used for the analysis.

The analysis was carried out based on the flow scheme in Fig. 15.

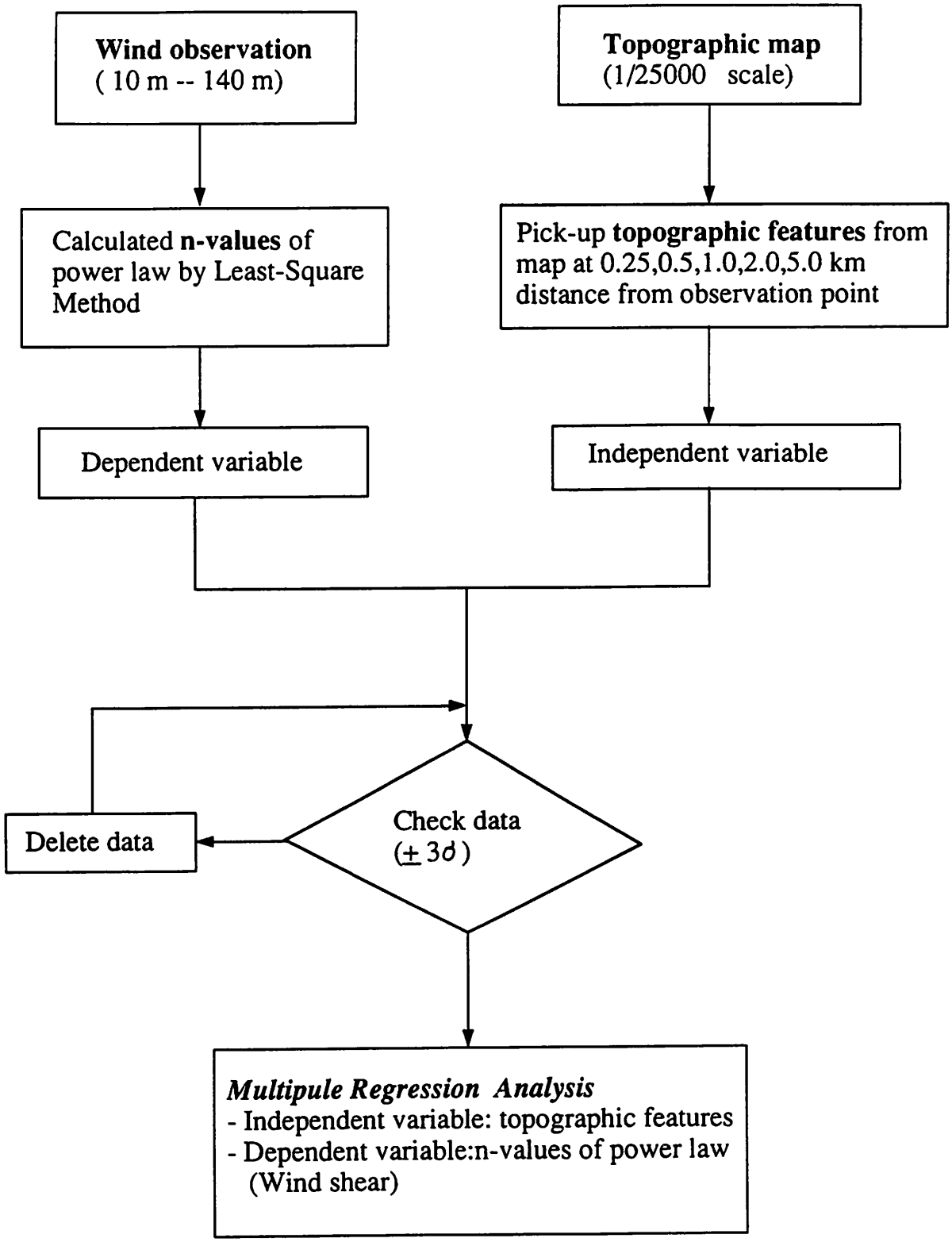

Fig. 15 Flow Scheme of Statistical Analysis

(iii) Topographic features

Fifty five independent variables with 15 kinds of topographic features were applied to this study. Each topographic feature at each wind direction was calculated at each sector of direction (V-shaped area) within 0.25, 0.5, 1.0, 2.0 and 5.0 kilometer radii from wind observation point. The numerical values of topographic features were defined as follows;

[MAX]: Maximum altitude in the each sector

[MIN]: Minimum altitude in the each sector

[UND]=[MAX]-[MIN]

[GP]={[MAX]-[Altitude of observation point]/[distance between observation point and the MAX point]

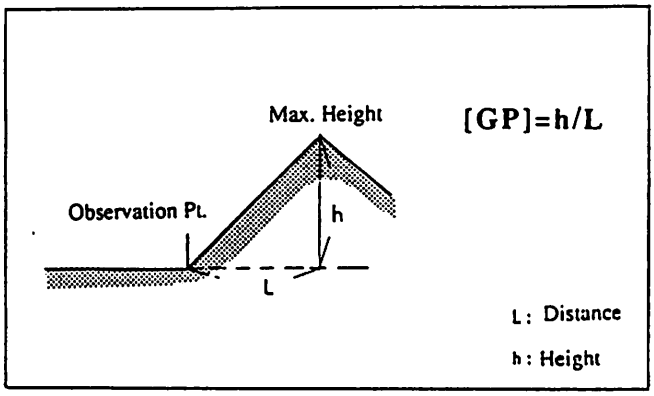

Definition of [GP]

[GM]={[Altitude of observation point]-[MIN]}/[distance between observation point and the MIN point]

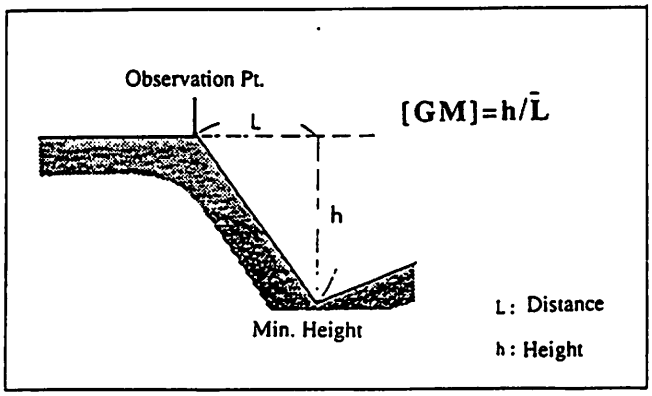

Definition of [GM]

[LOF]={[MAX]-[Altitude of observation point]/[UND]

[PRO]=[Altitude of observation point]/[Averaged Altitude of the area of 1.0 kilometer radius circle]

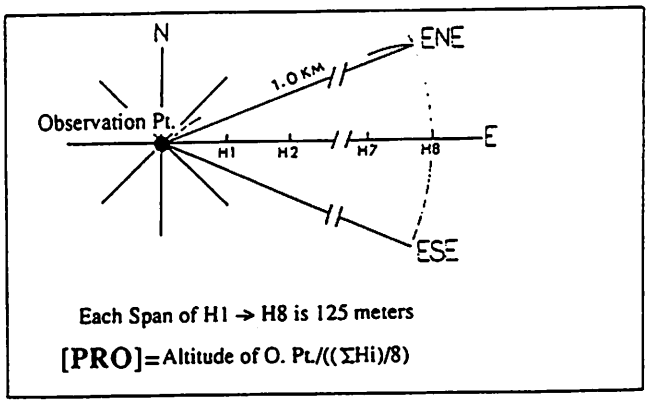

Definition of [PRO]

[OP-A or B or C]: The angle that there are no obstacles over certain height within angle of 22.5(the angle of one direction)

The heights of obstacles are defined as follows;

OP-A: 140 meters

OP-B: 70 meters

OP-C: 10 meters

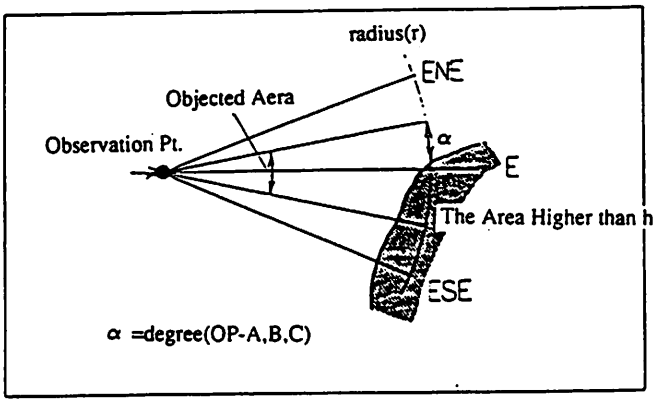

Definition of [OP-A,B,C]

[OP-V]=((tan ((AH-AO))/L)+90)/90

AO: Altitude of Observaton point

AH: (H1+H2+H3)/3

L : Radii of each sector(0.25, 0.5, ------5.0Km)

=tan (h/L)+90

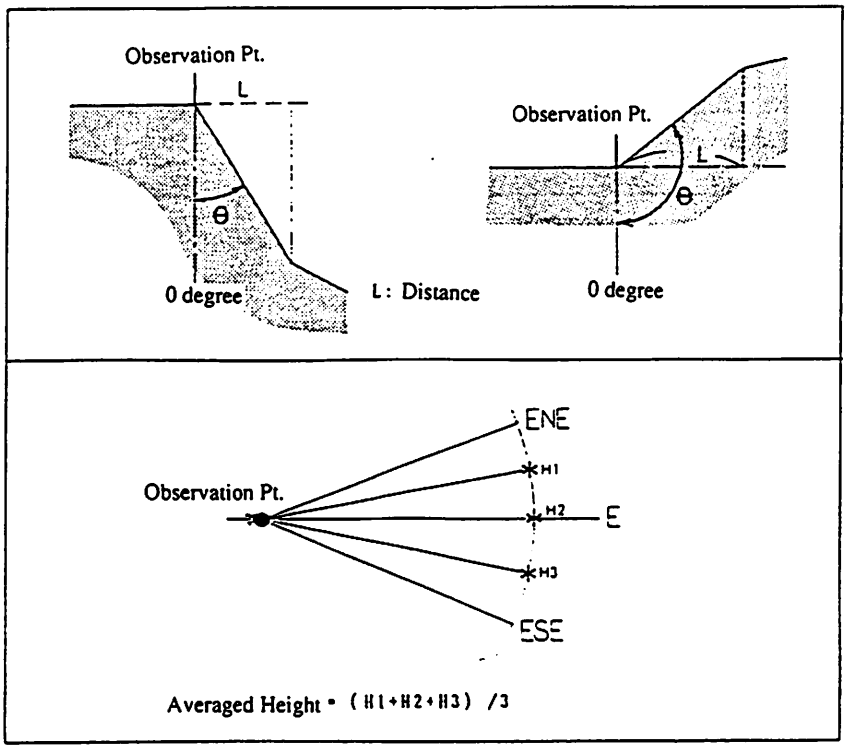

Definition of OP-V

[OBST-A or B or C]: The distance from observation point to obstacle.The heights of obstacles are defined as 140m, 70m and 10 m.

OBST-A:140 meters

OBST-B: 70 meters

OBST-C: 10 meters

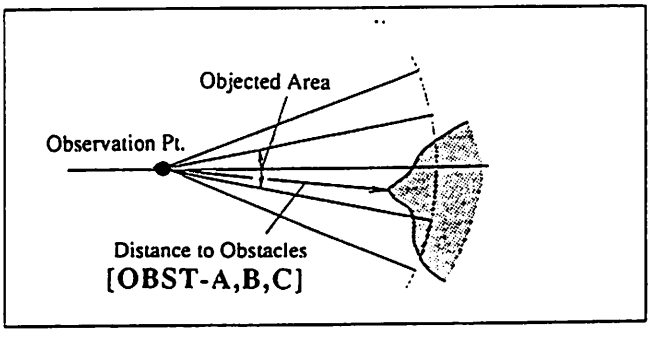

Definition of [OBST-A,B,C]

(d) Results of analysis

After checking for distribution of each independent variable, 16 independent variables with ten kinds and 37 samples were applied for the analysis. As the dependent variable, n-values based on six different conditions showed a similar tendency, therefor, one type of n-value(calculated by all wind speed data) represented all calculated n-values.

By using these independent variables and a dependent variable, Multiple Regression Analysis was performed. Two types of data sets(raw data set and general logarithm data set) were applied for the analysis. Table 3 and 4 show the fundamental valus of each variable.

(i) Regression by raw data

The results of Multiple Regression Analysis are shown in Table 5 and Table 6 . Table 5 shows the results based on all(16) independent variables and also shows the test of significance for the regression coefficient(F-ratio) and independent variables(t-ratio).

The F-ratio(3.09) at the Table 5 suggested that the R^2(coefficient of determination) of 72.1% was significant at 1%(α=0.01) level, on the contrary, only two independent variables could be found with a level of significance of 1%. The selected independent variables were [0.5MX](maximum height within the sector with 0.5 km radius) and [5.0MX].

Table 6 shows the results of Stepwise Regression. The R^2 statistics of 67.8% was smaller than that of the Table 5 , however, five independent variables with four kinds could be found with a level of significance of 1%(α=0.01) or six independent variables with five kinds independent variables with a level of significance of 5%(α=0.05).

The independent variables selected with a level of significance of 1% were [5.0MX], [5.0MX], [2.00GP], [OBST-A] and [2.00-OP-V].

Table 3 Fundamental Statistics of Variables(Raw Data)

NO. VARIABLE	MIN.	MAX.	AVERAGE	S.D	CO. of VA.	KURTOSIS	SKEWNEE
1.0.5MX	1.609	5.768	4.523	0.776	0.172	-1.317	4.206
2.5.0MX	1.609	6.985	5.435	1.090	0.201	-1.265	2.623
3.0.2MI	0.100	130.000	55.557	43.977	0.792	0.103	-1.425
4.0.2GM	0.001	3.000	0.290	0.689	2.375	3.594	12.571
5.0.25- UND	0.100	80.000	30.243	24.643	0.815	0.390	-1.058
6.2.0MI	0.100	130.000	31.673	42.437	1.340	0.861	-0.897
7.5.00- UND	5.000	920.000	288.027	213.572	0.742	0.953	0.819
8.PRO	0.001	60.000	3.828	10.190	2.662	5.026	27.258
9.2.00-GP	0.001	0.417	0.155	0.110	0.709	0.819	-0.164
10.DIST-SEA	160.000	20000.000	9385.406	9312.217	0.992	0.223	-1.970
12.0.50-LOF	0.001	1.000	0.474	0.382	0.806	0.263	-1.536
15.5.00-LOF	0.001	1.000	0.676	0.341	0.505	-0.730	-0.869
16.OBST-A	320.000	20000.000	8273.514	8795.718	1.063	0.616	-1.669
17.OBST-B	160.000	20000.000	5328.648	7874.023	1.478	1.381	-0.012
18.OBST-C	20.000	20000.000	1391.081	4541.415	3.265	4.023	15.244
25.2.00-OP-V	0.970	1.100	1.016	0.040	0.040	0.611	-1.031
26.GLn	1.200	6.300	2.592	1.196	0.462	1.557	1.933

Table 4 Fundamental Statistics of Variables(Logarithm Data)

NO.VARIABLE	MIN.	MAX.	AVERAGE	S.D	CO. of VA.	KURTOSIS	SKEWNEE
1.0.5MX	0.476	1.752	1.490	0.216	0.145	-2.916	13.039
2.5.0MX	0.476	1.944	1.666	0.261	0.157	-2.771	11.303
3.0.2MI	-2.303	4.868	2.852	2.489	0.873	-1.400	0.506
4.0.2GM	-6.908	1.099	-3.457	2.615	-0.757	-0.182	-1.278
5.0.25-UND	-2.303	4.382	2.470	2.115	0.856	-1.519	1.163
6.2.0MI	-2.303	4.868	0.643	3.179	4.946	0.232	-1.909
7.5.00-UND	1.609	6.824	5.302	1.017	0.192	-1.353	3.285
8.PRO	-6.908	4.094	0.084	1.726	20.597	-1.424	7.194
9.2.00-GP	-6.908	-0.875	-2.285	1.304	-0.571	-2.462	7.335
10.DIST-SEA	5.075	9.903	8.019	1.871	0.233	-0.242	-1.685
12.0.50-LOF	-6.908	0.000	-1.716	2.236	-1.303	-1.672	1.643
15.5.00-LOF	-6.908	0.000	-0.843	1.608	-1.908	-3.126	10.079
16.OBST-A	5.768	9.903	8.263	1.335	0.162	0.111	-1.345
17.OBST-B	5.075	9.903	7.469	1.513	0.203	0.521	-0.838
18.OBST-C	2.996	9.903	5.287	1.629	0.308	1.175	1.941
25.2.00-OP-V	-0.030	0.095	0.015	0.039	2.577	0.579	-1.087
26.N-LOG	0.182	1.841	0.868	0.401	0.462	0.669	0.284

Table 5 Result of Multiple Regression Analysis(Raw Data: All variables)

Dependent variable is: N-RAW
R^2 = 71.2% R^2(adjusted) = 48.2%

Source	Sum of Squares	df	Mean Square	F-ratio
Regression	36.691	16.000	2.293	3.09**
Residual	14.837	20.000	0.742	

Variable	Coefficient	s.e. of Coeff	t-ratio
Constant	13.171	8.414	1.570
0.5MX	-3.990	1.186	-3.360 **
5.0MX	3.702	1.104	3.350 **
0.2MI	0.012	0.015	0.831
0.2GM	0.251	0.374	0.671
0.25-UND	0.001	0.017	0.081
2.0MI	0.008	0.009	0.943
5.00-UND	-0.005	0.003	-1.590
PRO	0.039	0.019	2.050
2.00-GP	6.647	2.597	2.560*
DIST-SEA	0.000	0.000	0.174
0.50-LOF	1.484	0.828	1.790
5.00-LOF	-1.150	2.149	-0.535
OBST-A	0.000	0.000	2.420*
OBST-B	0.000	0.000	0.736
OBST-C	0.000	0.000	-0.041
2.00-OP-V	-14.704	8.101	-1.820

Table 6 Result of Stepwise Regression(Raw Data)

Dependent variable is: N-RAW
R^2 = 67.8% R^2(adjusted) = 57.0%

Source	Sum of Squares	df	Mean Square	F-ratio
Regression	34.916	9.000	3.880	6.31**
Residual	16.612	27.000	0.615	

Variable	Coefficient	s.e. of Coeff	t-ratio
Constant	16.770	6.223	2.690*
0.5MX	-2.827	0.482	-5.870**
5.0MX	2.604	0.439	5.930**
2.0MI	0.010	0.006	1.610
5.00-UND	-0.003	0.002	-1.720
PRO	0.037	0.014	2.570*
2.00-GP	6.288	1.984	3.170**
0.50-LOF	0.755	0.396	1.910
OBST-A	0.000	0.000	3.310**
2.00-OP-V	-17.185	5.770	-2.980**

(ii) Regression by general logarithm data

The results of Multiple Regression Analysis are shown in Table 7 and Table 8. The results of Table 7 which include all independent variables shows the R^2 of 76.8% with a level of significance of 1%. This value of R^2 is larger than that of analysis by raw data, however, only one independent variable could be found with a level of significance of 1%. Therefore, the results of Table 7 is not reliable.

Table 8 also shows the results of Stepwise Regression. The R^2 statistic of 67.8% was as same as the results of raw data and also significant at a level of 1%, however, only three independent variables with two kinds could be found at a level of significance of 1% on this analysis. The selected independent variables were [0.5MX], [5.0MX] and [2.00-GP].

Table 7 Result of Multiple Regression Analysis(Logarithm Data: All variables)

Dependent variable is: N-LOG
R^2 = 76.8% $\bar{R}^2$(adjusted) = 53.7%

Source	Sum of Squares	df	Mean Square	F-ratio
Regression	4.107	16.000	0.257	3.32*
Residual	1.239	16.000	0.077	

Variable	Coefficient	s.e. of Coeff	t-ratio
Constant	4.795	5.383	0.891
0.5MX	-6.794	1.511	-4.500**
5.0MX	0.461	3.962	0.116
0.2MI	0.087	0.053	1.670
0.2GM	-0.029	0.039	-0.748
0.25-UND	0.011	0.051	0.211
2.0MI	0.081	0.045	1.830
5.00-UND	0.648	0.753	0.861
PRO	0.302	0.143	2.110
2.00-GP	0.481	0.200	2.410*
DIST-SEA	0.124	0.111	1.120
0.50-LOF	0.048	0.058	0.839
5.00-LOF	-0.317	0.176	-1.800
OBST-A	0.239	0.173	1.380
OBST-B	-0.086	0.071	-1.210
OBST-C	0.045	0.062	0.727
2.00-OP-V	-5.892	3.024	-1.950

Table 8 Result of Stepwise Regression(Logarithm Data)

Dependent variable is: N-LOG
R^2 = 68.7% $\bar{R}^2$(adjusted) = 56.5%

Source	Sum of Squares	df	Mean Square	F-ratio
Regression	3.674	9.000	0.408	5.62**
Residual	1.672	23.000	0.073	

Variable	Coefficient	s.e. of Coeff	t-ratio
Constant	-1.723	2.544	-0.678
0.5MX	-4.705	1.052	-4.470**
5.0MX	3.935	1.107	3.550**
2.0MI	0.086	0.032	2.700*
PRO	0.087	0.084	1.040
2.00-GP	0.439	0.147	2.990**
DIST-SEA	0.123	0.087	1.410
5.00-LOF	-0.297	0.142	-2.090*
OBST-A	0.343	0.123	2.790*
2.00-OP-V	-6.510	2.361	-2.760*

(e) Concluding remarks

(i) The first trials of the statistical correlation analysis for the n-values of power law and topographical features has not achieve a reliable results yet, however, Stepwise Regression Analysis based on raw data suggested that a n-value of power law could be estimated by topographical features.

(ii) The results of Stepwise Regression based on raw data suggested that n-values of power law will be in proportion to numerical values of topographical features of [5.0MX], [2.00-GP] and [OBST-A]. This means n-values will increase with the increase of [5.0MX], [2.00-GP] and [OBST-A]. To the contrary, n-values would decrease with the increase of [0.5MX], [2.00-OP-V].

(iii) The more wind observation at various locations are necessary in order to find more reliable results of Multiple Regression Analysis and also verify the statistical models.

(iv) It is necessary to find out another topographical features that are strongly related to the change of n-values and also easy to convert to numerical values.

IEA WINDMEETING at FFA March 7-8 1991 **Participants**

M Berkelmans
Company: INTRON
Adress : Onderdoor 5 19
HOUTEN ~~Hanton~~ , Holland
Teleph : 03403-79580
Fax : 03403-79680

Jorgen Hojstrup
Company: Riso
Adress : DK 4000 Roskilde
Denmark
Teleph : +45 42371212
Fax : +45 46755619

Heiner Schmidt
Company: DWD-SWA
Adress : D-2000 Hamburg 36
PO Box ~~31190~~ 311190
Germany
Teleph : +49 40 3190822
Fax : +49 40 3190803

Gerd Tetzlaff
Company: UNI Hannover
Adress : D-3000 Hannover 21
Germany
Teleph : +49 511 7622620
+ 49 511 7623456

Augusto Aliberti
Company: ALENIA
Adress : Via Vitorchiano
81-00189 Roma
Italy
Teleph : +39 6 3339040
Fax : +39 6 333 9059

Stig Oye
Company: T V DK
Adress : DTH
bygn. 404
2800 Lyngby
Denmark
Teleph :
Fax :

Anders Wickström
Company: Kvaerner Turbin
Adress : Box 1005
681 01 Kristinehamn
Teleph : 0550-84800
Fax : 46 550 18998

Hans Ganander
Company: Teknikergruppen
Adress : Box 21
191 21 Sollentuna
Sweden
Teleph : 08 359455
Fax : 08 969987

Hans Bergström
Company: MIUU
Adress : Box 516
751 20 Uppsala
Sweden
Teleph : 018 542787
Fax : 018 544706

Ann-Sofi Smedman
Company: MIUU
Adress : Box 516
751 20 Uppsala
Sweden
Teleph : 018 542792
Fax : 018 544706

Ulf Högström
Company: MIUU
Adress : Box 516
751 20 Uppsala
Sweden
Teleph : 018 542800
Fax : 018 544706

Björn Montgomerie
Company: WEST
Adress : Via Archimede
Zona Industriale
741 00 Taranto
Italy
Teleph : +39 0 994769208
Fax : +39 0 4718566

Danny Winkelaar
Company: The Netherlands Energy Research Institute ECN
Adress : P O Box 1
1755 ZG Petten
The Netherlands
Teleph : +31 22464233
Fax : +31 22463214

Henry Parkinson
Company: ETSU
Adress : B156
Harwell Lab, Didcot, OXON
Ox11 ORA
UK
Teleph : 0 235 433462
Fax : 0 235 432923

Masanori Higashino
Company: Chiyoda Dames & Moore
Adress : 5-38-3 Kamata, Ota-Ku
Tokyo, 144 Japan
Teleph : 03 37342121
Fax : 03 37342126

Unsal Hassan
Company: Garrad Hassan
Adress : Cincorde House
9-11 St Stephens St
Bristol, UK
Teleph : 0272 250518
Fax : 0272 250517

Enzo Dalpane
Company: Riva Calzoni
Adress : V Emilia Ponente
72 40100 Bologna
Italy
Teleph : 051 527658
Fax : 051

Sören M Petersen
Company: Riso
Adress : DK-4000 Roskilde
Denmark
Teleph : +45 42371212
Fax : +45 2360609

S-E Thor

Company: FFA
Adress : Box 11021
161 11 Bromma
Sweden
Teleph : +46 8 7591370
Fax : +46 8 253481

Frits Verhey

Company: TNO
Adress : P O Box 342
7300 AH Apeldoorn
The Netherlands
Teleph : +31 55 ~~493394 231~~ 493493231
Fax : +31 55 419837

Dennis Elliot

Company: PNL
Adress : K6-07 P O Box 999
Richland WA 99352 USA
Teleph : 509 376 7860
Fax : 509 376 5217

B Maribo Pedersen

Company: DTH
Adress : DTH byggn 404
2800 Lyngby Denmark
Teleph : +45 42884622
Fax : +45 42882421

IEA-Implement Agreement R+D WECS
Topical Expert Meetings

1. Seminar on Structural Dynamics, Munich, October 12, 1978
2. Control of LS-WECS and Adaptation of Wind Electricity to the Network, Copenhagen, April 4, 1979
3. Data Acquisition and Analysis for LS-WECS, Blowing Rock, North Carolina, Sept. 26-27, 1979
4. Rotor Blade Technology with Special Respect to Fatigue Design Problems, Stockholm, April 21-22, 1980
5. Environmental and Safety Aspects of the Present LS WECS, Munich, September 25-26, 1980
6. Reliabiltiy and Maintenance Problems of LS WECS, Aalborg, April 29-30, 1981
7. Costings for Wind Turbines, Copenhagen November 18-19, 1981
8. Safety Assurance and Quality Control of LS WECS during Assembly, Erection and Acceptance Testing, Stockholm, May 26-27, 1982
9. Structural Design Criteria for LS WECS, Greenford, March 7-8, 1983
10. Utility and Operational Experiences and Issues from Mayor Wind Installations, Palo Alto, October 12-14, 1983
11. General Environmental Aspects, Munich, May 7-9, 1984
12. Aerodynamic Calculational Methods for WECS, Copenhagen, October 29-30, 1984
13. Economic Aspects of Wind Turbines, Petten, May 30-31, 1985
14. Modelling of Atomospheric Turbulence for Use in WECS Rotor Loading Calculation, Stockholm, December 4-5, 1985
15. General Planning and Environmental Issues of LS WECS Installations, Hamburg, December 2, 1987
16. Requirements for Safety Systems for LS WECS, Rome, October 17-18, 1988
17. Integrating Wind Turbines into Utility Power Systems, Herndon (Virginia), April 11-12, 1989
18. Noise Generationg Mechanisms for Wind Turbines, Petten, November 27-28, 1989
19. Wind Turbine Control Systems, Strategy and Problems, London, May 3-4, 1990
20. Wind characteristics of Relevance for Wind Turbine Design, Stockholm, March 7-8, 1991
21. Elektrical Systems for Wind Turbines with Constant or Variable Speed, Göteborg, October 7-8, 1991